

**Investigating the treatment of chloride-infested
archaeological iron objects**

Melanie B. Rimmer

Thesis submitted to Cardiff University
in candidature for the degree of PhD

June 2010

UMI Number: U585375

All rights reserved

INFORMATION TO ALL USERS

The quality of this reproduction is dependent upon the quality of the copy submitted.

In the unlikely event that the author did not send a complete manuscript and there are missing pages, these will be noted. Also, if material had to be removed, a note will indicate the deletion.



UMI U585375

Published by ProQuest LLC 2013. Copyright in the Dissertation held by the Author.
Microform Edition © ProQuest LLC.

All rights reserved. This work is protected against
unauthorized copying under Title 17, United States Code.



ProQuest LLC
789 East Eisenhower Parkway
P.O. Box 1346
Ann Arbor, MI 48106-1346

Declaration

This work has not previously been accepted in substance for any degree and is not concurrently submitted in candidature for any degree.

M. Rimmer 18/6/2010

M. Rimmer

Date

This thesis is being submitted in fulfilment of the requirements for the degree of PhD.

M. Rimmer 18/6/2010

M. Rimmer

Date

This thesis is the result of my own independent investigation, except where otherwise stated. Other sources are acknowledged by explicit references.

M. Rimmer 18/6/2010

M. Rimmer

Date

I hereby give consent for my thesis, if accepted, to be available for photocopying and inter-library loan, and for the title and summary to be made available to outside organisations.

M. Rimmer 18/6/2010

M. Rimmer

Date

Summary

Archaeological iron objects become infested with chloride ions during burial. These enhance electrochemical corrosion, acidify the pore solution and form hygroscopic β -FeOOH.

Controlling chloride-induced corrosion requires <15% relative humidity (RH); this is difficult to achieve in practice. Iron objects are at significant risk when dry storage is not maintained.

Alkaline deoxygenated solutions remove chloride ions from objects. A large quantitative dataset was needed to evaluate the chloride extraction efficiency, the relationship between chloride concentration and corrosion rate and the risks posed by aqueous treatments.

Using 120 archaeological iron nails as sample material, and recording chloride extraction behaviour for each individual object, three treatments were tested; nitrogen-deoxygenated 0.1M NaOH (20°C); and alkaline sulphite (0.1M NaOH/0.05M Na₂SO₃) at 20°C and 60°C. Objects were subsequently digested to measure residual chloride.

Chloride extraction efficiency was 60–99% in most cases; 87% of treatments resulted in residual chloride levels <1000 ppm. Accelerated corrosion tests showed that treated objects were more stable than untreated. Post-treatment scanning electron microscopy identified chloride ions in corrosion products or within slag inclusions, but none at the metal/corrosion interface.

The transformation of synthetic β -FeOOH showed that 0.5M NaOH or 0.1M NaOH/0.05M Na₂SO₃ (60°C) produced the maximum transformation (c.50%) to α -FeOOH and/or α -Fe₂O₃. It could not be confirmed whether this reaction occurs on objects.

Risk to objects was evaluated by assessing physical damage during treatment and modelling chemical residues. Less than 2% of objects experienced total fragmentation; 69% experienced no change. The most likely chemical residue from alkaline sulphite is Na₂SO₄; this poses no threat to objects at RH <76%.

The research reported here is a substantial addition to the body of data about desalination treatment. It improves understanding of the benefits and risks of treatment in relation to developing improved conservation strategies for highly chloride-contaminated objects.

Acknowledgements

This research was funded by a Collaborative Doctoral Award from the Arts and Humanities Research Council (AHRC). Their financial assistance is gratefully acknowledged.

Foremost thanks go to my supervisors, David Watkinson (Cardiff University) and Quanyu Wang (The British Museum). Their advice, support and encouragement have been invaluable.

At The British Museum, my thanks go to all the staff of the Department of Conservation and Scientific Research for their welcome and support during my time in London. Nigel Meeks provided assistance and training for scanning electron microscopy and sample preparation. Aude Mongiatti gave advice on health and safety, and Stephen Gallagher and Larry Carr provided administrative assistance. Fleur Shearman provided advice on conservation issues and Ana Tam discussed her MSc project on iron conservation with me. David Saunders (Keeper) and Catherine Higgitt (Head of Science) were welcoming and supportive throughout the project. J.D. Hill (Directorate) took me and all the collaborative award holders at The British Museum under his wing.

This thesis would not have been possible without the generous provision of sample material by Helen Ganiaris (Museum of London), Niall Sharples (Cardiff University) and Evan Chapman (National Museums Wales). X-ray diffraction was carried out at the National Museum Wales (Cardiff) with the help of Amanda Valentine and Tom Cotterell. David Thickett (English Heritage) provided gas sensing equipment.

Finally I would like to thank all those who have supported and encouraged me over the past three years, especially my parents.

To my grandfathers

Dr Norbert Werner († 2000)

Thomas Rimmer († 2010)

Table of Contents

| | |
|--|----|
| Summary | 3 |
| Acknowledgements | 4 |
| List of Figures | 12 |
| List of Tables | 17 |
| Chapter 1 – Introduction | 19 |
| 1.1 Why preserve iron objects?..... | 19 |
| 1.2 How do you solve a problem like iron? | 20 |
| 1.2 Research aims and objectives | 22 |
| 1.3 The advantages of collaborative working | 23 |
| 1.4 The structure of this thesis..... | 24 |
| Chapter 2 - Chloride-induced iron corrosion | 26 |
| 2.1 Corrosion processes | 26 |
| 2.1.1 Atmospheric corrosion | 28 |
| 2.1.2 Marine corrosion | 31 |
| 2.1.3 Corrosion in soil | 32 |
| 2.2 Corrosion products..... | 35 |
| 2.2.1 Goethite, α -FeOOH..... | 36 |
| 2.2.2 Lepidocrocite, γ -FeOOH | 36 |
| 2.2.3 Akaganéite, β -FeOOH | 37 |
| 2.2.4 Green rusts..... | 41 |
| 2.2.5 Ferrous hydroxychloride, β -Fe ₂ (OH) ₃ Cl | 43 |
| 2.2.6 Hematite, α -Fe ₂ O ₃ | 44 |
| 2.2.7 Magnetite, Fe ₃ O ₄ | 44 |
| 2.3 Transformation of corrosion products | 45 |
| 2.3.1 Goethite to hematite | 46 |

| | |
|---|-----------|
| 2.3.2 Akaganéite to goethite and/or hematite..... | 46 |
| 2.3.3 Ferric oxyhydroxides to magnetite..... | 48 |
| 2.4 Post-excavation corrosion..... | 49 |
| 2.5 Unanswered questions..... | 52 |
| Chapter 3 - Conservation approaches to archaeological iron..... | 54 |
| 3.1 Preventive conservation..... | 54 |
| 3.2 Active conservation..... | 58 |
| 3.2.1 Current attitudes to desalination treatment..... | 61 |
| 3.3 Defining success in iron conservation..... | 63 |
| 3.3.1 Modelling treatment outcomes..... | 64 |
| 3.4 Desalination treatment variables..... | 67 |
| 3.4.1 Chloride removal mechanism..... | 67 |
| 3.4.2 pH and concentration..... | 69 |
| 3.4.3 Deoxygenation..... | 69 |
| 3.4.4 Temperature..... | 70 |
| 3.4.5 Diffusion and solution changes..... | 71 |
| 3.4.5 Conclusion..... | 72 |
| Chapter 4 – Experimental treatment of archaeological iron objects..... | 73 |
| 4.1 Introduction..... | 73 |
| 4.2 Objects for testing..... | 74 |
| 4.3 Methodology..... | 75 |
| 4.3.1 Considerations for treatment methodology..... | 75 |
| 4.3.2 Experimental desalination treatment..... | 77 |
| 4.3.3 Statistical assessment methods..... | 79 |
| 4.4 Results of experimental treatments..... | 81 |
| 4.4.1 Chloride extraction during treatment..... | 81 |

| | |
|--|------------|
| 4.4.2 Extraction efficiency | 91 |
| 4.4.3 Comparison of samples | 92 |
| 4.4.4 Comparison of treatments..... | 94 |
| 4.4.5 Comparison of sites | 104 |
| 4.4.7 Measuring treatment outcome without digestion | 109 |
| 4.5 Evaluating treatment outcome | 111 |
| 4.5.1 Analysis of sample cross-sections..... | 112 |
| 4.5.1.1 Sample selection | 112 |
| 4.5.1.2 Results | 113 |
| 4.5.1.3 Discussion..... | 120 |
| 4.5.1.4 Conclusion | 121 |
| 4.5.2 Accelerated corrosion testing..... | 122 |
| 4.5.2.1 Post-treatment assessment – a problem..... | 122 |
| 4.5.2.2 Accelerated corrosion testing method | 124 |
| 4.5.2.3 Results | 125 |
| 4.5.2.4 Relationship of chloride content and weight gain | 137 |
| 4.5.2.5 Conclusion of accelerated corrosion tests..... | 139 |
| 4.5.3 The probability of long-term outcome | 140 |
| 4.6 Summary..... | 142 |
| Chapter 5 – The transformation of akaganéite..... | 144 |
| 5.1 Introduction..... | 144 |
| 5.2 Methodology | 145 |
| 5.2.1 Manufacturing akaganéite..... | 145 |
| 5.2.2 Methodology for transformation testing | 146 |
| 5.3 Results of transformation tests | 148 |
| 5.3.1 Temperature | 148 |

| | |
|--|------------|
| 5.3.2 Solution concentration | 150 |
| 5.3.3 Seeding..... | 152 |
| 5.4 Discussion | 153 |
| 5.5 Conclusion | 156 |
| Chapter 6 – The risks of desalination treatment | 157 |
| 6.1 Short term risk – change to objects during treatment | 157 |
| 6.1.1 Methodology for assessing change | 160 |
| 6.1.2 Results of photographic analysis | 163 |
| 6.1.3 Discussion | 164 |
| 6.1.4 Probability of short-term outcome..... | 165 |
| 6.1.5 Conclusion on damage from treatment | 166 |
| 6.2 Long-term risk – treatment residues..... | 167 |
| 6.2.1 Methodology | 168 |
| 6.2.2 Results – formation of residues..... | 170 |
| 6.2.3 Results – the effect of residues on iron corrosion..... | 170 |
| 6.2.4 Discussion | 175 |
| 6.2.4.1 Sodium sulphate | 176 |
| 6.2.4.2 Ferrous sulphate | 177 |
| 6.2.5 Conclusion on risk from treatment residues | 178 |
| 6.3 The effect of rinsing..... | 179 |
| 6.3.1 Methodology | 179 |
| 6.3.2 Results..... | 180 |
| 6.4 Summary..... | 182 |
| Chapter 7 – General discussion..... | 184 |
| 7.1 Experimental treatment | 184 |
| 7.2 Location, nature and effect of residual chloride | 185 |

| | |
|---|------------|
| 7.3 Probability of treatment outcomes..... | 189 |
| Chapter 8 – Conclusion..... | 193 |
| 8.1 Conclusions from experimental work | 193 |
| 8.2 Decision-making in iron conservation | 195 |
| 8.3 When should objects be treated? | 196 |
| 8.4 Recommendations for treatment and storage | 197 |
| 8.5 Further work..... | 198 |
| Bibliography | 200 |
| Appendix 1: Experimental methods..... | 212 |
| 1.1 Manufacturing akaganéite | 212 |
| 1.2 Transformation experiments..... | 213 |
| 1.3 Desalination of objects | 213 |
| 1.3.1 Nitrogen-deoxygenated NaOH | 214 |
| 1.3.2 Alkaline sulphite..... | 215 |
| 1.4 Digestion of objects | 215 |
| 1.5 Climate chamber tests..... | 217 |
| Appendix 2: Analytical methods | 218 |
| 2.1 X-ray diffraction..... | 218 |
| 2.1.1 Sample preparation | 218 |
| 2.1.2 XRD method | 218 |
| 2.2 Cross-section analysis..... | 219 |
| 2.2.1 Sample preparation | 219 |
| 2.2.2 SEM analysis method | 220 |
| 2.2.3 Raman microscopy..... | 220 |
| 2.3 Chloride measurement..... | 220 |
| 2.3.1 In alkaline solutions | 221 |

| | |
|--|------------|
| 2.3.2 In sulphite-containing solutions | 222 |
| 2.3.3 In sulphide-contaminated solutions | 222 |
| 2.3.4 In solutions from digested nails..... | 222 |
| 2.4 pH measurement..... | 223 |
| Appendix 3: Statistical methods | 224 |
| 3.1 Descriptive statistics..... | 224 |
| 3.1.1 Measures of central tendency | 224 |
| 3.1.2 Measures of distribution | 224 |
| 3.2 Inferential statistics | 225 |
| 3.2.1 Correlation (Pearson Product Moment, r)..... | 225 |
| 3.2.2 Coefficient of variation (r^2) | 226 |
| 3.2.3 Analysis of variance (ANOVA) (F)..... | 226 |
| 3.2.4 Chi-squared test (χ^2)..... | 227 |

List of Figures

| | |
|---|----|
| Figure 1: Schematic diagram of corrosion morphology, adapted from Neff et al. (2005). The Dense Product Layer (DPL) retains the approximate shape of the object and contains cracks and magnetite/maghemite veins. The Transformed Medium (TM) includes soil minerals. | 34 |
| Figure 2: Archaeological iron nail showing a bubble-like structure formed during exposure of the object to 75% RH. The bubble is 2 mm across and probably composed of akaganéite. .. | 40 |
| Figure 3: The tip of an Anglo-Saxon spearhead where the formation of akaganéite crystals has resulted in a large flake of the corrosion layers being detached..... | 51 |
| Figure 4: A model showing the lifespan of an unconserved archaeological iron object. As corrosion continues, the value of the object decreases until it is effectively destroyed. | 65 |
| Figure 5: Modelled treatment outcomes. Treatment occurs at T1. Successful treatments are those that result in improved value at time T2. | 66 |
| Figure 6: Chloride ion content of digested nails from eleven archaeological sites. | 75 |
| Figure 7: Histogram showing final solution concentration for all the objects in the three experimental treatments. | 82 |
| Figure 8: Histogram of chloride ions extracted by the three treatments. Bin width is 500 ppm. | 82 |
| Figure 9: Extraction of chloride ions from objects in nitrogen-deoxygenated 0.1M NaOH (dNaOH)..... | 84 |
| Figure 10: Extraction of chloride from objects treated in 0.1M NaOH/0.05M Na ₂ SO ₃ solution (AS20). | 85 |
| Figure 11: Extraction of chloride from objects treated in 0.1M NaOH/0.05M Na ₂ SO ₃ at 60°C (AS60). | 86 |
| Figure 12: Chloride extraction in dNaOH treatment showing percentage of extracted chloride in each bath..... | 88 |
| Figure 13: Chloride extraction in AS20 showing percentage of extracted chloride in each bath. | 89 |
| Figure 14: Chloride extraction in AS60 as percentage of extracted chloride in each bath. | 90 |
| Figure 15: Histogram of total chloride content of the objects in the three desalination treatments. Bin size is 500 ppm..... | 93 |

Figure 16: Extracted and residual chloride data for objects treated with dNaOH. Extraction % is given on the secondary axis. The data is arranged in order of increasing extraction % within each site.95

Figure 17: Extracted and residual chloride data for objects treated in AS20. The data is arranged in order of extraction % (secondary axis) within each site.96

Figure 18: Extracted and residual chloride data for objects treated in AS60. Data is arranged in order of increasing extraction % within each site.97

Figure 19: Histograms showing extraction % for the three treatments. All three distributions are negatively skewed. Top: dNaOH. Middle: AS20. Bottom: AS60.98

Figure 20: Histogram of residual chloride for all objects in the three treatments. Bin size is 200 ppm.100

Figure 21: Scatter graph of extraction % and residual chloride, showing that there is a negative correlation between the two variables ($r = -0.486$, $r^2 = 0.2364$).101

Figure 22: Scatter graph showing extraction % and total chloride. Objects with extraction % < 60% are likely to contain less than 2000 ppm total chloride ($r = 0.4597$, $r^2 = 0.2113$).101

Figure 23: Scatter graph of extracted chloride and total chloride. Objects between the two lines contained less than 1000 ppm residual chloride ($r = 0.9749$, $r^2 = 0.9504$).103

Figure 24: Histogram of total chloride of the samples from the three sites.105

Figure 25: Histogram of extraction % of the treated objects from each site. Bin size is 5%. 105

Figure 26: Scatter graph of residual chloride and final solution concentration of objects ($r = 0.463$, $r^2 = 0.2144$).107

Figure 27: CAE_16 before treatment in dNaOH. This object is thickly encrusted with soil and performed poorly during the treatment, with an extraction of only 25%.108

Figure 28: CAE_34 before treatment in AS20. This object is also thickly encrusted with soil, but it had a good extraction of 84%.108

Figure 29: Scatter graph of extracted and residual chloride for the treated objects. There is no significant relationship between the two variables ($r = 0.13$, $r^2 = 0.0169$).110

Figure 30: Scatter graph of residual chloride and final solution concentration, by treatment ($r = 0.4631$, $r^2 = 0.2144$).110

Figure 31: BOR_1693.2. SEM image (top) showing fresh corrosion on the polished surface located near cracks in the corrosion structure (arrowed). The EDX map (bottom) shows high

levels of Cl in these areas. Cl is also located on the metal/corrosion interface and along the outer edge of the sample.....115

Figure 32: Figure 2: CAE_27.2. SEM image (top) and EDX map of chlorine (middle). The bottom image was taken several weeks after the top, and shows the development of Cl-containing corrosion products.115

Figure 33: CAE_27.2. SEM image of an area located at the base of a deep corrosion profile. This area contained Cl in two different concentrations, as shown by the EDX map. Both were identified as β -FeOOH by Raman spectroscopy. The arrow indicates the location of the banded structure at the boundary.....115

Figure 34: Raman spectrum of the chlorine-containing corrosion product shown in Figure 33. When compared with the reference spectrum, the product is identified as akaganéite.117

Figure 35: CAE_27.1. Backscattered electron image (top) and EDX spectrum (bottom), showing chlorine present in very small quantity in slag inclusions (analysis location indicated by arrow).....117

Figure 36: CAE_45.1. Backscattered electron image (top) and EDX map for chlorine (bottom) of a treated nail, showing fresh surface corrosion caused by chlorine located around internal slag inclusions.....118

Figure 37: BWB83_44.1. Backscattered electron image (top) and EDX map for chlorine (bottom) of the treated nail. Low levels of chlorine were located within the corrosion structure, but there were no associated fresh corrosion growths.....118

Figure 38: BWB83_44.2. Secondary electron image (top) and EDX map for chlorine (bottom), showing a band of crystals containing chlorine on the edge of the sample.118

Figure 39: Results of accelerated corrosion testing for untreated objects. Ambient RH at the time of weight measurement is given on the secondary axis.127

Figure 40: BOR_6151 before (left) and after (right) accelerated corrosion testing. This untreated object was completely fragmented during the test.128

Figure 41: CAE_48 before (left) and after (right) accelerated corrosion testing.....128

Figure 42: Results of accelerated corrosion testing for dNaOH objects. Ambient RH at the time of weight measurement is given on the secondary axis.129

Figure 43: Results of accelerated corrosion testing for AS20 objects. Ambient RH at the time of weight measurement is given on the secondary axis.....129

| | |
|--|-----|
| Figure 44: Results of accelerated corrosion testing for halved Bornais objects treated in dNaOH. Ambient RH at the time of weight measurement is given on the secondary axis... | 131 |
| Figure 45: Results of accelerated corrosion testing for halved Bornais objects treated in AS20. Ambient RH at the time of weight measurement is given on the secondary axis. | 131 |
| Figure 46: BOR_1698. The treated half on the left showed no change during the accelerated corrosion test, while the untreated half on the right began to fragment..... | 132 |
| Figure 47: Results of accelerated corrosion testing for halved Billingsgate objects treated in dNaOH. Ambient RH at the time of weight measurement is given on the secondary axis... | 133 |
| Figure 48: Results of accelerated corrosion testing for halved Billingsgate objects treated in AS20. Ambient RH at the time of weight measurement is given on the secondary axis. | 133 |
| Figure 49: Results of accelerated corrosion testing for halved Caerwent objects treated in dNaOH. Ambient RH at the time of weight measurement is given on the secondary axis.. | 135 |
| Figure 50: Results of accelerated corrosion testing for halved Caerwent objects treated in AS20. Ambient RH at the time of weight measurement is given on the secondary axis. | 135 |
| Figure 51: CAE_45.1 (left) and CAE_45.2 (right). Both show signs of instability, but CAE_45.2 is more fragmented..... | 137 |
| Figure 52: Scatter graph showing correlation between chloride content and total weight gain during the accelerated corrosion test ($r = 0.534$, $r^2 = 0.286$). The data has been organised to reflect the final solution concentration. | 137 |
| Figure 53: X-ray diffraction spectrum for pure synthetic akaganéite. The green bars represent peaks of reference spectrum. | 146 |
| Figure 54: Transformation of akaganéite to goethite in room temperature solutions..... | 149 |
| Figure 55: Transformation of akaganéite to goethite and hematite in heated solutions. Hematite only occurred in the presence of sulphite ions..... | 149 |
| Figure 56: Transformation of akaganéite to goethite in varying concentrations of NaOH (60°C)..... | 151 |
| Figure 57: Transformation of akaganéite to goethite and hematite in varying concentrations of alkaline sulphite (60°C). Hematite occurred in the presence of 0.1M Na ₂ SO ₃ only..... | 151 |
| Figure 58: Transformation of akaganéite seeded with goethite in heated solutions. | 153 |
| Figure 59: Transformation of akaganéite seeded with magnetite in heated solutions. | 153 |

Figure 60: Examples of objects falling into each of the four change categories. Left: Before treatment. Right: After treatment. A = BOR_6510 (dNaOH), B = BWB83_40 (AS20), C = BOR_6750 (AS20), D = CAE_14 (dNaOH).162

Figure 61: Weight measurements of Fe, Na₂SO₄ and a mix of both at 75% RH. Weight gain for the mixture (bottom graph) is minimal over 16 days.171

Figure 62: Weight measurement of Na₂SO₄ and Fe/Na₂SO₄ at 90% RH. Hydration is rapid in both cases.172

Figure 63: Weight measurements for FeSO₄·7H₂O and Fe/FeSO₄·7H₂O. The 7-hydrate does not gain noticeable weight. Very slow weight gain is occurring in the mixture.....173

Figure 64: Hydration of FeSO₄·4H₂O and Fe/FeSO₄·4H₂O at 75% RH. Hydration of ferrous sulphate is complete within 1 day with no further weight change. The mixture gains weight more slowly. The line has been extrapolated in two places due to failure of the software to record for short periods of time during this test.174

Figure 65: Weight gain caused by including NaCl in a mixture of Fe and FeSO₄. At 75% RH weight gain is rapid and continuous, with much greater weight gain than any other test. .175

Figure 66: pH changes as a result of rinsing Nail 1 in deionised water. The rinse water was not stirred.....180

Figure 67: pH changes as a result of rinsing Nail 2 in deionised water. The rinse water was not stirred.....180

Figure 68: pH change as a result of rinsing Nail 3 in deionised water. The rinse water was stirred using a magnetic stirring rod.....181

Figure 69: Rinsing nail 2, showing development of orange corrosion on the surface after rinsing. The product was very powdery and non-adherent and identified as lepidocrocite.181

Figure 70: Graphical representation showing the probability of the treatment outcomes in order of decreasing desirability (left to right).....190

Figure 71: Diagram of set-up for dNaOH treatment.....214

Figure 72: Nitrogen-deoxygenated desalination in progress. The gas from the cylinder (right) flows through both Stewart boxes and out via the gas bubbler at the back.215

Figure 73: Testing weight measurements in climate chamber using 100g weight.217

Figure 74: XRD analysis of standardised goethite/akaganéite mixtures.219

List of Tables

| | |
|--|-----|
| Table 1: Common corrosion products that are discussed in this study. The information is taken from Cornell & Schwertmann 2003 and Scott & Eggert 2009. | 28 |
| Table 2: Hypothetical treatment outcomes for evaluation using data in this study. Short-term damage and long-term stability are both considered in evaluating overall outcome. .. | 66 |
| Table 3: Chloride testing for sample objects from eleven archaeological sites. | 74 |
| Table 4: Parameters of the experimental treatments carried out in this study. | 77 |
| Table 5: Descriptive statistics for the extraction of chloride ions in the three experimental treatments. | 83 |
| Table 6: Descriptive statistics for the three experimental treatments. S.D = standard deviation. I-Q range = interquartile range. | 92 |
| Table 7: Descriptive statistics for treated objects by site origin. The data from all three treatments has been combined. | 104 |
| Table 8: Samples of archaeological iron examined by SEM-EDX. Extracted chloride during treatment and chloride content as determined by digestion are given. | 113 |
| Table 9: Data for objects subjected to accelerated corrosion testing. Weight gain at the end of the test is given as % of weight of object, and chloride content was determined by digestion. Final solution concentration for the treated objects is also given. | 126 |
| Table 10: Probability of long-term stability of treated objects based on residual chloride data. | 141 |
| Table 11: Parameters for transformation testing of akaganéite and akaganéite mixtures. | 147 |
| Table 12: Results of transformation tests of pure akaganéite. Proportions are subject to an error of approx. 10% (see Appendix 2.1.2). | 148 |
| Table 13: Results of transformation of akaganéite seeded with goethite or magnetite. Seeding was 10 wt%, but the XRD software recorded this as 16% goethite or 17% magnetite. | 152 |
| Table 14: pH of NaOH solutions used in akaganéite transformation tests. | 155 |
| Table 15: Criteria for assessing change to objects during desalination treatment. | 161 |
| Table 16: Results of photographic analysis of change to objects during treatment. | 163 |
| Table 17: Probability of damage during treatment based on change analysis. | 166 |

Table 18: Solutions evaporated to dryness to simulate treatment residue formation. Results of the product analysis are given.....169

Table 19: Solid-state experiments to evaluate the effect of residues on iron corrosion. Compounds 1 and 2 were mixed and exposed to the given RH at 20°C in the climate chamber.170

Table 20: Transition RH and deliquescence RH for the compounds in this study. RH values are given for 20°C. Note that the only hydrated form of NaCl, NaCl·2H₂O, is not stable at atmospheric pressure above a temperature of 0.1°C, and is therefore not relevant to this study. References: ¹Steiger & Asmussen 2008, ²Chou et al. 2002, ³Ehlers & Stiles 1965, ⁴Linnow & Steiger 2007.....175

Table 21: Probability of treatment outcomes calculated using short and long-term outcome data developed in this study.....189

Chapter 1 – Introduction

'If these collections are so precious, why don't we take better care of them?' The next level of logic is, of course, 'If we don't take care of them, why should we keep them?'

Sonderman 1996

1.1 Why preserve iron objects?

Archaeological iron objects are an important part of our heritage. Iron has been used to make a vast range of objects, including weaponry, tools, ornaments and structures. It is a source of information about human capability, technological achievement, and many aspects of past societies. Iron objects form a part of the excavated material archive without which the past would be much more difficult, if not impossible, to interpret. Our inability to observe the past directly means that our ideas about it must be derived from the material evidence of past human activities (Fowler 1992; Shanks 1992).

The advent of new techniques of analysis and interpretation means that the interpretation of a site or object assemblage may change with time. Retaining the records and material archive from an excavation allows future interpretation to occur (Grossman 2006: 5), and this assumes long-term or indefinite storage. It is at this stage that conservation usually begins, and its principle purpose as far as archaeological material is concerned must be the preservation of the material record so that it can continue to provide information about the past. As archaeological excavations often involve the destruction of sites, the impact of that destruction is mitigated by retaining the material evidence and preserving it for the future. The wider world benefits from the conservation and interpretation of a shared past which contributes to national, cultural or social identity, as well as providing economic benefits in the form of the heritage industry (Fowler 1992; Smith 2006)

The retention of large archaeological material archives has caused storage problems for museums across the UK (Merriman & Swain 1999). Unlike museums which employ strict collecting policies, archaeologists are trained to retain everything they find, no matter how small or insignificant it may appear (Sonderman 1996). This leads to museums expending significant resources to preserve material which may receive very little use. A survey of

museum archaeological archives showed that only a few requests to work with archive material were made per year (Merriman & Swain 1999). Much archaeological material in archives is never used, and interest in some sites is so low that publications may never be read (Shanks 1992: 70)

The placement of material into a museum or archive presumes that the material has some value and should be preserved. As funding for research excavations decreases and more and more is preserved in situ, the extant material record from previous excavations may become more important as a source of material for research (Nelson & Shears 1996). For archaeological iron objects, however, entry into an archive does not guarantee long-term preservation.

1.2 How do you solve a problem like iron?

Iron is one of the most reactive metals used in the past, and this causes problems with its conservation. Extracting iron from iron-oxide bearing rocks through the input of heat and reducing conditions removes iron from its usual oxidised state (Scott & Eggert 2009). The return of iron metal to its mineral state is a natural chemical reaction. In that sense, iron rusts, and there is ultimately no escape from this fact.

Excavated iron objects are often no longer made of iron metal. The iron has begun its transformation back into the raw materials from which it was created, and although the objects excavated by archaeologists bear a relationship to the original, an irreversible chemical change has occurred. Changes continue to occur after objects are excavated and placed in museums for storage, analysis, display and safe-keeping. As long as an object contains a remnant of metal, it will be chemically inclined to continue the processes of oxidation and corrosion.

This is not to say that human intervention cannot extend the lifespan of an object. Altering the conditions in which an object is stored can retard the natural processes of corrosion, and can do so for a very long time. This maintains the information value for a longer period of time and allows for future reinterpretation. The goal of increasing lifespan underlies the research into the conservation of archaeological iron objects reported in this thesis.

Preventive conservation methods regulate the environment in order to increase lifespan. The degree of regulation can be balanced against the need for access and the available resources. But the fact that the conservation of archaeological iron is still acknowledged as a significant problem for museums and archaeological archives (Cronyn 1990; Keene 1994; Knight 1997; Selwyn 2004; Schmutzler & Ebinger-Rist 2008; Scott & Eggert 2009) suggests that preventive conservation has not been a sufficient solution for iron conservation to date.

Why is it that the solutions offered by preventive conservation do not appear to be ensuring the reasonable survival of archaeological iron objects? A full discussion is in Chapter 3, but the main issue is that a theoretical approach does not always work in practice. Although environmental control can prevent iron corrosion, factors such as resource availability, lack of time and other practical constraints mean it is not always possible to implement the strict and ongoing humidity control required to preserve objects. In a world of unlimited resources, preventive conservation would be sufficient for the preservation of iron objects, but this is not the world which conservators, and the objects they seek to preserve, inhabit.

The main reason why archaeological iron objects are problematic is post-excavation corrosion induced by chloride ion contamination of objects. Not only do chloride ions increase corrosion rates substantially, they also lower the critical humidity levels at which corrosion can begin to occur (Cai & Lyon 2005; Watkinson & Lewis 2005a, 2005b). This increases the difficulty of maintaining environmental conditions sufficiently to prevent corrosion. The problem of chloride-contaminated artefacts is the focus of this thesis.

It is also possible to remove chloride ions by means of chemical desalination treatment. Such treatments have existed for many years, but have been generally rejected in Britain in favour of preventive methods in the last few decades (Knight 1997). One reason for this is the lack of reliable empirical data on the effects of desalination, both positive and negative. Although studies were carried out on treatment mechanism (North & Pearson 1978b; Gilberg & Seeley 1982; Selwyn et al. 2001), effectiveness (Rinuy & Schweizer 1982; Watkinson 1982, 1996) and long-term outcomes (Keene & Orton 1985; Selwyn & Logan 1993; Keene 1994), no method was fully tested for effectiveness, and no single method ever came into common usage.

Preventive conservation became the preferred method for iron conservation partly as an acknowledgement of the principle of minimum intervention (Cronyn 1990: 9). This principle may appear to reject any desalination treatment in favour of preventive control, assuming that less intervention is always the better option. However, the principle of minimum intervention as a statement is incomplete (Caple 2000: 65); a goal for conservation must first be established, and then the means of achieving it assessed. For archaeological iron, the goal is to eliminate the effects of chloride contamination and stabilise the object so that it can continue to provide information about the past.

Environmental control, although theoretically capable of achieving this goal, does not always do so in practice. To achieve the consistently low relative humidity required for stabilisation (Watkinson & Lewis 2005b) requires considerable resources and constant maintenance. With limited resources available, it may not always be possible to achieve adequate provision of desiccated storage for iron objects, and without proper maintenance, desiccated storage is at risk of failure. This leads to rapid corrosion and eventual destruction of objects. In these cases, the use of desalination treatments to achieve the conservation goal can be considered as a valid option.

If desalination treatments are to be considered as an alternative or additional conservation measure for archaeological iron, more data is needed to support an evaluation of the benefits and risks. The purpose of this thesis is to provide well-supported quantitative data on the effectiveness and risks of selected desalination treatments, to help conservators decide whether desalination treatments can form a part of their overall iron conservation strategies.

1.2 Research aims and objectives

This research is designed to provide quantitative, statistically evaluated data on the effectiveness of desalination treatment for archaeological iron objects which can then be discussed relative to the preservation of archaeological iron and the design of treatment protocols. Its objectives are:

- To carry out selected aqueous desalination treatments and quantitatively measure their effectiveness in removing chloride ions.

- To use archaeological material (iron objects from terrestrial excavated sites) as sample material.
- To measure residual chloride content of objects after treatment by means of acid digestion.
- To provide sufficient data for statistical evaluation.
- To examine the link between treatments, chloride content of objects and corrosion rate.
- To examine the effects of treatment solutions on corrosion products, especially those that contain chloride ions.
- To critically evaluate the risks of treatment, both in the short and long term.

By fulfilling these objectives, this research will provide a quantitative, properly evaluated dataset on the effectiveness and outcomes of selected desalination treatments. Providing enough data to allow statistical evaluation will overcome the problems of small and unrepresentative data sets (Rinuy & Schweizer 1982; Watkinson 1996; Al-Zahrani 1999; Wang et al. 2008; Watkinson & Al-Zahrani 2008) and gives a strong basis for evaluating treatment outcomes. An examination of the effect of treatment on corrosion rate allows the benefits of treatment to be properly assessed alongside a considered analysis and appraisal of the risks involved, and will aid conservators in their decision-making.

1.3 The advantages of collaborative working

This thesis is the result of a Collaborative Doctoral Award funded by the Arts and Humanities Research Council (AHRC). The council and the research community are developing collaborative projects to cross interdisciplinary boundaries, to develop new partnerships and create research synergy.

Heritage science is a fruitful area for collaborative working (Williams 2009). Many conservation problems are related to physical and chemical processes and require the application of scientific principles and theories. The solutions, however, cannot lie solely in the domain of science, but must be applicable to and usable by conservators and their institutions. Answers cannot be found on the basis of science alone, but must also account for the special concerns and situations of conservators and the unique character of the material for which they are responsible. Ethical and practical concerns may limit the types of

analysis that are possible or the treatments or conservation solutions which science can supply (Muñoz Viñas 2005).

For this project, collaborative working was particularly useful, as the author is neither a conservator by training nor had direct experience of working in a museum environment. The participation of The British Museum in this research was very valuable in supplying expertise and insight into the conservation aspects of the research. Part of the research was carried out on the premises of the museum in the Department of Conservation and Scientific Research for one year (2009), where the author had many opportunities to talk to practising conservators and conservation scientists, and gain an insight into the workings of the museum and how this might affect the conservation strategy that could be developed.

The museum also benefits from participating in a collaborative research project. The British Museum has carried out several small-scale studies of desalination treatments over the past decade (Wang et al. 2008; Tam 2009), in an attempt to determine whether desalination should be reconsidered as a conservation option. It was realised that the museum had neither the time nor the resources to commit to the extensive, in-depth study needed to answer this question. Collaborating with Cardiff University in this doctoral research allowed the museum to contribute to the shaping of the research project to address their questions and concerns about desalination treatment. Although the research was designed as a standalone academic study and could have been executed as such, the involvement of the museum in the project has, it is hoped, increased its practical relevance to the community of conservation professionals.

1.4 The structure of this thesis

The thesis is structured to address the research objectives given above. An overview of the corrosion problem and relevant research is presented (Chapter 2), which forms a basis for the following discussions about conservation options, treatment mechanisms and the evaluation of treatment success (Chapter 3). The experimental treatment of archaeological iron objects and methods for assessing the success of the treatments are presented in Chapter 4. This is supplemented by experiments on the ability of treatment solutions to remove chloride ions from chloride-bearing corrosion products, which has an impact on the development of treatment methods (Chapter 5). The assessment of short and long-term risk

follows in Chapter 6. These three chapters report all the experimental work undertaken to fulfil the research objectives. In Chapter 7, a discussion of all the experimental results is presented and the benefits and risks of treatments evaluated. Chapter 8 provides a summary and conclusion, including recommendations for treatment directed at conservators and areas for further research.

Chapter 2 - Chloride-induced iron corrosion

Conservation aims for reasonably stable health rather than no change at all.

Pye 2001: 28

The corrosion of iron is, at its most basic, the return of the metal to the iron minerals from which it was extracted. The wide range of uses of iron and its alloys has led to a significant body of scientific study of iron corrosion reactions and products, and in this chapter the most relevant areas of this work are summarised in the context of archaeological iron. There are common areas between corrosion science and conservation (Cole et al. 2004), particularly as regards the study of corrosion products and their properties. Working with modern iron and steel, however, the corrosion science and engineering viewpoint is concerned primarily with understanding the earliest phases of corrosion processes, methods of slowing down or preventing corrosion on clean metal surfaces, and calculating the service life of iron alloys. Conservators are faced with iron objects that are already significantly corroded and whose corrosion products are important to the integrity and value of the object; they retain its shape and may contain mineral-replaced organic pseudomorphs (Cronyn 1990). This means that some corrosion science, particularly that dealing with thin oxide films, may be only of limited relevance. This section reviews the most relevant research to form a basis for understanding why chloride-contaminated iron is subject to severe corrosion processes and how desalination treatments could contribute to improving its stability.

2.1 Corrosion processes

Iron corrosion is, at its most fundamental, the oxidation of iron to ferrous (Fe^{2+}) ions according to reaction [1] (North & MacLeod 1987: 69). As with all redox reactions, the loss of electrons from iron must be balanced by a corresponding reduction. For archaeological iron, the two most common reactions are the reduction of hydrogen [2] and the reduction of oxygen [3] (North & MacLeod 1987: 69).





Hydrogen reduction has been connected with corrosion in marine contexts, and will be discussed briefly below. For the majority of terrestrial buried iron with which this study is concerned, enough oxygen and water is present to allow reaction [3] to be the main cathodic reaction, although exceptions may occur in anoxic waterlogged conditions. Where oxygen reduction is the cathodic reaction, the combination of reaction [1] and [3] gives the overall electrochemical corrosion reaction [4] (North & MacLeod 1987: 69).



Where these two reactions occur in the same place, the initial product is ferrous hydroxide, $\text{Fe}(\text{OH})_2$. Further oxidation of ferrous ions produces ferric ions [5]. A variety of further compounds can then form (Table 1), depending on local conditions of pH and redox potential, oxygen concentration, presence of other ionic species, presence of liquid water, thickness of corrosion layers and other variables (Scott & Eggert 2009: 95).

Corrosion products are also subject to further alteration according to surrounding conditions. They may be inherently metastable and transform slowly over time. Changes in environmental conditions alter the thermodynamic stability of corrosion products and lead to transformation to other compounds. Intermediate and unstable compounds such as the green rusts (see section 2.2.4 below) may occur during reactions. As much of the nature of corrosion and its products is dependent on environmental conditions, the discussion below is separated into the three environments most likely to be encountered by conservators working on iron.

Table 1: Common corrosion products that are discussed in this study. The information is taken from Cornell & Schwertmann 2003 and Scott & Eggert 2009.

| Product | Formula | Crystal structure |
|-------------------------------------|---|--------------------------|
| Goethite | $\alpha\text{-FeOOH}$ | Orthorhombic |
| Akaganéite | $\beta\text{-FeOOH}$ | Monoclinic |
| Lepidocrocite | $\gamma\text{-FeOOH}$ | Orthorhombic |
| Magnetite | Fe_3O_4 | Cubic |
| Hematite | $\alpha\text{-Fe}_2\text{O}_3$ | Hexagonal (rhombohedral) |
| Maghemite | $\gamma\text{-Fe}_2\text{O}_3$ | Cubic |
| Ferrous hydroxychloride | $\beta\text{-Fe}_2(\text{OH})_3\text{Cl}$ | Monoclinic? |
| Green rust 1 (Cl^-) | $\text{Fe(II)}_3\text{Fe(III)}(\text{OH})_8\text{Cl}\cdot n\text{H}_2\text{O}$ | Rhombohedral |
| Green rust 1 (CO_3^{2-}) | $\text{Fe(II)}_4\text{Fe(III)}_2(\text{OH})_{12}\text{CO}_3\cdot 2\text{H}_2\text{O}$ | Rhombohedral |
| Green rust 2 (SO_4^{2-}) | $\text{Fe(II)}_4\text{Fe(III)}_2(\text{OH})_{12}\text{SO}_4\cdot n\text{H}_2\text{O}$ | Hexagonal |
| Ferrous chloride dihydrate | $\text{FeCl}_2\cdot 2\text{H}_2\text{O}$ | Monoclinic |
| Ferrous chloride tetrahydrate | $\text{FeCl}_2\cdot 4\text{H}_2\text{O}$ | Monoclinic |

2.1.1 Atmospheric corrosion

The importance of iron and its alloys in the construction and engineering industries has led to much research into the corrosion of iron in terrestrial atmospheres. The primary mechanism is that which occurs through a wet/dry cycle, first modelled by Evans and Taylor (1972). The wetting and drying of metal surfaces under atmospheric conditions leads to cycles of oxidation and reduction, and the reduction of corrosion products may contribute to the cathodic reaction.

During the wetting stage, iron is dissolved at the anode and the electrons produced are consumed by the reduction of iron oxyhydroxides (FeOOH), to magnetite (Fe_2O_3). During the drying stage, Fe_2O_3 is reoxidised to FeOOH until the water has evaporated and electrochemical reaction ceases. This original model has been modified and expanded, particularly regarding the important role of atmospheric pollutants such as sulphur dioxide (SO_2) and chloride ions (Cl^-).

Dünnwald and Otto (1989) studied the wet/dry corrosion of iron in the presence of SO_2 and suggested that the formation of sulphuric acid (H_2SO_4) during the wet phase played a

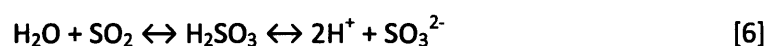
significant role. Their modification suggests that the acid reacts with iron to produce iron sulphate (FeSO_4), followed by transformation to $\text{Fe}(\text{OH})_2$ and finally oxidation in air to $\text{Fe}(\text{OH})_3$ during the drying period. Further water loss leads to FeOOH formation, primarily goethite ($\alpha\text{-FeOOH}$) and lepidocrocite ($\gamma\text{-FeOOH}$). This process may take several days. Reduction of FeOOH during the next wetting cycle depended on electrochemical potential. Magnetite formation occurred only at potentials lower than -0.5 V (SCE) from lepidocrocite, and from goethite at potentials less than -0.9 V (SCE) . At more positive potentials, Dünwald and Otto suggest that $\text{Fe}(\text{OH})_2$ is the primary reduced state of the corrosion layers and it reoxidises to $\text{Fe}(\text{OH})_3$ on drying, and that any magnetite does not reoxidise to FeOOH . Stratmann and Hoffmann (1989) suggested that the conversion of lepidocrocite and goethite to magnetite was a solid-state reversible reaction involving the movement of protons (H^+), allowing FeOOH to become a semi-conductor capable of transferring electrons and allowing corrosion of the iron substrate.

Stratmann and Hoffmann (1989) also showed that as rust layers age, the proportion of lepidocrocite, the more easily reduced oxyhydroxide, falls in favour of goethite production; this is supported by recent observations that rust layers become more electrochemically stable over time (Antony et al. 2007). The involvement of iron oxyhydroxides in atmospheric corrosion, particularly lepidocrocite, the unstable and poorly crystalline ferroxihite ($\delta\text{-FeOOH}$) and ferrihydrite ($\text{Fe}_2\text{O}_3 \cdot n\text{H}_2\text{O}$) as a source of electrons has been confirmed by the recent studies of Monnier et al. (2007) and Neff et al. (2006). The formation of $\text{Fe}(\text{OH})_3$ is also supported by Song et al. (2002).

Other studies of the corrosion layers formed on wet/dry corroded iron show that magnetite layers can transform to goethite and/or lepidocrocite (Keiser et al. 1982), with the presence of sulphate ions promoting goethite formation. Oxygen reduction to hydrogen peroxide (H_2O_2) has also been suggested (Keiser et al. 1982) but Song et al. (2002) detected very little hydrogen peroxide during the observation of iron hydroxide films. Garcia (2005) found traces of hematite in rust films on steel, suggesting that it formed from solution transformation of FeOOH .

One of the most critical factors in atmospheric corrosion is the formation of the liquid water film on the iron surface which allows electrochemical corrosion to occur. The relative

humidity (RH) at which surface water films occur has been called the critical RH. Cai and Lyon (2005) showed that even at 95% RH, insufficient surface water films form on iron surfaces to allow detectable corrosion. Atmospheric pollutants such as sodium chloride (NaCl) and sulphur dioxide (SO₂) play an important role in promoting corrosion by lowering the critical RH. Both SO₂ and NaCl increase atmospheric corrosion by about the same amount, although the calculated activation energy for reactions involving NaCl is lower (Cai & Lyon 2005). A further modification to the corrosion cycle was proposed, involving the formation of sulphurous acid (H₂SO₃), rather than sulphuric acid [6], and subsequent oxidation of sulphite to sulphate ions [7] as a controlling rate reaction (Cai & Lyon 2005). This reaction is catalysed by transition metals such as iron, and the reaction therefore becomes easier as ferrous ions are liberated by anodic dissolution.



Where chloride ions were present, the diffusion rate of water and/or oxygen through the oxide film seemed to be the rate controlling factor, but Cai and Lyon (2005) discovered that the thickening of the oxide film did not reduce the rate of reaction as would normally be expected for a diffusion-controlled reaction. This suggests that chloride ions are regenerated during the corrosion reaction, perhaps through the formation of an iron/chloride complex and subsequent hydrolysis (Duncan 1988; Cai & Lyon 2005) or through the acid regeneration cycle proposed by Askey et al. (1993) (see section 2.4). The role of chloride ions in corrosion is discussed further below.

Many of these studies have involved very thin oxide films, which are far removed from the bulky and complex corrosion layers found on buried objects. However, an understanding of the early stages of oxide formation is useful. The initial corrosion processes and the resulting layers may have application to archaeological iron, since fissured and cracked corrosion layers allow ingress of oxygen, water and pollutants to the metal surface which may induce similar reactions to those on atmospherically corroded iron. The active role of rust layers in corrosion cycles on archaeological iron has not been confirmed, but it cannot be ruled out. The complexity of the corrosion process and its changing profile according to time and prevailing conditions is evident from this brief review.

2.1.2 Marine corrosion

As this study deals primarily with terrestrial iron objects, marine corrosion is described only briefly. Marine environments range from the open sea to complete burial in marine sediments, and corrosion profiles vary as a result. In open water, thick encrustations form on cast iron objects through the action of marine organisms which concrete the iron (North & MacLeod 1987). This leads to rather different corrosion processes to those on terrestrial, wrought iron objects. Hydrogen reduction [2] as a cathodic reaction has been thought to play a significant role in iron corrosion in marine conditions. North (1982) claimed that hydrogen evolution is the main cathodic reaction because corrosion rates did not seem to be influenced by oxygen levels, and significant quantities of gas appear when marine concretions are broken open (North 1982).

As hydrogen reduction involves the removal of H^+ ions, it should be accompanied by an increase of pH. For thermodynamic reasons, it is also expected to occur at the metal surface (Turgoose 1985). In many marine concretions, however, low pH is found, as well as high concentrations of chloride ions from the seawater. Low pH probably occurs due to hydrolysis of ferrous ions [8, 9], which produces H^+ . The concentration of positive ions at the metal surface causes negatively charged chloride ions to move inwards to balance the charge (Turgoose 1985).



This two-stage formation of $Fe(OH)_2$ and the acidification of iron with chloride ion migration have been demonstrated experimentally (Ouyang et al. 2004; Ouyang & Xu 2005). The local acidification near the metal surface also increases corrosion rate as an autocatalytic reaction (Ouyang & Xu 2005). The experiments demonstrated that as long as iron dissolution at the anode produced positive ions, chloride ions diffused towards the positive charge. This tends to support the concept of chloride ions being held at anode sites as a counter ion.

The concentration of positive charge and low pH at the metal surface of a concreted iron object is not consistent with the reduction of hydrogen at this surface, and led Turgoose (1985) to conclude that the cathodic reaction must take place some distance from the metal

surface, within the concreted corrosion products, and that this cathodic reaction must be the reduction of oxygen [3]. This is supported by Carpenter and MacLeod (1993), who found correlations between the calculated corrosion rate of iron cannon from shipwrecks and the levels of dissolved oxygen in the water. Hydrogen evolution may still play a separate role through the action of bacteria, which are known to colonise marine iron (Jones 1996). These bacteria, of which there are many types, produce sulphide ions which react with the metal, produce sulphur which catalyses hydrogen evolution, and also produce the hydrogenase enzyme for catalysing hydrogen reduction (Jones 1996: 376). Marine corroded iron may therefore contain iron sulphide corrosion products which are not typically found on terrestrial objects (Refait et al. 2003b).

Whatever the specific reactions that occur, the concretions formed by marine growths on iron objects result in micro-environments which may be very corrosive given their low pH and high chloride ion content. The character of marine corrosion and the fact that the majority of research into its mechanisms and conservation treatment has focused on cast iron makes it difficult to draw conclusions for the different character of terrestrial iron.

2.1.3 Corrosion in soil

In the majority of soil environments, sufficient oxygen and water is present to make oxygen reduction the main cathodic reaction, although the reduction of corrosion products such as lepidocrocite cannot be ruled out. The earliest studies done specifically on archaeological objects from soil environments were carried out by Turgoose (1982b, 1985, 1993). When iron objects are first buried, anode and cathode reactions exist on the surface (Oguzie et al. 2004), but as corrosion proceeds, the corrosion crust separates the two reactions. Anodic dissolution of iron continues to take place at the metal/corrosion interface, but oxygen reduction is relocated towards the outer corrosion products where oxygen is more plentiful (Turgoose 1982b). The differential access of oxygen and the availability of water are important controlling factors in soil corrosion, according to experiments on modern iron buried in soils (Angelini et al. 1998). Charge may be conducted both through corrosion products which are semi-conductors (e.g. magnetite) and through a pore solution containing ions, including chloride and sometimes sulphate ions. In both cases a positive charge accumulating at the metal surface causes the inward diffusion of negatively charged

chloride ions, which then create a strongly acidic ferrous chloride (FeCl_2) solution at the metal/corrosion interface (Turgoose 1985; Réguer et al. 2007a).

Since Turgoose first developed this model, aspects of it have been confirmed and developed. High chloride regions have been mapped using spectrographic techniques and found to be primarily concentrated at the metal/corrosion interface (Réguer et al. 2005; Wang 2007a). Fully mineralized objects contain very little chloride (Watkinson 1983); as the corrosion reaction producing excess positive ions ceases when all the metal is consumed, chloride ions are released and slowly diffuse out of the object again.

Excavated objects show a typical morphology of voluminous orange/brown corrosion products on the outer part of objects, and grey/black corrosion products in the inner part. These grey/black corrosion products were thought to be magnetite (Turgoose 1982b) and delineate the 'original surface' of the object (Bertholon 2004, 2007). The location of magnetite close to the metal surface was thought to show a lack of oxygen transport to the inner part of the object, resulting in less oxidised corrosion products, and acidification at the metal surface pushing conditions towards the range of stability for magnetite (Turgoose 1982b).

More recent studies have revised the composition of the typical corrosion morphology of buried objects (Figure 1). Neff et al. (2004; 2005) showed that the inner, dark part of the corrosion products was composed of goethite with strips or patches of magnetite and maghemite ($\gamma\text{-Fe}_2\text{O}_3$). They confirmed that this Dense Product Layer (DPL) contained no extraneous soil minerals and probably represented the shape of the original object. The outer part of the corrosion profile (Transformed Medium, TM) was composed primarily of goethite and contained soil minerals (Neff et al. 2005). The DPL contains numerous cracks with a pore-size of 6 to 300 μm , permitting the movement of water and ions through the DPL to the metal surface (Chitty et al. 2005). These cracks can also contain deposited minerals such as calcite. The cracks are thought to form during the corrosion process, due to oxide expansion during the formation of the corrosion layer. The formation of cracks in corrosion layers increases overall corrosion rate by permitting more water and oxygen ingress towards the iron surface (Turgoose 1982a; Scully 1990; Selwyn et al. 1999).

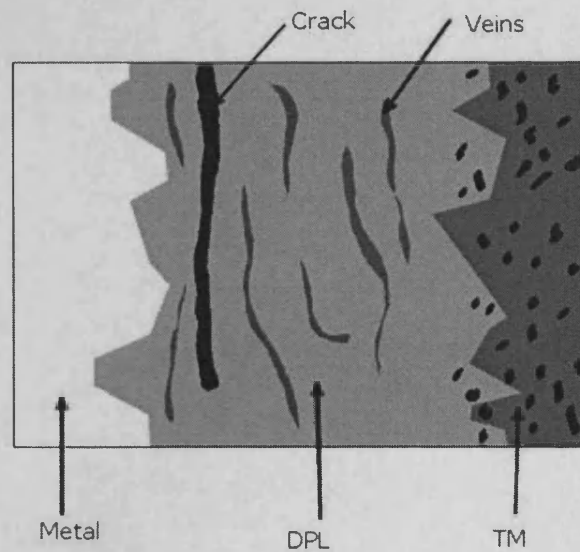


Figure 1: Schematic diagram of corrosion morphology, adapted from Neff et al. (2005). The Dense Product Layer (DPL) retains the approximate shape of the object and contains cracks and magnetite/maghemite veins. The Transformed Medium (TM) includes soil minerals.

The presence of the magnetite/maghemite veins is also related to crack formation. The initial corrosion product is likely to be α -FeOOH, given high oxygen availability in the early stages of corrosion (Neff et al. 2005). As corrosion progresses, the generation of Fe^{2+} at the metal surface causes the potential to drop into a region where neither magnetite nor goethite are stable. The excess Fe^{2+} ions diffuse outwards until they meet a crack or pore, where oxygen levels are higher and the potential increases sufficiently for magnetite/maghemite formation. The TM forms through dissolution of the DPL phases and reprecipitation in the soil (Neff et al. 2005). Chloride-containing corrosion products such as β -FeOOH and other more unusual corrosion products form according to the local composition of the soil, e.g. iron carbonates (Matthiesen et al. 2003; Neff et al. 2005) or phosphates (McGowan & Prangnell 2006). The occurrence of these corrosion products can be modelled using potential/pH diagrams for specific conditions. Bacterial action in anaerobic soils may cause the formation of unusual corrosion products such as iron sulphides (Novakova et al. 1997).

The new model of corrosion in soil is consistent with known morphology and processes, but Chitty et al. (2005) stated that the magnetite/maghemite veins were not connected to the

metal. This implied that both the cathodic and anodic reactions took place at the metal/DPL interface (Neff et al. 2005), as the relocation of cathodic reactions to the outer corrosion products requires a connection to the metal through a semi-conducting corrosion product such as magnetite. Studies carried out using oxygen tracers (Vega et al. 2004; Vega et al. 2005) appeared to confirm the view that oxygen diffusion through the pore solution to the metal surface was the rate controlling factor for buried iron. However, relocating the cathodic reaction to the metal surface once again contradicts the apparent charge accumulation which is responsible for chloride movement into objects, and the presence of acidic solutions which are found in chloride-contaminated objects. If the cathodic reaction takes place at the metal surface, the production of Fe^{2+} and H^+ at the metal surface should be balanced by OH^- production from the reduction of oxygen [3].

An alternative was suggested by Reguer et al. (2007a), where some of the magnetite/maghemite veins are connected to the metal surface and allow charge transfer from the outer parts of the corrosion products where oxygen reduction is occurring. Such localised connection between the outer layers and metal would explain why chloride ions are often highly localised. Oxygen diffusion would still be a rate-controlling factor, diffusing partway into the object and to areas of the object where there are no connections to the outer layers. It is premature to suggest that no connections exist between the magnetite/maghemite veins and the metal based on the small cross-sections of an object that can be viewed by a scanning electron microscope. It is also possible that corrosion products such as lepidocrocite and goethite, which were found in the DPL (Neff et al. 2005) could act as semi-conductors as suggested for atmospheric corrosion (Antony et al. 2007; Monnier et al. 2007). In either case, the concentration of chloride ions at the metal/DPL interface is well-attested, and can only be explained by at least some areas of positive charge accumulation at anodic sites. It is this accumulation of chloride ions that desalination methods must address if they are to be successful.

2.2 Corrosion products

The iron-oxygen system is extremely complex, with a large variety of possible products, polymorphs, structures and transformations, stable in a large variety of conditions. This is one of the reasons why their formation, behaviour and interactions are very difficult to predict; they depend not only on the corrosion product chemistry, but also crystal

properties, size, hydration and local conditions (Navrotsky et al. 2008). It is not possible to give a full review of all the research carried out on iron corrosion products here, nor is it necessary. A comprehensive overview is provided by Cornell and Schwertmann (2003). The corrosion products that are relevant to this work are briefly reviewed to facilitate interpretation of the experimental design and results.

2.2.1 Goethite, α -FeOOH

Goethite (α -FeOOH) is a ferric oxyhydroxide and is one of the most common iron corrosion products. It is a primary constituent of the corrosion layers on buried archaeological objects (Neff et al. 2005). It is one of four polymorphs of FeOOH, the others being akaganéite (β -FeOOH), lepidocrocite (γ -FeOOH) and feroxyhyte (δ -FeOOH). The latter is an unstable and poorly crystalline compound which is not usually found as a corrosion product (Scott & Eggert 2009) and is not discussed further here.

Goethite is usually the end-product of the transformations of the other ferric oxyhydroxides, as it is the most stable (Cornell & Giovanoli 1990). It has an orthorhombic crystal structure and may appear in various crystal sizes; small goethite crystals can transform into larger ones through a dissolution/reprecipitation process called Ostwald-ripening (Stratmann & Hoffmann 1989). This process occurs over time, and older rust samples contain higher quantities of large goethite crystals (Stratmann & Hoffmann 1989). The presence of anions in the formation environment may also stimulate increased crystal size by decreasing the surface charge of the crystals (Frini & El Maaoui 1997).

Watkinson and Lewis (2005b) showed that goethite is capable of adsorbing chloride ions onto its surface, but the quantity is small, around 0.2 wt% (Turgoose 1982b) to 0.6wt% (Al-Zahrani 1999). Although nano-scale goethite crystals may have superparamagnetic properties (Olowe et al. 1990), in general goethite is considered non-magnetic, relatively non-reactive and a stable corrosion product phase.

2.2.2 Lepidocrocite, γ -FeOOH

Lepidocrocite is a second polymorph of FeOOH, and is found on atmospherically corroded iron (Neff et al. 2006; Monnier et al. 2007) and on terrestrial objects (Gilberg & Seeley 1981; Neff et al. 2005). It is less stable than goethite, although it shares its orthorhombic

arrangement (Table 1) (Cornell & Schwertmann 2003: 11), and can transform into the latter in the correct conditions. It may also become reduced to magnetite during atmospheric corrosion cycles, particularly in the presence of sufficient ferrous ions (Stratmann & Hoffmann 1989). Wang et al. (2007) identified lepidocrocite as the middle layer of a three-layered corrosion morphology on iron corroded in a simulated soil pore solution, and showed that it formed primarily on the underside of samples where oxygen access was poorer than on the upper surface, where goethite was the main product. Lepidocrocite is considered a possible risk to iron, as it dissolves in the presence of acid and contributes to the oxidation of iron (Wang et al. 2007). Its reduction to Fe^{2+} or magnetite may be the cathodic reaction in some atmospheric corrosion cycles (Stratmann & Hoffmann 1989). Lepidocrocite has been identified on some archaeological objects (Neff et al. 2005), but the extent to which it may pose a threat to their stability is not known.

2.2.3 Akaganéite, β -FeOOH

Akaganéite is a ferric oxyhydroxide, but unlike lepidocrocite and goethite, it has a tunnel structure similar to that of hollandite ($\text{BaMn}_8\text{O}_{16}$), with a body-centred cubic arrangement (Cornell & Schwertmann 2003: 10, 20-22). The tunnels contain halide ions, usually chloride, and adsorbed chloride ions on the crystal surfaces. It was first identified by Weiser and Milligan (1935) in nature, and its involvement in active corrosion on iron objects was first reported by Zucchi et al. (1977).

The structure and formula of akaganéite has been revised most recently by Stahl et al. (2003), who suggest the overall chemical formula of $\text{FeO}_{0.833}(\text{OH})_{1.167}\text{Cl}_{0.167}$, and showed that of the possible tunnel sites, only two thirds are occupied by chloride ions. Akaganéite crystals tend to be small, with typical crystal sizes of 0.1 – 1 μm (Stahl et al. 2003). The different crystal structure makes akaganéite less dense than the other ferric oxyhydroxides (Cornell & Schwertmann 2003) and its greater volume can cause significant pressure on overlying corrosion layers as it forms.

Although Bland et al. (1997) report finding akaganéite that did not contain significant levels of chloride ions, all other reports suggest that chloride or other halide ions are essential for its formation and stability. There is some dispute as to how much chloride akaganéite contains in its tunnels and absorbed on the surface of the crystals. Cornell and

Schwertmann (2003) give the typical chloride content of akaganéite as 2 – 7 mol%; at a minimum, 0.25 – 0.5 mmol mol⁻¹ seems to be essential for its stability (Ellis et al. 1976). Reports of synthesised akaganéite give chloride contents of 3.0% to 6.24 mass% (Wang et al. 2007), and 2.28 – 6.4% (Keller 1970). Watkinson and Lewis (2005a) suggest that while naturally-formed akaganéite may have 0.3 – 5% chloride ion content, synthetic akaganéite can contain up to 17%.

Wang (2007b) identified akaganéite on metal coupons without direct contact with a source of chloride ions, and suggested that akaganéite formation was possible in low-chloride environments. However, the samples were in an enclosed space with high concentrations of FeCl₂, and Watkinson and Lewis (2005a) have previously reported that metal not in direct contact with chloride ions could suffer from chloride-induced corrosion through the formation of a vapour phase of hydrochloric acid (HCl) in high humidity conditions. Hydrochloric acid is volatile at high concentrations (Lide 1996), and this may well explain instances of akaganéite formation where there is no direct source of chloride ions.

Formation of akaganéite is suggested to require chloride ion concentrations of at least 2 – 3.6 M (Selwyn et al. 1999), but this was not determined experimentally. The formation of akaganéite from FeCl₂ and NaOH solutions by Rémazeilles and Refait (2007) showed that the end product depended on the ratio of [Cl⁻]/[OH⁻], with akaganéite formation only occurring if this ratio exceeded 8. Concentration of the reactants also influenced formation; akaganéite only formed above chloride ion concentrations of 1.6 M and was the sole reaction product at concentrations greater than 3.2 M (Rémazeilles & Refait 2007). The reaction proceeded via several intermediate products: β-Fe₂(OH)₃Cl and two types of green rust (see section 2.2.4 and 2.2.5). Reaction speed is significantly influenced by the access of oxygen (Rémazeilles & Refait 2007).

Also important to akaganéite formation is the concentration of ferrous ions. Rémazeilles and Refait (2007) found that varying Fe²⁺ concentration influenced akaganéite formation independently of chloride ion concentration. In conditions of high Cl⁻ but low Fe²⁺, lepidocrocite and goethite formation was favoured. This is likely to be because the intermediate products that lead to akaganéite formation do not form in low Fe²⁺. Instead, Fe(OH)₂ forms, which then favours chloride-free end products (Rémazeilles & Refait 2007).

The process was demonstrated for formation on solid iron as well as from solution. The recognition that ferrous ion concentration influences akaganéite formation is important when considering the purpose of treatment, which must also seek to remove or fix free Fe^{2+} as well as dealing with excess chloride ions (Knight 1997).

Both the formation of akaganéite and its crystallinity are influenced by pH (Cai et al. 2001). Well-formed akaganéite crystals occur only at pH less than 2, with crystallinity decreasing as pH increases, and akaganéite disappearing entirely by pH 6. The requirement of low pH led Cai et al. (2001) to suggest that the incorporation of chloride ions into the akaganéite structure is the result of extra protonation. The additional protonation of akaganéite was confirmed by Stahl et al. (2003), but it has usually been viewed as a result of the additional negative charge from the chloride ions, rather than vice versa.

The particle shape of akaganéite depends on the method of synthesis (Cai et al. 2001; Cornell & Schwertmann 2003; Ishikawa et al. 2005), and this may be the source of much of the conflicting information about the chemical and physical properties of akaganéite. Oxidation of Fe^{2+} ions produces rod-shaped particles, while hydrolysis of Fe^{3+} ions gives smaller spindle-shaped particles (Ishikawa et al. 2005). Cigar-shaped particles were reported by Cornell and Giovanoli (1990). Stirring during manufacture leads to smaller particle size overall, due to breaking up of aggregates (Stahl et al. 1998). Washing of akaganéite in water also leads to smaller particles by preventing conglomeration (Stahl et al. 1998).

Particle size and morphology is also influenced by the presence of foreign anions and cations during formation (Frini & El Maaoui 1997; Cai et al. 2001; Cornell & Schwertmann 2003; Ishikawa et al. 2005; Kamimura et al. 2005; Kwon et al. 2005). The effect depends on their concentration; e.g. increasing concentrations of SO_4^{2-} reduced the crystallinity of akaganéite, produced more porous crystals and gave a higher surface area (Ishikawa et al. 2005). Anions including HPO_4^{2-} and SO_4^{2-} may also be incorporated into the akaganéite structure during manufacture (Ishikawa et al. 2005), whereas substitution of cations such as Mn^{2+} appears to be minimal (Cai et al. 2001). Akaganéite has also been manufactured by mixing iron powder with ferrous chloride and exposing to high humidity (Turgoose 1985; Al-Zahrani 1999; Watkinson & Lewis 2005a). This method is considered to be more similar to the process of akaganéite formation on objects, although the extent to which crystals

formed by this method differ to those produced in solution and those on objects has not been established.

On archaeological objects, akaganéite has been observed in two forms: long thin crystals forming at RH levels less than 50-60%, and bubble shapes formed above this RH (Wang 2007b, 2007a). These forms are likely to correspond to the formation of akaganéite from solid FeCl_2 at lower RH, in which case rod-shaped crystals are formed, and formation from a liquid solution of FeCl_2 at RH above the deliquescence point of $\text{FeCl}_2 \cdot 4\text{H}_2\text{O}$, around 55% (Turgoose 1982a). In this case akaganéite forms as the liquid bubble oxidises and dries, forming bubble-shaped structures as seen in Figure 2.



Figure 2: Archaeological iron nail showing a bubble-like structure formed during exposure of the object to 75% RH. The bubble is 2 mm across and probably composed of akaganéite.

Anion exchange of structural chloride with fluoride, bromide and hydroxide ions is possible. Cai et al. (2001) showed that hydroxide ions are small enough to exchange with tunnel chloride, suggesting that the high pH reduces the excessive protonation of akaganéite and allows chloride ions to be released. This is contrasted with akaganéite in water, where only surface chloride (up to an equilibrium concentration of 0.24 mmol g^{-1}) could be released. In the presence of hydroxide, this equilibrium increased to 1.2 mmol g^{-1} at 55°C , with lower values for fluoride and bromide exchange (Cai et al. 2001). Substitution of hydroxide ions into akaganéite led to more rapid collapse of the tunnel structure on heating (Cai et al. 2001), and may be important for allowing the transformation of akaganéite in alkaline

solutions. However, the picture is unclear and unconfirmed; more work is required to clarify whether tunnel chloride is replaced by hydroxide ions, and to examine the proportion of chloride that can be released by ion exchange. The most recent work on the replacement of structural and adsorbed chloride in akaganéite crystals suggests that there is some reduction of chloride ions in the tunnels without requiring transformation, down to a chloride content of about 1 mass% (Réguer et al. 2009). This ion exchange occurs more slowly than the removal of surface-adsorbed chloride ions, which can be achieved readily by washing in neutral and alkaline solutions (Al-Zahrani 1999).

Akaganéite is hygroscopic, and this is an important aspect of its role in post-excavation corrosion. Although Stahl et al. (2003) confirmed that there was no H₂O inside the akaganéite tunnels, water does adsorb to the surface of akaganéite through hydrogen bonds and weak charge transfer bonds (Kaneko & Inouye 1979). This is confirmed when akaganéite is heated to less than 150°C; the initial mass loss is that of surface dehydration of akaganéite and is reversible (Chambaere & Degrave 1985; Stahl et al. 1998). Watkinson and Lewis (2005a, 2005b) showed that akaganéite is hygroscopic even at low RH, and that adsorption of water is faster than desorption. Aqueous washing of akaganéite until no more chloride was extracted removed surface-adsorbed chloride and reduced its affinity for water (Watkinson & Lewis 2005a). The role of akaganéite in post-excavation corrosion (see section 2.4) and the effectiveness of treatments in removing chloride ions from it are important factors to consider when developing a conservation treatment.

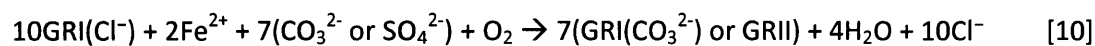
2.2.4 Green rusts

The green rusts are a group of corrosion products which are characterised by mixed Fe valencies and a variety of anion contents. They are generally intermediate and unstable products of corrosion formation or transformation reactions. They were first identified as a corrosion product on steel (Butler & Beynon 1967) but the majority of our understanding of these compounds comes from more recent research (Refait & Génin 1994; Refait et al. 1997; Refait & Génin 1997; Refait et al. 1998; Refait et al. 2003a; Refait et al. 2003b). Three types of green rust (GR) were identified by Refait et al. (1997), depending on their anion content and crystal structure. Green Rust One (GRI) has a rhombohedral structure and may contain either chloride or carbonate ions (Oh et al. 2002). In the former case, the chemical

formula is reported as $\text{Fe(II)}_3\text{Fe(III)(OH)}_8\text{Cl}\cdot n\text{H}_2\text{O}$ with an average oxidation state of Fe of +2.25. In the presence of carbonate ions, a more oxidised rust (average state +2.33) with formula of $\text{Fe(II)}_4\text{Fe(III)}_2(\text{OH})_{12}\text{CO}_3\cdot 2\text{H}_2\text{O}$ forms. The sulphated Green Rust Two (GRII) ($\text{Fe(II)}_4\text{Fe(III)}_2(\text{OH})_{12}\text{SO}_4\cdot n\text{H}_2\text{O}$) also has this higher oxidation state but forms a hexagonal structure (Refait et al. 1997) (Table 1).

$\text{GRI}(\text{Cl}^-)$ has an alternating layer structure, with sheets of Fe(OH)_2 -like structures which contain some Fe(III) and are therefore positively charged. These are interspersed with negatively charged layers of chloride ions and water molecules (Refait et al. 1998). The Fe(II)/Fe(III) ratio varies from 2.2 to 3 (Refait et al. 1998). Its overall oxidation state may increase due to continuing structural intercalation of chloride ions, leading to loss of additional electrons from ferrous ions. This reaction appears to be possible only with the chloride ion due to its small size and single charge.

Because it has a lower overall oxidation state, $\text{GRI}(\text{Cl}^-)$ may be transformed into either of the other GR in the presence of the appropriate anion, ferrous ions and oxygen [10] (Refait & Génin 1994).



This reaction determines whether akaganéite, which can only form from $\text{GRI}(\text{Cl}^-)$, develops. In a solution containing either sulphate or carbonate ions, the chlorinated GR would transform according to reaction [10], the end products of which tend to be lepidocrocite and/or goethite (Refait & Génin 1994; Oh et al. 2002). Higher concentrations of sulphate ions also favour goethite formation over lepidocrocite, as the anion extends the reaction time (Frini & El Maaoui 1997). Refait et al. (2003b) identified a sulphated green rust on steel piles corroded in marine conditions for 25 years. Here, the green rust formed the outer layer of a three-layered corrosion profile, with magnetite next to the metal and an intermediate layer of iron oxyhydroxides. No $\text{GRI}(\text{Cl}^-)$ was found, despite the surrounding water having a much higher chloride than sulphate ion content, confirming the preferential formation of green rusts with sulphate ions. The reason why green rust was found in the outer layer of the corrosion products is not clear, but it showed that the outer zone of the corrosion products was 'active' and continuously forming and transforming, demonstrating that, as with atmospheric corrosion, the rust layers themselves may partake in continued reactions.

In the case of marine corrosion, sulphate-reducing bacteria may also play a part in leading to green rust formation on the outer, colonised surface (Génin et al. 1992). Green rusts are rarely observed on archaeological iron, due to their instability in oxygenated atmospheres, but they may be important intermediaries in the corrosion process.

2.2.5 Ferrous hydroxychloride, $\beta\text{-Fe}_2(\text{OH})_3\text{Cl}$

Ferrous hydroxychloride is an uncommon compound, but some studies suggest it may play a role in iron corrosion. It is formed by mixing $\text{FeCl}_2 \cdot 4\text{H}_2\text{O}$ and NaOH , and is a precursor of $\text{GRI}(\text{Cl}^-)$. It can then form an over-chlorinated green rust which leads to akaganéite formation (Refait & Génin 1997; Rémazeilles & Refait 2007). $\beta\text{-Fe}_2(\text{OH})_3\text{Cl}$ will only form in the presence of a chloride ion concentration of at least 1.5 M, and in acidic conditions of pH 4 to 6. Its formation depends on the $[\text{Cl}^-]/[\text{OH}^-]$ ratio, which must be greater than 1, and greater than 4 for akaganéite to form as the end product. Its structure is thought to be similar to that of the copper corrosion product atacamite, $\text{Cu}_2(\text{OH})_3\text{Cl}$ (Réguer et al. 2005).

Although not stable in air (Réguer et al. 2007a), ferrous hydroxychloride has been reported on archaeological iron in a few instances. It was located near the metal/DPL boundary (Réguer et al. 2005; Réguer et al. 2007a; Réguer et al. 2007b), where two distinct Cl-containing phases were identified. One, with a lower concentration of Cl in the range 5-8 mass% was identified as akaganéite. The second phase had much higher Cl content in the range 15-20 mass%, and X-ray absorption studies showed that it was associated with a Fe(II) valence and was identified as ferrous hydroxychloride. $\beta\text{-Fe}_2(\text{OH})_3\text{Cl}$ and a small amount of a second form $\gamma\text{-Fe}_2(\text{OH})_3\text{Cl}$ (hibbingite) were also identified on an iron artefact from a marine context (Rémazeilles et al. 2009).

Thermodynamic stability calculations confirm that ferrous hydroxychloride is only stable in a limited range of conditions: anoxic, slightly acidic and under certain chloride concentrations (Rémazeilles et al. 2009), which may explain its limited quantity and position deep beneath corrosion layers in transverse profiles through archaeological nails (Réguer et al. 2005).

Once exposed to oxygen, it is likely to transform into akaganéite and/or goethite, and so its identification is only possible with careful sample preparation. The fact that it transforms so easily means that ferrous hydroxychloride is unlikely to be present on objects that have been exposed to the atmosphere for any significant period of time. With the recent

discovery that ferrous hydroxychloride may be a constituent of corrosion layers on both terrestrial and marine objects during burial and immediately after excavation, further study is required into the frequency of its appearance, its formation conditions, effect on corrosion rate and response to desalination treatment. Whether ferrous hydroxychloride promotes corrosion and, if so, under which RH conditions, are crucial questions for the understanding of corrosion and storage of iron in controlled humidity conditions.

2.2.6 Hematite, α -Fe₂O₃

Hematite (α -Fe₂O₃) has a close-packed hexagonal lattice (Cornell & Schwertmann 2003) containing only ferric (Fe³⁺) ions. It is rarely found on archaeological objects, as it forms most readily in high-temperature conditions, e.g. from the thermal transformation of akaganéite and goethite. It is possible for goethite to transform to hematite at lower temperatures if the crystal size is small (see section 2.3.1). Hematite is common in nature as it is one of the most stable iron oxides and the end-product of many transformation pathways, but on archaeological iron objects it usually only occurs if the objects are from a burnt context e.g. house fires or cremations (Scott & Eggert 2009). It is generally considered a stable end-product of corrosion and is not likely to pose a threat to the survival of iron objects.

2.2.7 Magnetite, Fe₃O₄

Magnetite (Fe₃O₄) is a mixed ferrous-ferric oxide which is stable under a wide range of conditions. It is part of the corrosion product mixture found in the inner corrosion layers (section 2.1.3) (Neff et al. 2005). It occurs in a variety of crystal forms with an inverse spinel structure and has magnetic properties (Scott & Eggert 2009). As it contains some ferrous ions, further oxidation is possible, usually to hematite. It is denser than the ferric oxyhydroxides. For this reason reduction of corrosion products to magnetite is the aim of some conservation treatments for iron, e.g. plasma treatment. By transforming bulky iron oxyhydroxides to magnetite, microcracks open in the corrosion structure, increasing the porosity and improving the diffusion rate of chloride ions out of the object. However, there is considerable debate about the extent to which reduction to magnetite can be achieved in different conditions (see Chapter 3). As a semi-conductor, magnetite may play a part in

connecting anodic and cathodic reactions when these are separated by corrosion layers, but otherwise it is not considered a threat to the stability of iron objects.

2.3 Transformation of corrosion products

The iron oxide/hydroxide system is complex and includes a multitude of forms. Many iron corrosion products are fine-grained, and some are poorly crystalline, making them hard to characterise by spectrographic methods (Neff et al. 2004; Rémazeilles & Refait 2007).

Factors such as particle size and hydration play a key role in determining which are stable in any given conditions (Navrotsky et al. 2008). Thus preparation methods of corrosion profiles such as aqueous polishing and the speed with which a profile is examined must be considered in relation to how the preparation process may have altered the original corrosion profile.

In general, iron oxides are least soluble at neutral pH, and solubility increases in both alkaline and acid conditions (Cornell & Schwertmann 2003). Reducing conditions enhance solubility through reductive dissolution, and solubility increases in dilute solutions (Cornell & Schwertmann 2003). Small particles tend to have higher enthalpy and free energy (ΔG) than larger ones, and tend towards greater hydration (Navrotsky et al. 2008). Particle shapes and morphologies that have high surface area tend to be more soluble and reactive (Cornell & Schwertmann 2003). Transformations may occur during burial and following excavation of archaeological iron, which may influence the reactivity of the object and its corrosion products. Transformations may also occur as the result of desalination treatment.

Both solid-state (topotactic) and dissolution/reprecipitation transformations of iron corrosion products are possible. Most of the FeOOH polymorphs, except goethite, are thermodynamically metastable and have similar entropy, enthalpy and free energy (Navrotsky et al. 2008), making interconversions possible with only minor changes in environmental conditions. Not all transformations observed under laboratory conditions may be possible in nature, nor are consistent results always obtained (Cornell & Schwertmann 2003). However, it is important to know the possible conditions under which transformations can occur. Most important to the conservation of archaeological iron is the possibility of transforming chloride-containing corrosion-inducing products into passive oxides in treatment environments. Equally, the stability under treatment conditions of

corrosion products which constitute the information-bearing corrosion layers in archaeological objects is important for retention of heritage value. The possible transformations of akaganéite, goethite and magnetite are therefore briefly reviewed.

2.3.1 Goethite to hematite

Although goethite is the most stable iron oxyhydroxide, dehydroxylation to hematite, α -Fe₂O₃, may occur in elevated temperatures beginning at 85°C (Cornell & Giovanoli 1990) according to reaction [11].



Similarities in structure between goethite and hematite mean that interconversion is easily possible, as the dehydroxylation reaction removes H₂O pairs without disrupting the anion array (Cornell & Schwertmann 2003). This reaction can occur in solution (Cornell & Schwertmann 2003) or as a solid-state thermal transformation (Cudennec & Lecerf 2005). In the latter case it occurs around 270°C, without significant structural modification or intermediate compounds. Although hematite is thermodynamically more stable, kinetic factors mean that goethite may become the more stable phase if particle size is small (Navrotsky et al. 2008). Hydrated hematite surfaces tend to behave like goethite and may initiate reaction at temperatures only slightly higher than ambient. In this case, the reaction may occur as a dissolution/precipitation reaction. Garcia (2005) suggests that hematite forms from goethite on atmospherically corroded iron, where hematite was found in small quantities, probably through solution transformation from the iron oxyhydroxides.

As both goethite and hematite do not induce corrosion, their interconversion is not a significant concern in terms of object stability. However, as goethite constitutes an important part of the information-bearing corrosion layers, its alteration may not be desirable. The presence of hematite on archaeological objects may be evidence of cremation or other important archaeological contextual information. Its alteration to goethite in desalination treatment would therefore be undesirable.

2.3.2 Akaganéite to goethite and/or hematite

Akaganéite transformation is possible to hematite and goethite under a variety of conditions. Solid-state transformation to goethite is possible because collapsed akaganéite

tunnels resemble goethite blocks, requiring little rearrangement. This change begins to occur under heating to temperatures of greater than 150°C (Stahl et al. 1998) with no intermediate products, although Chambaere and Degrave (1985) observed an amorphous phase during the transformation of akaganéite to hematite at higher temperatures. The temperature required for full transformation to hematite depends on particle size and hydration, but is at least 310°C. These temperatures are not reached during aqueous desalination treatment, which are limited to a maximum of 100°C, but they may occur during high-temperature plasma treatment (Chapter 3).

In solution, akaganéite transformation occurs through a dissolution/reprecipitation process (Cornell & Giovanoli 1990, 1991). In acid conditions, akaganéite appears to be a stable phase, which is why it forms at anode sites in chloride rich environments after excavation, and only transforms slowly if seeded with goethite or hematite crystals (Cornell & Schwertmann 2003). At room temperature and in neutral pH conditions, transformation is also slow and can take up to a year to complete (Cornell & Giovanoli 1991).

The transformation of akaganéite in alkaline solution is particularly relevant to the research in this thesis assessing the chloride extraction ability of alkaline washing methods. In 1 M potassium hydroxide (KOH) at 70°C, transformation to goethite was completed in 48 hours (Cornell & Giovanoli 1990, 1991). Formation of hematite alongside goethite was dependent on OH⁻ concentration. Between 0.5 M and 2 M only goethite formed; outside this range, some hematite formed, the amount dependent on OH⁻ concentration and the shape of the crystals (Cornell & Giovanoli 1990). Lower concentrations of KOH also reduced the reaction rate. Rod-shaped crystals reacted more slowly than cigar-shaped crystals, and more hematite resulted (Cornell & Giovanoli 1990). Both products nucleated during the initial reaction stage (24 hours), and the ratio of goethite to hematite did not change. Nor was there any indication that hematite formation was a secondary transition from goethite. The proportion of the final products appears to depend on the extent of nucleation during the initial stages (Cornell & Giovanoli 1990). Seeding with either goethite or hematite crystals did not change the proportions of the end products. The rate-determining step is akaganéite dissolution; the addition of silicate ions retarded the reaction by stabilising the akaganéite crystals against dissolution (Cornell & Giovanoli 1990). No intermediate transformation products were detected. Goethite formation seems to occur more readily and under a wider

range of conditions; most likely this is because hematite formation requires a higher activation energy due to the need for dehydration.

Akaganéite samples made by the solid-state method of mixing iron powder with ferrous chloride were immersed in alkaline solutions by Al-Zahrani (1999) and these produced different results to those of Cornell & Giovanoli (1990). Pure akaganéite transformed completely to goethite within 4 months in both 0.5M NaOH and 0.5M NaOH/0.5M Na₂SO₃ solutions at room temperature, and partially transformed to a mixture of mostly magnetite and some goethite in deionised water heated to 70-100°C. When seeded with magnetite, partial transformation to only magnetite occurred within a week, with the maximum transformation (around 80%) in mildly alkaline solutions (pH 8.5-10.5). Above this pH only around 25% transformation occurred. Washing in water at room temperature for a year caused over 80% of the akaganéite to transform to magnetite. The results of Al-Zahrani (1999) therefore contradict previous work, as seeding with magnetite did affect the transformation of akaganéite. The reasons for this discrepancy are not clear.

The transformation of akaganéite in alkaline desalination solutions is an important factor in assessing the performance of the treatments, and this is an area in which further experimentation is needed (see Chapter 5).

2.3.3 Ferric oxyhydroxides to magnetite

The reduction of the bulky ferric oxyhydroxides (goethite, akaganéite, lepidocrocite) to magnetite has been cited as a desirable result of desalination treatment of iron, opening up pores and improving chloride ion release (North & Pearson 1978b; Selwyn 2004). Although treatments such as alkaline sulphite (Chapter 3) were initially suggested to be able to reduce ferric compounds to magnetite, it is unlikely that this is the case in the majority of treatment/object combinations. Only strong reducing agents such as hydrazine are capable of direct reduction of ferric oxyhydroxides (Cornell & Schwertmann 2003). According to Ishikawa et al. (1998), ferric oxyhydroxides may be transformed to magnetite, but only in the presence of high ferrous ion concentration and in oxygen-free conditions. The extent of reduction depends on the ratio of $[\text{OH}^-]/[\text{Fe}^{2+}]$, with the maximum magnetite yield at a ratio of 2, with akaganéite as the precursor. Lepidocrocite and goethite underwent less reduction, as akaganéite is more soluble than the other ferric oxyhydroxides (Cornell &

Schwertmann 2003: 217). The reaction occurs through dissolution/reprecipitation, as dissolved species of $\text{Fe}(\text{OH})_2$ react with those of FeOOH through a complicated reaction sequence involving a variety of complex ions (Ishikawa et al. 1998).

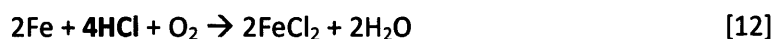
Although it is in theory possible for large quantities of ferrous ions to be present on archaeological objects, these will be washed out or fixed during treatment. Gilberg and Seeley (1981) determined that reduction to magnetite was not a significant occurrence during alkaline sulphite treatment, and although it was observed by Gil et al. (2003), electrolysis was required to lower the potential enough to form magnetite from FeOOH . In either case, it is not certain that magnetite formation is a desirable consequence of treatment, as it involves dissolution of already existing rust layers which may contain important information, such as the shape of mineral-replaced organic material. It may also weaken the dense corrosion product matrix that retains the object shape, which is now known to contain significant amounts of goethite (Neff et al. 2005).

2.4 Post-excavation corrosion

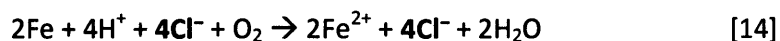
Once excavated from their buried soil environments, archaeological iron objects may undergo further and rapid change. All objects that have a remaining metal core (Watkinson 1983) will be subject to oxidation of the metal in the presence of water and oxygen [1], but in most ambient conditions this reaction is slow without the presence of corrosion accelerators. Objects containing sufficiently high concentrations of chloride ions, however, may suffer from very rapid corrosion. This was first studied systematically by Turgoose (1982b, 1982a), although it had been known for nearly a century that iron was subject to rapid corrosion after excavation. Upon excavation objects contain an acidic ferrous chloride solution in their pores and at the metal/DPL interface. As objects dry in more oxygenated atmospheric conditions, this solution may become visible on the surface as droplets, called 'weeping', and harden into shells of akaganéite (Selwyn et al. 1999; Wang 2007b, 2007a). The formation of fresh corrosion in the shape of spherical shells containing chlorine on polished cross-sections of iron nails was attributed to drawing out of the iron chloride pore solution (Réguer et al. 2005; Réguer et al. 2007a; Réguer et al. 2007b).

The pore solution may have several effects on iron corrosion. While still liquid, it increases corrosion rate by providing an electrolyte for corrosion, allowing charge transfer between

anode and cathode. Its acidity accelerates corrosion. Hydrochloric acid may dissolve already present corrosion products (Turgoose 1982b; Cornell & Giovanoli 1988). An acidic corrosion cycle was suggested by Askey et al. (1993), involving the attack by hydrochloric acid on the metal, forming iron hydroxides and releasing hydrochloric acid again to continue the cycle, according to reactions [12] and [13].



Although hydrochloric acid appears to be carrying out direct attack of the iron metal, if FeCl₂ is fully dissociated in water, the chloride ions in the corrosion cycle do not directly participate in any of the corrosion reactions, which remain a reaction of iron, oxygen and H⁺ ions [14, 15]. The chloride ions are present only to balance the charge (Selwyn et al. 1999).



Chloride ions are not consumed by this reaction, although subsequent formation of akaganéite would consume some chloride ions by incorporating them structurally. Unless chloride levels are low, however, this does not appear to remove enough chloride to halt their effect on iron (Turgoose 1982a). This non-consumption is unique to chloride ions; sulphate ions, for example, may also increase the electrolytic strength of the solution, but they are gradually consumed during corrosion reactions by forming insoluble sulphate-containing corrosion products such as Fe(OH)SO₄ or Fe₂(OH)₄SO₄ (Graedel & Frankenthal 1990; Selwyn et al. 1999)

The formation of akaganéite in itself causes further problems for excavated iron objects. Due to its hygroscopicity, it attracts water even when ambient RH is low. Watkinson and Lewis (2005a) showed that even at RH as low as 15%, unwashed akaganéite is capable of attracting sufficient water to enable the corrosion of iron in contact with it. Although the experiments of Watkinson and Lewis (2005a, 2005b) were carried out with powdered compounds and therefore represent a worst case scenario, it demonstrates the power of akaganéite to initiate corrosion at RH which otherwise would be considered non-hazardous

to objects. Even solid ferrous chloride (FeCl_2) is less hygroscopic than $\beta\text{-FeOOH}$. It does not deliquesce until 55.9% RH (Selwyn et al. 1999) and its hydration from $\text{FeCl}_2 \cdot 2\text{H}_2\text{O}$ to $\text{FeCl}_2 \cdot 4\text{H}_2\text{O}$ occurs around 20% RH. The less hydrated form is not corrosive to iron. Iron in contact with $\text{FeCl}_2 \cdot 4\text{H}_2\text{O}$ begins to corrode appreciably from 25% RH, whereas with akaganéite corrosion can be observed at 15% and is rapid at 25% (Watkinson & Lewis 2005b, 2005a). Thickett (2005) and Wang (2007b) have observed that corrosion increases significantly above c. 50%, probably due to the deliquescence of solid $\text{FeCl}_2 \cdot 4\text{H}_2\text{O}$.

A further effect of akaganéite is the promulgation of stress within the corrosion layers as it forms. As one of the most bulky corrosion products it forms elongated particles within the corrosion structure (Selwyn et al. 1999), causing stress and leading to cracking and flaking of the outer corrosion products. This can easily be observed where flakes are removed from objects and an orange powder identified as akaganéite is seen in the resulting scar (Figure 3). It is suggested that this expansion is the primary cause of object fragmentation after excavation, and is the direct result of the rapid formation of akaganéite (Scott & Eggert 2009: 101). However, the dissolution of the metal as active corrosion proceeds must also reduce the adhesion of the corrosion layers to the metal core, leading to further lamination and spalling.



Figure 3: The tip of an Anglo-Saxon spearhead where the formation of akaganéite crystals has resulted in a large flake of the corrosion layers being detached.

2.5 Unanswered questions

Despite all the research reviewed here, there are still many unanswered questions that are important for understanding the corrosion and treatment of archaeological iron objects.

First, although several values for chloride ion concentration required for akaganéite formation are given in the literature, it is not clear how these may relate to the situation on objects. Chloride ions are usually localised in pits and crevices, and the concentration of chloride in these areas has not been measured.

Second, there is no empirical data that describes the relationship between chloride concentration and actual corrosion rate of objects. Although North and Pearson (1978a) have postulated that objects with 1000 ppm or more of chloride are at significant risk, this value is not based on any sound experimental work. Although we can therefore assume that objects with high chloride levels are most at risk, the relationship is not at present quantified.

Third, many of the properties of akaganéite appear to be determined by its crystal form and method of manufacture. There have been no studies of the morphology and properties of akaganéite formed on objects compared to synthetically prepared crystals. The differing results of Al-Zahrani (1999) and Cornell and Giovanoli (1990) on the transformation of akaganéite may be related to different manufacturing methods, but this hypothesis requires testing. There is thus no clear information about which reactions may or may not occur on archaeological objects.

It appears from the majority of the literature surveyed that it is primarily free and surface-adsorbed chloride that causes corrosion problems. Free chloride in solution is both an electrolyte and a source of akaganéite formation, while chloride ions adsorbed onto the surface of akaganéite seems to be the primary reason for its high hygroscopicity and corrosiveness. Washed akaganéite was not found to corrode steel at 98% RH (Wiesner et al. 2007). The role of the chloride ions inside the tunnel structure of akaganéite, however, is poorly understood. It is crucial to the structural integrity of the β -FeOOH crystals; Cai et al. (2001) suggest that it is the loss of structural chloride ions under heating that causes the collapse of the akaganéite structure, but this is contradicted by Stahl et al. (2003). Anion exchange with OH^- and the transformation of akaganéite to goethite and hematite have

been observed under laboratory conditions, but it is not known whether such reactions are possible on archaeological objects without the input of an electrolytic current to lower the potential (Gil et al. 2003).

It is a matter of dispute whether the tunnel chloride in akaganéite is a threat to the stability of archaeological iron. Given that it is bound within the tunnels, it is reasonable to suppose that it plays no direct role in corrosion reactions. However, if akaganéite crystals are transformed or dissolved, the tunnel chloride can be released, and may then pose a threat. Release is possible if pH is low, dissolving the corrosion products (Turgoose 1982a; Cornell & Giovanoli 1988). Akaganéite may also be inherently metastable, and transform slowly to goethite over time. Thickett has observed the transformation of akaganéite to goethite on archaeological objects at 40% RH in the presence of ethanoic acid (D. Thickett, *pers.comm.* 12/04/2010), whereas a sample of synthetic akaganéite stored for 23 years inside a stoppered glass bottle did not appear to have transformed to goethite at all (Watkinson & Lewis 2005a). The conditions of metastability are therefore not known. Given this lack of information, it may be safest to assume that all akaganéite is a threat, but that the primary threat comes from surface-adsorbed chloride rather than tunnel-bound chloride. There is thus a question mark about whether any desalination treatments for iron need to transform akaganéite into other corrosion products to release tunnel-bound chloride. If transformation of akaganéite to release all structural chloride is possible, it would be of benefit in ensuring the long-term stability of objects and would be one reason to support the use of desalination treatments. If it is not possible, desalination treatment can still improve the stability of iron by removing surface-adsorbed chloride, although leaving the possibility of later chloride release open.

Chapter 3 - Conservation approaches to archaeological iron

In the far-from-ideally-protective world that most objects live in, too little treatment is a real source of danger.

Appelbaum 2007: 305

Although corrosion is a natural process and is ultimately inevitable, there are various methods available by which the rapid corrosion induced by chloride ions can be controlled and reduced. These methods fall into two categories – preventive methods, where the object is untouched and the environment controlled to prevent or hinder corrosion, and active conservation methods, in which attempts are made to reduce corrosion rates by direct action on the object that involves changing its composition by removing or changing corrosion products or by adding materials like inhibitors or coatings. A review of which methods have and have not been successful is needed to inform current approaches to the conservation of iron.

3.1 Preventive conservation

The use of preventive conservation methods has increased significantly in the last few decades in Britain in all areas of conservation (Keene 2002: 2). It was recognised that environmental control was a key factor in extending the lifespan of all heritage objects, without interfering directly with the object and risking undesired change or irreversible treatment (Cronyn 1990: 196). Preventive conservation can include controlling light levels, relative humidity (RH), temperature, storage methods and materials, the length of time an object is on display and the frequency with which it is handled. The control of these areas is a form of risk management, where the risks to objects are identified and eliminated or mitigated as much as possible to increase the objects' lifespan, depending on the available resources. The management of risk through preventive conservation methods has been systematically evaluated (Ashley-Smith 1999). Such methods can be applied where information on the effects of risk factors on the objects is well-quantified.

For chloride-contaminated archaeological iron, the main environmental risk factors are access to humidity and oxygen, the primary reaction components that allow corrosion to occur. Controlling either or both of these slows down the corrosion process. Lowering temperature would also theoretically slow down corrosion rates, but it is not a commonly used method. The experience of deep-freeze storage in Germany has shown that although it can help to preserve iron objects for a period of a few years, long-term cold storage is actually damaging, and is therefore not a suitable storage solution except for short periods of time (Schmutzler & Ebinger-Rist 2008).

Oxygen-free storage has been attempted as an approach to corrosion control, with some success (Mathias et al. 2004). However, there are inherent problems with a method which requires objects to be sealed in oxygen-free containers. This limits the accessibility of the object, the possibilities for display and analysis are reduced, and good seals are needed to exclude oxygen. Even where an effective system is found, oxygen-free storage is more suitable as a short-term preventive measure while more permanent conservation solutions are found (Mathias et al. 2004).

The most common approach to environmental control for iron is reducing the relative humidity (RH) both in storage and display cases. Simple, cheap and easy to use methods for reducing RH are available, such as the common desiccant silica gel. Sachets or cassettes of silica gel are dried in warm ovens until they contain no water. When placed in a sealed environment such as that created in a snap fit polyethylene box, the silica gel removes water from the air until an equilibrium point is reached. This will be determined by the water in the iron, the leakage of the box seal, the amount of water in the objects and the amount of silica gel included. Simple colour card sensors can be used to roughly indicate the humidity in the container. Other options for desiccation include large or small mechanical dehumidifying units capable of reducing RH in whole showcases or rooms.

For environmental control to be effective, the relationship between RH and corrosion and the threshold humidity values below which corrosion is slow or does not occur must be known. For objects contaminated with chloride ions, corrosion can begin at 15% RH where akaganéite is present (Watkinson & Lewis 2005a), and so a 'no-corrosion' threshold RH value has been assigned to 12% RH. Below c. 30% RH corrosion is thought to be quite slow,

but a rapid increase in corrosion rate occurs around 50% RH (Thickett 2005). Such work provides guidelines for what may be expected to occur when objects are exposed to various RH levels, and makes it possible to adjust RH depending on the nature of the material and its risk level – e.g. 12% or less for very highly contaminated material, below 30-35% for material at lower risk.

The management of risk based on selected RH values has been demonstrated by the conservation of the *SS Great Britain*, where an RH value of 22% was selected as being practically achievable while slowing down corrosion significantly (Watkinson & Lewis 2004; Watkinson & Tanner 2008). The RH can be adjusted up or down if necessary to balance cost against the conservation of the ship. Desiccating the ship to 22% RH has increased its predicted lifespan from 25 years to at least 100 years (Watkinson & Tanner 2008). The corrosion thresholds currently used are based on modelling corrosion using powders (Watkinson & Lewis 2005a). There is not enough quantitative data on actual corrosion rates of objects as a function of ambient RH, nor of the relationship of corrosion rates to chloride ion content.

Additional important factors when considering the use of silica gel for the desiccation of iron is the longevity of silica gel as a buffer, which depends on the external RH and the air exchange rate of the box. In the majority of cases in the UK, Stewart boxes are used for iron storage. Thickett and Odlyha (forthcoming) have measured the air exchange rates of storage boxes, which allow calculations to be made of the length of time a certain quantity of silica gel can buffer against external RH. This should help to improve predictions of silica gel longevity.

The difficulty with silica gel is the need to monitor RH in the controlled space and change the gel when it rises above the desired threshold limit. The card indicators that are often used to monitor RH in storage boxes suggest lower RH values by up to 10% than is actually the case (Thickett & Odlyha forthcoming). While other monitoring systems, such as digital sensors, are more accurate, they are too expensive to put in every storage box and require regular calibration for accuracy. Checking and changing silica gel in the many hundreds of storage boxes in an archaeological archive requires significant manpower and time, and as the work-load of conservators and museum assistants is increasingly taken up with

exhibitions and loans, changing silica gel in iron stores as often as needed may not be possible. This leads to iron being exposed to RH levels above the desired thresholds for a considerable amount of time despite the use of silica gel.

The use of mechanical dehumidification systems brings advantages – once set up, the dehumidifier works consistently to a selected RH, rather than gradually allowing the RH to increase as with silica gel. However, there are also disadvantages, notably in the space required for the installation of such systems, their cost and mechanical maintenance, and the power they consume. For certain projects, such as the *SS Great Britain*, a system of plant dehumidification is the most sensible option (Watkinson & Tanner 2008), but for many museum stores, often in buildings which are not designed for the purpose, desiccating whole rooms may not be a sensible or cost-effective undertaking. In The British Museum, for example, only a small percentage of stores where iron is located can feasibly be desiccated (Shearman 2003), so the rest of the collection must either be desiccated using silica gel or remain exposed to the ambient RH conditions. Oversights, accidents or other unforeseen events may lead to further exposure of objects to dangerously high RH levels.

Iron stored using desiccation methods is susceptible to RH changes whenever it is taken out of storage to be examined or conserved. For objects with high levels of chloride contamination, even short periods at higher RH such as those that may be found in conservation or analytical laboratories can be enough to restart rapid corrosion. With mechanical dehumidification systems, there is always the risk that a mechanical fault may occur, and in this case all the iron in the case or room is then exposed to higher RH levels which may lead to corrosion. Even supposedly well-maintained dry storage such as that described by Keene (1994) is not necessarily sufficient to prevent iron corrosion. The survey of iron at the Museum of London maintained at 18-20% RH did not show significantly less corrosion susceptibility than iron in ambient storage at higher RH. This was attributed to pockets of high humidity within the pores of the object (Keene 1994: 259), but this theory remains unproven. As 18% RH should slow corrosion appreciably, the actual RH prevailing during storage may actually have been higher; the accuracy of the RH sensors and recording devices used in the study was not recorded, and even small inaccuracies of 5% may be sufficient to increase corrosion significantly in the presence of chloride ions (Watkinson & Lewis 2005b). This underlines the difficulty in properly maintaining low humidity stores if

recording systems are unreliable, and in assessing the success of treatments solely from condition surveys where other variables are difficult to control.

Due to these factors, relying on low humidity storage alone to preserve archaeological iron is a strategy with potentially high risk (Knight 1997). Indeed, although widely practiced, the fact that there is still perceived to be a problem with the conservation of archaeological iron suggests that preventive conservation strategies are not providing sufficient corrosion protection for collections of unstable archaeological iron in the current context of resource availability.

3.2 Active conservation

The active approach to iron conservation is to reduce the risk of rapid post-excavation corrosion by attempting to extract some or all of the chloride ions which are the root of this problem. Early attempts to prevent iron corrosion after excavation involved fairly drastic measures, including high temperatures and complete stripping of the corrosion products (e.g. Rosenberg 1917). Research into iron corrosion mechanisms and treatments developed from the 1960s onwards. The increasing recognition that the corrosion layers contained archaeological information (Cronyn 1990), and that high temperature treatments changed the metallographic structure of the objects (Tylecote & Black 1980), led to new developments, particularly in low temperature aqueous treatments. In 1975 North and Pearson published the alkaline sulphite treatment for marine iron (North & Pearson 1975, 1978a; 1978b). This was soon adopted for use for terrestrial iron as well, and was regarded as one of the more successful methods, a view that was supported by small-scale testing (Skinner 1980; Rinuy & Schweizer 1981; Rinuy & Schweizer 1982; Watkinson 1996).

Non-aqueous treatments were also attempted, such as a mixture of lithium hydroxide (LiOH) and ethanol or similar solvents, which was first used in the 1970s for modern steel surfaces and then tested for archaeological materials (North & Pearson 1978b; Watkinson 1982; Oddy 1987). It was thought that the use of non-aqueous treatment was an improvement as it did not introduce water into objects to induce corrosion, but the treatment was not found to be any more effective than aqueous solutions (Watkinson 1982). The difficulty of disposing of large quantities of organic solvents means that non-aqueous treatments have not found general acceptance.

A large variety of other treatments were tested in the 1970s and 80s, including anhydrous ammonia, ethylene oxide, methanol, and various types of aqueous washing (see Oddy 1987; Knight 1997; Scott & Eggert 2009 for overviews). Many of these treatments were either found to be unsuccessful (Keene & Orton 1985; Keene 1994), or the chemicals involved were deemed too hazardous for use by conservators. An approach which appeared promising for some time was the use of ethylenediamine (Argyropoulos et al. 1997) together with sodium hydroxide solutions. This industrial corrosion inhibitor was thought to prevent the destabilisation of corrosion layers during long (8-12 months) immersion in sodium hydroxide solutions. However, further research showed that ethylenediamine forms soluble complexes with ferrous ions, and is therefore as likely to stimulate corrosion as it is to inhibit it (Selwyn & Argyropoulos 2005). A second amine which had been proposed as a desalination treatment, hydroxylamine, has recently been found to be unsuitable because it oxidises Fe^{2+} ions and dissolves magnetite (Wiesner et al. 2007).

By the 1990s, the use of desalination treatments had declined significantly. Conservators were reporting mixed success with these treatments. In some cases, treatments caused changes to the objects, sometimes amounting to severe damage. There were reports that corrosion products were softened or changed by treatment, particularly in alkaline solutions (Selwyn & Logan 1993; Selwyn & Argyropoulos 2005). In other cases, the objects continued to decay after treatment, suggesting that treatments had not been successful (e.g. Beaudoin et al. 1997). There were concerns about the removal of corrosion products by treatments, particularly as interest in mineral-replaced organic pseudomorphs increased. Additionally, more stringent rules about chemical disposal, reduced staff time for working on large collections of unconserved iron, the prioritization of other types of artefact and the huge increase in excavation in the 1980s as rescue archaeology took off, resulted in less and less time available for applying treatments and assessing their effects. The allocation of resources from developer-funded archaeology for conservation was not sufficient to allow for rigorous conservation treatment of iron finds, and so iron often slipped low on the priority list (Ganiaris 2009).

However, collection surveys showed that, although there were some exceptions, on average the use of a desalination treatment could improve the lifespan of archaeological iron collections and reduce the risk of renewed corrosion, particularly treatments that were

alkaline and deoxygenated such as alkaline sulphite or the nitrogen Soxhlet method (Scott & Seeley 1987). Suzanne Keene carried out two collection surveys of treated objects at the Museum of London, and found that treatments did improve the overall lifespan of the objects, although they did not always prevent further corrosion (Keene & Orton 1985; Keene 1994). Using analysis methods used for assessing data from clinical trials (Keene 1994), Keene was able to show that alkaline sulphite and sodium hydroxide were most successful in extending the lifespan of objects. Other reports of alkaline sulphite treated objects seem to confirm its general effectiveness (Aoki 1987; Selwyn & Logan 1993; Gasteiger 2008). A French study of 5000 artefacts treated in 0.5M NaOH/0.5M Na₂SO₃ found a recorrosion rate of only 0.02% (Loeper-Attia & Weker 1997). The data from collection surveys must be viewed with caution, as consistent measurement of the condition of objects relative to the original condition is challenging, but the cumulative picture does suggest an improvement in object survival through alkaline deoxygenated treatment.

In continental Europe, treatment research and usage by conservators continued, partly due to the continuing investigation of plasma treatments as a conservation method (de Graaf et al. 1995; Arnould-Pernot et al. 1997; Dussere 1997; Oswald 1997; Kotzamanidi et al. 1999; Kotzamanidi et al. 2002; Schmidt-Ott & Boissonas 2002; Schmidt-Ott 2004). Plasma formed from gases such as hydrogen is used to reduce the corrosion products and/or remove them. Concerns were raised over the high temperature used during such treatments (Tylecote & Black 1980; Scharff & Huesmann 1998), which was known to cause changes to the metallographic structure of the objects. Modern plasma methods have adopted lower temperatures, around 80°C (Schmidt-Ott 2004), in order to loosen the outer corrosion to aid in the recovery of the original surface. Plasma treatment alone is not able to remove chloride ions without using unacceptably high temperatures (Schmidt-Ott & Boissonas 2002). Its use prior to desalination may improve the removal of chloride ions by opening up the corrosion products and improving access of the treatment solution (Oswald 1997; Schmidt-Ott 2004), but the extent to which this pre-treatment is beneficial is not clear (Drews et al. 2004). Plasma treatments, even in their improved form, have not made a resurgence among British conservators to date, probably due to continued fears of the implications of plasma treatment on metallographic detail, coupled with the high cost of the equipment and its inconclusive results.

Desalination treatments also remained in use in continental Europe, particularly in Germany, Switzerland and France (Scott & Eggert 2009), and research into improving the treatments also continued. Schmidt-Ott and Oswald (2006) carried out research on whether lower concentrations of the chemicals used in alkaline sulphite treatment would be equally effective in extracting chloride. They concluded that alkaline sulphite concentrations could be reduced from the 0.5M NaOH/0.5M Na₂SO₃ used by North and Pearson (1975) to 0.1M NaOH and 0.05M Na₂SO₃, and this does not reduce the rate of extraction (Mathias 1994; Wang et al. 2008). The lower concentration of Na₂SO₃ was a particularly significant change, but a logical one, given that the only action of sulphite ions in the solution was now known to be deoxygenation, not reduction (Gilberg & Seeley 1982). In this case it is only necessary to have sufficient concentration of sulphite ions present to deoxygenate the solution for the period of the treatment. Reducing the necessary treatment concentrations made the application of alkaline sulphite safer and less environmentally hazardous, while maintaining equal extraction levels.

A 2009 survey of German conservators showed that 40% were still using desalination treatments regularly, and of these, although alkaline sulphite predominated, there was still a wide variety of other treatments in use, from simple washing to plasma treatment (Eggert & Schmutzler 2009). Of the 60% of respondents who did not treat iron in the German survey, reasons given included a lack of time, a lack of knowledge or equipment, and uncertainty about the effectiveness of the treatments (Eggert & Schmutzler 2009). Use of alkaline sulphite is also still common in France (Scott & Eggert 2009: 162). British conservators are therefore somewhat unusual in Europe in rejecting desalination as a conservation option.

3.2.1 Current attitudes to desalination treatment

Why have British conservators almost universally stopped using desalination treatments that are still finding a reasonable level of use on the continent? Several important reasons can be summarized. A lack of good quality empirical data on the function and effectiveness of treatments is a significant factor (Scott & Eggert 2009: 161). It is not particularly surprising that conservators are reluctant to use a treatment about which they do not have sufficient information to judge whether the possible risks outweigh the expected benefits.

The majority of information is anecdotal or not available in sufficient quantity to be statistically significant. Studies carried out on treatment efficiency (Rinuy & Schweizer 1981; Rinuy & Schweizer 1982; Watkinson 1982, 1996; Al-Zahrani 1999; Guilminot et al. 2008; Watkinson & Al-Zahrani 2008) have provided some useful data, but sample numbers are often small, usually no more than twenty objects, and this makes it difficult to be confident about the treatment outcomes. Treatment function has also been evaluated (North & Pearson 1975; North & Pearson 1978b; Gilberg & Seeley 1982; Ouahman et al. 1997; Guilminot et al. 2008), but almost no data is available about what actually happens to objects and their constituent corrosion products during a desalination treatment. Much of what is available is based on theory rather than experiment and observation. Although the role of chloride ions and β -FeOOH in corrosion is well known and has been described above, there is almost no information available on threshold chloride levels linked to corrosion rates.

The focus on preventive conservation may have discouraged or disguised the need for further study of interventive methods (Pye 2001: 34). The trend towards preventive methods may stem partly from a fear of doing too much, or causing damage to an object through treatment that could be considered unnecessary (Appelbaum 2007: 188-9). Although such caution is appropriate, it does not take into account the losses that occur to objects when preventive conservation methods fail. Conservators may feel less personally responsible for these than if an object is damaged during an active desalination treatment, but failing to carry out treatments which would benefit objects is also ethically problematic (Appelbaum 2007: 286-7), especially if preventive conservation methods are proving inadequate.

Treatments are accused of not 'stabilising' objects and of damaging objects. These objections are investigated in this thesis, but there is a need to define what conservators mean by 'stability'. It may be assumed to mean 'no change' but this is not a realistic expectation when dealing with processes of corrosion, which are thermodynamically inevitable. 'Reasonably stable health', 'managed change', or 'enhanced lifespan', are more appropriate terms for thinking about what conservation of iron objects is aiming to achieve. All objects have a finite lifespan, but there is an unwillingness to consider what an acceptable lifespan for an object might be (Ashley-Smith 1999).

Damage to objects can only be quantified in relation to the perceived value of an object. Change to an object becomes damage only when it has some meaningful impact on the value of that object (Ashley-Smith 1999; Muñoz Viñas 2005; Appelbaum 2007). Further discussions on this subject are in chapter 6, but the potentially detrimental side-effects of desalination treatment must be weighed against the deterioration and loss of value caused by corrosion when preventive measures are inadequate or not functioning, and therefore not achieving the expected maintenance of an object's value (Appelbaum 2007).

Resource availability also plays an important role in determining conservation decisions. With only limited resources available, time-consuming interventive conservation may not always be possible. Preventive methods are also resource-intensive, and it is partly a lack of available resources for environmental maintenance which results in the failure to prevent corrosion in storage. Resources may limit the ability of conservators to carry out desalination treatments. The use of desalination treatment to stabilise iron objects and reduce the need for long-term high-maintenance storage may, however, justify the initial resource outlay, if the treatments are generally successful. In providing data on treatment effectiveness, this study will enable conservators to consider how their resources can best be applied to maximise the lifespan of objects.

3.3 Defining success in iron conservation

If the effectiveness of treatments is to be determined, a definition of what constitutes success in iron conservation is required, based on the objects' value, lifespan and the practical limits of what treatments can achieve. If success means 'no corrosion', then it is almost impossible to achieve; corrosion is a thermodynamically inevitable process, and long-term survival of any archaeological object cannot be guaranteed (Ashley-Smith 1999). Only the total removal of oxygen and water from the object environment could prevent corrosion reactions from occurring. Although this may be theoretically possible, it would prevent access, study or use of the objects, and is not a viable long-term option for archaeologists, conservators or curators.

The rapid corrosion caused by chloride contamination of iron objects is not an acceptable situation either. The excavation of objects only to allow them to disintegrate shortly afterwards could be considered ethically problematic (Stanley-Price 1989). Success in iron

conservation must therefore strive to preserve value for a reasonable period of time while accepting that the objects eventually degrade. What this time period is depends on individual situations and is difficult to measure, but the goal of increasing lifespan of objects is a standard by which conservation methods can be evaluated.

A successful treatment, therefore, is one which substantially increases the lifespan of the object, maintaining its value for a longer period of time. This does not require that no damage is caused to the object by the treatment, but rather that any damage caused is outweighed by the increase in lifespan and maintenance of object value. An unsuccessful treatment is one in which the lifespan is not increased, or where the treatment causes damage sufficient to outweigh the benefits of an extended lifespan. It is these definitions of success and failure which will be used to assess the overall outcome of desalination treatments in this thesis. The same terms could also be used to assess the success or failure of preventive conservation methods, which are also intended to increase lifespan and may therefore be judged on whether this has been accomplished.

3.3.1 Modelling treatment outcomes

A model for understanding the difference desalination treatment can make to an object's lifespan is necessary to allow assessment of treatment success. Both short and long-term outcome must be considered. Short-term outcome is that relating to damage during the treatment. Long-term outcome is the effect of the treatment on the corrosion rate, and therefore the lifespan of an object.

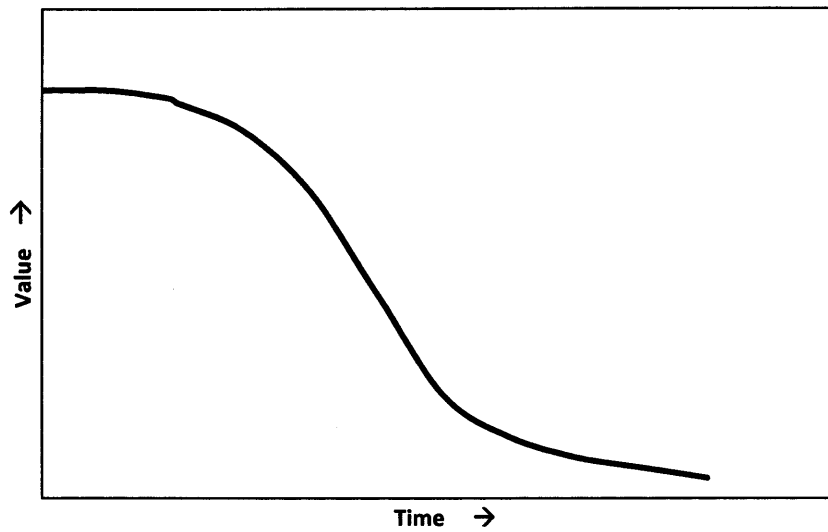


Figure 4: A model showing the lifespan of an unconserved archaeological iron object. As corrosion continues, the value of the object decreases until it is effectively destroyed.

The modelled life of an untreated and unstable object is shown in Figure 4, based on similar models in Ashley-Smith (1999). As time passes, the object loses value, until, at some point, it has lost so much of its value that it is effectively destroyed. No attempt is made to define value except that it is related to the ability of an object to relate information about the past. It decreases as an object corrodes, is disfigured by flaking and akaganéite growth, and eventually disintegrates, although the relationship between corrosion and value decrease cannot be quantified. However, an object that is severely corroded is unlikely to contain as much value as one that is stable and only lightly corroded, and so reducing corrosion rate must help to maintain value.

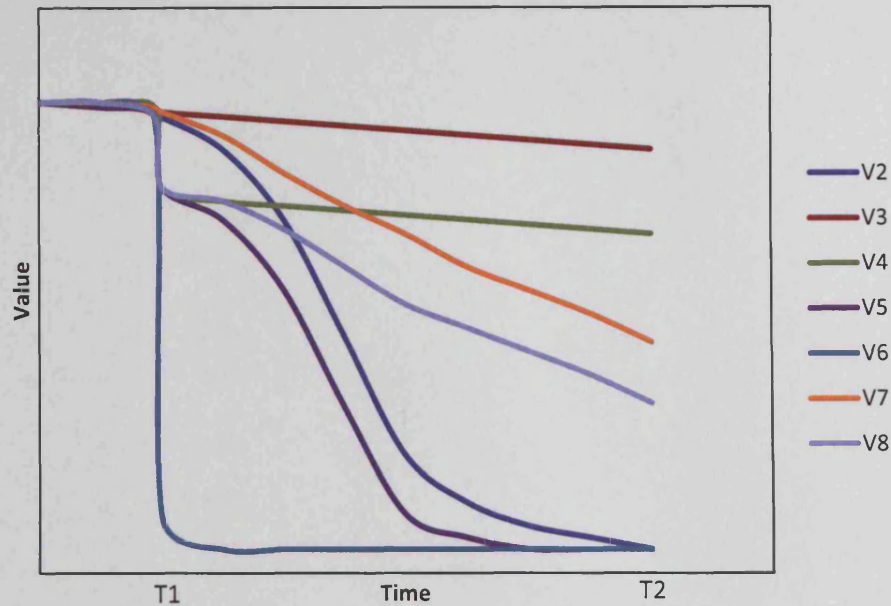


Figure 5: Modelled treatment outcomes. Treatment occurs at T1. Successful treatments are those that result in improved value at time T2.

Figure 5 shows some possible short and long term outcomes of treatment as they might impact on the object in Figure 4. The point at which treatment occurs is designated T1. The value outcomes are given in Table 2, and range from a large reduction in corrosion rate with no damage to the object during treatment (V3) to total loss during treatment (V6).

Table 2: Hypothetical treatment outcomes for evaluation using data in this study. Short-term damage and long-term stability are both considered in evaluating overall outcome.

| Outcome | Damage (short-term) | Corrosion rate change (long-term) | Overall outcome compared to untreated object at T2 |
|---------|---------------------|-----------------------------------|--|
| V2 | No damage | Unaltered | No change |
| V3 | No damage | Significantly reduced. | Highest value increase |
| V4 | Some damage | Significantly reduced | Intermediate value increase |
| V5 | Some damage | Unaltered | Value decreased |
| V6 | Total loss | N/A | Object lost |
| V7 | No damage | Some reduction | Intermediate value increase |
| V8 | Some damage | Some reduction | Intermediate value increase |

These hypothetical outcomes illustrate how treatment may be evaluated in relation to short and long-term effects. Treatments that result in an improvement in value at time T2 can be considered as successful – there has been an increase in lifespan. These are modelled outcomes, and a wide range of changes to corrosion rate, and therefore expected lifespan, is possible. Any number of intermediate states between the optimal V3 and the worst V6 are possible, but by categorising outcomes into these types, it is possible to evaluate the likelihood of each outcome based on the results of this study. The calculation of short and long-term outcome probability should help to shed light on whether desalination treatment is likely to have an overall beneficial effect compared to taking no action (see Chapter 7).

3.4 Desalination treatment variables

This study is concerned with alkaline deoxygenated desalination treatments, as these appear to offer the best effectiveness (Rinuy & Schweizer 1981; Rinuy & Schweizer 1982; Keene & Orton 1985; Selwyn & Logan 1993; Keene 1994; Loeper-Attia & Weker 1997; Al-Zahrani 1999). Within this group of treatments, a range of methods have been used, and no one treatment protocol has been established. The main variables in operating alkaline desalination treatment are temperature, solution volume, method of deoxygenation, chemical concentration and pH, length of treatment and frequency of solution changes. The methods used by Al-Zahrani (Al-Zahrani 1999; Watkinson & Al-Zahrani 2008) appear to offer the most successful outcomes to date, with greater than 95% chloride extraction using both alkaline sulphite (0.5 M NaOH/0.5 M Na₂SO₃) and nitrogen-deoxygenated 0.5 M NaOH. Since that study, further work on treatment variables has suggested improvements to the treatment procedure. In order to select a method for experimental treatment in this thesis, research on treatment variables is reviewed in relation to the mechanism by which alkaline deoxygenated treatments extract chloride ions from objects.

3.4.1 Chloride removal mechanism

To stabilise objects, chloride ions must be removed from within the pores of objects, the surface of akaganéite and other corrosion products, and if possible from within the structure of akaganéite. On recently excavated objects which have not yet dried out, chloride ions are contained in a liquid ferrous chloride solution at the metal/corrosion interface and in the pores of the corrosion matrix as well as in akaganéite and β -Fe₂(OH)₃Cl.

As objects dry out after excavation, this solution is likely to form akaganéite, and so the majority of chloride ions may be in solid form. The proportion of these various forms of chloride is not known.

Any ferrous chloride solution present should be washed out by successive changes of a treatment solution. It is not known whether $\beta\text{-Fe}_2(\text{OH})_3\text{Cl}$, if present, is transformed by alkaline treatment, although it can be reduced by electrolytic treatment (Guilminot et al. 2008). As it is unstable in oxidising conditions, it is unlikely to be present on objects which have been exposed to the atmosphere for any length of time. In this case it is akaganéite which is the main solid form containing chloride ions. Surface-adsorbed chloride ions on akaganéite can be removed by washing in neutral solutions (Al-Zahrani 1999; Cai et al. 2001; Watkinson & Lewis 2005a); the rate of removal is increased in alkaline conditions. The optimum pH for removal of surface-adsorbed chloride is not known. The mechanism is likely to be the replacement of surface-adsorbed chloride with hydroxide ions (Selwyn & Argyropoulos 2005), and in this case, higher concentration of OH^- ions is assumed to offer improved replacement.

The possibility of ion exchange or transformation of akaganéite to remove structural (tunnel-bound) chloride from akaganéite has been discussed in Chapter 2. Al-Zahrani (1999) found that optimum transformation occurred in moderate pH conditions (pH 8.5 - 10.5), but the influence of treatment variables has not been fully examined. Transformation to goethite and/or hematite is considered a desirable outcome of treatment to reduce the future corrosion threat (Watkinson & Al-Zahrani 2008), but it has only rarely been observed on objects. Where it has been observed it appears to require the presence of electrolytic current (Gil et al. 2003) or high temperatures or pressures (Drews et al. 2004; de Vivies et al. 2007). An investigation of transformation of akaganéite in various concentrations of treatment solutions at various temperatures was carried out, and is reported in Chapter 5.

Although the chloride corrosion mechanism is theoretically the same for all iron objects, every archaeological object is different, with variable corrosion morphologies, chloride concentrations and distributions. It is therefore vital to measure the chloride extraction rate for individual objects rather than groups of objects in order to understand the full range of treatment variability and efficiency. Individual objects may respond well or poorly to the

same treatment method, and this variation needs to be assessed and quantified if treatment outcomes are to be properly evaluated.

3.4.2 pH and concentration

High pH appears to be an important component of successful treatments. The extraction of chloride is significantly better with sodium hydroxide (NaOH) than in neutral solutions (Al-Zahrani 1999; Watkinson & Al-Zahrani 2008). As well as removing surface-adsorbed and possibly structural chloride on akaganéite, hydroxide ions are highly mobile and diffuse easily into objects. They are able to replace chloride as the counter-ion in corrosion and may fix free ferrous ions as insoluble ferrous hydroxide ($\text{Fe}(\text{OH})_2$). Sodium hydroxide, as a strong base which is fully dissociated in water, produces high pH even at relatively low concentrations. Most sodium hydroxide and alkaline sulphite treatments use 0.5M NaOH (e.g. Watkinson 1982; 1983; Keene 1994; Al-Zahrani 1999; Selwyn & Argyropoulos 2005; Liu & Li 2008), producing a pH of 13.7. Work carried out by Wang et al. (2008) and Schmidt-Ott and Oswald (2006) showed that 0.1M NaOH (pH 13.0) produces similar extraction behaviour to the higher concentration. In general, low concentrations of solutions are to be preferred wherever possible for health and safety and cost reasons. Other alkaline solutions such as sodium carbonate, sodium sesquicarbonate, sodium hydrogencarbonate and sodium sulphite are not as effective at removing chloride ions from objects (North & Pearson 1978b; Watkinson & Al-Zahrani 2008), which is attributed to the higher mobility of the OH^- ion.

3.4.3 Deoxygenation

The positive charge at the centre of actively corroding objects attracts chloride ions and makes their removal more difficult. Deoxygenated treatment solutions overcome this problem by depriving the corrosion reaction of oxygen, halting the corrosion process. This removes the electrochemical charge at the centre of the object and frees chloride ions from their counter-ion role, allowing them to diffuse out of the object more easily.

Deoxygenation of treatment solutions was suggested by Gilberg and Seeley (1981) and shown by Al-Zahrani (1999) to improve chloride extraction significantly.

Various methods of deoxygenation are available. Both nitrogen gas and sodium sulphite ions have been tested and found to be similarly effective in deoxygenating solutions (Al-

Zahrani 1999). Sodium sulphite is an oxygen scavenger which deoxygenates solutions by reacting with oxygen to form sulphate ions [16].



The oxygen scavenger hydroxylamine has been tested but it attacks magnetite during the treatment, and is therefore not suitable for use with archaeological material (Wiesner et al. 2007). Other methods of removing oxygen from the treatment solution have been considered, such as heating the treatment solution or using a vacuum to remove oxygen (Eggert 2009), but so far no data is available on their effectiveness. The apparent success of a high temperature-high pressure aqueous treatment (Drews et al. 2004) may be partly attributable to a lack of oxygen in the solution under these conditions; further investigation is merited.

As the role of sodium sulphite is only to remove oxygen and not to reduce corrosion products as initially thought (Gilberg & Seeley 1982), it is only necessary for sufficient sulphite ions to be present to remove oxygen for the duration of the treatment. In a reasonably well-sealed container, 0.05M Na₂SO₃ is sufficient for this purpose (Schmidt-Ott & Oswald 2006). As with NaOH, the reduced concentration of Na₂SO₃ in treatment solutions is an improvement on health and safety and environmental grounds. It may also reduce the risk of chemical residues forming after the treatment. Using nitrogen gas to deoxygenate solutions is a further option, as this eliminates a chemical deoxygenator entirely (Al-Zahrani 1999; Watkinson & Al-Zahrani 2008). This thesis will determine whether nitrogen deoxygenation is more or less efficient than the use of sulphite ions (Chapter 4), and whether the introduction of sulphite ions poses a risk to objects (Chapter 6).

3.4.4 Temperature

Elevated temperatures (50-70°C) are commonly used to increase extraction rates by speeding up diffusion of ions. Schmidt-Ott & Oswald (2006) assert that heating the treatment solution increases the extraction rate tenfold, presumably based on calculations of the effect of temperature on diffusion rates, but provide no empirical data. It is not clear whether heating treatments serves solely to increase diffusion rates, or whether higher temperatures may also increase the proportion of structural chloride released from akaganéite, or improve the access of the treatment solution to deep-seated chloride ions.

North and Pearson (1978b) modelled the effect of temperature on marine artefacts and suggested that raising the temperature to 80°C for a short time would produce a permanent increase in chloride extraction rates, probably due to dehydration of corrosion products and microcrack formation.

No research is available on the possibly damaging effect of increased temperature on objects. Heating of treatment solutions may cause mechanical damage and the dissolution of corrosion products (Selwyn 2004; Selwyn & Argyropoulos 2005). If heating promotes the formation of cracking as suggested by North and Pearson (1978b), then this might be expected to cause the unwanted removal of corrosion products. Al-Zahrani (1999) experienced high chloride extraction at room temperature over only two months, which suggests that high temperature treatment solutions are not needed, and may therefore be considered an unnecessary risk. Room temperature and heated treatment solutions will be compared in this research to establish what the benefits and risks of heated solutions are (Chapter 4 and 6).

3.4.5 Diffusion and solution changes

Chloride extraction is a diffusion-controlled process (North & Pearson 1978b; Selwyn et al. 2001). Maximising the diffusion rate of chloride ions out of the object shortens the treatment time. Changing the solution at intervals maintains a high diffusion gradient between the chloride level in the artefact and the chloride level in solution. As chlorides diffuse into the wash solution from the artefact, the diffusion rate slows down as the solution equilibrates with the artefact. Diffusion-controlled systems follow distinct extraction patterns, with about 75% of the chloride extraction for any one wash occurring during the initial 14 to 21 days (Watkinson 1982). Published graphs for alkaline treatments suggest that the diffusion rate slows considerably after the first 10 – 14 days in each solution (Reguer et al. 2007c; Liu & Li 2008; Wang et al. 2008). Solution changes at 14 day intervals have been found to be equally effective to more frequent changes (Schmidt-Ott & Oswald 2006; Wang et al. 2008). As the treatment progresses, subsequent baths will have a substantially lower chloride concentration and diffusion rate, suggesting that the majority of chloride is extracted in a short period of time. Treatment is usually considered complete when the chloride content of the solution is less than 5 ppm (Loeper-Attia & Weker 1997;

Wang et al. 2008), although this guideline can only be followed if a reliable method of chloride measurement is available.

The ratio of object weight to solution volume will play a role in determining the speed with which chloride levels between the object and solution equilibrate. Watkinson (1982) found that an object weight to solution volume of between 1:4 and 1:9 was optimal. The volume of solution appears to have a minimal effect on overall extraction efficiency provided it is maintained at no less than 1:4.

3.4.5 Conclusion

There has been little systematic study of treatment variables to achieve optimum chloride extraction. The information available suggests that NaOH concentrations of 0.1M provide comparable chloride extraction to higher concentrations. The concentration of sulphite ions can be reduced to 0.05M, or substituted with nitrogen gas. These two deoxygenation methods will be compared in this study. The importance of heating solutions is not clear, and will also be evaluated here. Solution changes appear to be the best way of maximising diffusion rates, and changes at approximately 14 day intervals are suggested. These treatment guidelines will be used to carry out the experimental treatments. Although it is possible that this treatment methodology is not the optimal method for chloride extraction, the literature reviewed suggest that this set of variables is both representative of current desalination practice and should provide a reasonable level of chloride extraction for evaluation.

Chapter 4 – Experimental treatment of archaeological iron objects

Conservators have an obligation to carry out treatments that have been shown to retard deterioration... Treatments that retard deterioration are the ones that quantitative science can address most clearly.

Appelbaum 2007: 277

4.1 Introduction

To accurately evaluate the effectiveness of treatment, the residual chloride content of objects after treatment needs to be measured. Instrumental neutron activation analysis (INAA) can be used to determine chlorine content non-destructively (Selwyn & Argyropoulos 2006) but this method was not available for this research. The only option available for measuring residual chloride content was by means of object digestion in nitric acid. This method was used by Watkinson (1996) and Al-Zahrani (Al-Zahrani 1999; Watkinson & Al-Zahrani 2008) to compare residual chloride content with extracted chloride. This method allows quantitative evaluation of treatment efficiency. Watkinson (1996) found that alkaline sulphite was the most effective chloride extraction method, with an average extraction rate of $87\% \pm 7$. Al-Zahrani (1999) produced extraction efficiencies of $97\% \pm 3$ from iron objects using alkaline sulphite, and $99\% \pm 1$ using nitrogen-deoxygenated sodium hydroxide.

The results from Al-Zahrani appear promising, but the sample size for the tested treatments was small (7 – 17 objects for each treatment), and concerns have been raised regarding the method used to digest the objects, where some chloride may have been lost to the atmosphere through the volatilization of hydrochloric acid (Scott & Eggert 2009). In order for efficiency data to be of use to conservators, treatments must be tested on a large number of objects to allow statistical evaluation of the results and to account for the variability of archaeological iron objects. Providing a substantial body of treatment data, including residual chloride content, from archaeological iron objects is a primary objective of this research.

4.2 Objects for testing

Destructive testing for residual chloride used objects which could be sacrificed; primarily, bulk iron with low archaeological value from sites that had been published. Artefacts were sourced from the National Museum Wales (Cardiff), the Museum of London and Cardiff University. Small numbers of untreated objects from eleven different archaeological sites were digested to evaluate the likelihood that they would contain enough chloride to be suitable for desalination tests. Three sites with the highest chloride levels were chosen: Bornais (BOR), Billingsgate (BWB83) and Caerwent (CAE) (Table 3, Figure 6).

Table 3: Chloride testing for sample objects from eleven archaeological sites.

| Site code | Site name | Number of nails tested | Mean Cl content (ppm) |
|------------------|---|-------------------------------|------------------------------|
| BA84 | Bermondsey Abbey, Southwark | 2 | 66 |
| BC72 | Baynard's Castle, London | 3 | 150 |
| BIG | Biglis, Glamorgan | 3 | 268 |
| BOR | Bornais, Western Isles, Scotland | 3 | 6748 |
| BWB83 | Billingsgate, London | 3 | 1961 |
| CAE | Caerwent, Glamorgan | 3 | 1721 |
| PDN81 | Pudding Lane, London | 2 | 181 |
| SEG | Segontium, Caernarfon, Gwynedd | 3 | 942 |
| SWA81 | Swan Lane, London | 4 | 399 |
| TEX88 | Thames Exchange Buildings, London | 3 | 1090 |
| VRY89 | Vintry, London | 3 | 1186 |

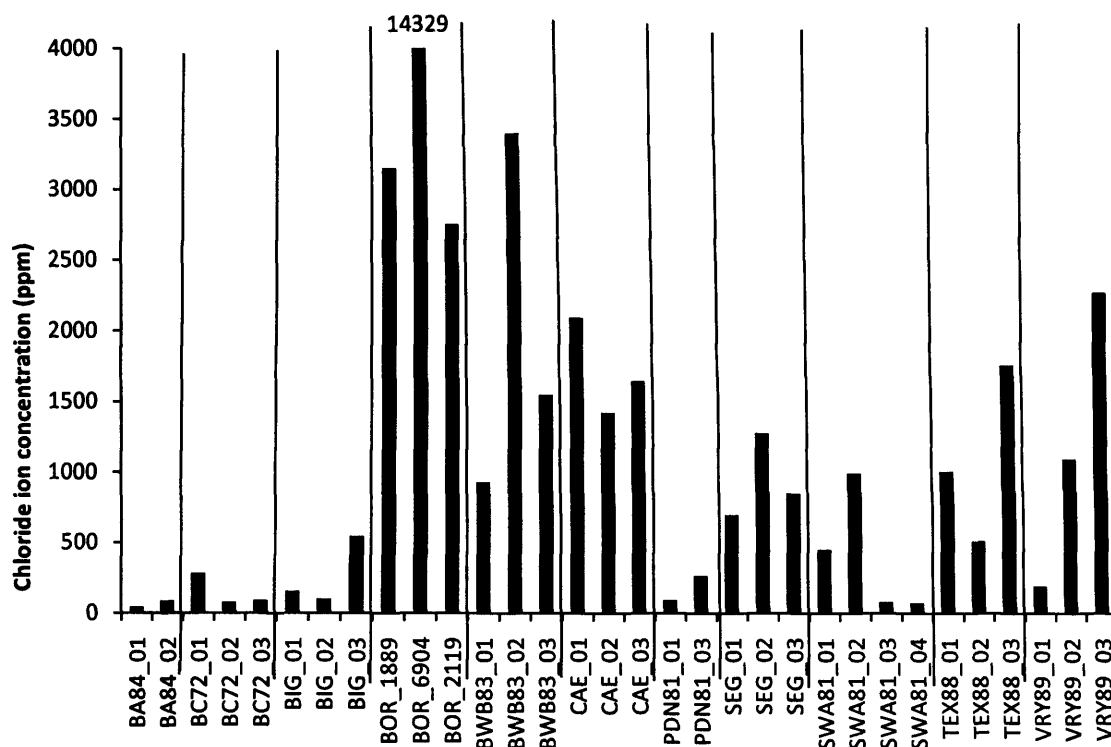


Figure 6: Chloride ion content of digested nails from eleven archaeological sites.

Once material had been received from the three sites, objects were selected for treatment. Two main criteria were used in selection: the presence of a metal core (assessed by X-ray radiography) and object integrity. Objects which were already significantly fractured or had suffered large amounts of flaking were rejected, as the chloride levels measured would not give an accurate picture of the chloride content of the original object. No prior preparation of the objects was undertaken; many retained soil products adhering to the surface. The majority of the objects were wrought iron nails ranging in weight from 1 to 25 g.

4.3 Methodology

4.3.1 Considerations for treatment methodology

The review of treatment variables carried out in Chapter 3 suggested which treatment methods should be tested: alkaline solutions of 0.1M NaOH, deoxygenated using nitrogen or sulphite ions, and tested at room temperature and heated. Other practical issues also needed to be considered in developing the treatment methodology:

- *Sample number:* A primary objective of the thesis is to treat enough samples to allow statistical analysis. No less than 100 samples are required.
- *Chloride measurement:* All objects needed to be treated in individual solutions to allow individual chloride concentrations to be calculated. This significantly increases the amount of work involved in measuring chloride and changing treatment solutions, but offers an opportunity for precise quantitative assessment of treatment success for individual objects, and a proper assessment of chloride extraction outcomes.
- *Time:* The two factors above both mean that each treatment carried out involves a significant time investment. With only limited time available for testing, only a few treatment variables can be investigated.
- *Safety:* lower concentrations of solutions are preferable for reasons of safety and cost-effectiveness.
- *Equipment:* the equipment available may limit the methods that can be used.
- *Comparability:* a valid comparison between alkaline sulphite and nitrogen-deoxygenated sodium hydroxide requires that external variables such as temperature and treatment time be kept equal. The requirements for running alkaline sulphite may influence the variables chosen for the sodium hydroxide treatment, and vice versa.

In a museum situation, all objects would be rinsed after treatment to try to remove residual treatment solution (Aoki 1987; Selwyn & Logan 1993; Keene 1994; Schmidt-Ott & Oswald 2006). This is considered important for the alkaline sulphite treatment, where the presence of sulphite or sulphate ions in the object is thought to promote corrosion. The influence of treatment residues on corrosion rate is tested in this thesis (Chapter 6). As all objects treated experimentally will be dissolved after treatment, rinsing was not included in the treatment method to avoid the extra time required (up to 16 weeks according to Keene 1994).

Drying methods may include simple air-drying with or without a desiccant, use of dry heat and elevated pressure and/or the use of an organic solvent such as acetone to drive off any remaining water (Selwyn & Logan 1993; Schmidt-Ott & Oswald 2006). As the majority of

objects in this study are to be digested after treatment, drying is not an important process, and will be carried out using silica gel to remove most of the water before digestion.

4.3.2 Experimental desalination treatment

Based on these considerations, three treatments were carried out: nitrogen-deoxygenated 0.1M sodium hydroxide at room temperature (dNaOH), 0.1M NaOH/0.05M Na₂SO₃ alkaline sulphite at room temperature (AS20), and 0.1M NaOH/0.05M Na₂SO₃ alkaline sulphite at 60°C (AS60) (Table 4). 48 objects were treated in each of the two room temperature treatments, and 24 objects in the 60°C treatment, giving a total of 120 objects treated. For the two room temperature treatments, nine nails were cut in half before treatment using a diamond rotating tool (Dremel). Only one half of each of these nails was treated, and the other was retained as a control, and for comparison during accelerated corrosion tests (section 4.5.2). Objects were photographed before and after treatment to provide a basic record of any changes occurring (see Chapter 6).

Table 4: Parameters of the experimental treatments carried out in this study.

| Treatment | NaOH concentration | Deoxygenation method | Temperature (±5°C) | Number of objects treated | Maximum treatment time (days) |
|-----------|--------------------|---------------------------------------|--------------------|---------------------------|-------------------------------|
| dNaOH | 0.1M | Nitrogen gas | 20 | 48 | 96 |
| AS20 | 0.1M | 0.05M Na ₂ SO ₃ | 20 | 48 | 96 |
| AS60 | 0.1M | 0.05M Na ₂ SO ₃ | 60 | 24 | 56 |

Objects were placed in individual screw-top HDPE flasks with a maximum volume of 125 ml. The treatment solutions had a volume of 100 ml (dNaOH) and 120 ml (AS20 and AS60). Lids were screwed on for AS20 and AS60; for dNaOH, the bottles were left open and placed in sealed Stewart boxes for nitrogen gas deoxygenation via a positive pressure system (see Appendix 1.3.1 for full details). The maximum object weight was 25 g, giving an object weight to solution volume ratio of no less than 1:4. Treatment solutions were changed approximately every 14 days. All chemicals used were AnalaR grade and dissolved using clean glassware and deionised water. Control samples of the treatment solutions were

checked for chloride content (see below); none was detected. Further details of method are in Appendix 1.3.

The degree of deoxygenation achieved by the two methods was measured using a dissolved oxygen meter (Hach HQ40d with LDO® probe). The probe uses a pre-calibrated sensor which measures oxygen concentration when dipped in aqueous solutions. AS20 and AS60 solutions were measured before each bath was started, and again at the end of each bath. Oxygen concentration in dNaOH solutions was measured after 24 hours exposure to the nitrogen atmosphere by briefly opening one of the containers and removing a control sample.

Chloride content of solutions was measured using a Radiometer Analytical PHM250 specific ion meter, with a detection limit of c. 0.5 ppm and an error of around 10% (see Appendix 2.3). The range of chloride measurement depended on calibration but was never more than 354 ppm; solutions with higher concentrations were diluted to fall within the appropriate range.

Objects were removed from treatment when two consecutive treatment solutions contained less than 10 ppm. Although some conservators have used 5 ppm as the cut-off point for treatment completion (e.g. Loeper-Attia & Weker 1997), this stringent criterion was not possible due to time constraints. After 96 days (56 days for 60°C treatment) objects were removed from the treatment solution regardless of the chloride ion concentration. Although this may result in some objects not completing the treatment, this is unlikely to interfere with the main objective of the study to examine the relationship between treatment, chloride content and corrosion rate. The implications of the time restriction for interpretation of the results will be considered. Chloride extraction is reported as a proportion of the weight of the object (ppm), except where the chloride concentration of the final bath is reported; this is given as ppm relative to the volume of solution.

After treatment, objects were dried using oven-dry silica gel as a desiccant for at least two weeks in a desiccating cabinet. Objects were then placed in 5M nitric acid (diluted from concentrated AnaLar nitric acid using deionised water) to digest. Digestion was carried out at room temperature in covered beakers or screw-top HDPE containers to minimize the possibility of chloride ion loss through the volatilization of hydrochloric acid (HCl). The lids

and covers of the containers were thoroughly rinsed and added to the solution before analysis. Further details may be found in Appendix 1.4.

Out of the 120 objects treated, 118 were digested and analysed for residual chloride (see Appendix 2.3). One object (CAE_29) from dNaOH was donated to another study, while one AS20 object (CAE_40) did not complete digestion in the time available. The extraction results from these two objects have been included in the analysis of the treatment but omitted from further statistical analysis.

4.3.3 Statistical assessment methods

One of the stated aims of this research was to provide sufficient data to allow statistical analysis of the sample. A statistically robust sample is more likely to provide information that is relevant to other groups of iron objects. Statistical analysis may also be misused or misinterpreted. A short summary of the issues regarding statistics and some of the precautions and caveats relating to their use in the following sections is presented here.

Statistics are of two kinds – descriptive and inferential. Descriptive statistics (such as measures of central tendency and variability) describe the sample at hand, whereas inferential statistics attempt to draw conclusions from the sample about the wider population. In order for such inferences to be valid, the sample used in the statistical analysis must be representative of that population.

Technically, this study could define the population as ‘every archaeological iron object’. To draw a representative sample from such a broadly defined population would be extremely difficult, as it would need to include large numbers of objects from many varied contexts. A fully representative sample in this sense was not possible for this study, and will in all likelihood never be possible.

The sampling strategy for this study was constrained by the material available for destructive testing. This confined the possible sample material to bulk iron from archaeological sites that had already been published or were deemed to be disposable by the archaeologists and curators holding them. The inclusion of sample material from three very different archaeological sites is an attempt to reduce the biased nature of the sample and broaden its applicability to other iron objects. As the problem of chloride-induced

corrosion is common to many archaeological sites, it is not wholly unreasonable to draw some conclusions about the treatments used and extend them to other artefacts. However, the use of inferential statistical methods has been limited to questions regarding only the sample, rather than attempting to draw statistical conclusions about all archaeological iron.

Many of the data distributions described below are of skewed samples, that is, the sample does not follow the normal distribution (Gaussian distribution or bell curve). Many statistical tests, including the Pearson Product Moment Correlation (r) and the analysis of variance (ANOVA) are designed to be used with normally distributed data. Their use for this study must therefore be approached with caution. They have been used where a numerical analysis of the data is helpful in determining whether a correlation or significant difference exists, but only very strongly significant results will be taken as probably true. The ANOVA test, particularly, may be problematic with skewed data as it relies on the comparison of means, which do not accurately describe skewed samples. The Pearson correlation coefficient is more robust against skewed data, and the effects of skew would be to reduce the value of r rather than artificially increase it. A fuller description of the statistical methods used and their limitations is found in Appendix 3.

Statistical significance is the probability that a given result is due to chance or random variability, and is usually taken either at the .05 (5% chance) or .01 (1% chance) level. Critical values for the calculated coefficients can be found in any statistics textbook. In general, an obtained value that is much greater than its critical value can be safely taken as significant, whereas obtained values very close to the critical value must be treated with caution, particularly given the issues of sample skew. Statistical significance is always in relation to a null hypothesis, which is rejected if the obtained value falls above the critical value. In all the tests described in the following sections, the null hypothesis is that there is no difference or no relationship between the data being examined. Separate null hypotheses have not been stated in the text for simplicity.

4.4 Results of experimental treatments

4.4.1 Chloride extraction during treatment

There was no difference between the ability of nitrogen gas and sulphite ions to deoxygenate the solutions. Measured oxygen content in alkaline sulphite solutions was 0.27 ± 4 mg/L at the beginning of each treatment solution, and was at the same level at the end. The concentration of sulphite ions was sufficient to keep the solution deoxygenated for the duration of each treatment solution. Deoxygenation with nitrogen gas achieved similar low oxygen content (0.35 ± 3 mg/L) within 24 hours of solutions being exposed to the nitrogen positive pressure. Both methods achieved a near total removal of oxygen from the treatment solutions.

In these experiments, the criterion used to determine whether a treatment was complete was that two consecutive solutions should have a measured chloride ion content of less than 10 ppm. Because of time restrictions, not all the objects reached this criterion before the treatment had to be terminated. Figure 7 shows the final treatment solution concentration for all the objects. The majority of the objects did have a final solution concentration of less than 10 ppm, and of these the majority did in fact meet the 5 ppm criterion. 12 objects (10%) did not reach the 10 ppm criterion, all but one of which were from the room temperature treatments (dNaOH and AS20) (Table 5). For 11% of objects treated at room temperature (11 out of 96 objects), the 96 days of treatment time were not sufficient, while for heated treatment, only 4% (1 out of 24 objects) needed an extraction period longer than eight weeks.

The amount of chloride ions extracted from objects varied widely, from 15 ppm (CAE_20, dNaOH) to over 15000 ppm (BOR_3654, AS60). The histogram of chloride extraction for all the treatments (Figure 8) shows a positively skewed distribution in favour of chloride extraction up to around 5000 ppm, with only 12 out of 120 objects extracting more than that. Table 5 gives descriptive statistics for the extraction of chloride of the three treatments. Mean and median extracted chloride is highest for AS60, and slightly lower for dNaOH and AS20.

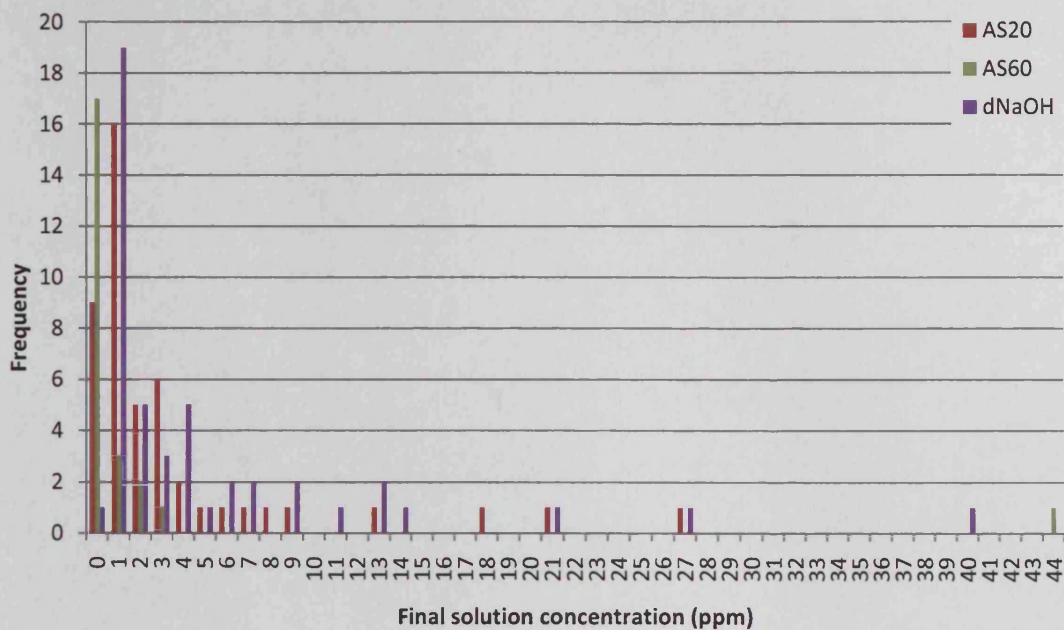


Figure 7: Histogram showing final solution concentration for all the objects in the three experimental treatments.

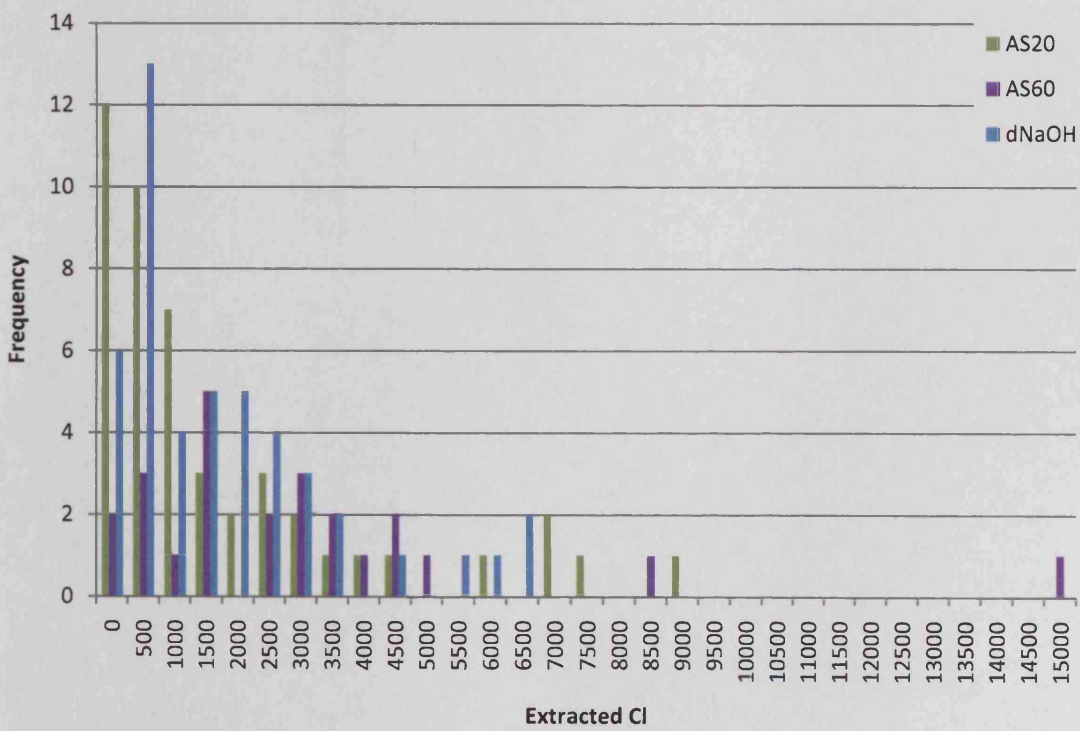


Figure 8: Histogram of chloride ions extracted by the three treatments. Bin width is 500 ppm.

Table 5: Descriptive statistics for the extraction of chloride ions in the three experimental treatments.

| | dNaOH | AS20 | AS60 |
|---|--------------|-------------|---------------|
| No. of samples | 48 | 48 | 24 |
| Mean Cl extracted (ppm) | 1990 | 2028 | 3269 |
| Standard deviation (ppm) | 1733 | 2283 | 3171 |
| Median Cl extracted (ppm) | 1542 | 1095 | 2854 |
| Range Cl extracted (ppm) | 6884 | 9335 | 14934 |
| | (15 – 6899) | (44 – 9379) | (130 – 15064) |
| Inter-quartile range (ppm) | 1936 | 2121 | 3244 |
| Mean % extracted in first solution | 68 | 67 | 88 |
| Median % extracted in first solution | 70 | 71 | 92 |
| Number (%) of objects not reaching completion criteria | 7 (15%) | 4 (8%) | 1 (4%) |

In all three treatments the majority of chloride was extracted in the first solution (Figures 9, 10, 11), with a median of 70-71% for room temperature treatments (Table 5). The heated treatment, AS60, appears to have greater extraction in the first solution (mean 88%, median 92%). There is, however, significant variation in the pattern of extraction between individual objects.

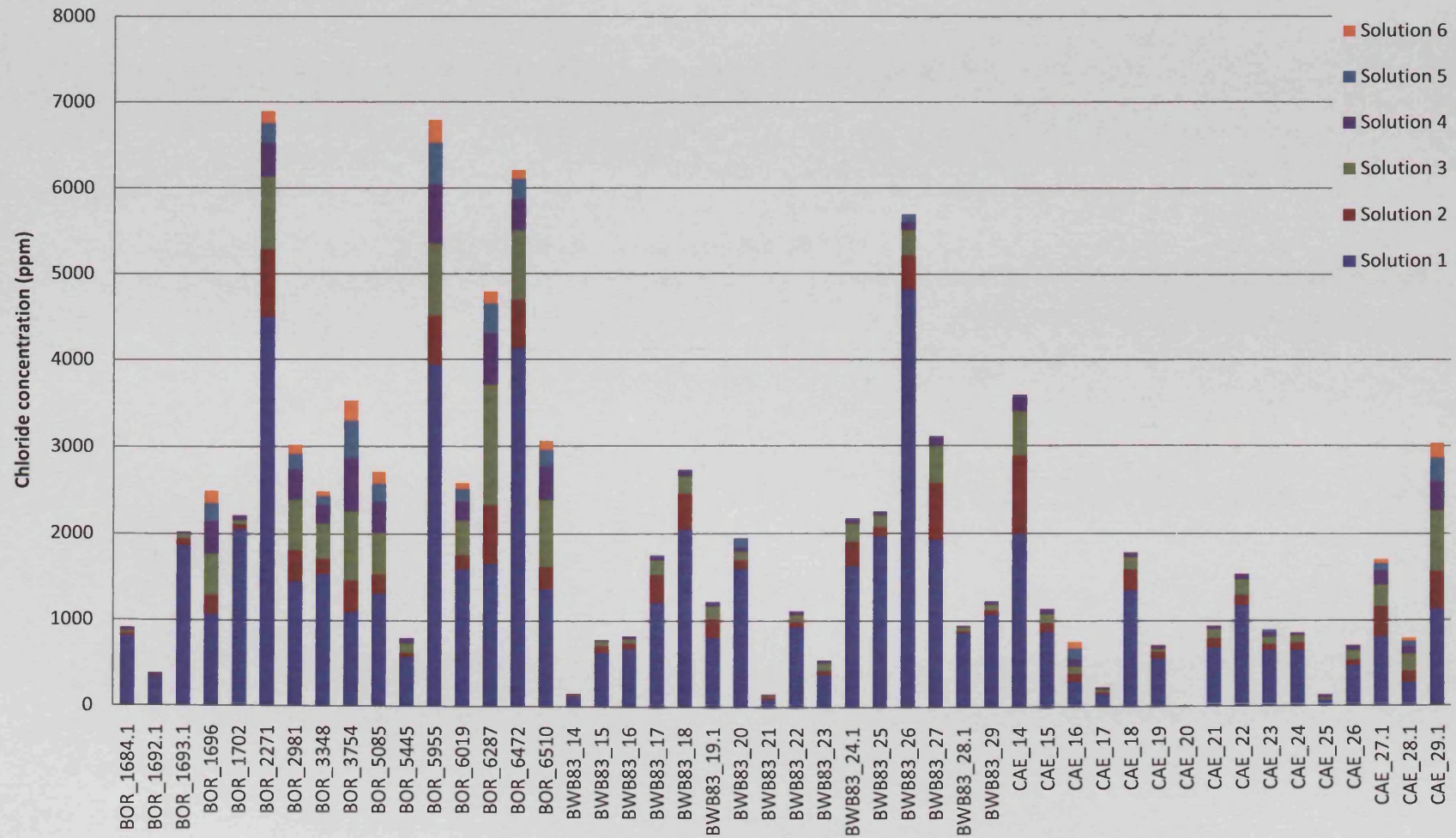


Figure 9: Extraction of chloride ions from objects in nitrogen-deoxygenated 0.1M NaOH (dNaOH).

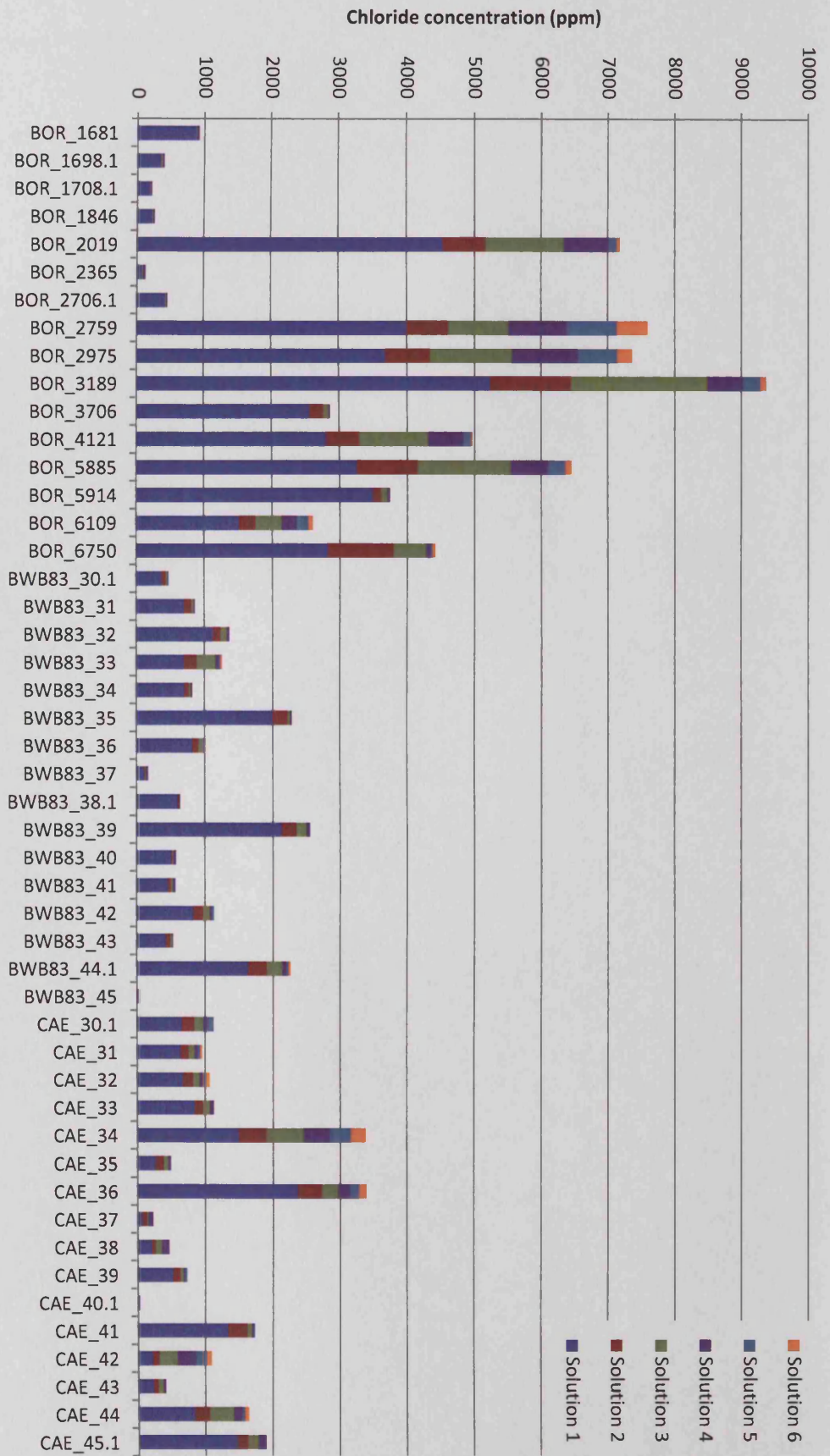


Figure 10: Extraction of chloride from objects treated in 0.1M NaOH/0.05M Na₂SO₃ solution (AS20).

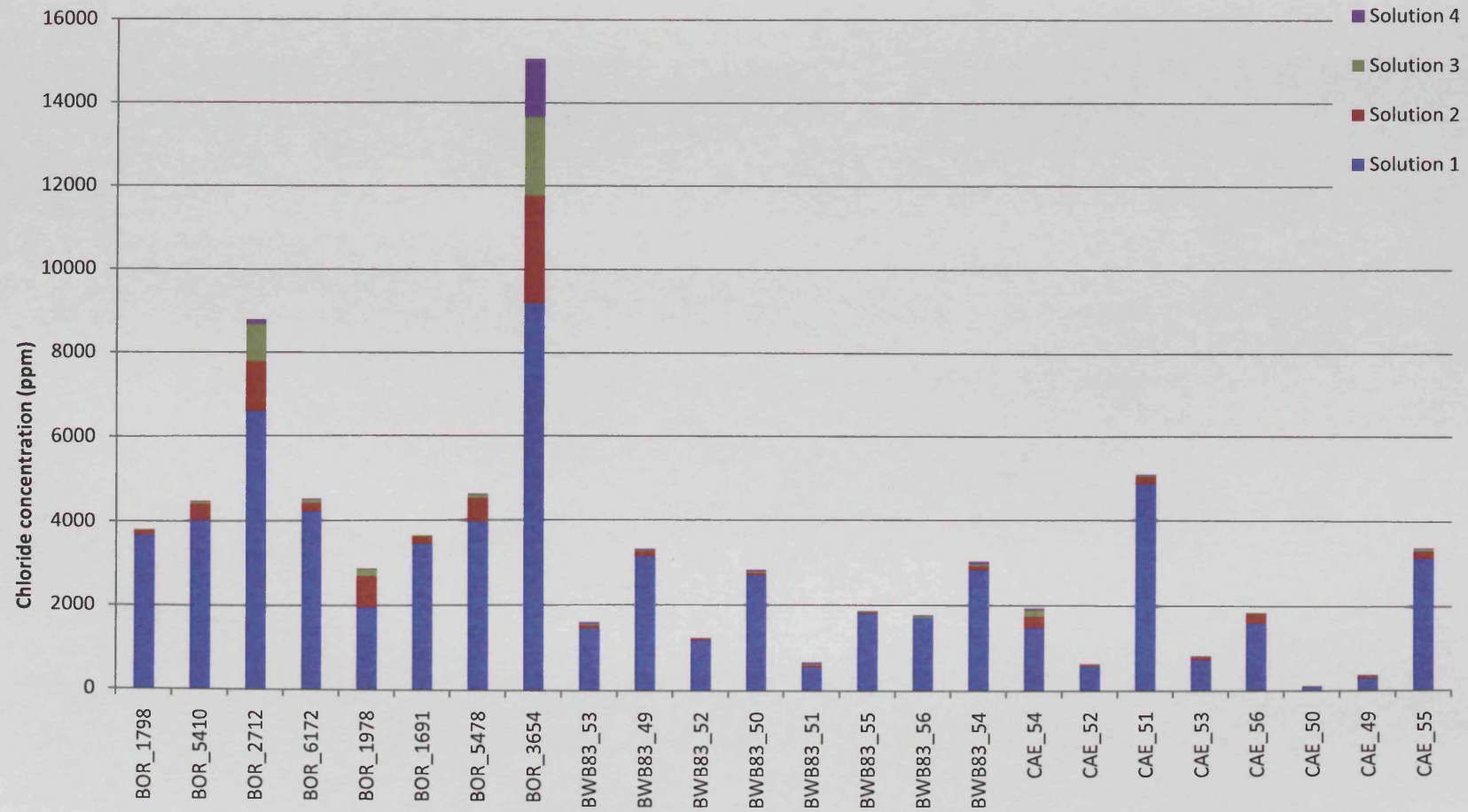


Figure 11: Extraction of chloride from objects treated in 0.1M NaOH/0.05M Na₂SO₃ at 60°C (AS60).

Figures 12, 13 and 14 show the pattern of extraction as % in each solution of the total chloride extracted. The % extracted in the first solution may be as high as 90% and as low as 20%. AS60 has the most consistent extraction with no object having a first solution extraction % of less than 60% (Figure 14); this may be related to the heating promoting faster diffusion of the soluble chloride in the initial treatment stages.

The amount of chloride extracted after the first solution is very low in some cases (a 'fast' extraction), in others a large proportion of the total amount extracted comes in the later baths (a 'slow' extraction). The distribution of extraction patterns is not related to the total chloride extracted – two objects with similar overall extraction may show different patterns (e.g. dNaOH, BOR_3754 and CAE_14 both extracted a total of around 3500 ppm, but the extraction occurred more slowly in the former object) (Figure 12). Although objects with high chloride extraction tend to have more chloride present in the later solutions (e.g. many of the Bornais objects, Figures 9, 10, 11) the converse is not true – objects with low total chloride extraction may also extract slowly (e.g. CAE_42, Figure 10). This suggests that the differences in extraction patterns between objects may have little to do with either the treatment itself or the total amount of chloride in the object, but rather are related to the morphological nature of the object corrosion layers. For example, Billingsgate objects usually have fairly rapid extraction patterns (Figures 12, 13, 14), and this may be related to the relatively thin corrosion products that the majority of these objects displayed. This issue will be discussed further below.

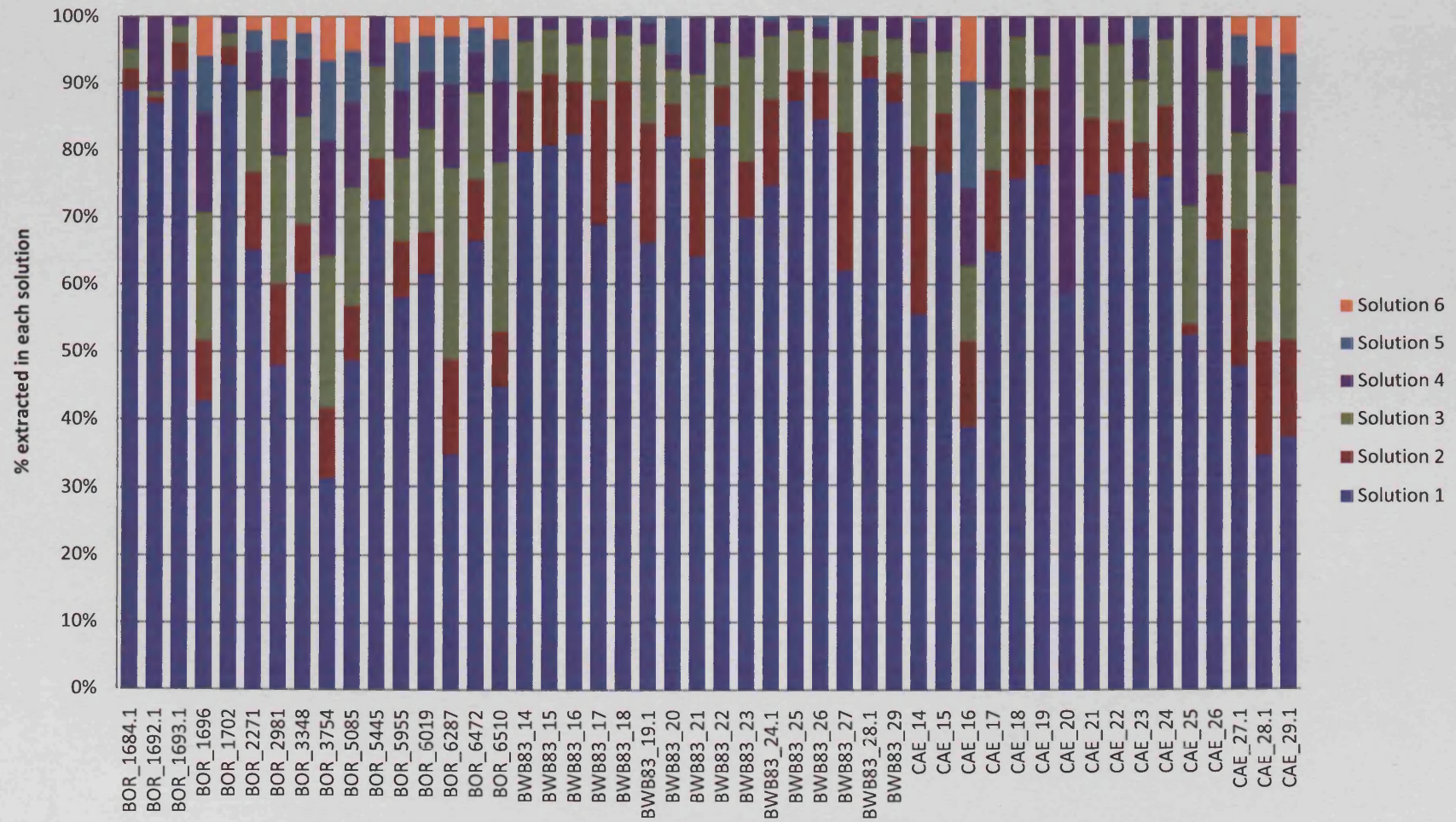


Figure 12: Chloride extraction in dNaOH treatment showing percentage of extracted chloride in each bath.

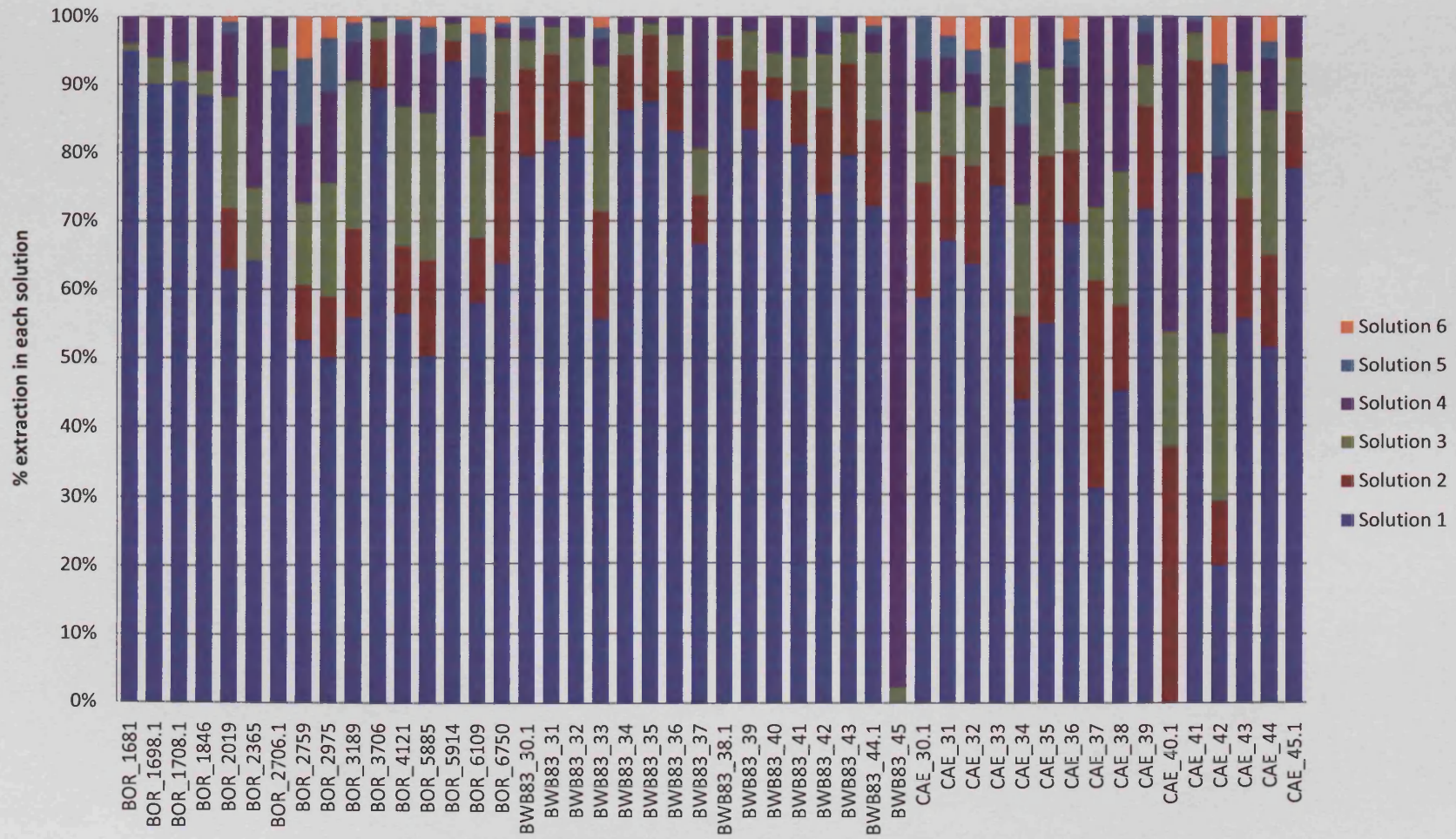


Figure 13: Chloride extraction in AS20 showing percentage of extracted chloride in each bath.

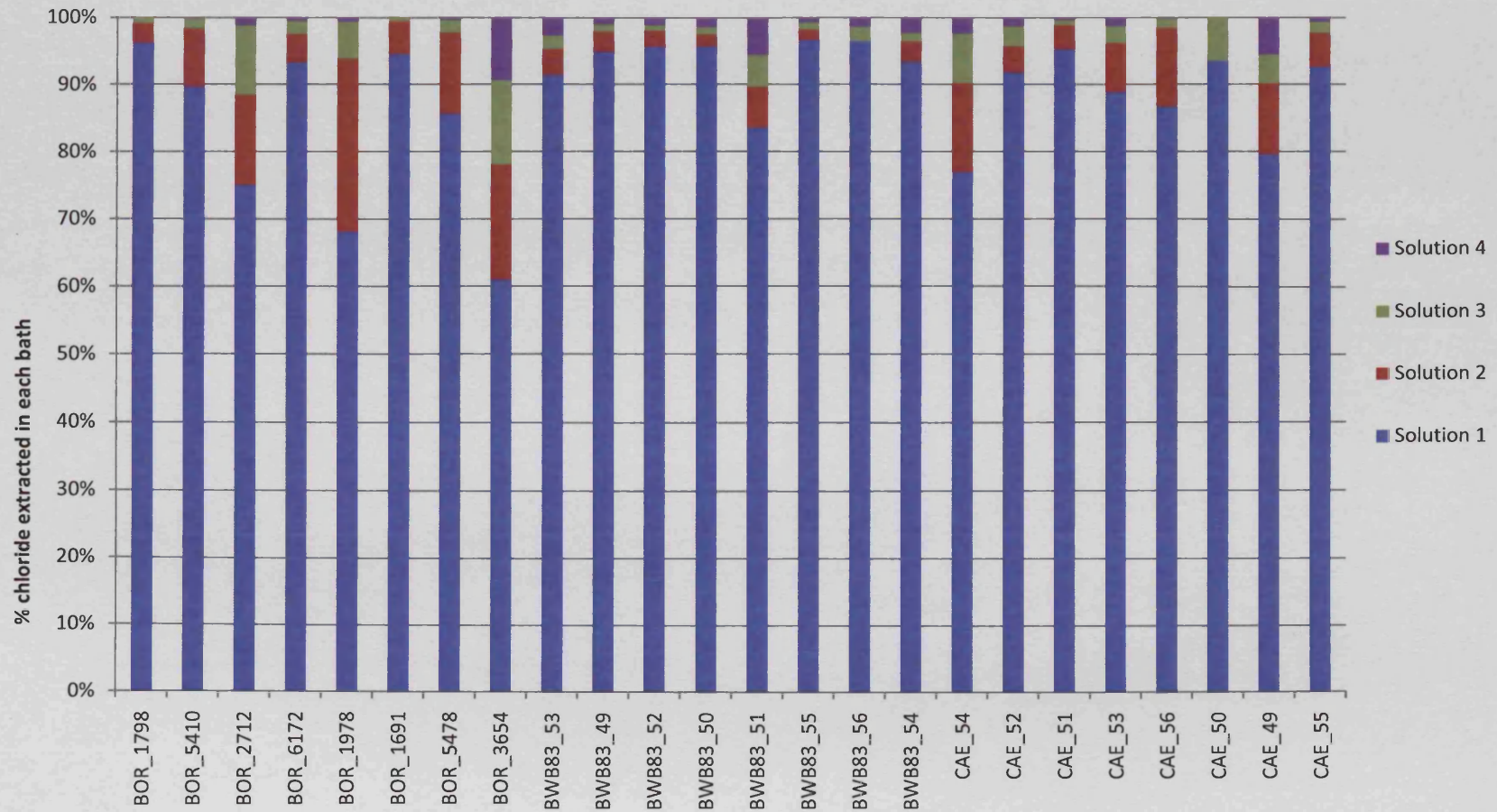


Figure 14: Chloride extraction in AS60 as percentage of extracted chloride in each bath.

For treatments carried out on objects in museum collections, the data on extraction presented above would be the only information available on the outcome of treatment. This leaves some very important unanswered questions. If treatment always extracts a consistent proportion of the chloride ions present in an object, then we might conclude that objects with high extracted chloride also contain more residual chloride than objects where only a small amount of chloride was extracted. This assumption has never been shown to be true. Indeed, the difference in the way the treatment proceeds (slow vs. fast extractions) suggest that the distribution and morphology of chloride ions and the corrosion layer morphology have an important role to play in determining the outcome of treatment. Objects with low chloride extraction may actually contain high residual chloride which was not accessible or extractable, for whatever reason. It is dangerous to make the assumption that treatments work the same way for all objects given the variability of objects and the variability with which they respond to treatment. This is why individual chloride measurement is important for understanding the behaviour of individual objects.

Without residual chloride data, the three treatments are also very difficult to compare. On the basis of Figure 8 it is tempting to conclude that of the two room temperature treatments, dNaOH is more effective because there were fewer objects with low chloride extraction (<500 ppm) than for AS20. This would only be an accurate assumption if the two samples were exactly the same and presented exactly the same range and frequency of total chloride content. As each object in the treatment samples is unique, this is not a valid assumption. AS20 may appear to have extracted less chloride overall than dNaOH, but there may have been more objects with low total chloride than dNaOH. Information about how much chloride the objects actually contain is therefore vital both to compare the samples and judge the success of the treatments. Total chloride content cannot be deduced from the treatment data; it must be measured. Without it, it is impossible to say whether any one of the three treatments is better than the others.

4.4.2 Extraction efficiency

Extraction efficiency in this study is defined as the amount of chloride extracted as a proportion of the total chloride in the object. Total chloride is the sum of extracted chloride measured during treatment and residual chloride as provided by digestion. With so many

objects, a statistical description of the data is vital to understand which of the differences are significant and which are due to random variation. Descriptive statistics for the three treatments are given in Table 6. Mean and median have been calculated as measures of central tendency, standard deviation (S.D.), range and interquartile range for variability. These are given for extraction %, residual chloride, and total chloride.

Table 6: Descriptive statistics for the three experimental treatments. S.D = standard deviation. I-Q range = interquartile range.

| | | dNaOH | AS20 | AS60 |
|--------------------------|-----------|--------------|--------------|---------------|
| No. of samples | | 47 | 47 | 24 |
| Extraction % | Mean | 74 | 77 | 84 |
| | Median | 79 | 83 | 89 |
| | S.D. | 22 | 23 | 19 |
| | Range | 93 | 87 | 82 |
| | I-Q range | (6 – 99) | (12 – 99) | (16 – 98) |
| Residual Cl (ppm) | Mean | 596 | 320 | 360 |
| | Median | 300 | 196 | 218 |
| | S.D. | 770 | 328 | 291 |
| | Range | 3859 | 1561 | 1031 |
| | I-Q range | (32 – 3891) | (37 – 1598) | (109 – 1140) |
| Total Cl (ppm) | Mean | 2587 | 2348 | 3629 |
| | Median | 1942 | 1293 | 3123 |
| | S.D. | 2028 | 2318 | 3309 |
| | Range | 8077 | 9310 | 15437 |
| | I-Q range | (201 – 8278) | (262 – 9572) | (768 – 16205) |

4.4.3 Comparison of samples

The similarity of the three samples is assessed in terms of their total chloride content (Table 6). Histograms for the total chloride content of the objects are given in Figure 15.

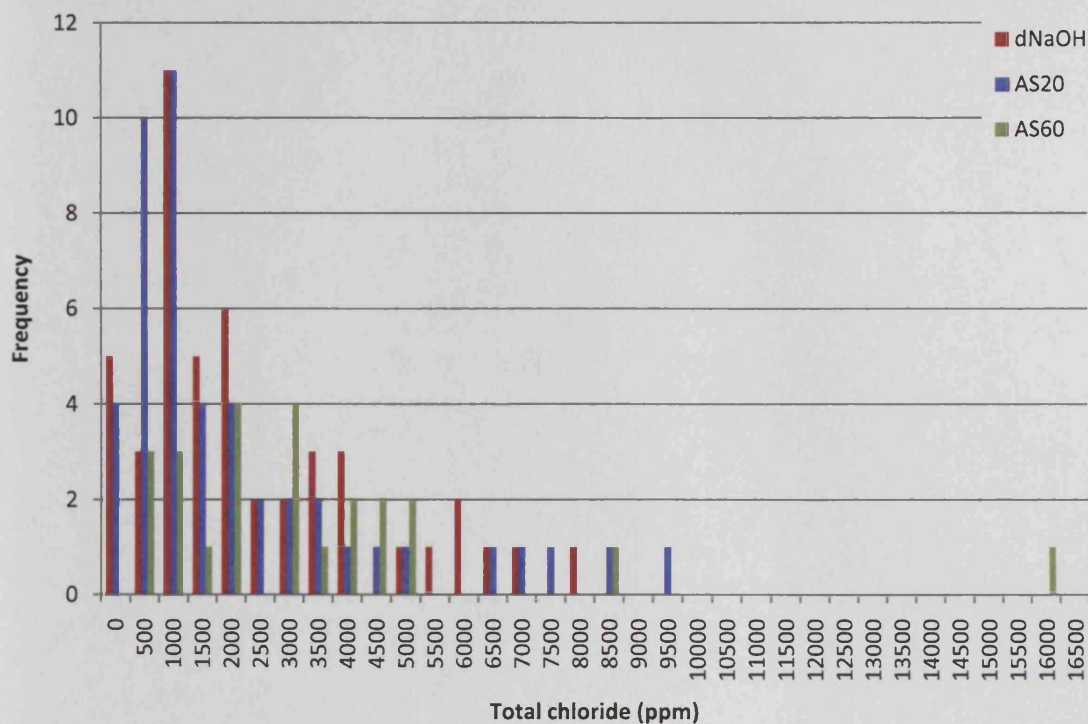


Figure 15: Histogram of total chloride content of the objects in the three desalination treatments. Bin size is 500 ppm.

The mean and median total chloride content show a difference of at least 500 ppm in all three cases (Table 6). Differing mean and median is an indication that the distribution of the data is skewed, and this is confirmed by the histogram (Figure 15). Apart from the outlier at 16000 ppm, all the objects have chloride content less than 10000 ppm, with the main cluster of samples less than 2500 ppm (Figure 15). Comparing the samples from the three treatments, we see that in general they have the same distribution, except that AS20 includes more objects in the 500-1000 ppm range, and AS60 includes no objects in the 0-500 ppm range and more objects in the 3000-5500 ppm range. An analysis of variance (ANOVA) shows that the three samples were not different to a statistically significant degree ($F = 2.26$, $F_{crit} = 2.7$ at .05 significance level), especially if the outlier at 16000 ppm is discounted from the analysis ($F = 0.63$ when excluded). Although there is some variation between the samples, it is accounted for by the general pattern of variation within each sample, and should have no significant effect on an assessment of the treatment outcomes. The three samples are similar enough to allow valid comparisons, an important piece of information that can only be determined by measuring total chloride content of the objects.

4.4.4 Comparison of treatments

Figures 16, 17 and 18 show the extracted and residual chloride in absolute ppm, and the extraction % for each object in the three treatments. Data is arranged in order of increasing extraction % within the objects from each site. Extraction efficiency covers a similar range and variability in all three treatments, except that AS60 has fewer low-efficiency extractions (Figure 18) leading to a higher mean and median (Table 6). dNaOH has more objects containing high residual chloride ion content (Figure 16), while the majority of AS20 and AS60 objects contain less than 1000 ppm residual chloride (Figure 17 and 18). Bornais objects in dNaOH had the worst treatment outcomes, containing more objects with higher residual chloride than any other group of objects (Figure 16).

The median extraction % is always higher than the mean by at least 5% (Table 6). Histograms of the extraction % for the three treatments confirm that the distribution of extraction % is negatively skewed (Figure 19). The majority of extraction efficiency lies between 63 and 99%, with a scatter of lower values. This is the case for all three treatments, except that the bulk of AS60 results begin at 77%. The long tail of low values is the reason that the mean extraction % is lower than the median, as the latter is less susceptible to the effect of skewed distributions and therefore a better description of the central tendency of these distributions. For the same reason, the full range is not a good descriptor of the general tendency of the data, whereas the interquartile range is a better reflection of where the majority of the data are grouped (Table 6). Standard deviation is more accurate than range, but is based on the mean and therefore assumes a normal distribution. Median extraction % and interquartile range are the most accurate descriptors of the tendency of the data.

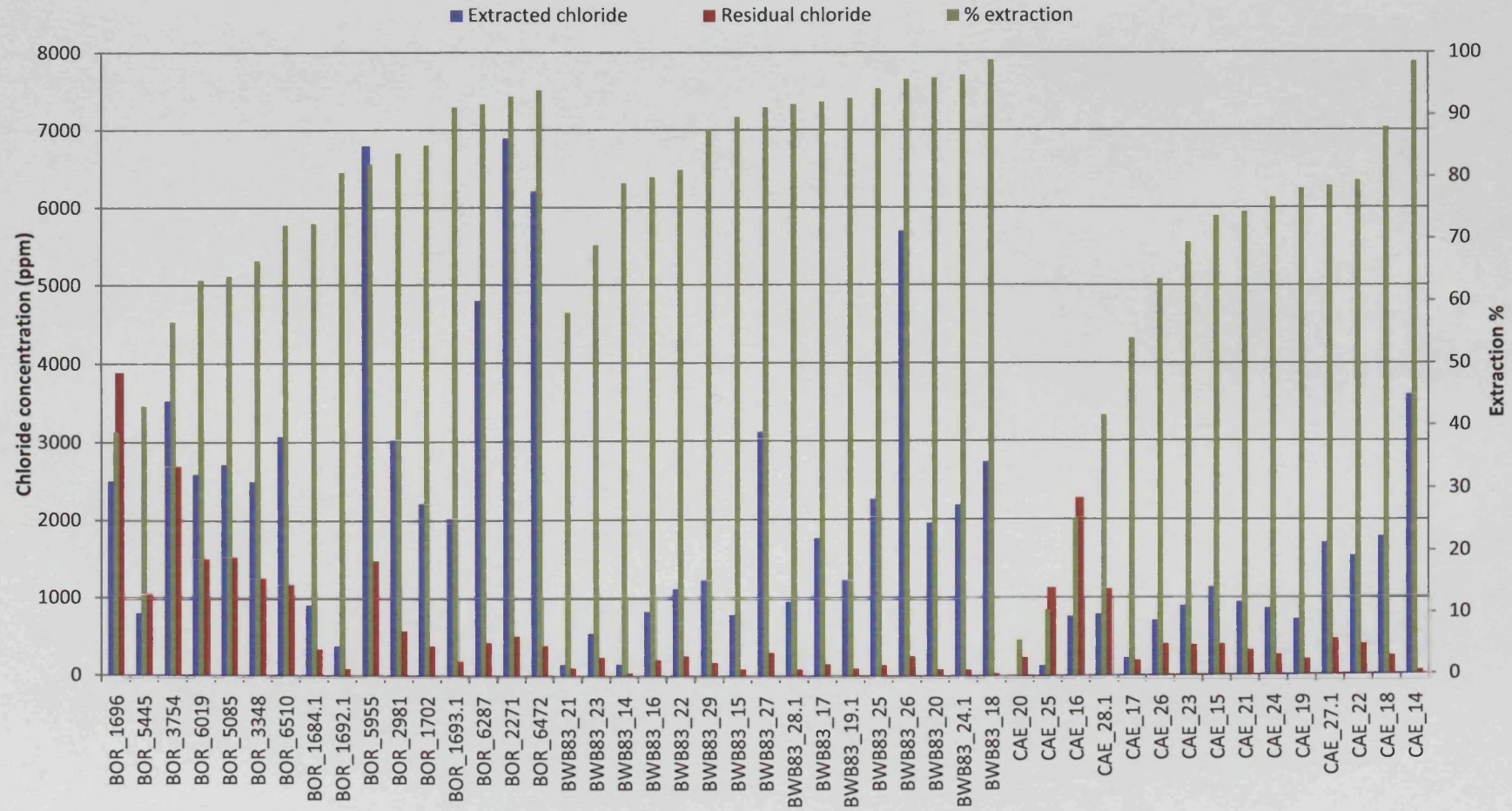


Figure 16: Extracted and residual chloride data for objects treated with dNaOH. Extraction % is given on the secondary axis. The data is arranged in order of increasing extraction % within each site.



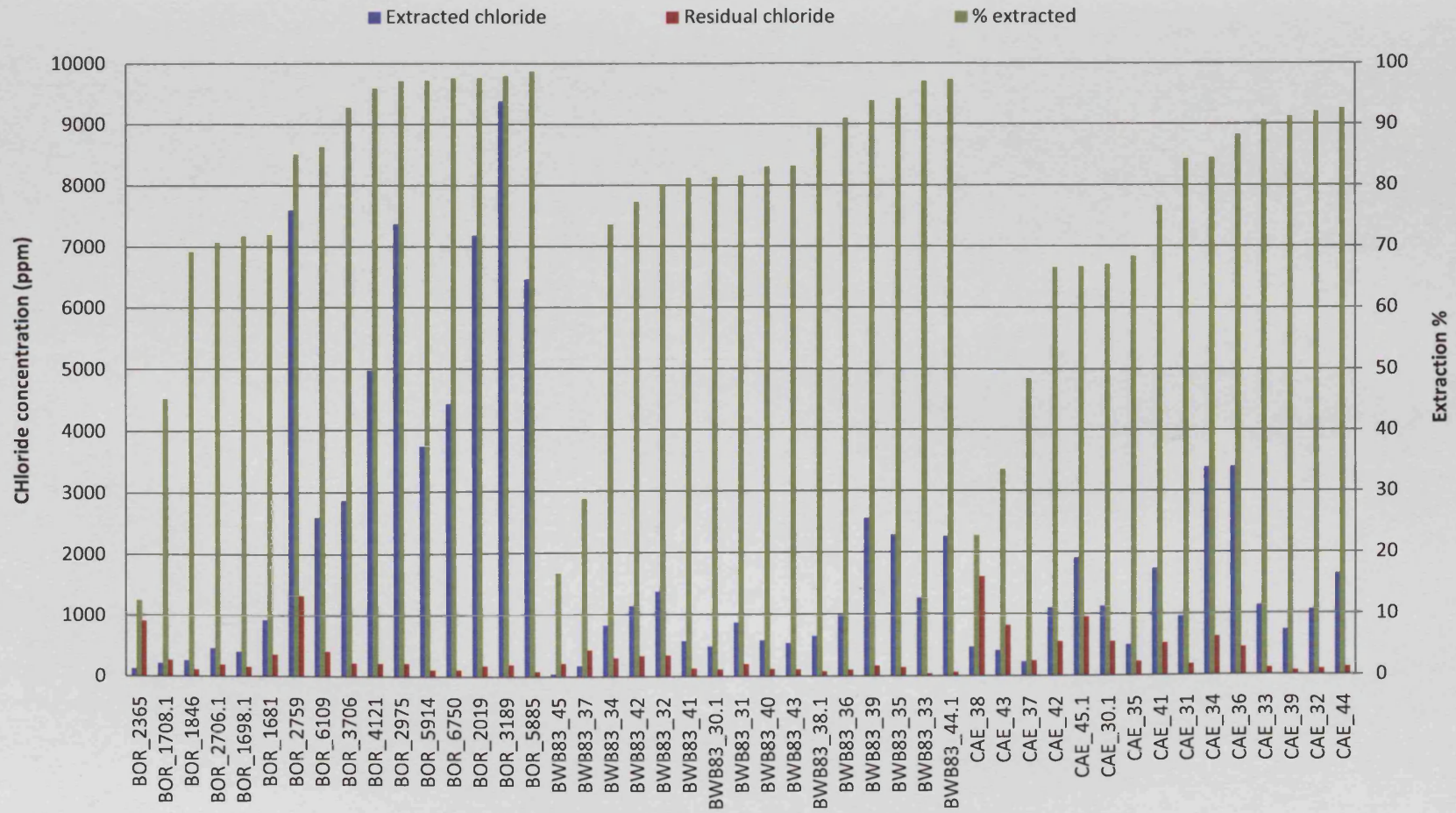


Figure 17: Extracted and residual chloride data for objects treated in AS20. The data is arranged in order of extraction % (secondary axis) within each site.

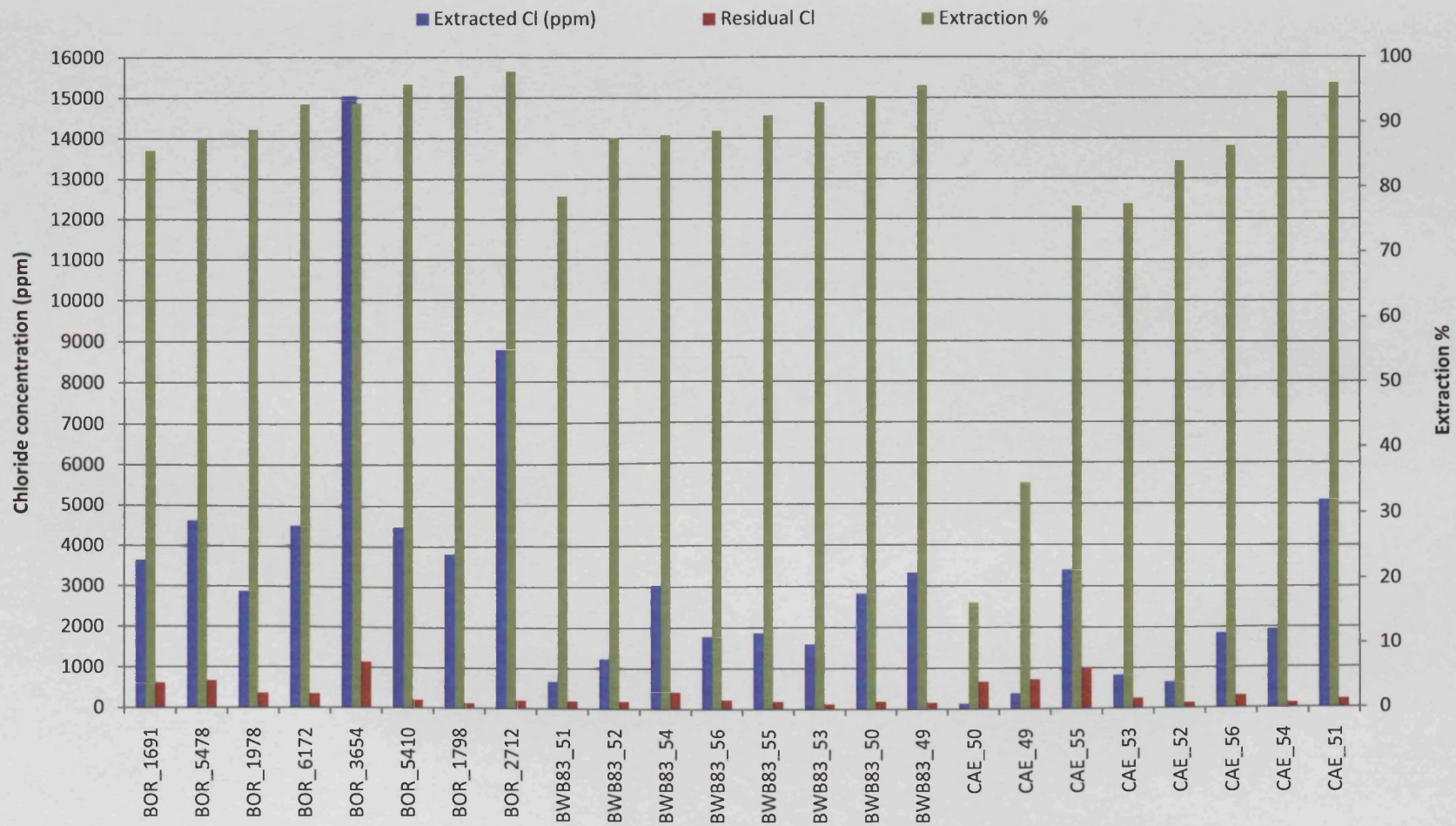


Figure 18: Extracted and residual chloride data for objects treated in AS60. Data is arranged in order of increasing extraction % within each site.

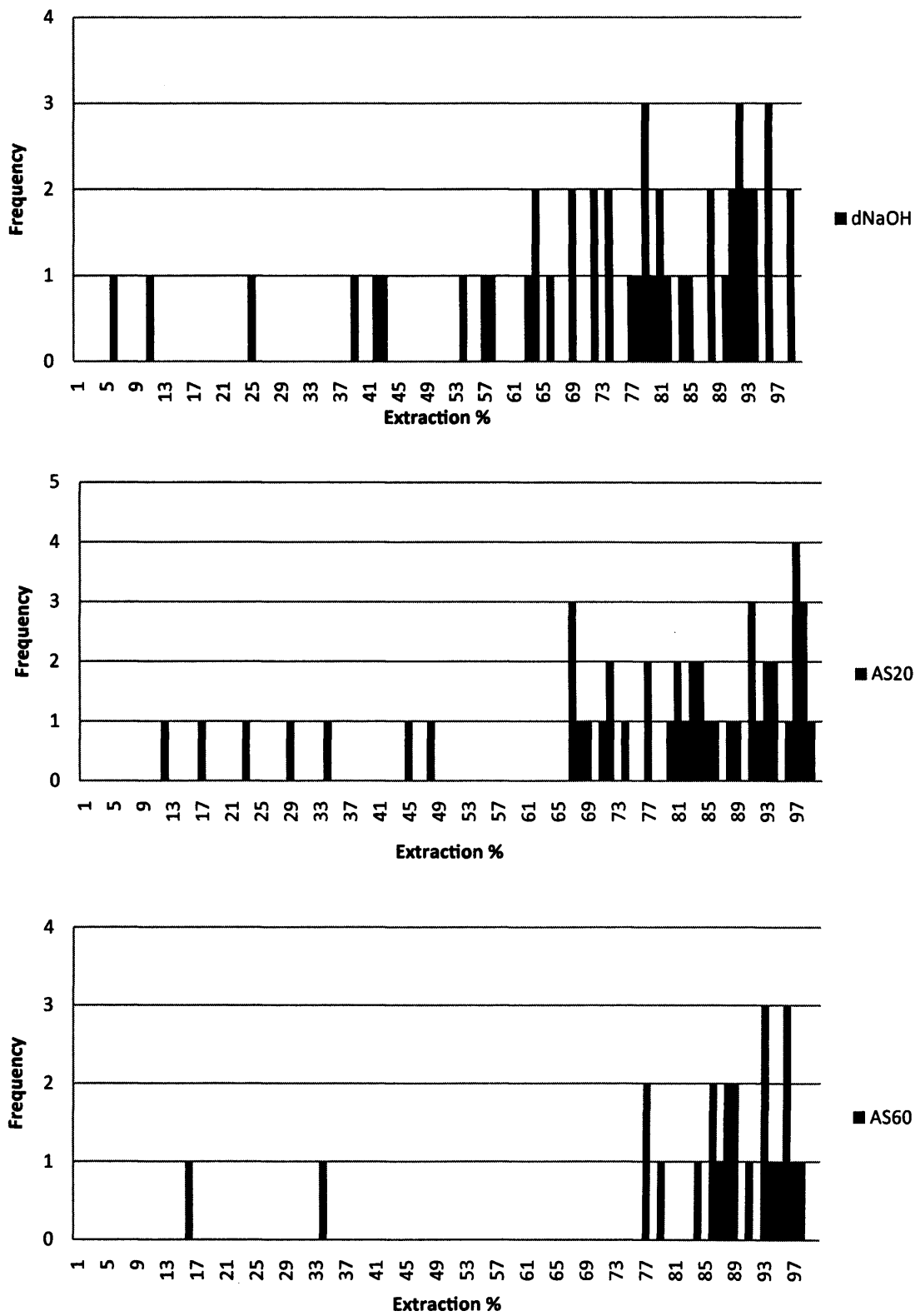


Figure 19: Histograms showing extraction % for the three treatments. All three distributions are negatively skewed. Top: dNaOH. Middle: AS20. Bottom: AS60.

To determine whether any of the treatments performed significantly better or worse than the others, extraction percentage can be compared. Looking only at the median % extraction suggests that dNaOH is the worst-performing treatment (median = 79%) and AS60 is the best (median = 89%) (Table 6). However, an ANOVA test shows that there is no statistically significant difference between the mean extraction % of the three treatments ($F = 1.68$, $F_{crit} = 2.7$ at .05 significance). Although it is still possible that the difference in extraction is significant, this cannot be shown from these samples, as the variability within each group precludes a definitive answer in this case. The statistical result is supported by the similarity of the three histograms of extraction % (Figure 19). None of the treatments stands out as being particularly successful or unsuccessful. This is not surprising, as the treatment mechanism is similar. The suggestion that increasing temperature substantially increases the proportion of chloride released cannot be substantiated using this data.

The measure of extraction % may, however, be flawed. Although it has been used in other treatment studies (Watkinson 1983; Al-Zahrani 1999), the percentage is dependent on the total chloride content, which varies dramatically. High or low total chloride content may skew extraction % such that it does not reflect the final state of the object in terms of its susceptibility to corrosion. Part of the reason why the median extraction % of AS60 appears to be slightly higher is that no objects in this treatment had total chloride less than 500 ppm (Figure 15). Objects with low total chloride are more likely to have low extraction percentage (Figures 16, 17, 18).

If susceptibility to corrosion depends on chloride ion content, then the more interesting issue is how many of the objects had their chloride levels reduced to a 'safe' limit – whatever such a limit might be (see section 4.5.3). Thus, an object with very high total chloride content may appear to have had a successful treatment with a high extraction %, but may still contain quite high levels of residual chloride. An example of this is BOR_3654 (AS60); although 93% of the chloride in the object was extracted, over 1000 ppm (similar to some untreated objects) remained (Figure 18). Conversely, an object with very low chloride ion content may not appear to have very good extraction % at all, but with low chloride to begin with its susceptibility to corrosion may not have changed much. For example, CAE_20 had the worst extraction at 6%, but the total chloride content of the object was only 254

ppm (Figure 16), a much lower chloride level than that of many other treated objects. Care must therefore be taken in interpreting extraction % data.

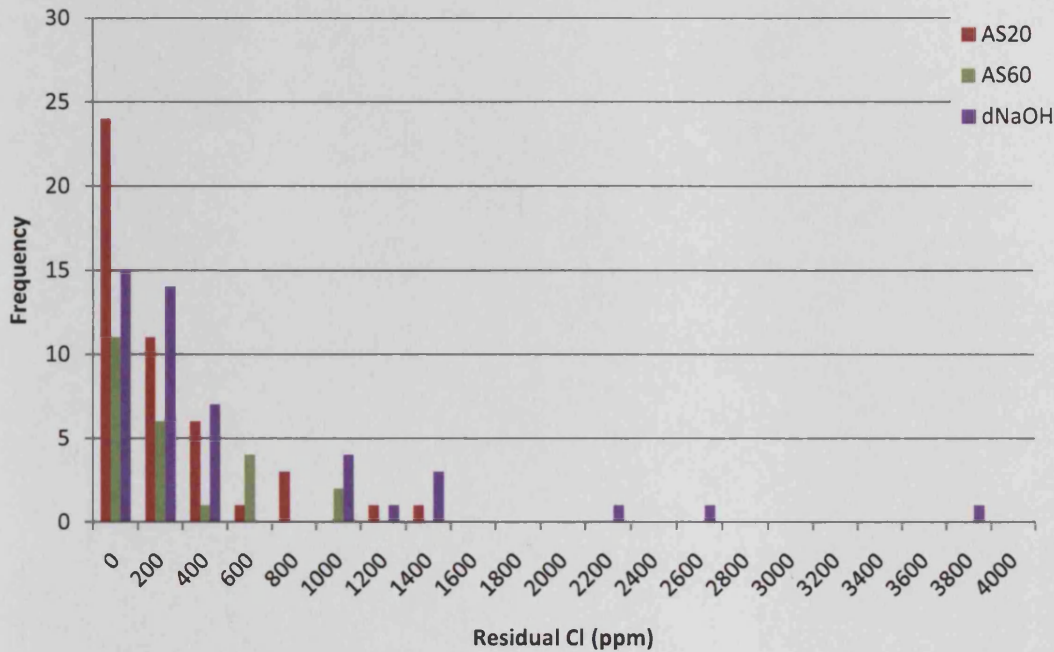


Figure 20: Histogram of residual chloride for all objects in the three treatments. Bin size is 200 ppm.

Figure 20 shows a histogram of the residual chloride content of the objects. Low residual chloride levels (less than 200 ppm) are always the most common, and frequency decreases up to 1400 ppm. All of the outliers in the higher regions of residual chloride stem from the dNaOH treatment, but with so few samples remaining in this region it is not possible to draw any conclusions from this. It may be related to individual corrosion morphology (see section 4.4.5). The three outliers in Figure 20 did have poor extraction % compared to the median for the treatment (25, 57 and 39%), but not the worst extraction %.

To further investigate the relationship between extraction % and residual chloride content, a scatter diagram of the two variables is shown in Figure 21, and the correlation (r) and coefficient of variation (r^2) were calculated. The correlation coefficient is -0.486 for all the treatments taken together, indicating a significant negative relationship ($r_{crit} = 0.254$ at .01 significance), but the scatter plot and a low r^2 of 0.2364 show that the relationship is not very strong. Although there is a grouping of samples that have high extraction % and low residual chloride, outside of this group there is a large scatter with no observable pattern.

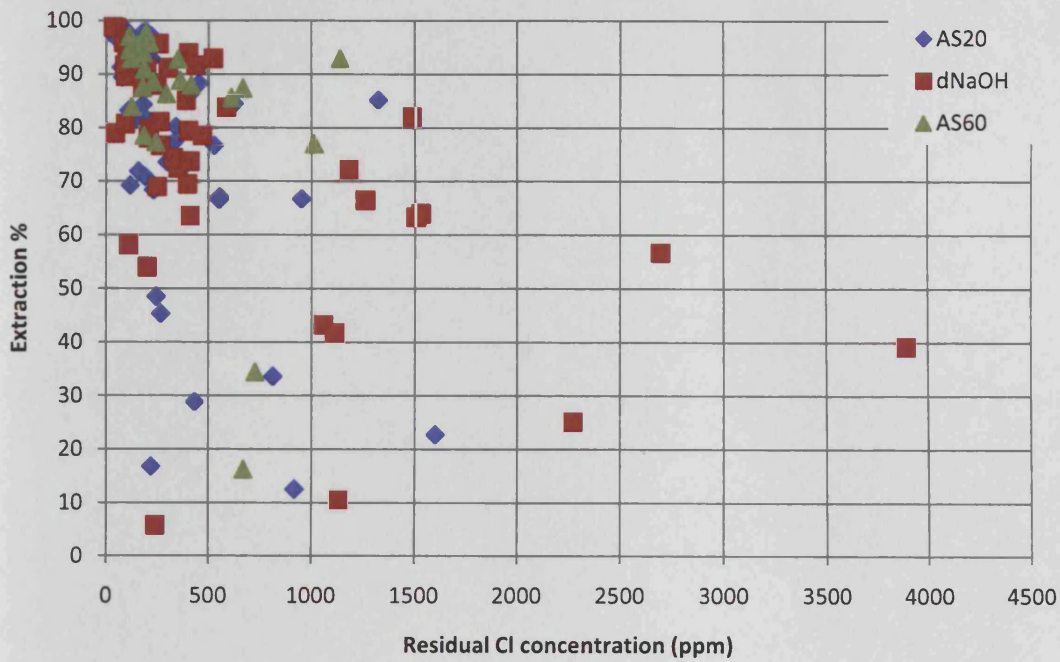


Figure 21: Scatter graph of extraction % and residual chloride, showing that there is a negative correlation between the two variables ($r = -0.486$, $r^2 = 0.2364$).

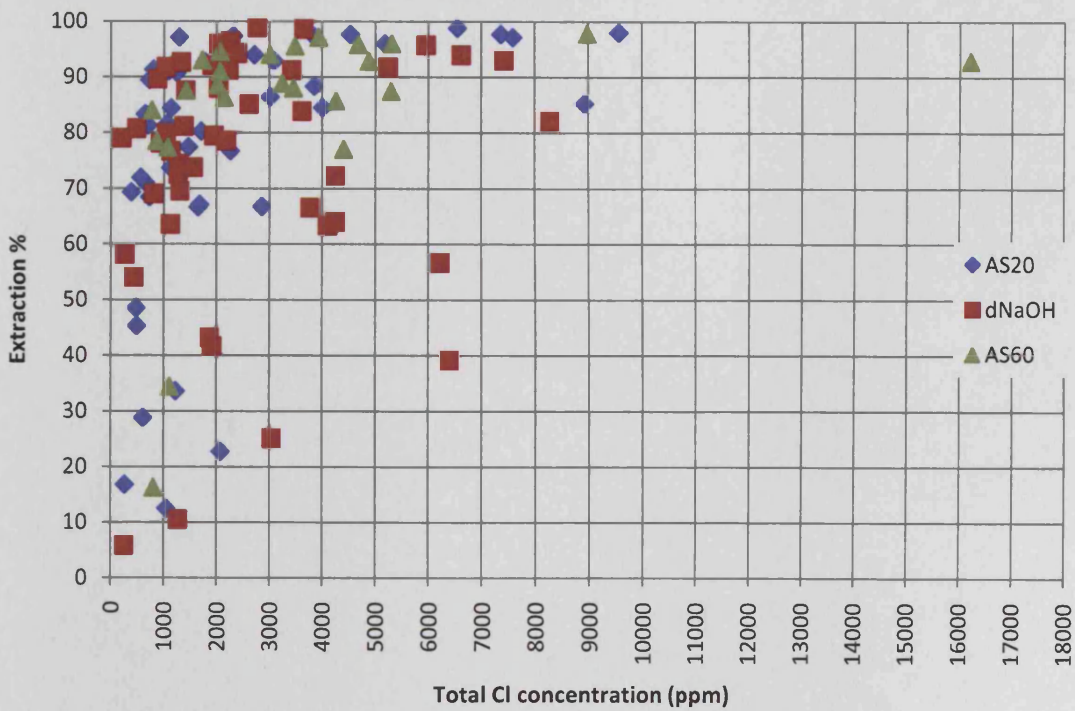


Figure 22: Scatter graph showing extraction % and total chloride. Objects with extraction % < 60 are likely to contain less than 2000 ppm total chloride ($r = 0.4597$, $r^2 = 0.2113$).

Extraction % seems to be more closely related to total chloride content, at least for low values. Figure 22 shows that the objects falling outside of the main range of extraction % from 60-99% tend to have low total chloride content, reinforcing the care needed when using extraction % alone as a guide to treatment success. Treatment may appear to be less successful for objects with low chloride levels, and since it is high chloride levels which are most detrimental to objects, it is the effect of treatment on high chloride objects which is of most concern.

Figure 23 shows that, compared to the total chloride content of objects, residual chloride content is quite small. The solid black line shows perfect extraction, i.e. 100% of the total chloride is removed (extracted chloride = total chloride). All of the treated objects fall below this line, as none had 100% extraction. The dotted line shows the boundary where residual chloride is equal to 1000 ppm, which has been suggested as a boundary value for high-risk corrosion (North & Pearson 1978a) (see section 4.5.3). Almost all the treated objects in this study fall between these two boundaries, and they do so at all total chloride contents. Only 15 out of 118 objects (13%) retain more than 1000 ppm chloride after treatment.

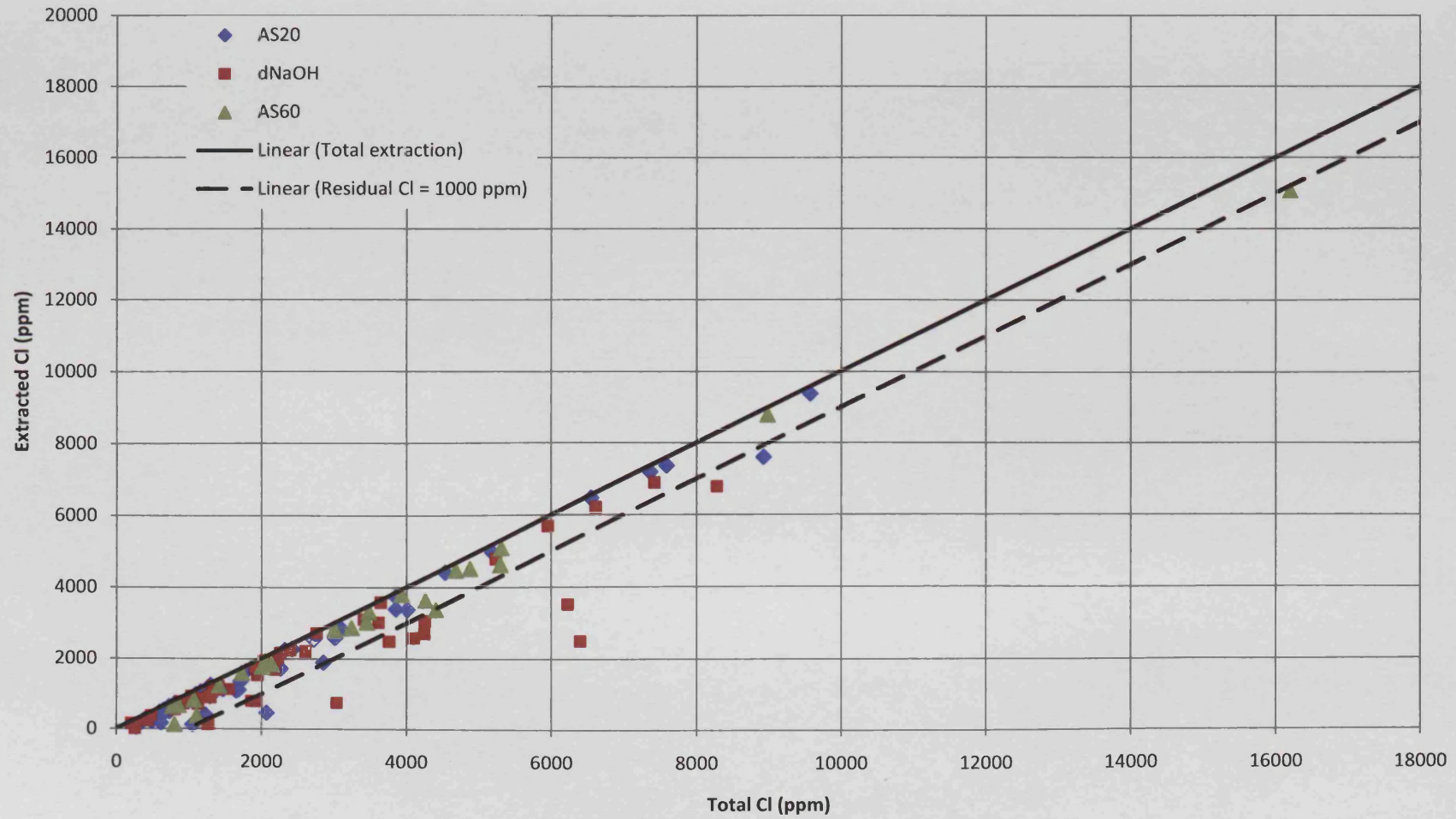


Figure 23: Scatter graph of extracted chloride and total chloride. Objects between the two lines contained less than 1000 ppm residual chloride ($r = 0.9749$, $r^2 = 0.9504$).

4.4.5 Comparison of sites

Two questions relating to the archaeological site of the objects can be examined – how big are the differences between the sites in terms of chloride ion content and extraction, and does any site have significantly better or worse extraction efficiency?

An ANOVA test was performed to compare the differences between the total chloride ion content of the objects from the three sites. This gave an F value of 25.28 ($F_{crit} = 2.70$ at .05 significance level), showing that there is more variability between the mean total chloride of the three sites than is accounted for by their internal variability. The mean total chloride of all the objects by site is given in Table 7, and this shows that it is the Bornais objects which are the source of the difference, both in mean and median. The median chloride content of Bornais objects is about three times greater than that of Billingsgate and Caerwent objects, which only have a 33 ppm difference.

Table 7: Descriptive statistics for treated objects by site origin. The data from all three treatments has been combined.

| | | Bornais (BOR) | Billingsgate (BWB83) | Caerwent (CAE) |
|---------------------------|--------|--------------------------|---------------------------------|---------------------------|
| No. of samples | | 40 | 40 | 38 |
| Extraction % | Mean | 80 | 84 | 67 |
| | Median | 86 | 89 | 77 |
| Residual Cl (ppm) | Mean | 656 | 171 | 490 |
| | Median | 359 | 152 | 361 |
| Total Cl (ppm) | Mean | 4602 | 1661 | 1803 |
| | Median | 4247 | 1389 | 1422 |
| Extracted Cl (ppm) | Mean | 3946 | 1490 | 1324 |
| | Median | 3298 | 1227 | 952 |

The different distributions of total chloride are confirmed by the histogram (Figure 24). The ranges for Billingsgate and Caerwent overlap, while Bornais objects have a larger distribution which extends to higher chloride contents. This is not a surprising difference, as the site of Bornais is located close to the sea and the soils in the area are therefore likely to contain high levels of chloride ions.

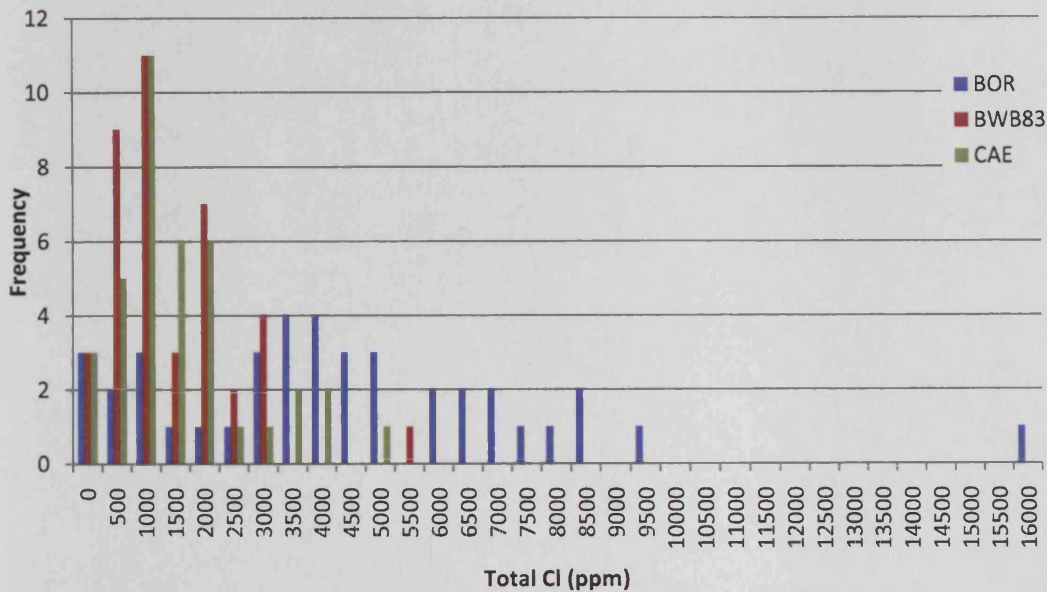


Figure 24: Histogram of total chloride of the samples from the three sites.

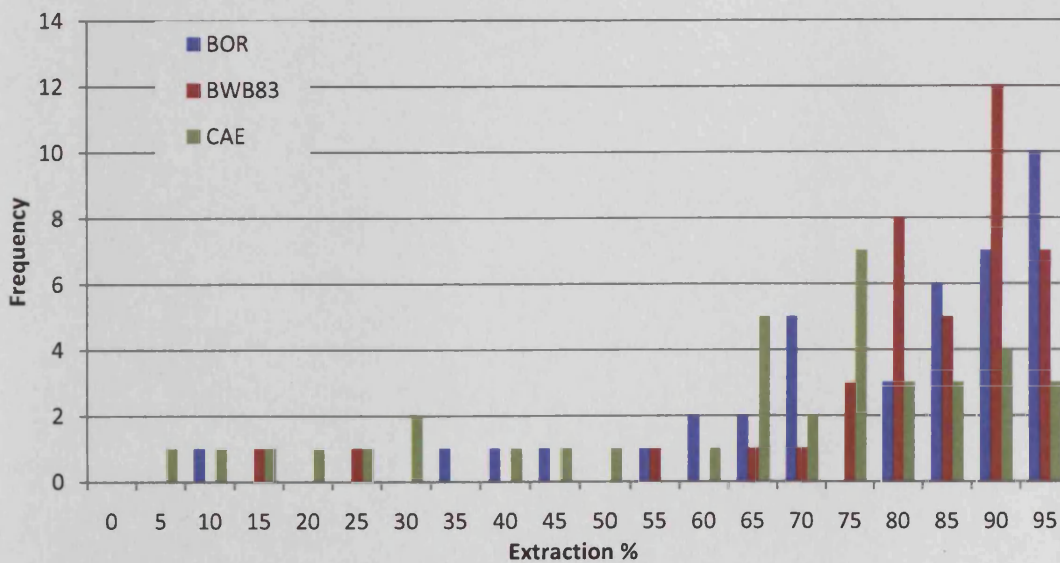


Figure 25: Histogram of extraction % of the treated objects from each site. Bin size is 5%.

Extraction % is evaluated on a site-by-site basis using data from all the treatments together, on the assumption, as discussed above, that the differences between the treatments are not statistically significant. The histogram (Figure 25) shows that Bornais and Billingsgate have more objects at higher extraction % than Caerwent, which spreads more across the range of extraction %. An ANOVA analysis shows that this difference is significant ($F = 6.745$, $F_{crit} = 3.98$ at .01 significance). Looking at the mean and median % extraction (Table 7), it is Caerwent nails which have lowest extraction % mean and median, and this is confirmed by a post-hoc Scheffé analysis, which shows that the difference in mean between Bornais and Billingsgate nails is not significant ($C = 0.82$, $C_{crit} = 2.32$ at .05 significance), but differences between Caerwent and Bornais ($C = 2.71$) and Caerwent and Billingsgate ($C = 3.52$) are.

A contributing factor to the difference between sites is that of the twelve nails that did not complete the treatment (Table 5), more than half (7) were from Caerwent. The correlation between final solution concentration and residual chloride is shown in Figure 26, and has a calculated r of 0.463 and r^2 of 0.2144. This is a statistically significant relationship ($r_{crit} = 0.2540$ at .01 significance). The scatter plot (Figure 26) shows that objects with a final solution concentration of 5 ppm or less are unlikely to have high residual chloride concentration. Above 5 ppm there is a large scatter of data, but half of the objects that did not reach the specified treatment goal of 10 ppm did have residual chloride greater than 1000 ppm. The relationship is by no means consistent however; the object with the highest residual chloride content (BOR_1696) had a final solution concentration of only 5.6 ppm. In general though, it is true that lower final solution concentrations mean that residual chloride content is likely to be low. Billingsgate objects were the least likely to have a final solution concentration of more than 5 ppm, and also have no objects with chloride content > 500 ppm.



Figure 27: CAE_16 before treatment in dNaOH. This object is thickly encrusted with soil and performed poorly during the treatment, with an extraction of only 25%.



Figure 28: CAE_34 before treatment in AS20. This object is also thickly encrusted with soil, but it had a good extraction of 84%.

A second reason for poor extraction efficiency may be a greater proportion of bound chloride in the Caerwent objects, which could not be removed by the treatment. An ANOVA test of residual chloride levels by site showed that there is a significant difference ($F = 8.92$) between the means of the three sites. Post-hoc analysis shows that the mean of Billingsgate is significantly lower; Caerwent residual chloride levels are on a par with those of Bornais objects. This is confirmed by the median (Table 7); Bornais and Caerwent objects have almost the same residual chloride median value. However, total chloride values for Bornais

are statistically higher than those of Caerwent as established earlier. The conclusion is that Caerwent nails are retaining more chloride than would otherwise be expected from their total chloride ion content, which is more similar to Billingsgate nails. As the Caerwent objects were excavated in the 1980s, there has been ample time for akaganéite formation, whereas the site of Bornais was only excavated in the early 2000s, and thus a greater proportion of the chloride present may still be in soluble form.

It is not possible to distinguish from the data presented whether the residual chloride was in a bound or soluble form. If a higher proportion of bound chloride leads to the apparently poor performance of these nails, this may not be significant for the future performance of the object in terms of corrosion, as bound chloride is not as strongly implicated in promoting corrosion as soluble chloride (Wiesner et al. 2007). The corrosion performance of treated objects is investigated in section 4.5.2.

4.4.7 Measuring treatment outcome without digestion

This study has used measured residual chloride as the basis of treatment evaluation. However, residual chloride is not typically available as a measure of treatment success, as it requires destruction of the object. A method of estimating residual chloride without needing residual chloride data would be helpful for conservators. The colour of treatment solutions has previously been thought to correlate to chloride content (Bradley 1988), but this has been refuted (Wang et al. 2008), and no such correlation was observed here. The colour of treatment solutions tended to become lighter as the treatment proceeded regardless of the chloride concentration.

Only two of the chloride content measures used in this study are available without measuring residual chloride: total extracted chloride and the concentration of chloride in the treatment solutions, specifically the final treatment solution. Which of these provides a better indication of the residual chloride content?

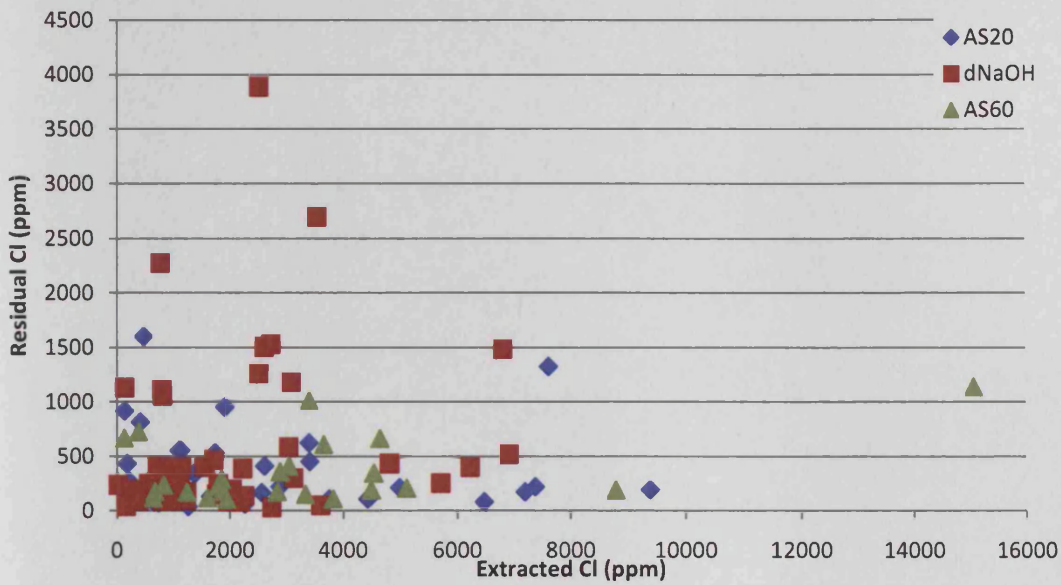


Figure 29: Scatter graph of extracted and residual chloride for the treated objects. There is no significant relationship between the two variables ($r = 0.13$, $r^2 = 0.0169$).

Figure 29 shows the correlation of extracted chloride and residual chloride. There is no obvious linear relationship between extracted chloride and residual chloride, and a low correlation coefficient of $r = 0.13$, which is not significant at .05 level ($r_{crit} = 0.1946$) confirms this. The residual chloride level in an object cannot be predicted from the extracted chloride.

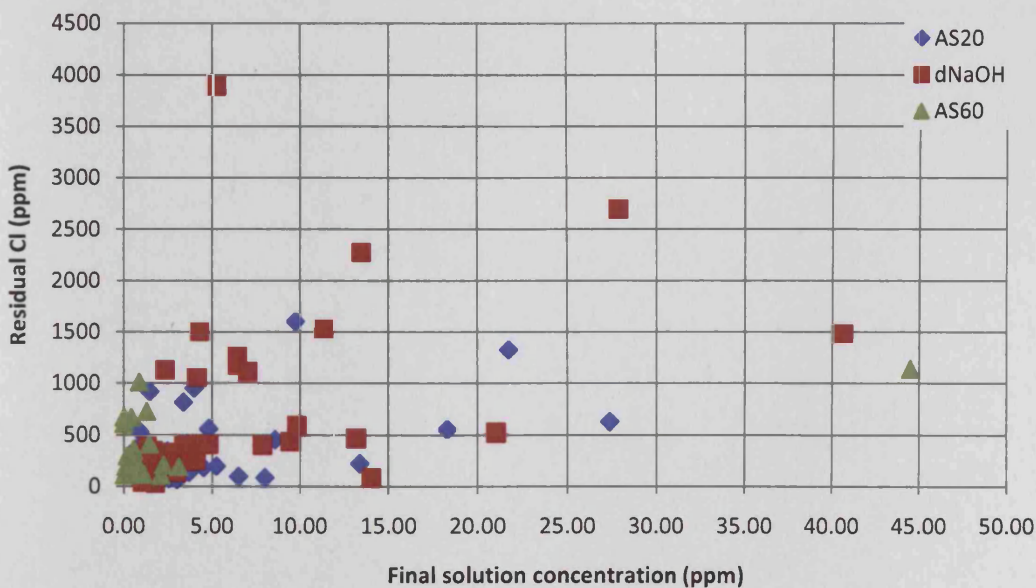


Figure 30: Scatter graph of residual chloride and final solution concentration, by treatment ($r = 0.4631$, $r^2 = 0.2144$).

Figure 30 shows that there is a correlation between final solution concentration and residual chloride content. This correlation works best in one direction only. It is possible to say from the data that achieving less than 5 ppm chloride in the final solution increases the likelihood that the object will contain chloride levels less than 500 ppm, irrespective of the total chloride content of the object. Of the 94 objects with final solution concentration < 5 ppm, only 13 (14%) had a residual chloride concentration of more than 500 ppm, and only 4 (4%) had a residual chloride content of > 1000 ppm. Measuring the final solution concentration and continuing the treatment until the concentration is less than 5 ppm offers a reasonably high probability (86%) that residual chloride levels will be less than 1000 ppm. The opposite statement, that high concentration in the final solution results in high residual chloride levels, is less well supported by the data, as the scatter is considerable. Therefore, conservators wishing to estimate residual chloride content of a treated object should use the final solution concentration as a guide. Although the correlation is not perfect and subject to significant error at high levels of final solution concentration, continuing treatment until the final solution concentration is less than 5 ppm is likely to mean low residual chloride levels.

4.5 Evaluating treatment outcome

Assessing the effect of desalination treatment on the corrosion of iron objects has always been difficult. It requires knowledge of pre and post-treatment chloride content and the long-term response of treated and untreated objects to specific environmental conditions. Residual chloride is helpful but does not give any direct information about the long-term stability of objects. Any object containing akaganéite or other chloride-bearing corrosion products will contain some residual chloride, but this may not pose a significant threat to the future stability of the object.

Two methods were used to evaluate the effects of the desalination treatment on the objects. Scanning electron microscopy, coupled with energy-dispersive spectroscopy (SEM-EDX) was used for detailed analysis of cross-sections of treated and untreated nails. This provided micro-scale assessment of the location of chloride within the corrosion structure. Larger numbers of objects, both treated and untreated, were subjected to accelerated corrosion testing for several weeks to give an indication of the effect of removing chloride

ions on the corrosion of objects. Both methods will contribute to understanding the impact that treatment has on the stability of iron objects.

4.5.1 Analysis of sample cross-sections

4.5.1.1 Sample selection

Of the eighteen halved nails treated in nitrogen-deoxygenated sodium hydroxide (dNaOH) and room temperature alkaline sulphite (AS20), four were selected for SEM-EDX analysis (Table 8). Those with the highest extracted chloride from each site and treatment were chosen which would be most likely to provide detectable contrasts between the treated and untreated halves. At the time the analysis was undertaken, there was no information on residual chloride levels of objects, but the data is included in Table 8 for reference.

As chloride ions are very soluble in water, no aqueous lubricants could be used during sample preparation for SEM-EDX analysis. A small transverse section was cut from each sample using an Isomet diamond saw and an oil-based lubricant (Buehler ISOCUT), and set in epoxy resin, such that the inner, freshly cut face of the sample could be analysed. The surface was ground and polished down to a finish of 1 μm using white spirit as the lubricating agent. A few drops of Industrial Methylated Spirits (IMS) were used to clean the sample surface of any white spirit residues after polishing (see Appendix 2.2.1 for further details). The samples were then carbon-coated.

SEM-EDX analysis was carried out at The British Museum (Department of Conservation and Scientific Research) using a Hitachi S-4800 field-emission scanning electron microscope equipped with energy dispersive X-ray spectrometry (EDX), running at an accelerating voltage of 20 kV (see Appendix 2.2.2). Both spot identification and area mapping were used to locate and map elements, from a magnification of x60 up to x4500. The detection limit for chlorine (Cl) is c. 0.2%, and the relative precision is 10% in the concentration range 5-20%, deteriorating as the detection limit is approached. The mapping resolution is 512x416 pixels.

Table 8: Samples of archaeological iron examined by SEM-EDX. Extracted chloride during treatment and chloride content as determined by digestion are given.

| Sample | Treatment used | Chloride removed relative to the weight of nail (ppm) | Residual chloride content of the nail (ppm) |
|------------|----------------|---|---|
| BOR_1693.1 | dNaOH | 2029 | 195 |
| BOR_1693.2 | Untreated | - | 1388 |
| BWB83_44.1 | AS20 | 2255 | 61 |
| BWB83_44.2 | Untreated | - | 106 |
| CAE_27.1 | dNaOH | 1709 | 467 |
| CAE_27.2 | Untreated | - | 1652 |
| CAE_45.1 | AS20 | 1902 | 950 |
| CAE_45.2 | Untreated | - | 425 |

Once chlorine-containing corrosion products were identified, Raman spectroscopy was used on the polished sections using a Jobin Yvon Infinity spectrometer with a green laser (532 nm with maximum power of 1.2 mW at the sample) to identify their form. The analysis was run with a laser power of 0.3 mW to avoid burning the corrosion products (Appendix 2.2.3). The analytical spot size was c. 5 μm in diameter. The resulting Raman spectra were identified by comparison with a British Museum in-house reference database and published data (de Faria et al. 1997; Neff et al. 2004). Due to time constraints, the analysis was restricted to a very small number of samples, and was used only to confirm the identity of some of the chlorine-containing corrosion products located by SEM analysis.

4.5.1.2 Results

Between polishing and the completion of analysis, the samples were kept in a desiccating chamber with silica gel at RH of $10\% \pm 5$ (measured using a digital sensor). Even at this low humidity, fresh corrosion appeared on some of the polished surfaces. This has been noted below where it occurred. Table 8 indicates the quantity of chloride ions extracted from the treated half of each nail and the chloride content of both the treated and untreated halves as determined by digestion of the samples from which the cross-sections were taken. This provides a rough guide to the performance of the treatment and the different chloride levels of the samples.

BOR_1693

This sample had a thin layer of corrosion products surrounding a substantial metal core. Corrosion product growths appeared on the polished surface of the untreated half of this nail, BOR_1693.2. EDX analysis showed that these new corrosion products contained chlorine, and originated in areas where chlorine-containing corrosion products were present in the structure (Figure 31). The chlorine-containing growths on the surface appear to be associated with a void in the corrosion product structure. Chlorine was also identified along the metal/corrosion interface and as a thin band along the outer edge of the sample.

BOR_1693.1, treated in dNaOH, showed no sign of fresh corrosion product growth on the surface. Although chlorine was identified in three places only low levels were found compared to the untreated half, and the residual chloride analysis showed that the treated half contained seven times less chloride than the untreated half (Table 8). The chlorine identified by EDX was not located along the metal/corrosion product interface, but within patches of corrosion product. Sodium was also picked up in low quantities in many places in the treated half, but was not seen in the untreated half. The most likely origin of sodium is the remains of the treatment solution, which was not rinsed from the objects after treatment, although it was not detected in any other treated nail. It was not possible to determine the form of sodium, but it is likely to be sodium carbonate, which occurs when sodium hydroxide reacts with carbon dioxide during drying (Watkinson & Al-Zahrani 2008).

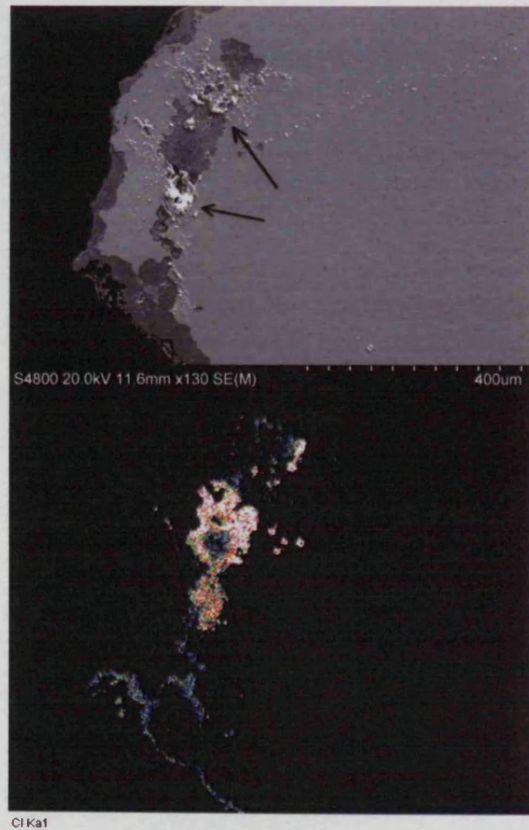


Figure 31: BOR_1693.2. SEM image (top) showing fresh corrosion on the polished surface located near cracks in the corrosion structure (arrowed). The EDX map (bottom) shows high levels of Cl in these areas. Cl is also located on the metal/corrosion interface and along the outer edge of the sample.

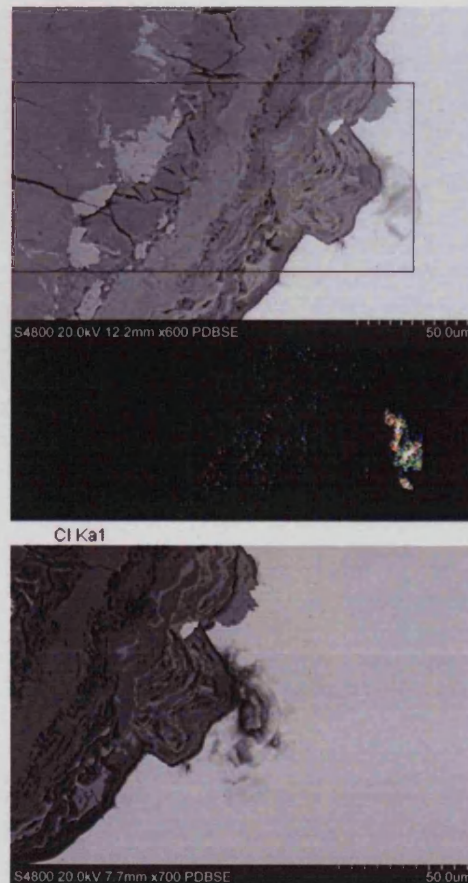


Figure 32: Figure 2: CAE_27.2. SEM image (top) and EDX map of chlorine (middle). The bottom image was taken several weeks after the top, and shows the development of Cl-containing corrosion products.

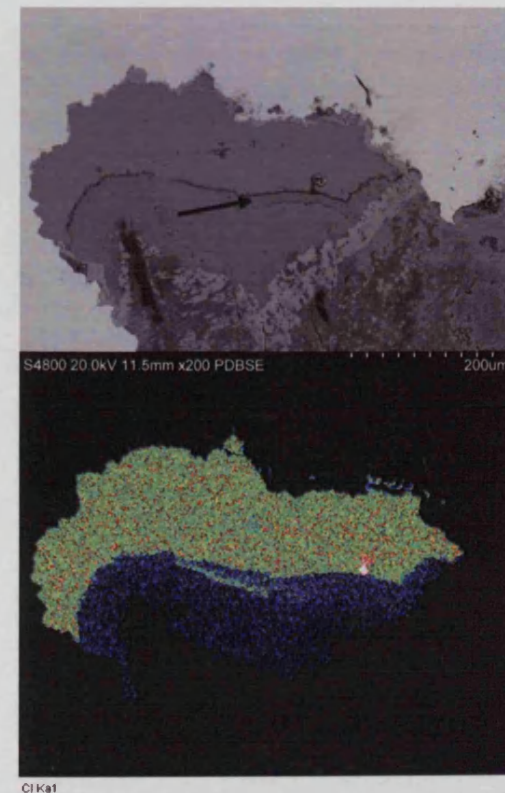


Figure 33: CAE_27.2. SEM image of an area located at the base of a deep corrosion profile. This area contained Cl in two different concentrations, as shown by the EDX map. Both were identified as β -FeOOH by Raman spectroscopy. The arrow indicates the location of the banded structure at the boundary.

CAE 27

This sample had thicker corrosion products than the other nails, particularly in one corner of the untreated half, CAE_27.2. Chlorine was located in several areas by EDX analysis. At the base of a sequence of deep corrosion products a small quantity of chlorine was found and imaged twice several weeks apart. The small patch of chlorine distribution expanded and became fresh corrosion product extending out onto the metal surface (Figure 32), similar to that found on BOR_1693.2 (Figure 31). In another area, a patch of corrosion product was located, also deep in the corrosion structure and located next to the metal/corrosion interface. When mapped, it was found that this area contained corrosion products with two different concentrations of chlorine (Figure 33). There was a sharp interface between the two areas of corrosion product, with a banded structure (arrowed in Figure 33) suggesting that the front may have moved over time. Small patches of fresh corrosion products grew on this sample over a period of weeks, containing very high levels of chlorine.

Raman analysis was carried out on the chlorine-containing areas shown in Figure 33, and on the fresh corrosion products formed on the surface. The two areas in Figure 33 were both identified as akaganéite (β -FeOOH) (Figure 34). The analysis of the fresh corrosion products on the surface produced a spectrum with a broad peak at 710 cm^{-1} , suggesting that these corrosion products are an unknown and perhaps amorphous form of iron hydroxide or oxyhydroxide (Wang 2007b).

CAE_27.1, treated in dNaOH, was not found to contain chlorine in the sampled areas, except in one area, where spot analysis located chlorine in a deep pit associated with a slag inclusion (Figure 35). There was no new corrosion product growth, and no areas where chlorine was found within the corrosion structure. Residual chloride analysis showed that the treated sample contained less than 500 ppm chloride ions, three times less than the untreated half.

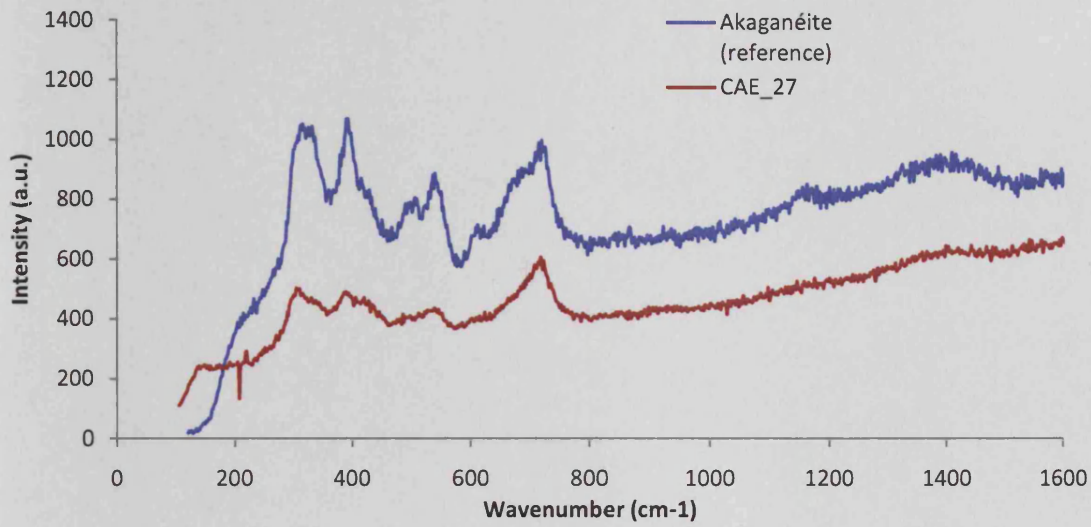


Figure 34: Raman spectrum of the chlorine-containing corrosion product shown in Figure 33. When compared with the reference spectrum, the product is identified as akaganéite.

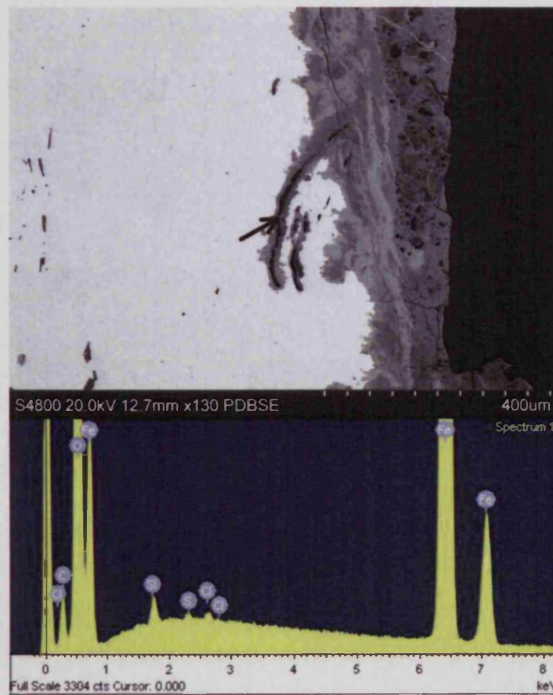


Figure 35: CAE_27.1. Backscattered electron image (top) and EDX spectrum (bottom), showing chlorine present in very small quantity in slag inclusions (analysis location indicated by arrow).

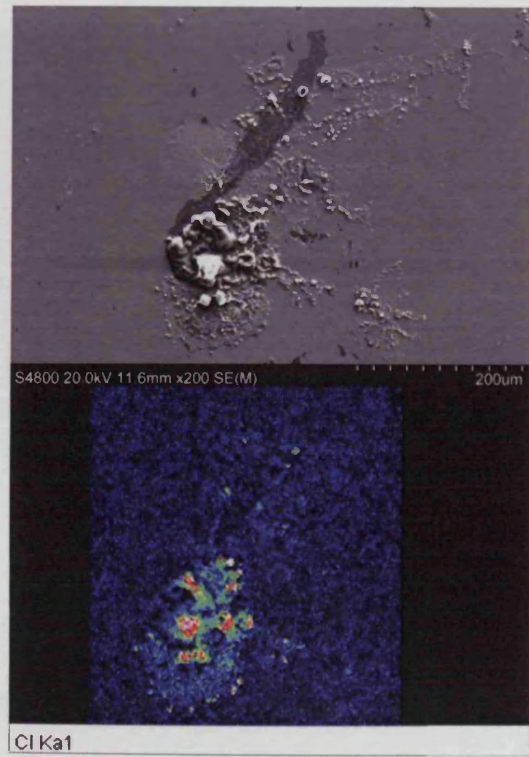


Figure 36: CAE_45.1. Backscattered electron image (top) and EDX map for chlorine (bottom) of a treated nail, showing fresh surface corrosion caused by chlorine located around internal slag inclusions.

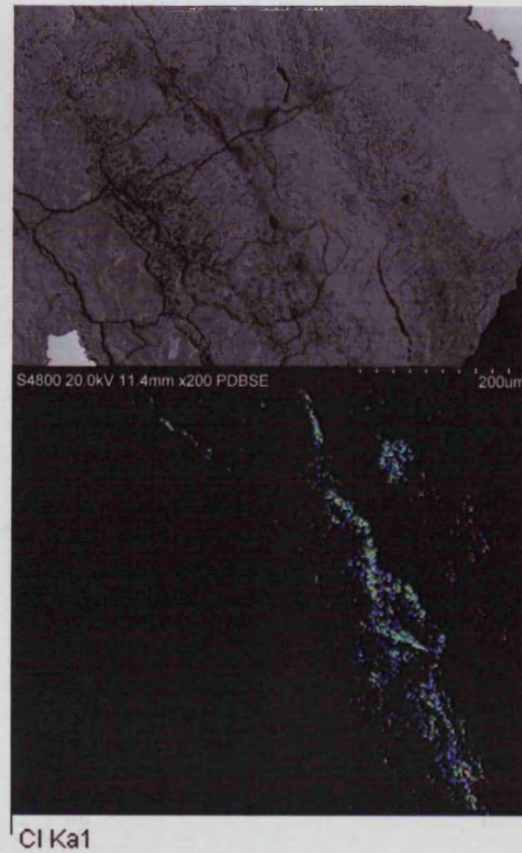


Figure 37: BWB83_44.1. Backscattered electron image (top) and EDX map for chlorine (bottom) of the treated nail. Low levels of chlorine were located within the corrosion structure, but there were no associated fresh corrosion growths.

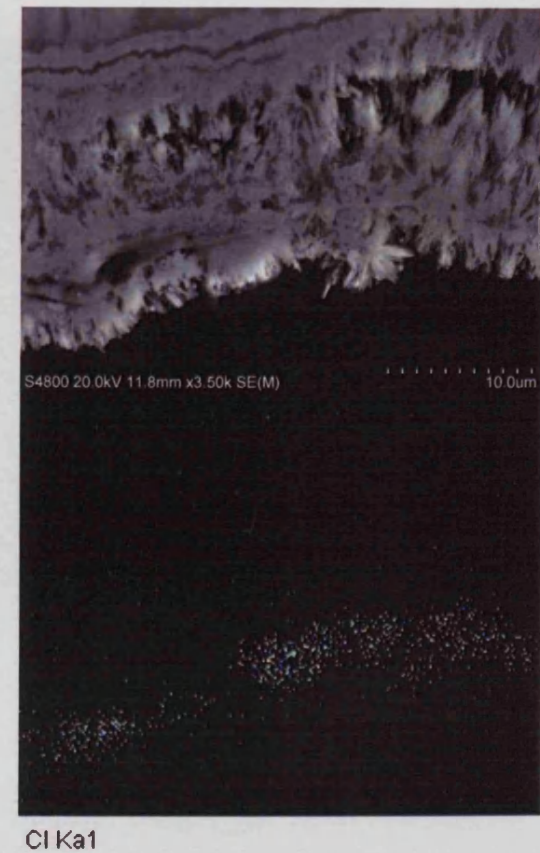


Figure 38: BWB83_44.2. Secondary electron image (top) and EDX map for chlorine (bottom), showing a band of crystals containing chlorine on the edge of the sample.

CAE 45

The untreated half of this nail, CAE_45.2, showed significant development of fresh corrosion products on the polished surface similar to those in Figure 31. Under magnification, this was found to be distributed both at the metal/corrosion interface and around slag inclusions in the centre of the metal. Chlorine-containing corrosion products were associated with these slag inclusions, and fresh corrosion had also formed near cracks in the corrosion products. Chlorine-containing corrosion products and fresh corrosion growths were also found near the outer edge of the sample.

In the treated sample, CAE_45.1 (AS20), fresh corrosion had occurred on the polished surface near internal slag inclusions (Figure 36), similar to those in the untreated half. EDX analysis showed that the corrosion products associated with the slag inclusions contained high levels of chlorine, as did the fresh corrosion on the surface. The metal/corrosion interface and the outer layer of corrosion products were free of chlorine, and no fresh corrosion products formed here. This suggests that the treatment was effective in the outer layers of corrosion and on the metal/corrosion interface, but could not access chloride ions in the internal structure surrounded by metal. Residual chloride analysis confirmed that this sample contained significant amounts of chloride ions even after desalination treatment (Table 8).

BWB83 44

This nail showed thin and coherent corrosion products around a substantial metal core. BWB83_44.2 was the only untreated sample not to display fresh corrosion product growth on the surface. Although small quantities of chlorine were found as part of corrosion products in the structure of the nail, no areas with high chlorine or renewed corrosion could be identified. Residual chloride analysis subsequently showed that this sample contained only very low chloride levels (Table 8).

BWB83_44.1, treated in AS20, showed no fresh surface corrosion products. Areas of chlorine-containing corrosion product were found, but none showed any renewed corrosion or growth of new corrosion products, and all were located away from the metal/corrosion interface (Figure 37). Chlorine was also identified on the outermost edge of the cross-

section. When imaged at x4500, a very thin band about 1-2 μm thick of blade-like crystals containing chlorine was located at the very edge of the sample (Figure 38). The corrosion products below this band contained very little chlorine. This thin band was also seen in BOR_1693.1, BOR_1693.2 (Figure 31) and CAE_27.2. An attempt was made to identify the crystal structure using Raman spectroscopy, but the resin interfered with measurements at the very edge of the sample and prevented a spectrum from being acquired.

4.5.1.3 Discussion

SEM-EDX analysis was able to identify chlorine in both treated and untreated nails, and showed clear differences between treated and untreated samples. All but one of the untreated samples developed fresh corrosion products on the polished surface, which contained high levels of chlorine. Their formation on the untreated surface suggests that there were free chloride ions in the structure of the corrosion products, which on contact with oxygen formed corrosion products. This may be similar to the process that leads to 'weeping' on iron objects, where an acidic solution of iron and chloride ions dries and reacts with oxygen to form bubbles or shells of akaganéite (Selwyn et al. 1999). The same phenomenon was observed by Reguer et al. (2007a) and attributed to the drying of the pore solution containing chloride ions. This explains why it occurred during storage at low RH. The fresh products were found near cracks in the structure or at the interface between the metal and the corrosion products, both areas where iron and chloride ion-containing solutions are likely to be present in an actively corroding object.

By contrast, none of the treated objects showed this substantial development of fresh corrosion, and in general the polished surfaces did not undergo alteration. The exception was in the treated half of CAE_45, where fresh corrosion did develop near internal slag inclusions and their associated corrosion products. It is likely that the treatment solution was not able to penetrate into these areas, which are deep inside the object and surrounded by very dense metal. This suggests a reason why objects may re-corrode after treatment; if chloride ions remain deep in the structure where the treatment cannot access, they can then act as a catalyst for further corrosion at a later date. In this case, the structure of the metal may play an important role in how effective a treatment can be; iron with a large number of slag inclusions may be more susceptible to recurring corrosion from deep within the structure than iron that has few slag inclusions. Chlorine was also still

present in low levels in the outer corrosion layers, presumably as part of chlorine-containing corrosion products such as akaganéite, although adsorption onto goethite is also possible (Turgoose 1982b; Al-Zahrani 1999). However, as there was no fresh development of corrosion products in these areas, and the levels were very low, this does not appear to pose the same level of risk as the chloride in untreated samples.

Although desalination treatment may not remove chloride ions in sealed areas such as slag inclusions as observed in this study, it seems to have been successful in removing chloride present at the metal/corrosion interface and free chloride ions present in cracks in the corrosion structure. The SEM data and the behaviour of the polished samples suggest that desalination treatment significantly reduces the risk of new corrosion occurring, even if some chloride remains in the structure of the corrosion products. In the majority of cases, reducing the concentration of chloride ions and removing them from the metal/corrosion interface made a clear difference to the object's vulnerability to fresh corrosion.

4.5.1.4 Conclusion

The analysis of treated and untreated cross-sections of iron objects using SEM-EDX analysis was an effective method of assessing treated and untreated iron objects, although a larger sample number would have provided confirmation of the points made above. The formation of fresh corrosion products on nearly all the untreated samples, compared to almost none of the treated samples, showed that treatment has a positive impact on the stability of iron. The method could be expanded to gain insight about the specific action of treatment solutions. It could be used to locate areas of chlorine and akaganéite in the structure of untreated samples as demonstrated in this study. The sections could then be treated in desalination solutions and then reanalysed, allowing a direct comparison of the same areas to note any change. SEM-EDX analysis could also shed light on the effect of treatments on corrosion product structure, its coherence and porosity, issues that have rarely been analysed in detail. This was not attempted in this small study due to time pressure and the limited number of samples, and would also need to be carried out on the same sample before and after treatment.

Although SEM-EDX analysis is limited to elemental analysis of the corrosion products, the changed distribution and concentration of chlorine in the treated and untreated sections

has provided an insight into the effects and limitations of desalination treatment. It has also indicated how the corrosion behaviour of iron objects may be altered by desalination treatment, but with so few samples no firm conclusions can be drawn about the overall behaviour of chloride-contaminated objects before and after treatment. Therefore, further assessment of the corrosion behaviour of whole objects is required.

4.5.2 Accelerated corrosion testing

4.5.2.1 Post-treatment assessment – a problem

Assessing how well a treatment has worked involves more than an understanding of extraction efficiency. The behaviour of objects after treatment, their corrosion rate and susceptibility to RH changes is the most important measure of whether a treatment has positively influenced an object's lifespan. Direct measurement of object corrosion rates has never been carried out on a large scale, and this lack of information hinders a full evaluation of treatment benefits.

The length of time required to measure corrosion is the most important reason why corrosion rate measurements on objects have not been attempted. Even for objects with high chloride levels that corrode relatively rapidly, the actual rate may still be quite low. It may take months or years to observe enough change to determine the differences between treated and untreated objects. Measuring the corrosion rate of a large enough sample of objects covering a range of chloride levels and treatment patterns would take several years at the least, and require constant monitoring of RH and temperature conditions and a reliable corrosion rate measurement method. Very few research projects are able to carry out measurements on large groups of objects over such a long period of time. In this study, time was an important limiting factor, and long-term studies under ambient conditions could not be considered as an option.

To facilitate assessments of corrosion rate over a shorter period of time, enhanced RH conditions were tested as a way of increasing corrosion rate enough to measure over a time-scale of weeks to months rather than years. Temperature was not increased, to see if it was possible to measure corrosion rates using only high RH as a reaction accelerant. Weight gain was used as an indirect measurement of corrosion rate. As objects corrode, they pick

up oxygen and moisture from the air and incorporate it into the corrosion products, increasing the weight of the object.

Many materials also hydrate and dehydrate, adsorbing surface water depending on their hygroscopicity. This hydration/dehydration occurs constantly as RH changes. In order to separate out the effects of hydration of objects from the weight gain from corrosion, a fixed weight baseline had to be established at a stable RH.

Objects were desiccated using a large quantity of dry silica gel until the weight was stable. This was assumed to have dehydrated the object completely, and took about three weeks. An object was then placed in the climate chamber (Vötsch VC4018, see Appendix 1.5) and the RH increased to 75% (20°C). Weight was measured continuously for a period of five weeks. Over this time, total weight gain was 0.016 g for an object weighing 17.5 g, or less than 0.1% weight gain. On subsequent desiccation, it was found that all the weight gain was attributable to hydration of the object. In fact, the object lost further weight, indicating that the object had not been fully dehydrated to begin with.

This test showed two problems: first, the difficulty of dehydrating objects to a stable weight, even with completely dry silica gel and over several weeks. It would be possible to overcome the hydration effect by hydrating objects to a set RH in the chamber before the beginning of the test, and then returning to this humidity at the end of the corrosion test, using the dynamic balance to assess when the weight is stable and calculating the difference. However, the tested object showed no sign of corrosion over the time of the test. For corrosion to be detected by this method, very long test times would be needed, at least several months per object. The climate chamber and balance used to monitor weight gain can only measure corrosion rate for one object at a time, so this method of measuring corrosion was unfeasible for this study.

Corrosion reactions use up oxygen, so that in a sealed vessel, the consumption of oxygen is also an indication of corrosion rate. A method of measuring corrosion via oxygen concentration was trialled using gas sensing equipment (Gas Sensor Solutions 450 oxygen analyser). A ruthenium complex sensor, whose fluorescence under LED illumination is quenched by the presence of oxygen, is enclosed with the object in a sealed container and used to measure oxygen concentration over time. Boiling tubes with ground glass stoppers

and silicon grease were used, and the RH controlled to $50\% \pm 5$ using conditioned silica gel. Two tubes were flushed with nitrogen gas before sealing as controls to check whether the seals held. 10 untreated objects were tested, but no drop in oxygen levels could be detected within three weeks. Although this method has been successful elsewhere (Thickett et al. 2008), it was therefore not suitable for this study. The fact that untreated objects did not corrode detectably under the conditions of the test (50% RH and 20°C) shows that at room temperature, all corrosion reactions are likely to be slow.

As neither method produced detectable corrosion at room temperature within an acceptable time period, a study at high temperature was necessary to evaluate corrosion behaviour. Increasing temperature speeds up reaction rates significantly and should allow detectable corrosion within a short period of time. However, it is not possible to extrapolate from the behaviour of archaeological iron objects at high temperature to real time reaction rates. This is a significant drawback of accelerated studies.

A study under accelerating conditions could, however, indicate the relative differences between treated and untreated iron objects and evaluate them with regard to chloride content. If all the objects are aged under the same conditions, their behaviour can be compared, and with a large enough sample, general trends determined. Although this provides no guidance for how the actual lifespan of an object is affected by treatment, it would be possible to assess the extent to which extracting chloride ions reduced the susceptibility of the objects to corrosion under accelerated conditions. With so little information on this subject, it was important to obtain some information on the relative relationship of chloride levels of untreated and treated objects to observed corrosion under the conditions of the test.

4.5.2.2 Accelerated corrosion testing method

Given that no extrapolation to real-time conditions is possible, both temperature and RH were increased substantially to produce the maximum amount of corrosion within the time available. 75°C and 75% RH were chosen as the test conditions, using a temperature and humidity controlled oven to carry out the test. 75% RH was used as ferrous chloride within the objects would become liquid through deliquescence and promote the most aggressive types of corrosion. Adsorbed surface chloride on akaganéite would also attract significant

water and promote corrosion under these conditions. Objects containing only bound chloride in the structure of akaganéite should be easily distinguished. 75°C was chosen as a high enough temperature to accelerate corrosion reactions significantly, without altering the corrosion products or straining the capabilities of the equipment available.

To measure the corrosion rate indirectly, the objects were weighed at regular intervals, but removing them from the high RH of the accelerated corrosion test would also change the weight of the object through hydration/dehydration, depending on the ambient conditions. The RH in the laboratory space could not be controlled. To overcome this problem, objects were allowed to acclimatise to the ambient RH for 24 hours after removal from the oven before the weight was measured. By treating all the objects the same way for each measurement the relative fluctuations of RH should be distinguishable from the linear increase in weight due to corrosion, although very low weight increases from corrosion may not be detectable due to the uncertainty deriving from this method. Ambient RH was recorded using a Hanwell sensor (RH $\pm 2\%$).

Nine objects from the two room temperature desalination treatments were available for accelerated corrosion testing, along with the treated and untreated cut halves of nails, and several untreated objects; a total of 62 objects. (One of the cut nails, CAE_29, was donated to another study and was not available for this test.) The test took place over 63 days at 75°C ± 0.5 and 75% ± 3 RH in a Sanyo-Gallenkamp temperature/humidity controlled oven (model BR185H/RO). Objects were weighed before the test and at weekly or fortnightly intervals on a Sartorius A200s analytical balance (± 0.0001 g). Weight gain was calculated as a % of the initial weight of the object before the test. The effects of the accelerated corrosion were also recorded photographically. After the accelerated corrosion test was completed, the objects were digested in nitric acid according to the same method given in Appendix 1.4 and residual chloride content measured.

4.5.2.3 Results

The 62 objects subjected to accelerated corrosion conditions are divided into groups for discussion. Whole treated and untreated nails are discussed first followed by the halved nails from dNaOH and AS20. Data is given in Table 9.

Table 9: Data for objects subjected to accelerated corrosion testing. Weight gain at the end of the test is given as % of weight of object, and chloride content was determined by digestion. Final solution concentration for the treated objects is also given.

| AS20 | | | | dNaOH | | | | Untreated | | |
|------------|--------------------------|------------------------|----------------------------|------------|--------------------------|------------------------|----------------------------|------------|--------------------------|------------------------|
| Object | % Weight gain at 63 days | Chloride content (ppm) | Final solution conc. (ppm) | Object | % Weight gain at 63 days | Chloride content (ppm) | Final solution conc. (ppm) | Object | % Weight gain at 63 days | Chloride content (ppm) |
| BOR_2975 | -0.21 | 219 | 13.36 | BOR_1702 | -0.20 | 388 | 1.29 | BOR_1848 | 1.06 | 980 |
| BOR_6109 | -0.41 | 410 | 3.55 | BOR_6287 | 1.81 | 435 | 9.42 | BOR_2021 | 4.43 | 2968 |
| BOR_6750 | -0.06 | 108 | 1.87 | BOR_6472 | 0.36 | 399 | 7.84 | BOR_5615 | 3.89 | 1717 |
| BWB83_33 | -0.16 | 37 | 1.81 | BWB83_16 | -0.45 | 209 | 1.20 | BOR_6151 | 4.35 | 3509 |
| BWB83_35 | -0.14 | 139 | 0.95 | BWB83_20 | 0.21 | 82 | 14.01 | BWB83_46 | 2.50 | 1461 |
| BWB83_39 | 0.00 | 165 | 1.71 | BWB83_27 | -0.02 | 300 | 1.05 | CAE_46 | 1.52 | 950 |
| CAE_34 | 2.52 | 622 | 27.35 | CAE_17 | -0.69 | 198 | 1.28 | CAE_47 | 1.63 | 1245 |
| CAE_36 | 0.70 | 451 | 8.57 | CAE_18 | -0.08 | 244 | 3.71 | CAE_48 | 16.01 | 1019 |
| CAE_41 | -0.65 | 527 | 0.87 | CAE_24 | -0.22 | 263 | 2.95 | BOR_1692.2 | 0.24 | 223 |
| BOR_1698.1 | -0.11 | 158 | 0.61 | BOR_1692.1 | -0.06 | 92 | 1.50 | BOR_1693.2 | 2.01 | 1388 |
| BOR_1708.1 | -0.04 | 266 | 0.82 | BOR_1693.1 | -0.11 | 195 | 1.53 | BOR_1684.2 | -0.04 | 466 |
| BOR_2706.1 | -0.07 | 191 | 0.46 | BOR_1684.1 | -0.20 | 347 | 1.64 | BWB83_19.2 | -0.57 | 99 |
| BWB83_30.1 | -0.01 | 110 | 1.65 | BWB83_19.1 | -0.19 | 97 | 0.94 | BWB83_24.2 | -0.13 | 565 |
| BWB83_38.1 | -0.03 | 77 | 1.19 | BWB83_24.1 | -0.07 | 80 | 1.77 | BWB83_28.2 | 0.23 | 495 |
| BWB83_44.1 | -0.14 | 61 | 2.98 | BWB83_28.1 | -0.01 | 86 | 1.41 | CAE_27.2 | 4.40 | 1652 |
| CAE_30.1 | 1.02 | 553 | 4.79 | CAE_27.1 | -0.50 | 467 | 13.17 | CAE_28.2 | 2.75 | 2507 |
| CAE_45.1 | 0.41 | 950 | 3.97 | CAE_28.1 | 4.98 | 1112 | 7.01 | BOR_1698.2 | 0.49 | 208 |
| | | | | | | | | BOR_1708.2 | 0.25 | 209 |
| | | | | | | | | BOR_2706.2 | 0.23 | 365 |
| | | | | | | | | BWB83_30.2 | 0.17 | 177 |
| | | | | | | | | BWB83_38.2 | 0.54 | 493 |
| | | | | | | | | BWB83_44.2 | -0.28 | 106 |
| | | | | | | | | CAE_30.2 | 0.19 | 1049 |
| | | | | | | | | CAE_45.2 | 2.37 | 425 |

Figures 39, 42 and 43 show the weight change of untreated objects and treated objects from dNaOH and AS20. Some objects lost weight during the accelerated corrosion test. Decreases in weight can be correlated to desorption of water from the objects due to a low ambient RH. However, some objects show a drop in weight in the first measurement (after 14 days) that does not correlate to a drop in RH; in fact, the RH increased between the pre-test weight and the first measurement. The most likely reason is that the objects were not all acclimatised to the ambient RH before the pre-test measurement. Some objects were stored in polyethylene bags within a cardboard box in a closed cupboard, and so the storage RH had not equilibrated to the very low ambient RH (30%) recorded in the room.

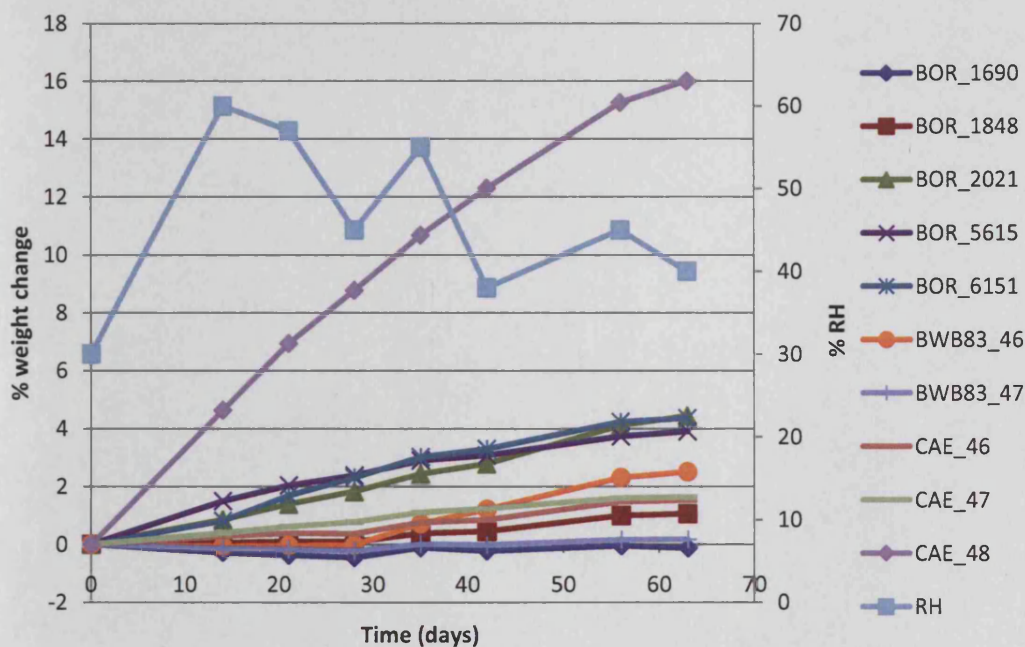


Figure 39: Results of accelerated corrosion testing for untreated objects. Ambient RH at the time of weight measurement is given on the secondary axis.

Untreated objects do not strongly reflect the changing RH conditions (Figure 39). Instead, weight increased steadily for most of the objects over the test period in a roughly linear fashion. The greatest weight change of any object tested is +16.0% of the untreated object CAE_48. The other untreated objects had weight gain ranging from -0.1 to +4.3%. Corrosion could be easily observed on these objects. Flaking and fragmentation occurred, and weeping of a dark orange/brown solution could be observed on many of the objects. Some (e.g.

BOR_6151 (Figure 40) disintegrated completely within the 63 day accelerated corrosion period. CAE_48, which had the greatest weight gain, was almost completely covered with small orange crystals, probably akaganéite, before the test, and experienced massive fragmentation and flaking over the whole object during exposure (Figure 41). BOR_1690 and BWB83_47 experienced the least weight gain (-0.13 and +0.17 respectively); the latter showed no changes, while BOR_1690 lost only a few fragments of the outer corrosion products. The lack of precision of the method makes it impossible to say conclusively whether these objects experienced corrosion during the test period. However, the majority of the untreated objects experienced catastrophic damage in the 63 day period of the test.



Figure 40: BOR_6151 before (left) and after (right) accelerated corrosion testing. This untreated object was completely fragmented during the test.

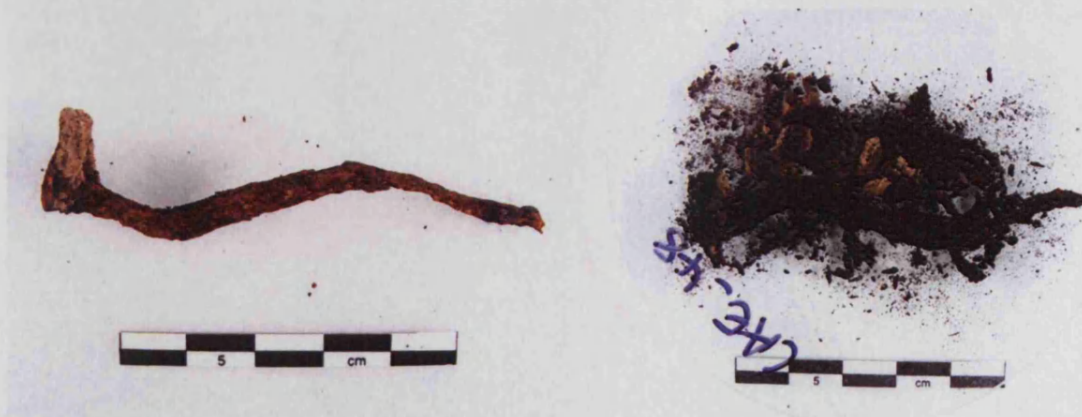


Figure 41: CAE_48 before (left) and after (right) accelerated corrosion testing.

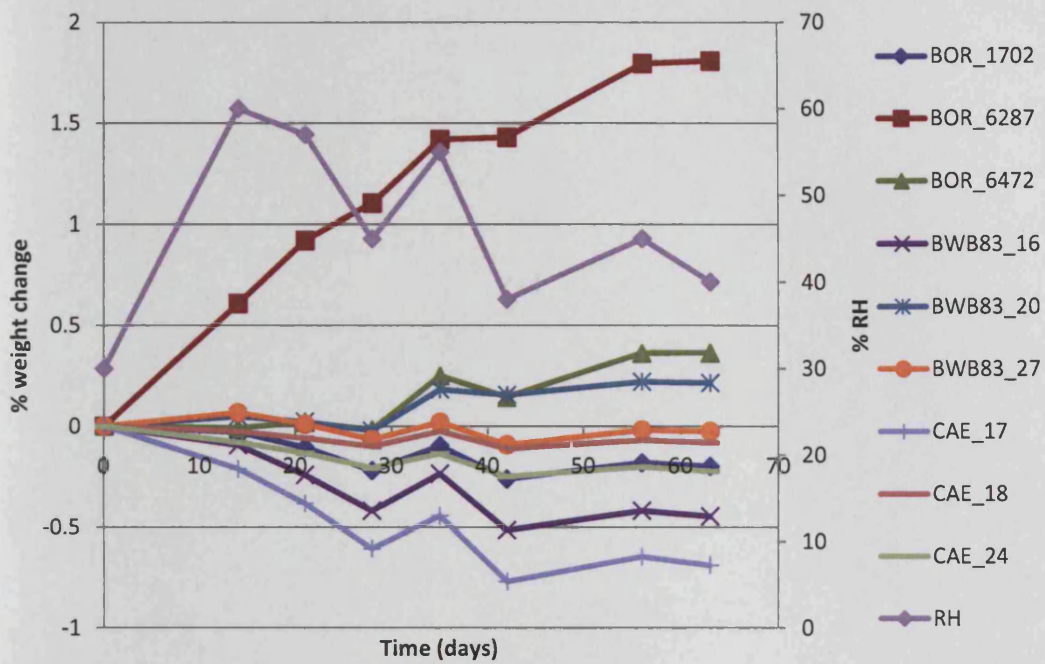


Figure 42: Results of accelerated corrosion testing for dNaOH objects. Ambient RH at the time of weight measurement is given on the secondary axis.

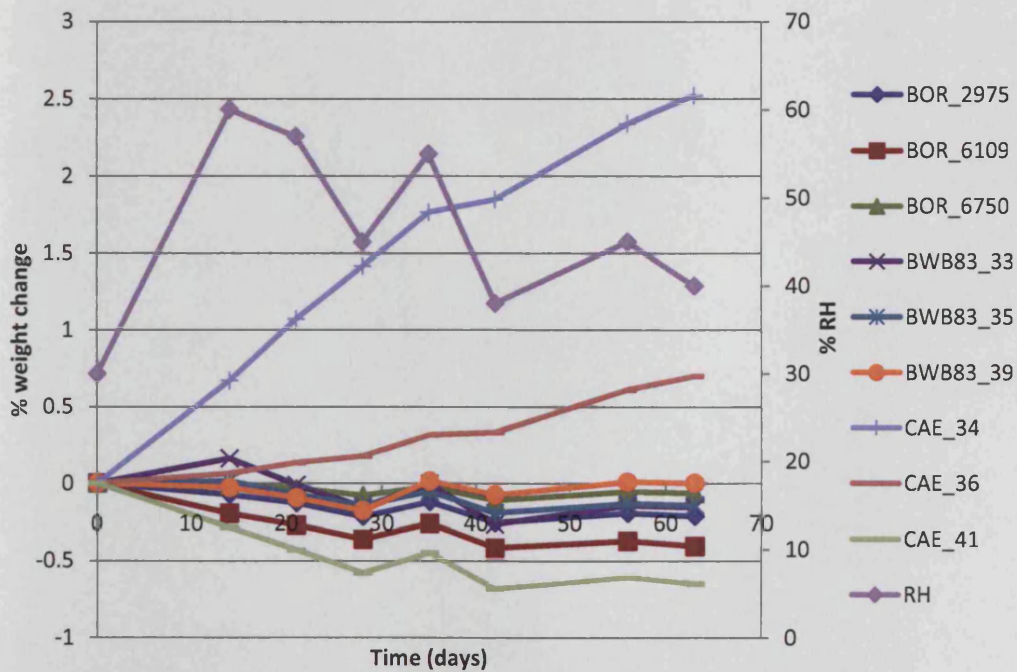


Figure 43: Results of accelerated corrosion testing for AS20 objects. Ambient RH at the time of weight measurement is given on the secondary axis.

Of the objects treated in dNaOH, only three showed positive weight change (BOR_6472, BOR_6287 and BWB83_20), ranging from +0.2 to +1.8% after 63 days (Figure 42). The other objects showed some fluctuation from humidity changes, but no overall weight gain could be detected. These objects showed no obvious visual changes during the accelerated corrosion period. Because of the uncertainty surrounding the role of humidity, corrosion of objects less than or very close to 0% change cannot be ruled out, but it is of a different order of magnitude to objects displaying clear weight gain.

AS20-treated objects also show a range of positive and negative weight change, but only two objects (CAE_34 and CAE_36) show a definite increase in weight, up to +2.5% (Figure 43). The other seven objects present only RH-linked fluctuations, and showed no visible corrosion.

The nails cut in half before treatment were also exposed to accelerated corrosion conditions. It is assumed that the corrosion morphology of the two halves is similar. It must be noted, however, that chloride concentrations of the two halves are not exactly the same. The chloride content of each half is given in Table 9. Their behaviour is discussed grouped by the three sites from which the nails came. Those with the suffix .1 were treated, those with .2 are untreated.

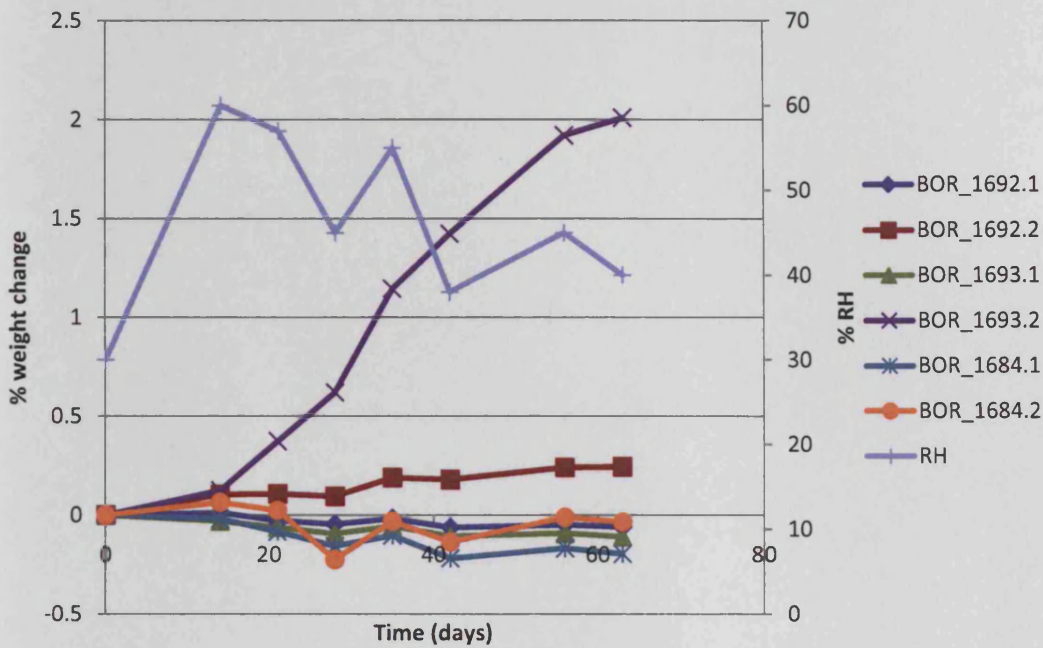


Figure 44: Results of accelerated corrosion testing for halved Bornais objects treated in dNaOH. Ambient RH at the time of weight measurement is given on the secondary axis.

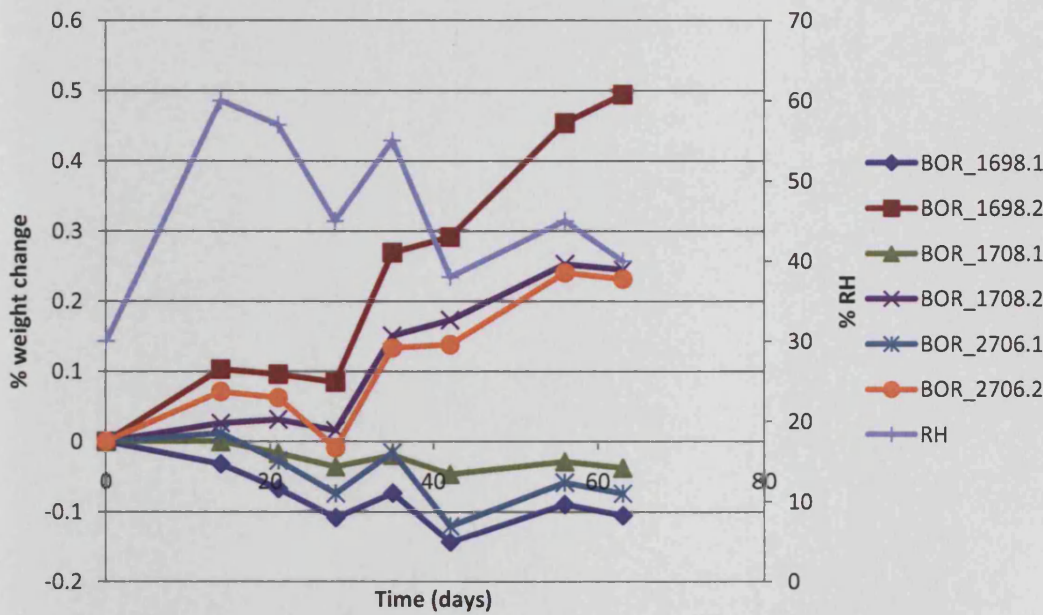


Figure 45: Results of accelerated corrosion testing for halved Bornais objects treated in AS20. Ambient RH at the time of weight measurement is given on the secondary axis.

The Bornais nails which responded to the accelerated corrosion conditions with positive weight gain were all untreated halves (Figures 44 and 45). All the treated halves had

negative weight change. The object in this group with the largest weight increase (BOR_1693.2, +2.0%, Figure 44) also had the highest chloride content, of 1388 ppm (Table 9). The other objects that exhibited positive change had chloride concentration in the range 208 – 466 ppm, which is not much different to the treated halves, which range from 92 – 359 ppm. Weight gain for the untreated halves other than BOR_1693.2 was quite low, up to +0.49% (BOR_1698.2, Figure 45), but the positive trend is easily distinguishable from the treated halves, whose weight fluctuates with ambient RH. All of the untreated halves showed visual signs of corrosion, including cracking, flaking, formation of fresh corrosion products and fragmentation of the object (Figure 46). BOR_1684.2 fragmented into pieces, despite showing no significant weight gain, underlining the imprecision of the weight gain method. None of the treated halves showed visual signs of corrosion or gained weight. Even though the residual chloride levels of treated objects are similar to those of some of the untreated halves, they show less susceptibility to corrosion under the test conditions.

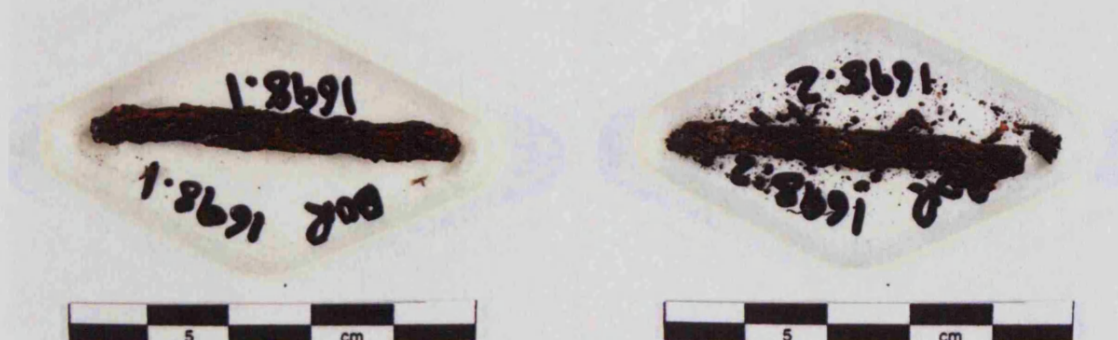


Figure 46: BOR_1698. The treated half on the left showed no change during the accelerated corrosion test, while the untreated half on the right began to fragment.

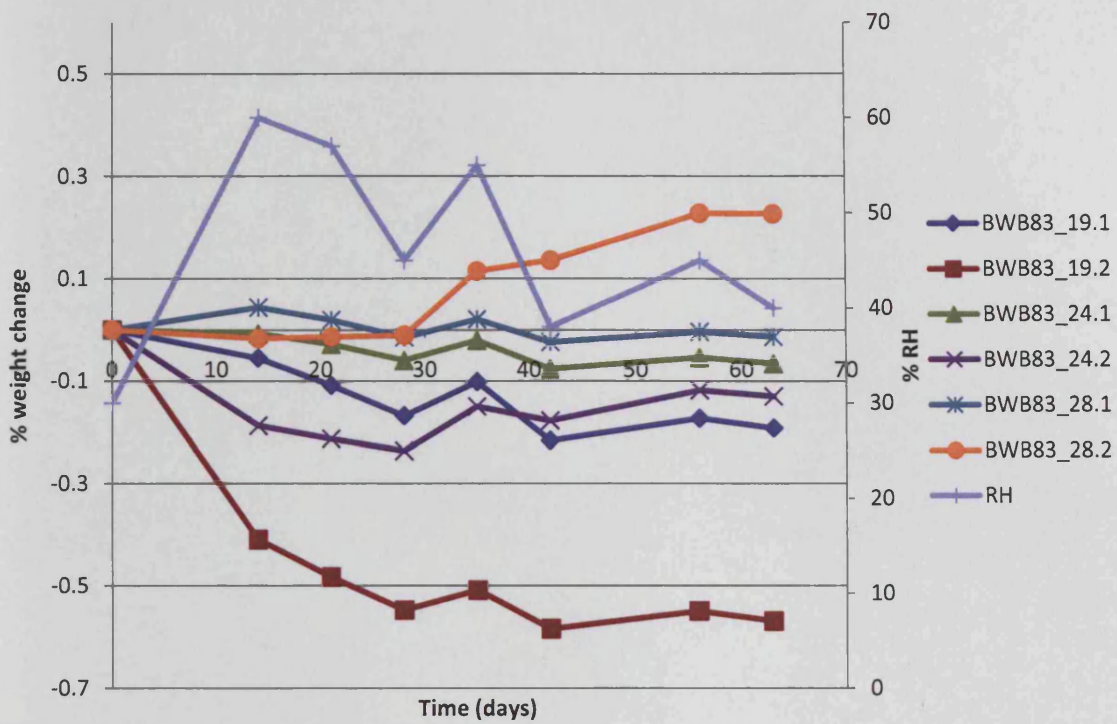


Figure 47: Results of accelerated corrosion testing for halved Billingsgate objects treated in dNaOH. Ambient RH at the time of weight measurement is given on the secondary axis.

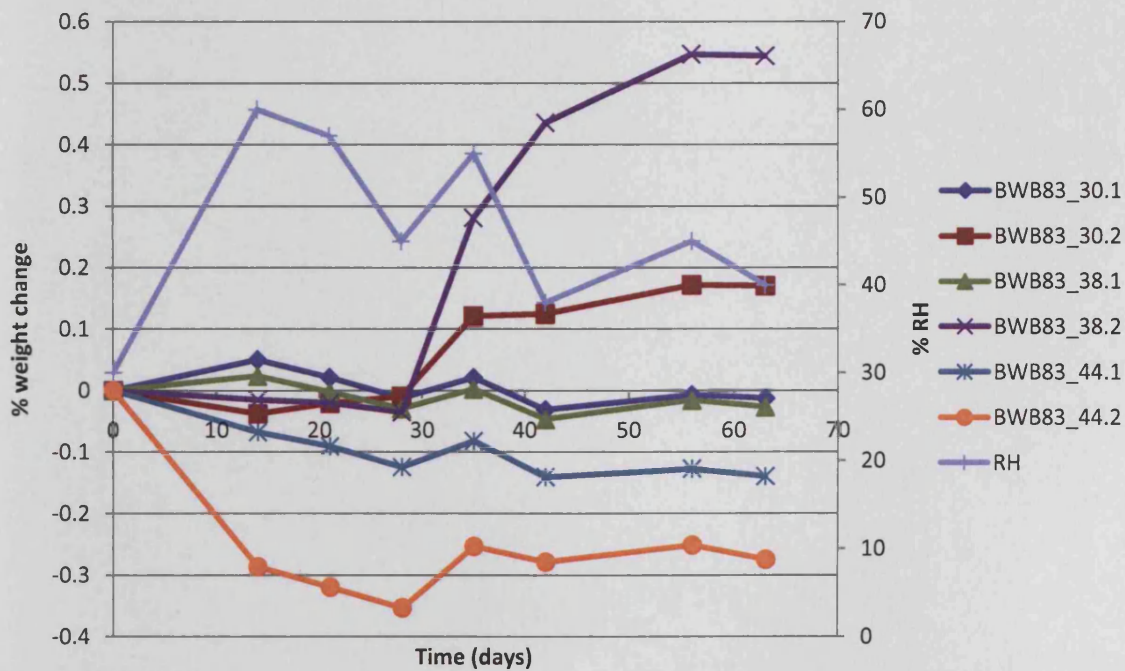


Figure 48: Results of accelerated corrosion testing for halved Billingsgate objects treated in AS20. Ambient RH at the time of weight measurement is given on the secondary axis.

Billingsgate nails did not generally react strongly to the accelerated conditions (Figure 47 and 48) – the maximum weight gain was +0.5% (BWB83_38.2, Figure 48). Again, none of the treated halves show detectable weight increase or visual corrosion. Some of the untreated halves show a small positive trend (e.g. BWB83_28.2, Figure 47; BWB83_30.2, Figure 48). Chloride levels in these objects are no higher than 565 ppm; treated halves contain less than 110 ppm. Visually, the untreated Billingsgate objects showed less change than Bornais, with flaking or limited fragmentation only. The behaviour of BWB83_38.2 is somewhat unusual (Figure 48); initially it loses weight with ambient RH decreases, but after 28 days it begins to gain weight rapidly. This may be the result of initial slow corrosion opening up a crack which then allowed rapid ingress of water and oxygen towards the centre of the object and increasing the corrosion rate.

Objects from Caerwent behave in more complex ways. Three of the four halves from dNaOH showed rapid linear weight gain, of +2.7 to +5.0% (Figure 49). Only CAE_27.1 (treated) did not show weight gain or visual change (Figure 49), and had the lowest chloride content of 467 ppm (Table 9). The three halves that gained weight had chloride ion content in the range 1112 to 2507 ppm, although the highest chloride content (CAE_28.2) does not correspond to the highest overall weight gain, which belongs to a treated object (CAE_28.1) (Figure 49). Only 42% of the total chloride of CAE_28.1 was extracted by the treatment (Figure 16), leaving a significant amount (1112 ppm) to stimulate corrosion and resulting in visible flaking. In contrast, the treatment of CAE_27.1 extracted 79% of the total chloride (Figure 16), and this appears to have been sufficient to eliminate its susceptibility to weight gain; no visual corrosion was observed.

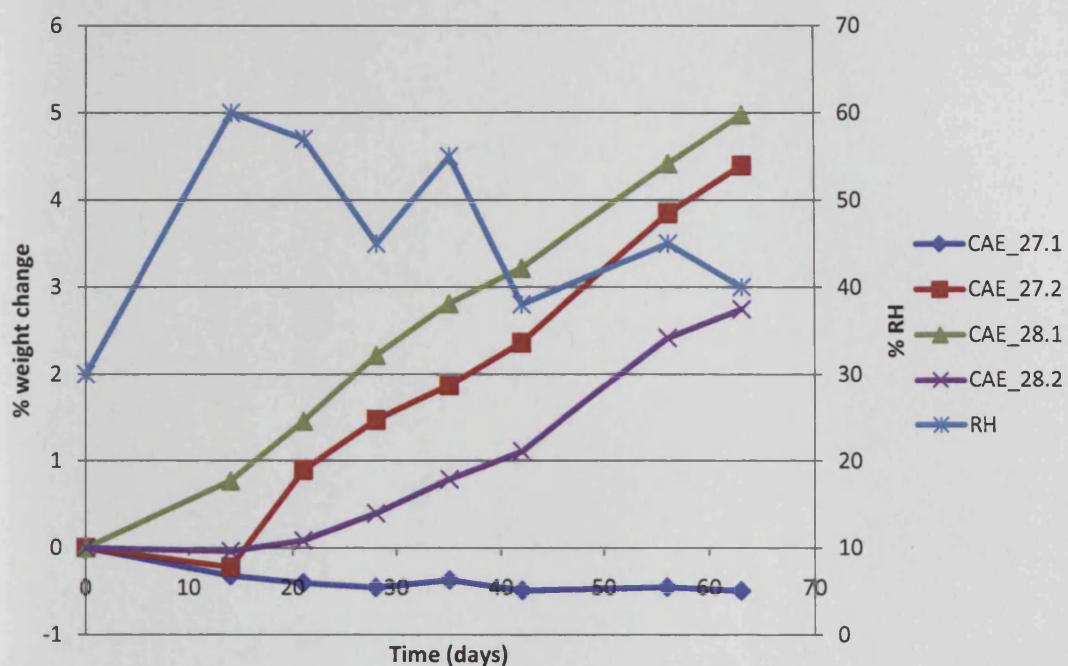


Figure 49: Results of accelerated corrosion testing for halved Caerwent objects treated in dNaOH. Ambient RH at the time of weight measurement is given on the secondary axis.

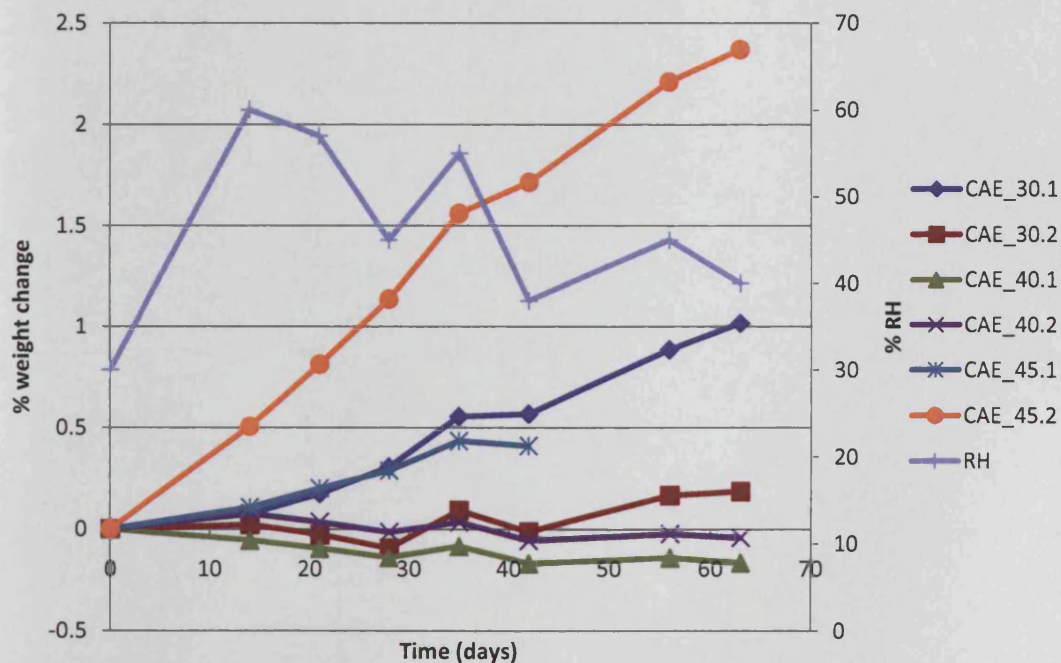


Figure 50: Results of accelerated corrosion testing for halved Caerwent objects treated in AS20. Ambient RH at the time of weight measurement is given on the secondary axis.

Looking at the AS20 halves of Caerwent objects (Figure 50), both halves of CAE_40 do not show any positive weight gain. No residual chloride ion data is available for this object, as it did not complete digestion, but only a very small amount of chloride was removed from CAE_40.1 (36 ppm, Figure 10), and further examination of the X-ray photograph shows that this object was completely mineralized. No visual change was observed during the test. The other four halves showed positive change, greatest for CAE_45.2 at +2.4% (Figure 50). The treated half (CAE_45.1) had lower weight change although still showing a positive trend. Curiously, however, CAE_45.2 contains less than half the amount of chloride ions than the treated half (Table 9). The 950 ppm remaining in CAE_45.1 after treatment (67% extraction, Figure 17) appears to be less damaging to this object than the 425 ppm in the untreated half. Visually, CAE_45.2 is totally fragmented, while the fragmentation of CAE_45.1 is more limited (Figure 51), although this may partly be related to the fact that CAE_45.1 had to be removed from the accelerated corrosion test twenty days early due to a technical error. The difference in weight gain between the treated and untreated halves of this object suggests that at least some of the chloride in the treated half is not playing a role in increasing corrosion, while the untreated half contains more soluble chloride which can stimulate the corrosion reaction.

The opposite appears to be true for CAE_30 (Figure 50). The treated half (CAE_30.1) gains more weight than the untreated half, but in this case it is CAE_30.2 which contains more chloride. The treated half, which had an extraction efficiency of 67% and retained 553 ppm chloride (Figure 17, Table 9) appears to be more susceptible to corrosion than the untreated half, which contained a total of 1049 ppm chloride, but only produced +0.2% weight gain (Figure 50). It is not clear why this is the case, but it indicates that untreated objects with relatively high chloride content are not necessarily susceptible to corrosion, whereas a single concentrated area of chloride that is not removed by treatment can lead to large weight gain and fragmentation.



Figure 51: CAE_45.1 (left) and CAE_45.2 (right). Both show signs of instability, but CAE_45.2 is more fragmented.

4.5.2.4 Relationship of chloride content and weight gain

The data suggests that there is a complex relationship between chloride content and weight gain. To assess this relationship more fully, total weight change at the end of the accelerated corrosion period was compared with the chloride content of the objects (Figure 52).

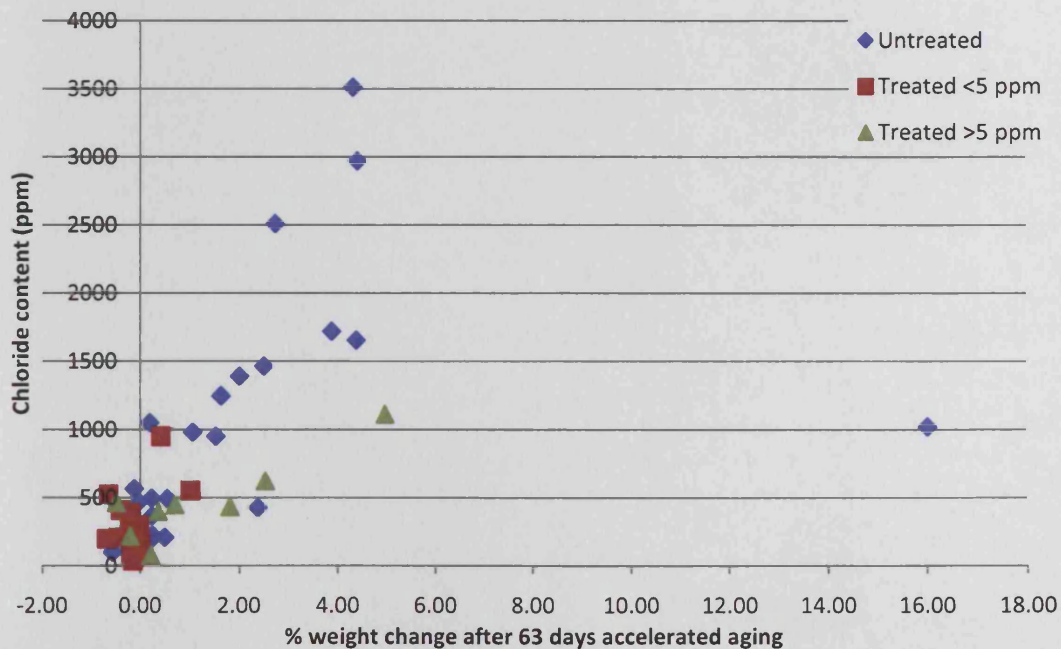


Figure 52: Scatter graph showing correlation between chloride content and total weight gain during the accelerated corrosion test ($r = 0.534$, $r^2 = 0.286$). The data has been organised to reflect the final solution concentration.

Although there is significant scatter, there is a positive correlation between high chloride levels and greater weight gain (Figure 52). Weight gain of greater than +1.0% is almost always associated with chloride content greater than 500 ppm. The majority of the objects with high chloride levels are untreated objects and these also tend to have greater weight gain. Treated objects, apart from one exception, have chloride content less than 1000 ppm, and of these, objects where the concentration of the final treatment bath was less than 5 ppm tend to cluster around 0 to -0.5% weight change, and usually have chloride content less than 500 ppm. Objects with a final bath concentration of > 5 ppm show a range of weight gain and chloride content (Figure 52). Almost all of the treated objects that had positive weight gain fall into this category, suggesting that there is a relationship between an incomplete treatment and the likelihood an object will corrode under the test conditions. The object with the highest overall weight gain (CAE_48, +16.0% weight gain) falls well outside the spread of the other data.

The strength of the relationship between chloride content and weight gain is statistically evaluated using the Pearson Product Moment Correlation (r). For the data shown in Figure 52, $r = 0.534$ ($n = 58$). This value is significant at the .01 significance level ($r_{crit} = .3248$). The coefficient of determination (r^2) is only 0.286; although the relationship exists, only a small amount of the variability in one factor is accounted for by variability in the other. However, removing the outlier CAE_48 increases the correlation to $r = 0.816$ and $r^2 = 0.666$, a strong linear relationship for the majority of the objects. The correlation coefficient may not be a particularly accurate measure of this relationship, due to the somewhat crude weight measuring methodology and the difficulty in distinguishing positive weight gain when objects corrode very slowly, but a relationship clearly exists between the two variables.

As an initial study the results of the accelerated corrosion test are striking, and support the hypothesis that chloride levels correlate to increased corrosion rate, even in archaeological iron objects with complicated morphology and unevenly distributed chloride in the structure. Some of the objects were completely destroyed by corrosion. In other cases only part of the object was affected showing that chloride-induced corrosion can be localised and still have a detrimental effect on the object.

The relationship between final bath concentration and weight gain of objects is also statistically significant ($r = 0.472$, $r^2 = 0.223$) at the .05 significance level ($r_{crit} = 0.3246$). This supports the hypothesis that incomplete treatment leads to continued susceptibility to corrosion. All but two of the objects that did complete treatment show no detectable weight gain under the test conditions (Figure 52), even though untreated or incompletely treated objects with similar overall chloride content do show weight gain.

The correlation of final solution concentration and weight gain may indicate the different effects of bound and soluble chloride. The residual chloride in objects that complete treatment does not appear to have a strong effect on corrosion behaviour, and may therefore represent bound chloride in akaganéite tunnels. Objects that do not complete the treatment still contain some soluble chloride in addition to this bound chloride, and it is likely that the soluble chloride fraction leads to weight gain compared to objects that did complete the treatment. For example, BOR_6287 and CAE_34, which had the greatest weight gain (+1.81% and +2.52%, respectively) of the whole treated objects (Figures 42 and 43), have similar chloride content (435 and 622 ppm, Table 9) to that of other treated objects which did not show positive weight gain (e.g. CAE_27.1, CAE_41, Table 9). For both BOR_6287 and CAE_34, the final bath contained more than 5 ppm (9.42 and 27.35 ppm respectively, Table 9). Untreated objects containing around 500 ppm (the same as some fully treated objects) showed detectable weight gain and corrosion behaviour, implying that at least some of the chloride is in soluble form and contributes to corrosion.

4.5.2.5 Conclusion of accelerated corrosion tests

The results from the accelerated corrosion test lead to several conclusions regarding desalination treatment and the relationship of chloride content to corrosion rate:

- Objects where treatments was incomplete (>5 ppm in final solution) are more likely to experience later corrosion, because they still contain some soluble chloride. This underlines the importance of measuring chloride extraction during treatment and continuing treatment until chloride levels in solution are low.
- Fully treated objects may contain up to about 500 ppm chloride ions without this appearing to cause any increased corrosion behaviour. In fact, the majority of the fully treated objects subjected to the accelerated corrosion test did not show any

enhanced corrosion behaviour, and were stable even under the harsh test conditions.

- Where weight gain did occur in fully treated objects (CAE_30.1 and CAE_45.1) this could be attributed to incomplete extraction due to inaccessible chloride. The SEM-EDX analysis of CAE_45.1 (section 4.5.1.2) showed that chloride was located deep within the metal along slag inclusions, and this may have resulted in its corrosion behaviour. As these two objects represent only 7% of the fully treated objects in the test (out of 27 objects that had a final solution concentration less than 5 ppm) it seems that in a large majority of cases (93%), a properly completed treatment does reduce the corrosion susceptibility of the objects.
- This accelerated corrosion test was short and the methodology somewhat crude. It is encouraging that useful results have been obtained despite these problems, and this suggests that more detailed study of the relationship of chloride to corrosion rate is likely to produce useful information.

4.5.3 The probability of long-term outcome

To evaluate the outcome of treatments according to the model in Chapter 3, a method of assessing the probability of long-term stability after treatment needs to be developed from the data in this chapter.

Residual chloride content is one possible measure. Although the relationship between chloride content and corrosion rate has not been quantified, the accelerated corrosion tests have established the existence of a correlation between high chloride content and high corrosion susceptibility. In order to relate residual chloride content to long-term outcome, some boundary values need to be determined above and below which corrosion is likely to occur. The only boundary values that have been proposed are by North and Pearson (1978a), who suggest that below 200 ppm, objects are stable, while above 1000 ppm is a high risk of rapid corrosion. In between these two values corrosion may occur but is slow. These values are based on the experience of the authors of treating archaeological iron rather than an empirical study. The 200 ppm boundary for stable objects was supported by Rinuy and Schweizer (1982), but no other evidence exists. In the absence of any further information, however, these boundary values provide an initial guide for relating residual

chloride content to long-term treatment outcome. These boundary values do not discriminate between bound and soluble chloride ions. The lower boundary, 200 ppm, is quite low and should include only objects that either have little soluble chloride or contain only bound chloride.

There are three categories of long-term outcome: optimum stabilisation, improvement in stability, and no stabilisation (see Chapter 3). These are simplifications of the wide range of possible outcomes, but if the boundary values are correct, an assessment using these boundaries should give an indication of how many objects have improved (200 – 1000 ppm) or optimum stability (<200 ppm) after treatment, and how many remain in the danger zone of >1000 ppm.

Residual chloride data from the three treatments is divided into these three bands in Table 10. Between 4% and 23% of objects remain in the >1000 ppm category after treatment. Between 32% and 51% of objects have residual chloride content of less than 200 ppm, while 45-46% of objects are in the intermediate category.

Table 10: Probability of long-term stability of treated objects based on residual chloride data.

| Long-term outcome | Residual Cl | dNaOH (n=47) | | | AS20 (n=47) | | | AS60 (n=24) | | |
|--------------------|--------------|--------------|----|----------------|-------------|----|----------------|-------------|----|----------------|
| | | n | % | P _r | n | % | P _r | n | % | P _r |
| Optimum stability | <200 ppm | 15 | 32 | 0.32 | 24 | 51 | 0.51 | 11 | 46 | 0.46 |
| Improved stability | 200-1000 ppm | 21 | 45 | 0.45 | 21 | 45 | 0.45 | 11 | 46 | 0.46 |
| No improvement | >1000 ppm | 11 | 23 | 0.23 | 2 | 4 | 0.04 | 2 | 8 | 0.08 |

Long-term treatment outcomes could also potentially be assessed using the results of accelerated corrosion experiments. However, the difficulty of distinguishing slow corrosion using the crude methodology employed in this thesis undermines the usefulness of this data for long-term predictions. The long-term behaviour of objects, including the possibility of chloride release from akaganéite over time, could not be evaluated using this short-term study. More accurate measurements of weight gain under accelerated corrosion conditions followed by measurements of chloride content could be used to improve on the boundary

values given by North and Pearson (1978a), and this should be an important objective of further work.

It is impossible to know whether the boundary values of 200 and 1000 ppm actually reflect the behaviour of objects in the long term. It does, however, contradict the view that desalination treatments do not make a difference to the behaviour of objects. The number of objects with high-risk levels of chloride is quite low after treatment, and the accelerated corrosion data indicates that this is beneficial in reducing corrosion susceptibility, although the behaviour of objects after treatment cannot be predicted with absolute certainty. This supports the information from collection surveys (Keene & Orton 1985; Selwyn & Logan 1993; Keene 1994; Loeper-Attia & Weker 1997) that alkaline desalination treatments cause a significant improvement in the long-term stability of objects. Although all methods of assessing long-term corrosion behaviour have problems, the cumulative picture supports the view that desalination treatment enhances stability and increases the lifespan of objects in a majority of, though not in all, cases. Low RH storage may still be deemed necessary due to the inability to predict treatment outcomes definitely, but the risks to objects from high RH are significantly reduced if the majority of chloride ions have been removed by desalination treatment.

4.6 Summary

The experimental treatments of archaeological iron reported in this chapter have fulfilled the objective of providing detailed, statistically significant data for the evaluation of desalination treatments. With 120 objects treated, the variability of object corrosion morphology did not prevent a strong general picture from emerging. All three treatments performed in similar ways, with the main difference being the reduced treatment time when solutions are heated. Statistical analysis of the data was an important tool in showing that all three treatments had similar chloride extraction ability and in identifying correlations. Analysing objects for residual chloride, although a destructive method, was the only way of properly assessing the effectiveness of treatments in removing chloride ions within the time frame of this thesis.

The evaluation of treated objects by SEM-EDX gave an initial insight into the difference that treatment made to the distribution of chloride ions and the behaviour of objects. It showed

that treatments were able to remove chloride ions effectively, although not able to reach chloride ions located deep within objects.

Accelerated corrosion testing of objects at high temperature and humidity proved to be the only feasible method for assessing object corrosion behaviour in this thesis. This data cannot be extrapolated to ambient conditions, but showed that desalination treatment reduced the corrosion susceptibility of objects under the accelerated conditions. Combining this data with residual chloride has confirmed the positive correlation of chloride levels and corrosion, and is an important contribution towards fulfilling the aims of the research.

Chapter 5 – The transformation of akaganéite

In real life, carrying out a treatment is a struggle for control in the face of unavoidable uncertainty.

Appelbaum 2007: 418

5.1 Introduction

The effect of treatment solutions on corrosion products is subject to considerable uncertainty. There are two issues to be considered. First, the effect on the information-bearing corrosion layers of being immersed in alkaline solutions for extended periods of time is not known. Change to corrosion layers may be detrimental to the object's value. Desalination treatments have sometimes been suggested to 'soften' the corrosion layers of objects (Argyropoulos et al. 1997; Selwyn & Argyropoulos 2005), but no information exists as whether the change is chemical transformation or mechanical destabilisation of the corrosion matrix. The many variations of corrosion products and morphologies on archaeological objects place a full scale study of the effects of treatment solutions on corrosion layers beyond the scope of this study.

Second, the ability of alkaline solutions to transform akaganéite into another iron oxide and thereby release structural chloride requires further research. Chapter 2 reported transformations that have been observed in laboratory conditions, but they have only rarely been observed on objects (Gil et al. 2003; Drews et al. 2004), and never in the case of an alkaline desalination treatment as used in this study. Furthermore, the changes occurring to synthetic akaganéite in alkaline solutions reported in the literature are not consistent, and there is considerable uncertainty as to which transformations may or may not occur. Much depends on the exact conditions under which the akaganéite is manufactured and treated.

Experimental work was designed to determine the behaviour of akaganéite under the treatment conditions used in this study. It follows on from experiments carried out by Al-Zahrani (1999), who tested transformation of akaganéite in alkaline and neutral solutions at various temperatures. The experimental treatments in this thesis use lower concentrations of chemicals than those tested by Al-Zahrani, and their effects require evaluation. Al-Zahrani also found that akaganéite contaminated with magnetite behaved differently to pure

akaganéite, contradicting other results reported in the literature (Cornell & Giovanoli 1990). Both pure akaganéite and akaganéite mixed with other corrosion products were tested in this study to determine if seeding influences the transformation outcome.

5.2 Methodology

5.2.1 Manufacturing akaganéite

Akaganéite was manufactured using the method of Turgoose (1985), Watkinson and Lewis (2005a) and Al-Zahrani (1999), which more closely replicates the formation conditions on archaeological iron objects than other methods. Iron powder (nitrogen-reduced, 99% purity) and ferrous chloride ($\text{FeCl}_2 \cdot 4\text{H}_2\text{O}$, AnaLar grade) were mixed in equal weight in Petri dishes and exposed to 92% RH in a desiccator cabinet. The powders were mixed once a week and the door of the cabinet opened at least once a week to ensure sufficient oxygen supply (see Appendix 1.1). After four months the product was analysed by X-ray diffraction (XRD) (see Appendix 2.1).

Initial results showed that the product contained akaganéite ($\beta\text{-FeOOH}$) and some excess ferrous chloride. To remove this, the powder was subjected to washing, half in deionised water and half in acetone. Further XRD showed that all the ferrous chloride was removed by both methods and the product was now 100% $\beta\text{-FeOOH}$ (Figure 53). Further XRD analysis of the akaganéite after 2 years stored in a screw-top glass jar in ambient conditions (15-25°C, 35-65% RH) showed that no spontaneous transformation had occurred: under these conditions, akaganéite did not appear to be metastable. Several samples of the synthetic akaganéite were digested in nitric acid and the chloride content measured using the specific ion meter (Appendix 2.3); this was found to be in the range of 7.0 – 7.8 wt%. As a final step in preparation of the akaganéite samples, the powder was gently ground in an agate mortar to break up aggregated particles.

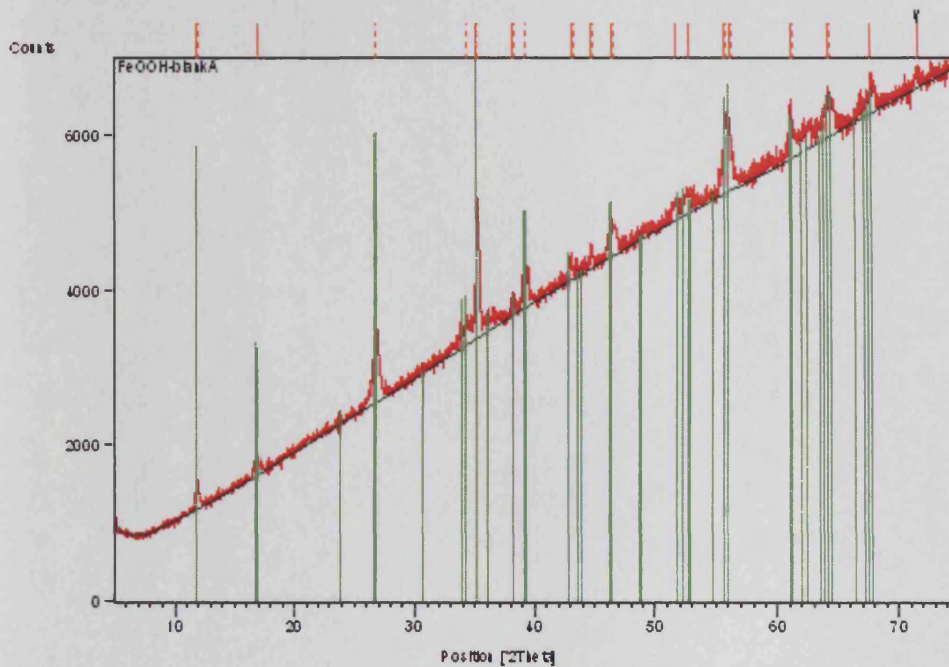


Figure 53: X-ray diffraction spectrum for pure synthetic akaganéite. The green bars represent peaks of reference spectrum.

5.2.2 Methodology for transformation testing

Three main variables were under investigation in these tests:

- Temperature: $20^{\circ}\text{C} \pm 5$ or $60^{\circ}\text{C} \pm 5$.
- Solution concentration: 0.1M to 1M NaOH, and 0.05M to 0.5M Na_2SO_3
- Seeding akaganéite with 10 wt% goethite or 10 wt% magnetite

The ratio of powder to solution was 1:25 (see Appendix 1.2). The tested solutions and product combinations are given in Table 11. The solution concentrations used for the seeded samples were the concentrations used in the actual treatment experiments, 0.1M NaOH and 0.1M NaOH/0.05M Na_2SO_3 .

Table 11: Parameters for transformation testing of akaganéite and akaganéite mixtures.

| Temperature (°C ± 5) | Solution | Treatment time | Akaganéite only | Akaganéite seeded with goethite | Akaganéite seeded with magnetite |
|-------------------------|----------------------------|-------------------|--------------------|---------------------------------------|--|
| 20 | 0.1M NaOH | 20 months | ✓ | | |
| | 0.1M/0.05M AS | 20 months | ✓ | | |
| | Deionised H ₂ O | 20 months | ✓ | | |
| 60 | 0.1M NaOH | 56 days | ✓ | ✓ | ✓ |
| | 0.5M NaOH | 28 days | ✓ | | |
| | 1M NaOH | 28 days | ✓ | | |
| | 2M NaOH | 28 days | ✓ | | |
| | 4M NaOH | 28 days | ✓ | | |
| | 0.1M/0.05M AS | 56 days | ✓ | ✓ | ✓ |
| | 0.1M/0.1M AS | 28 days | ✓ | | |
| | 0.5M/0.5M AS | 28 days | ✓ | | |
| | Deionised H ₂ O | 28 days | ✓ | ✓ | ✓ |

Due to equipment availability it was not possible to deoxygenate the majority of the sodium hydroxide samples with nitrogen gas as used for desalination of objects. Deoxygenation of the solution by boiling prior to adding the corrosion products was attempted, but the sample tubes were not airtight enough to prevent reoxygenation of the solutions within a short time. One sample of akaganéite in 0.1M NaOH was placed in a nitrogen-deoxygenated environment at room temperature for comparison with the oxygenated NaOH samples.

Samples were removed at consecutive time intervals: 1, 3, 5, 7, 14, 21, 28 and in some cases 56 days for heated treatments; 1, 2, 4, 8, 16 and 32 weeks for room temperature treatment, with a final sample analysed after 20 months. Samples were shaken to promote thorough mixing: every weekday (Monday to Friday) for heated samples and twice a week for room temperature samples. Control samples in deionised water were run at both temperatures with analysis at 7 and 28 days (heated) and 4 and 16 weeks and 20 months for room temperature. The powdered samples were filtered and air-dried, and then stored in screw-top glass vials for up to 6 weeks until analysis by X-ray diffraction (XRD) (see Appendix 1.2

and 2.1). Proportions of corrosion products given below have an associated error of about 10% (see Appendix 2.1.2 for further details).

5.3 Results of transformation tests

Results of the transformation tests are given in Table 12 and 13 and shown in Figures 54 to 59.

Table 12: Results of transformation tests of pure akaganéite. Proportions are subject to an error of approx. 10% (see Appendix 2.1.2).

| Temperature (°C ± 5) | Solution | % Akaganéite | % Goethite | % Hematite |
|----------------------------|----------------------------|--------------|------------|------------|
| 20 | 0.1M NaOH | 84 | 16 | |
| | 0.1M/0.05M AS | 81 | 19 | |
| | Deionised H ₂ O | 89 | 11 | |
| 60 | 0.1M NaOH | 70 | 30 | |
| | 0.5M NaOH | 47 | 53 | |
| | 1M NaOH | 76 | 24 | |
| | 2M NaOH | 81 | 19 | |
| | 4M NaOH | 81 | 19 | |
| | 0.1M/0.05M AS | 50 | 30 | 20 |
| | 0.1M/0.1M AS | 58 | 29 | 14 |
| | 0.5M/0.5M AS | 41 | 59 | |
| Deionised H ₂ O | 89 | 11 | | |

5.3.1 Temperature

At room temperature and over a period of 20 months, akaganéite transformed partially to goethite (α -FeOOH) in both 0.1M NaOH and 0.1M NaOH/0.05M Na₂SO₃ solution (Figure 54). 16-19% goethite appeared within the first month of treatment (Table 12), and no further change occurred. Goethite was confirmed after 2 weeks for alkaline sulphite and after 4 weeks in NaOH (Figure 54). It may have been present in earlier samples in very low quantities, but this could not be confirmed because of the difficulty in distinguishing the iron oxyhydroxides using XRD alone (Neff et al. 2004; Rémazeilles & Refait 2007; Navrotsky

et al. 2008). In deionised water, no transformation occurred during the first 16 weeks of the test, but after 20 months, approximately 10% goethite was detected (Table 12). The sample of nitrogen-deoxygenated 0.1M NaOH at room temperature resulted in c. 20% transformation of akaganéite to goethite after 57 days, the same result as for the oxygenated solution.

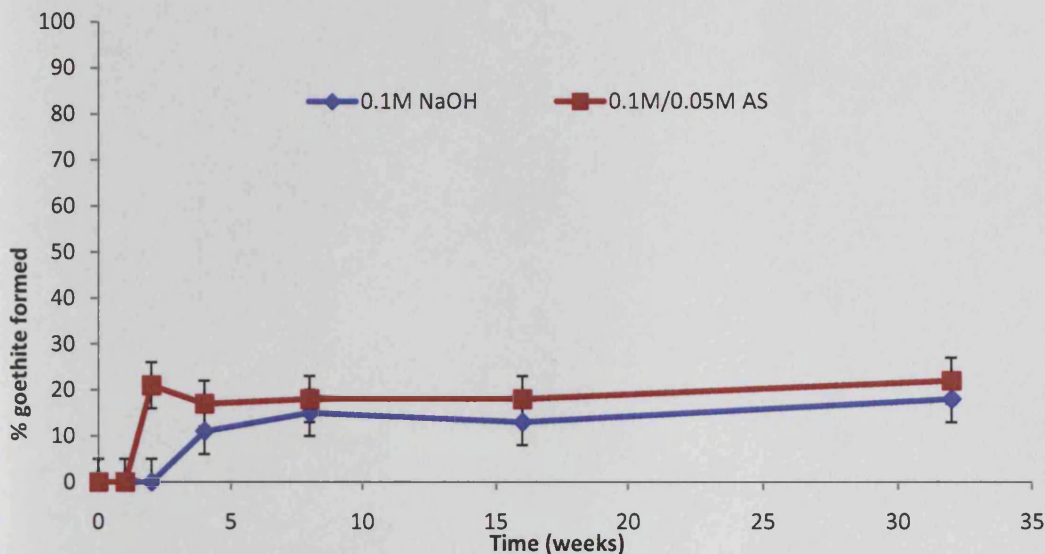


Figure 54: Transformation of akaganéite to goethite in room temperature solutions.

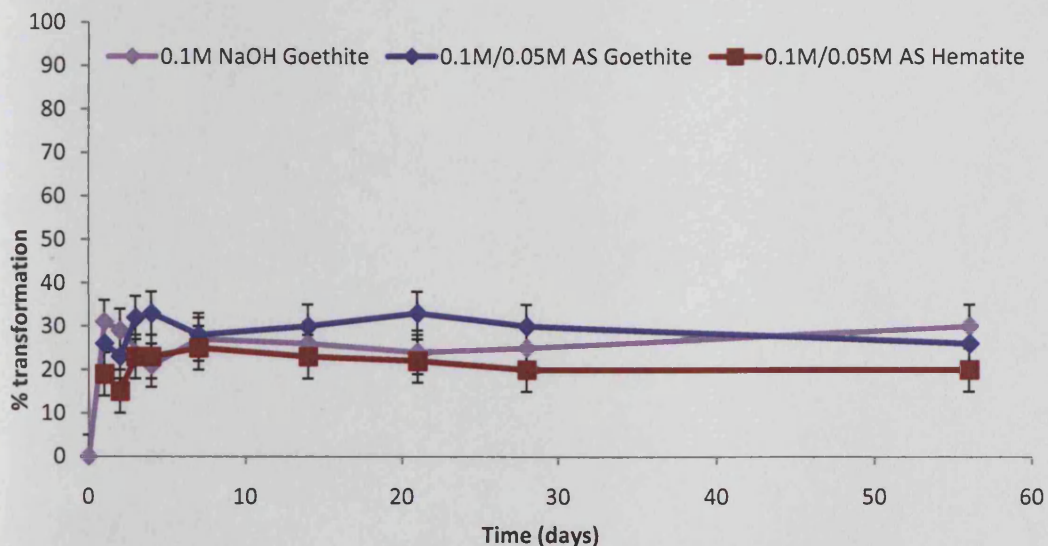


Figure 55: Transformation of akaganéite to goethite and hematite in heated solutions. Hematite only occurred in the presence of sulphite ions.

Samples heated to 60°C transformed more quickly, with some transformation occurring within 24-48 hours. A greater proportion of akaganéite transformed: in 0.1M NaOH, transformation resulted in approximately 30% goethite, while in 0.1M/0.05M alkaline sulphite, approximately 50% of the akaganéite transformed (Table 12, Figure 55). In the latter solution, both goethite and hematite appeared, with goethite predominating slightly (Figure 55). Both products appeared together (within the first 24 hours) and their proportion did not change during the treatment time. Heating deionised water produced c. 10% change within 28 days, although goethite was not present at 7 days (Table 12).

5.3.2 Solution concentration

Increasing the concentration of NaOH changed the proportion of akaganéite transforming to goethite (Table 12, Figure 56). The greatest transformation occurred in 0.5M NaOH, with about 50% goethite appearing; in all other concentrations of NaOH about 15-25% goethite appeared. Doubling the concentration of Na₂SO₃ to 0.1M while maintaining the same NaOH concentration (0.1M) did not alter the ratio of goethite to hematite or the amount of transformation that occurred (Figure 57, Table 12). Increasing the concentration of both to 0.5M eliminated hematite altogether, producing a c. 50% transformation to goethite only (Figure 57).

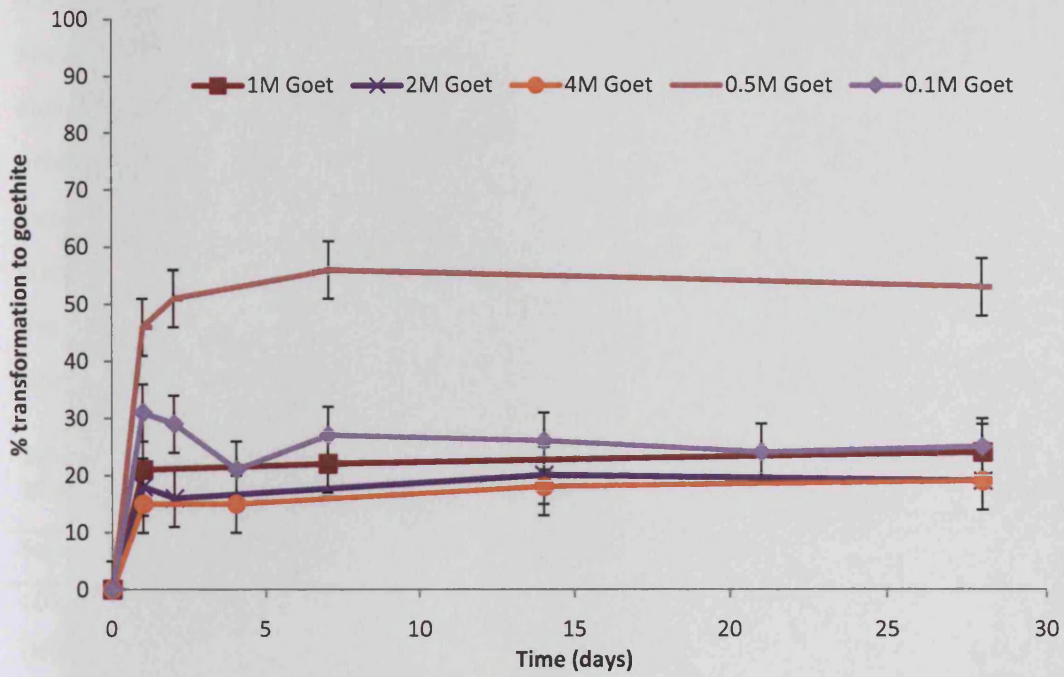


Figure 56: Transformation of akaganéite to goethite in varying concentrations of NaOH (60°C).

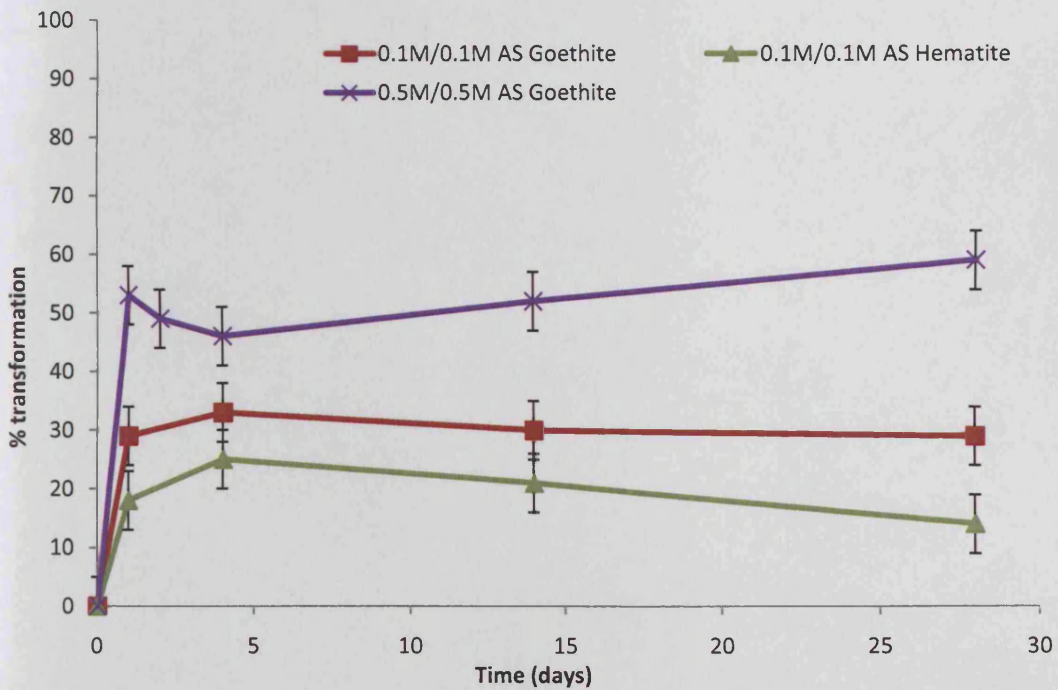


Figure 57: Transformation of akaganéite to goethite and hematite in varying concentrations of alkaline sulphite (60°C). Hematite occurred in the presence of 0.1M Na₂SO₃ only.

5.3.3 Seeding

Seeding with 10% goethite or magnetite produced very little alteration to the behaviour of akaganéite in both 0.1M/0.05M alkaline sulphite and 0.1M NaOH. In 0.1M NaOH, goethite proportion increased by 15% after 28 days, a similar increase as pure akaganéite (Table 13, Figure 58). In alkaline sulphite, seeding appeared to retard the transformation, increasing goethite by only 20% (compared to 30% transformation of pure akaganéite) and eliminating the formation of hematite that occurred in pure akaganéite under the same solution conditions.

Table 13: Results of transformation of akaganéite seeded with goethite or magnetite. Seeding was 10 wt%, but the XRD software recorded this as 16% goethite or 17% magnetite.

| Seeding | Solution | % Akaganéite | % Goethite | % Magnetite |
|-------------------------------------|-----------------|--------------|------------|-------------|
| 10% Goethite (XRD = 16%) | 0.1M NaOH | 69 | 31 | - |
| | 0.1M/0.05M AS | 64 | 36 | - |
| | Deionised water | 80 | 20 | - |
| 10% Magnetite (XRD = 17%) | 0.1M NaOH | 64 | 15 | 21 |
| | 0.1M/0.05M AS | 61 | 16 | 23 |
| | Deionised water | 73 | 11 | 16 |

When seeded with 10% magnetite, 15% goethite formed in 0.1M NaOH (Table 13, Figure 59), while the proportion of magnetite remained within the error limits of the XRD analysis, although there may have been a slight increase. No transformation to hematite occurred. In all cases, the transformation seemed to occur within the first 24 hours, and no further significant change occurred.

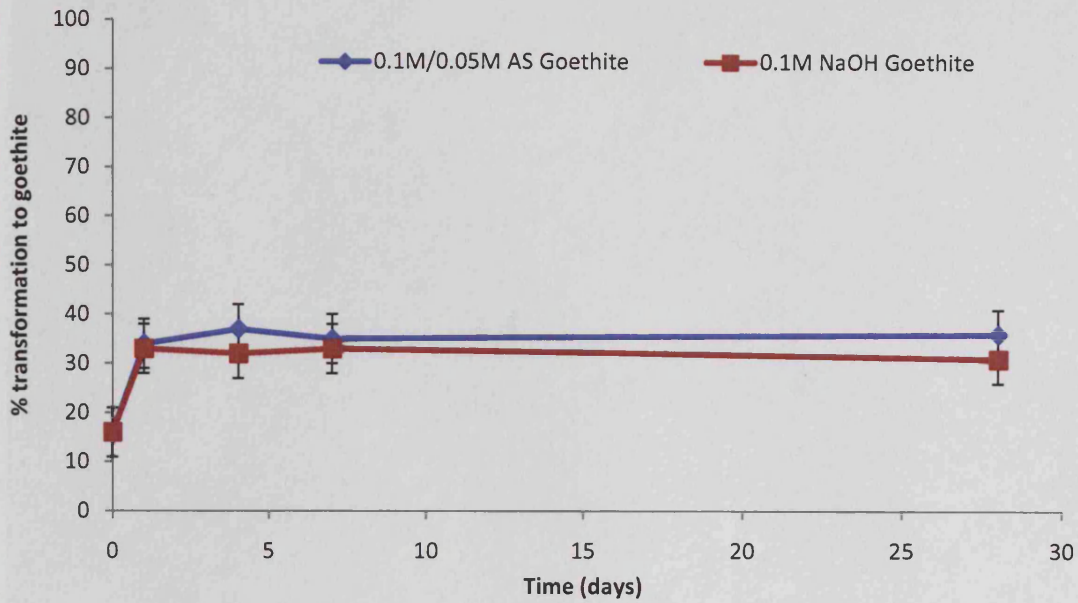


Figure 58: Transformation of akaganéite seeded with goethite in heated solutions.

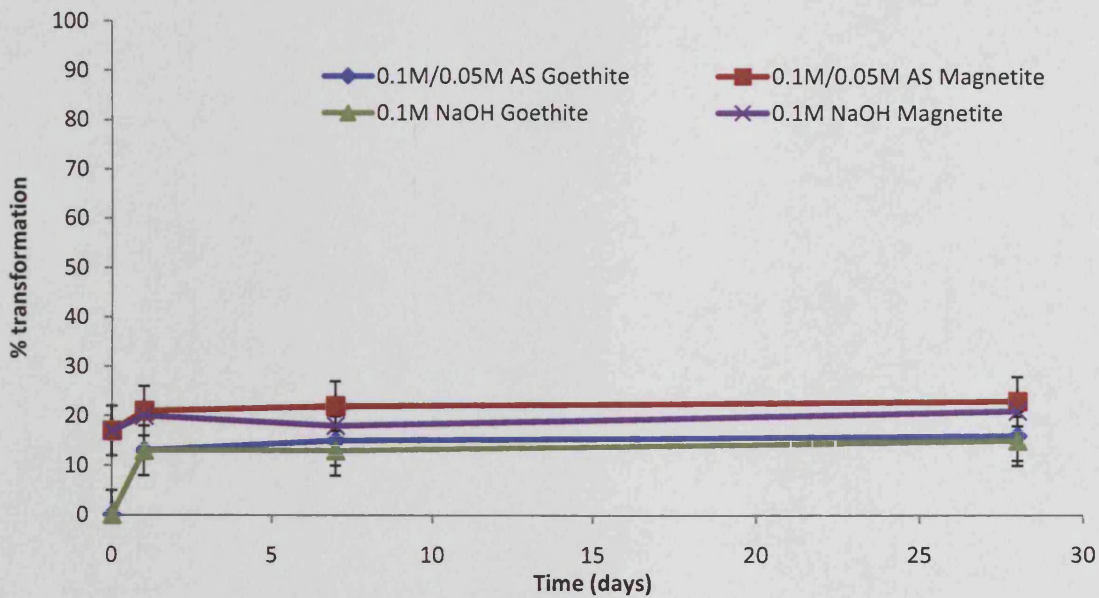


Figure 59: Transformation of akaganéite seeded with magnetite in heated solutions.

5.4 Discussion

The results obtained by the transformation tests above differ from those previously reported. Transformation in these experiments was always partial, with no more than 50% of akaganéite transforming to other corrosion products. Al-Zahrani (1999) found complete

transformation to goethite over four months, and almost complete transformation to magnetite and goethite in hot water (70-100°C). He also reported that seeding with magnetite resulted in transformation to magnetite rather than goethite, although Cornell and Giovanoli (1990) state that seeding with other minerals has no effect on transformation outcomes. In the tests reported here, seeding with magnetite had very little influence on the treatment outcome, with the amount of magnetite remaining essentially stable and transformation to goethite occurring instead.

At room temperature and 60°C, transformations occurred within a short period and then no further increase in the products was observed, suggesting that the lack of complete transformation is not related to the time of exposure to the treatment solution. According to the results of Al-Zahrani (1999) and Cornell and Giovanoli (1990) full transformation of akaganéite should have occurred within the time period evaluated here, and so some other factor must be influencing the outcome and resulting in incomplete transformation.

The consistent ratios between akaganéite and its transformation products suggest that kinetic factors may be preventing completion. As akaganéite transforms to goethite via a dissolution/precipitation pathway (Cornell & Giovanoli 1990) it is possible that an equilibrium is established between akaganéite and goethite. The release of chloride ions from akaganéite during the initial transformation may produce a solution containing sufficient chloride ion concentration to allow akaganéite to reform after dissolution rather than going to goethite. This may also explain why seeding does not increase the level of transformation. Further testing is needed to evaluate this hypothesis, by measuring chloride ion release from akaganéite during immersion, and either changing the solution at intervals to remove chloride or increasing the solution volume. Both Al-Zahrani and Cornell and Giovanoli used a greater ratio of solution to powder: 0.1g powder to 100 ml in Cornell and Giovanoli (1990), 0.5g to 100 ml in Al-Zahrani (1999). This much bigger ratio to that used in this study (1 g to 25 ml) may have played an important part in allowing full transformation to occur, and requires further investigation.

The role of solution concentration was not consistent with that reported in the literature. In Cornell and Giovanoli (1990), hematite formed in concentrations of heated KOH from 0.5 to 2M. Here, hematite did not occur in the presence of NaOH in the same concentration range,

but only when sodium sulphite was also present at 0.05 to 0.1M concentration. This suggests that sulphite ions are promoting the formation of hematite alongside goethite, but the mechanism is not clear. The transformation pathway of akaganéite can be influenced by the presence of anions including sulphate ions (Ishikawa et al. 2005), which result from the oxidation of sulphite ions. Although it is possible that the lack of oxygen induced by the presence of sulphite ions plays a role, the fact that no hematite was found in 0.5M sulphite concentration suggests otherwise. More work is needed to assess the influence of sulphite and/or sulphate ions on the transformation of akaganéite over a greater range of concentrations.

The role of pH is also different to that reported in the literature. According to Frini and El Maaoui (1997), hematite formation from akaganéite occurs in pH less than 12.8. All the NaOH concentrations in the tests performed here had pH >13 (Table 14), yet hematite formed in some cases. A greater range of pH needs to be examined to determine what effect pH has on transformation. More akaganéite transformed in 0.5M NaOH (pH 13.7) than in either higher or lower concentration.

Table 14: pH of NaOH solutions used in akaganéite transformation tests.

| NaOH concentration (M) | pH |
|------------------------|------|
| 0.1 | 13.0 |
| 0.5 | 13.7 |
| 1 | 14.0 |
| 2 | 14.3 |
| 4 | 14.6 |

The different manufacturing method of akaganéite used here may be responsible for some of the different results. It was not possible to obtain images of the akaganéite crystals produced or the transformed samples. Transmitting electron microscope (TEM) analysis may help to determine whether the product obtained by the solid manufacture method is significantly different to that produced by other methods. Akaganéite produced by the method used here was examined by Al-Zahrani (1999) and suggested to have tactoid crystals similar to crystals made by precipitation of FeCl₃. This could not be confirmed for the samples used here. However, the discrepancy between the results reported here and

those of Al-Zahrani (1999) also need further investigation, as the same manufacturing method was used.

5.5 Conclusion

The results of the transformation tests were somewhat ambiguous, giving different results to those which were anticipated from the literature. No treatment conditions produced transformation of more than 50% of the akaganéite. Heating the treatment increased the rate of transformation and slightly increased the amount of transformation that occurred compared to room temperature conditions, where about 20% transformation occurred. Seeding did not significantly increase the level of transformation. It appears, therefore, that although some transformation of akaganéite may be possible under the treatment conditions used in this study, full transformation is not expected. The differences with other reported data and the influence of solution volume, foreign anions and chloride ion concentration require further investigation.

According to the results of these tests, the best transformation conditions for akaganéite occur in 0.5M NaOH, or alkaline sulphite solutions with 0.1 – 0.5 M NaOH and 0.05 – 0.5M Na₂SO₃, both under heated conditions. If this is the case, decreasing the concentration of NaOH in treatment solutions may reduce the extraction of chloride ions from akaganéite. Leaving chloride ions in the structure of akaganéite does not pose an immediate corrosion risk, but if akaganéite is metastable and slowly transforms to another corrosion product, this structural chloride will be released and may pose later corrosion problems. It is not known how much akaganéite may form on objects, how long the transformation may take or how much chloride may be released by this process.

However, given that the manufacturing method and shape of akaganéite crystals appears to have a significant influence on its behaviour in treatment solutions, it is necessary to gain a better understanding of how these synthetically produced samples compare to those of akaganéite formed on archaeological objects, and so the results of this study cannot be directly extrapolated to the behaviour of treatments on objects. The study of the nature and behaviour of akaganéite on objects is likely to be a more fruitful approach in understanding the effect of treatment solutions than continued studies on synthetic akaganéite.

Chapter 6 – The risks of desalination treatment

Damage is usually associated with a loss of material, a loss of well-being or a loss of expectation. Not everything that people consider as damage results in a change of value. Not every change in physical or chemical properties results in loss.

Ashley-Smith 1999: 99

One of the objectives of this study is to consider the possible risks that treatments pose to objects, and how these might be quantified and evaluated. Short term risks during treatment include the immersion in solution causing mechanical change to the corrosion products, chemical changes induced by the treatment solution, or physical change caused by handling during solution changes. Long-term risks may be posed by residues of the treatment solution left in the object, but there is very little information available about the formation of compounds, what hazards they might pose, and their effects on objects.

Although intensive post-treatment rinsing has been a normal part of conservation procedure (e.g. North & Pearson 1978b; Keene 1994; Wang et al. 2008), there has been no study of the effectiveness of rinsing at removing chemical residues and any risks posed by the rinsing process itself. There are no clear guidelines on best practice for rinsing and drying of objects once treatment is complete.

Three aspects of risk are assessed in this chapter:

- Short-term risk: A qualitative assessment of the condition of the objects was undertaken using photographic records to determine the type and frequency of changes occurring during treatment.
- Long-term risk: The formation and behaviour of a range of treatment residues were modelled under controlled relative humidity (RH) and temperature conditions.
- The effect of rinsing: A small number of test objects were rinsed in deionised water to determine whether any detrimental outcomes occurred.

6.1 Short term risk – change to objects during treatment

Quantifying damage to objects is difficult, as changes to objects become damage only when there is a negative impact on the value of the objects (Ashley-Smith 1999). As so much of

the value of archaeological objects lies in their context as part of an assemblage belonging to a particular site (Berducou 1996), change to one or more objects must be evaluated in relation to its effect on the entire site as well as the individual objects. Placing too great an emphasis on individual objects when their value is partly or wholly collective may lead to an over-inflated sense of risk. Changes to objects occurring during treatment should not be described as damage without carefully considering whether the value of the object, the information it contains and the material archive of the archaeological site as a whole has been reduced.

The relationship between change and damage cannot be determined for the objects in this study, but it is possible to categorise change occurring to the objects due to the treatment procedures, without making statements about whether these changes represent damage. By determining how frequently various types of changes occur during treatment, conservators will be able to assess more easily whether changes which constitute damage in each individual situation are likely to occur.

Little direct data exists on whether desalination treatments are damaging to objects. Fragmentation of corrosion layers during treatment is widely reported, and seems to depend in part on the previous condition of the object (Wang et al. 2008). The 'softening' of corrosion products which has been mentioned (Selwyn & Logan 1993; Argyropoulos et al. 1997; Selwyn & Argyropoulos 2005) is described variously as increased porosity, fragility, and corrosion becoming 'mushy', but no analysis has been undertaken to determine what causes these apparent phenomenon. It is not known whether the softening refers to a mechanical change, such that the corrosion products fragment more easily, or a chemical change to the corrosion layers. The action of plasma treatments has sometimes been described as 'softening' corrosion layers (Scott & Eggert 2009: 137), which the analysis of Schmidt-Ott (2004) implies is a mechanical breaking of the outer corrosion products to expose the original surface. The terminology used to describe changes to corrosion layers is somewhat inconsistent and unqualified. Immersion in inert liquids of a similar surface tension to water would help to distinguish whether the changes are mechanical or chemical.

Hjelmhansen et al. (1992, 1993) suggested that during treatment in sodium hydroxide, objects underwent rapid oxidation-reduction reactions involving the metal substrate,

magnetite in the corrosion layers and ferrous ion species. These electrochemical reactions increased the porosity of the corrosion layers, and this might be related to the fragmentation seen during treatments (Selwyn & Argyropoulos 2005). Microstructural changes during immersion in sodium hydroxide and ethylenediamine solutions have also been observed on experimental corrosion samples, with the corrosion structure becoming more compact and cracking (Liu & Li 2008). This points to a change in the structure of the oxide layers, but there is no clear indication of what this change is.

The high pH of treatment solutions has been blamed for causing damage to corrosion layers. Argyropoulos et al. (1997) suggest that the pH of most treatment solutions is high enough to allow dissolution of corrosion products. Although the solubility of iron corrosion products is higher at alkaline pH than at neutral pH (Cornell & Schwertmann 2003), these values are calculated rather than empirically determined. Experiments to determine solubility constants for the iron oxyhydroxides show that it takes several years for goethite to achieve equilibrium solubility in alkaline conditions. The solubility of a compound says nothing about the rate at which dissolution occurs (Cornell & Schwertmann 2003: 201). It is not clear, therefore, that physical dissolution of corrosion products is a significant factor in the relatively shorter treatment times used by most conservators. It must be noted that the treatment of Argyropoulos et al. (1997) where 'softening' was noticed involved 8-12 month immersion in NaOH, rather than the 3-4 months used elsewhere (Keene 1994; Schmidt-Ott & Oswald 2006; Wang et al. 2008). Several studies have noted that heavily mineralized objects or those without a substantial metal core are at greater risk during desalination treatment (Bradley 1988; Selwyn & Logan 1993; Argyropoulos et al. 1997), although the reasons for this are not known. The original condition of objects was noted by Wang et al. (2008) to play a role.

6.1.1 Methodology for assessing change

The large number of objects in this study made it impossible to carry out full conditions assessments for each object. Objects were photographed before and after treatment. These photographs were then compared to give a qualitative analysis of the changes occurring during treatment.

Various types of changes were noted. Fragments were detached from objects during the treatment, either during immersion or during handling during solution changes. The objects were handled using plastic tweezers or, occasionally, nitrile-gloved fingers, but no supports or trays were used. Some objects appeared to have changed colour, particularly those from the site of Billingsgate, although colour changes on photographs cannot be directly compared due to differences in lighting conditions. Flakes of corrosion product and adhering soil particles were also removed from some objects by the treatments.

A method was needed to categorise the types of change so their frequency could be counted. This needed to be simple, rapid and use visual assessment only from the photographs, avoiding any judgement about the significance of changes in terms of damage. Changes to the corrosion products and the overall shape and coherence of the object needed to be considered, and the categories needed to be well-defined so they could be applied consistently without overlap.

A system of four categories was developed and is given in Table 15. The main criterion used to distinguish levels of change was the effect that removal of material had on the integrity of the object as a whole. Changes to the shape of the object are therefore the focus of category C and D, with D being sufficient fragmentation that the shape of the object is no longer recognisable. Category B changes are those where, although some removal of corrosion products has occurred, the overall shape and integrity of the object is not affected. Category A objects include those where no visible change has occurred, or only soil products have been removed. Although some of the objects appeared to display colour changes, these were not included as a separate group, as it was not always possible to distinguish whether the colour of corrosion products had actually altered or whether it was the action of desalination treatment in removing soil and dust, or the effects of lighting and camera type. Where colour change was the only visible difference, the objects have been

included in category A. Although the categories are broad, they provide an overview of the types of change that may occur and grade them into increasing levels of change, with A the lowest and D the highest. Examples of each type of change are given in Figure 60. Where an object experienced more than one type of change (e.g. soil removal plus category C fragmentation) it was graded into the worse of the two.

Table 15: Criteria for assessing change to objects during desalination treatment.

| Category of change | Description |
|---------------------------|--|
| A | No change OR loss of adhering soil products OR possible colour change. |
| B | Removal of flakes of corrosion products, but no effect on the overall shape of the object |
| C | Removal of up to three fragments which changes the overall shape of the object |
| D | Removal of sufficient fragments to destroy the original shape of the objects and/or total fragmentation of the corrosion layers. |

To carry out the comparison, the pre and post-treatment photographs of each object were imported into photo-editing software (Adobe Photoshop Elements) and compared. High resolution photographs had been taken from all sides of the object before and after treatment (usually between three and four photographs per object), and detail was viewed by zooming in on individual parts of the object. A qualitative judgement of the changes occurring to the object was made and a category assigned.

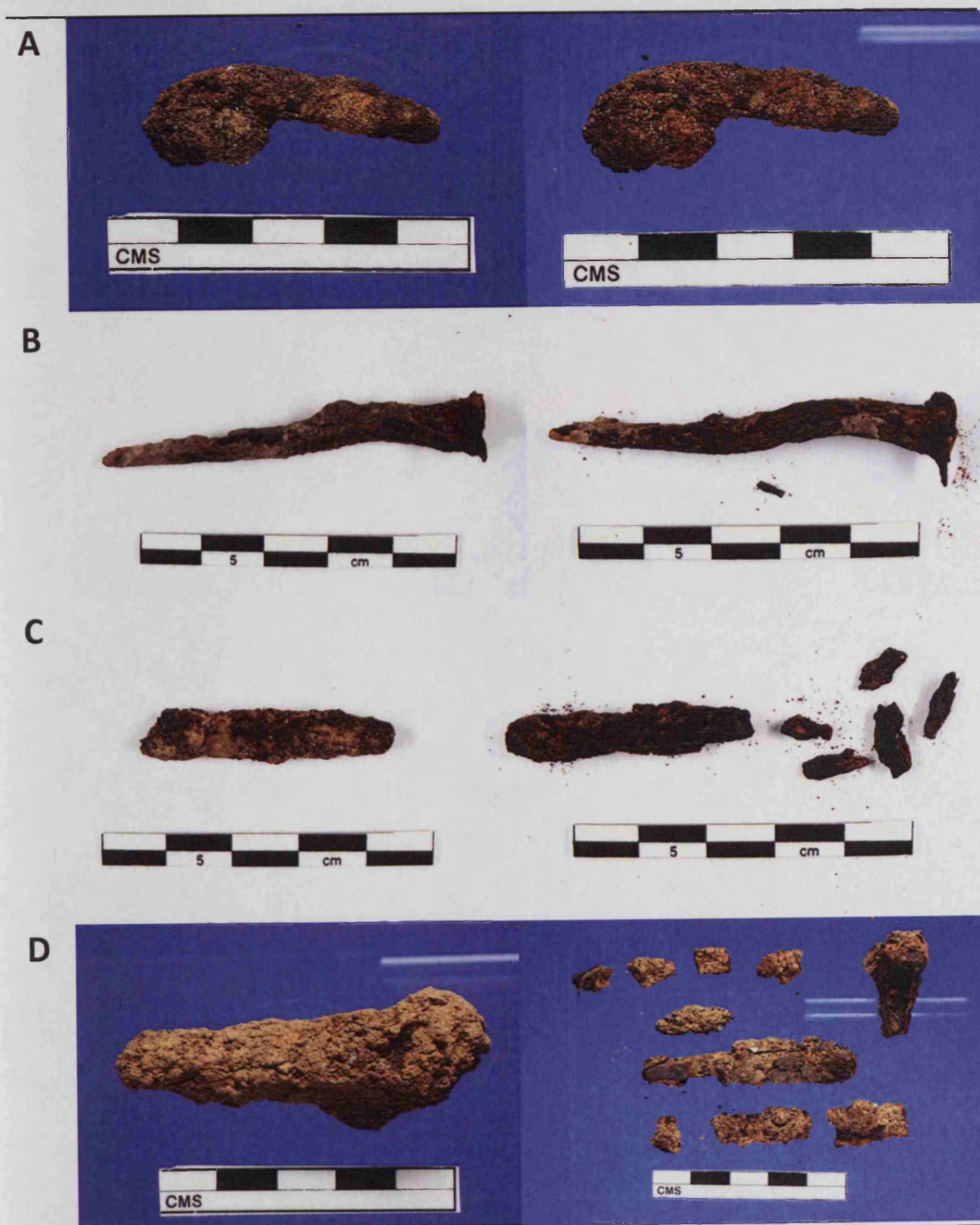


Figure 60: Examples of objects falling into each of the four change categories. Left: Before treatment. Right: After treatment. A = BOR_6510 (dNaOH), B = BWB83_40 (AS20), C = BOR_6750 (AS20), D = CAE_14 (dNaOH).

6.1.2 Results of photographic analysis

The results of the photographic analysis are given in Table 16.

Table 16: Results of photographic analysis of change to objects during treatment.

| Category | % of objects in change category | | | |
|----------|---------------------------------|-------------|-------------|-------------|
| | dNaOH (n=48) | AS20 (n=48) | AS60 (n=24) | All (n=120) |
| A | 73 | 69 | 62 | 69 |
| B | 21 | 21 | 21 | 21 |
| C | 4 | 8 | 17 | 8 |
| D | 2 | 2 | 0 | 2 |

For all three treatments, the majority of objects fall into category A, with either no change or only loss of soil or visual appearance, with no change to the integrity of the object. Only one object from each of dNaOH and AS20 was categorised as D, and no objects from AS60. Objects in category C, where there was some change to the integrity of the object but not full fragmentation are also uncommon, with only 8% of objects in this category overall, although AS60 had 17% objects in this category, more than either of the room temperature treatments. 21% of objects fell into category B for all three treatments.

Overall, the results suggest that most of the objects were not changed to a great extent by the treatments. Of the three treatments, AS60 appears to cause the most change to objects, with 38% of objects (B, C and D) experiencing some level of change to the corrosion layers or object shape (Table 16). It could be suggested that heating the treatment solution to 60°C is more likely to cause change to the objects (Selwyn 2004; Selwyn & Argyropoulos 2005). However, a chi-squared test (see Appendix 3) on the data reveals that at .05 significance, the difference between the treatments is not significant ($\chi^2_{\text{calc}} = 3.67$, $\chi^2_{\text{crit}} = 12.59$). Both dNaOH and AS20 have similar effects on the objects, with only slight variation in category A and C (Table 16). It does not seem that alkaline sulphite is more aggressive than sodium hydroxide, or causes more or different changes, despite the introduction of sulphite ions into the objects.

6.1.3 Discussion

With so little information available on the effects of treatment on objects immediately after the treatment, it is not possible to compare this data with previous work. Colour changes were seen most commonly on Billingsgate objects, and may be related to the unusual chemical composition of the urban soil environments from which the objects came, including water-logged and anaerobic sites. These sites may include iron sulphide corrosion products such as greigite (Fe_3S_4) which occur on objects when oxygen is absent and hydrogen sulphide is present (Scott & Eggert 2009). Iron sulphides are more reactive than the iron oxyhydroxides and may therefore have undergone some transformation during the treatment. Analysis of corrosion product composition using Raman spectroscopy would have been beneficial to evaluate this, but could not be completed due to time factors.

It was not possible to assess the claims that desalination treatment 'softens' corrosion products on objects. Although some fragmentation of the corrosion layers was observed, only one-third of objects experienced any fragmentation. This suggests that fragmentation may be linked more closely with the condition of individual objects than any chemical transformation of corrosion products. The nails selected for treatment were generally in good condition, with no obvious loose flakes, although some exhibited cracking and the presence of akaganéite. The claim of softening needs to be assessed more carefully using analytical techniques, e.g. hardness testing, but this was not possible in this study.

The observations made on the samples treated are on a macroscopic scale, and it cannot be ruled out that more detailed and microscopic analysis would have revealed other changes to a greater number of the objects, not visible in this overview. However, the anecdotal perception that immersing objects in desalination treatments causes them to 'fall apart' is not borne out by this study, as less than 2% of the objects suffered total disintegration. It is possible that in conservation practice where objects are not routinely treated, desalination treatment is only used when objects are already rapidly corroding and fragmenting. This is the case with treatment testing at The British Museum, where the objects selected for treatment were already in poor condition, and this was a major contributor to the flaking and fragmentation occurring during treatment (Tam 2009). Earlier treatments may also have been oxygenated, allowing corrosion to occur during treatment and further weakening the object, leading to fragmentation.

If the condition of objects has a bearing on the likelihood of object collapse or fragmentation on immersion, an argument can be made for treating objects before corrosion causes their condition to deteriorate significantly. There are other arguments for why early treatment may be advisable, which are discussed further in Chapter 8. A further factor may be the handling of objects when wet, which may increase the likelihood of fragmentation by disturbing the corrosion layers. Methods of reducing handling of objects such as the use of trays and supports are an important consideration in protecting objects during desalination.

6.1.4 Probability of short-term outcome

For the data on change during treatment to be used in the modelling of treatment outcomes, a relationship between change and value does need to be established. This is problematic, as discussed earlier, but categorisation into the three broad damage outcomes defined in Chapter 3 (no damage, some damage, total loss, Table 2) is attempted to allow treatment evaluation in these terms.

Category D objects, those which were totally fragmented by the treatment, are most easily defined as damage, as the object is no longer whole and reconstruction from such a state would be near to impossible. Category D objects can therefore be equated with the state of total loss of value. Category A objects were those which suffered no change or lost only soil products. With no obvious changes occurring, these would not be viewed as damaged.

It is the intermediate change categories B and C which are most difficult to assess. The point at which the removal of small flakes or fragments becomes a significant loss of value cannot be assessed on the available evidence. It would depend in large part on the type of object, whether there were any mineral-replaced organic materials preserved in the corrosion layers, the uniqueness of the object and its importance within the material archive, and other factors. To steer towards a cautious approach, categories B and C together will be taken to calculate the probability of 'some damage'. The reasoning is that in both categories, the object retains all or most of its shape and constituent parts, and that the flakes and fragments removed could be reattached. There is not a total loss of information, but some value could be lost by the removal of flakes and fragments.

Using these three categories, no damage (A), some damage (B and C), and total loss (D), the number of objects from the treated sample in each damage category were calculated. Table 17 presents the number and percentage of objects in each category for each of the three treatments. Probabilities (P_d) are simple conversions from %, and represent the likelihood that any one object would fall into each category.

Table 17: Probability of damage during treatment based on change analysis.

| | dNaOH (n=48) | | | AS20 (n=48) | | | AS60 (n=24) | | |
|--------------------|--------------|----|-------|-------------|----|-------|-------------|----|-------|
| | n | % | P_d | n | % | P_d | n | % | P_d |
| No damage | 35 | 73 | .73 | 33 | 69 | .69 | 15 | 62 | .62 |
| Some damage | 12 | 25 | .25 | 14 | 29 | .29 | 9 | 38 | .38 |
| Total loss | 1 | 2 | .02 | 1 | 2 | .02 | 0 | 0 | 0 |

This method of quantifying damage to objects is crude, as it is not based on detailed assessments of individual objects and an appreciation of how their value is decreased by removal of flakes or fragments. These probabilities will be used in the Chapter 7 to indicate how data such as this can make a helpful contribution to an overall assessment of treatment outcomes, but much more work is required to properly assess the complex relationship between change and damage. The use of this data in assessing treatment outcome is a preliminary attempt to make an overall assessment, but the limitations of the method are acknowledged.

6.1.5 Conclusion on damage from treatment

The qualitative assessment of change to objects as a result of treatment, although a rapid assessment with little detail, leads to two initial conclusions:

- The majority of objects (69%) were not significantly affected by desalination treatment. The frequency of change decreases with its severity: less than 2% of objects had their overall shape destroyed by treatment.
- There is no significant difference in change frequencies between treatments. Heated treatment does not increase the frequency of change. The main factors leading to change appear to be the condition of the object before treatment and, possibly, the amount of handling of the objects while wet.

Although the relationship between change and damage is complex, a simple relationship was established to allow the probability of levels of damage (no damage, some damage and total loss) to be calculated from the data in this section. This will contribute to an overall assessment of treatment outcomes in Chapter 7.

6.2 Long-term risk – treatment residues

Chemical residues from treatment solutions are a potential future risk factor for objects. Although several studies on desalination treatment mention the possible effects of residues (North & Pearson 1975; Turgoose 1993; Watkinson 1996), there has been no examination of the formation of residues or their effects on corrosion rate. Extensive rinsing programmes to remove the chemical solution, reduce pH to neutral and remove remaining anion may themselves be potentially detrimental. Exposure to oxygenated water, sometimes heated, could restart corrosion which has been inhibited during an oxygen-free treatment. The issue of chemical residues therefore must be addressed to determine whether rinsing programmes are in fact necessary.

Alkaline sulphite treatment produces Na^+ , OH^- and SO_3^{2-} ions. Atmospheric oxygen will react with SO_3^{2-} to form SO_4^{2-} . Any Fe^{2+} from pre-treatment corrosion will react with OH^- ions during treatment to produce insoluble $\text{Fe}(\text{OH})_2$ that later oxidises to other compounds. Upon completion of treatment Cl^- and Fe^{2+} concentrations in the alkaline sulphite solution and corroded iron matrix are expected to be low. Further Fe^{2+} may form if post-treatment corrosion occurs. Drying treated iron objects without washing will mean they contain Na^+ , OH^- , SO_4^{2-} and SO_3^{2-} , although some residual SO_3^{2-} could be removed by adsorption onto corrosion products during drying (Kaneko 1993).

Hygroscopic iron sulphate (FeSO_4) formation after treatment (Turgoose 1993) has been suggested as a high-risk residue. FeSO_4 is implicated in some atmospheric corrosion cycles (Schwarz 1965a, 1965b; Dünwald & Otto 1989), and is thought to increase corrosion rates significantly above 60% RH (Jones 1996; Selwyn et al. 1999). Since Fe^{2+} precipitates as insoluble ferrous hydroxide during treatment, renewed corrosion must supply Fe^{2+} to form FeSO_4 . However, FeSO_4 may not form, as oxidation of Fe^{2+} in SO_4^{2-} containing solutions favours goethite ($\alpha\text{-FeOOH}$) formation via an intermediate sulphate-containing Green Rust II (Refait & Génin 1994; Oh et al. 2002). The aggressive role of iron sulphate in atmospheric

corrosion of iron (Schwarz 1965a, 1965b; Stambolov 1985) has also been questioned (Weissenrieder et al. 2004; Cai & Lyon 2005). Although iron sulphate is occasionally found on objects due to sulphate ions in the burial environment, (Knight 1982) it has not been implicated in accelerating corrosion of excavated objects.

Currently there is no evidence either that iron sulphate forms on alkaline sulphite treated iron or that it offers a corrosion risk. Post-treatment drying may also form sodium sulphate (Na_2SO_4), but this has not been confirmed nor has its potential effect on iron objects been examined.

A series of experiments were undertaken to answer the most pressing questions: what residues are likely to form from treatment solutions, specifically alkaline sulphite, and what effect are these compounds likely to have on the corrosion of iron? Although not an exhaustive study of all possible residues, the most likely residues are addressed and their effects on iron in set RH conditions modelled using synthetic powders. This does not replicate directly the situation on objects after treatment, but should indicate which residues are of concern and need to be investigated further.

6.2.1 Methodology

The formation of residues was tested by evaporating solutions containing relevant ions from alkaline sulphite treatment and analysing the compounds formed. AnaLar grade reagents were used throughout, and X-ray diffraction (XRD) was carried out. Panalytical X'Pert High Score software was used to identify and calculate approximate quantities of the principal products (see Appendix 2.1).

Solution mixtures in Table 18 were evaporated to dryness over several days in an open container in the laboratory (35-60% RH approx. 20°C). They simulated:

- Oxidation of sulphite ions in atmospheric conditions.
- Formation of compounds from solutions containing Fe^{2+} , Na^+ , SO_4^{2-} and Cl^- ions that may occur on the surface of iron during post-treatment drying.
- Drying of alkaline sulphite ($\text{NaOH}/\text{Na}_2\text{SO}_3$) solutions containing both Cl^- and Fe^{2+} .

Reactions of various combinations of solid sodium sulphate, ferrous sulphate and sodium chloride with nitrogen-reduced iron powder were examined at 20°C ($\pm 0.1^\circ\text{C}$) and fixed RH

(±1%) in a Vötsch VC4018 climatic chamber (Table 19). A Mettler AJ100 balance (±0.0001 g) recorded weight change to file every 5 minutes to offer hydration, dehydration and corrosion data (see Appendix 1.5). All components were powders and mixed in the ratio 1:1 by weight and spread out in a plastic Petri dish to provide maximum surface area for reaction. Controls of Na₂SO₄, FeSO₄·7H₂O, FeSO₄·4H₂O and Fe were run. The instability of the balance from chamber vibration produces reproducible weight fluctuation (Appendix 1.5), but this makes very slow corrosion trends difficult to distinguish over the short time periods available for testing. Visual examination under low-power magnification was used to check for any signs of corrosion occurring.

Table 18: Solutions evaporated to dryness to simulate treatment residue formation. Results of the product analysis are given.

| Starting solution | Products on drying | Approximate proportions (±10%) |
|---|---|---------------------------------|
| 1M Na ₂ SO ₃ | Na ₂ SO ₄ | 64 |
| | Na ₂ SO ₃ | 36 |
| 1M FeCl ₂ ·4H ₂ O / 1M Na ₂ SO ₄ | FeSO ₄ ·7H ₂ O | 52 |
| | FeSO ₄ ·4H ₂ O | 17 |
| | NaCl | 30 |
| 0.1M NaOH / 0.05M Na ₂ SO ₃ / 0.05M FeCl ₂ ·4H ₂ O | Na ₂ SO ₄ | 49 |
| | NaCl | 47 |
| | γ-FeOOH | 4 |
| 1M NaOH / 1M Na ₂ SO ₃ / 0.1M FeCl ₂ ·4H ₂ O | Na ₆ (CO ₃)(SO ₄) ₂ | 56 |
| | Na ₂ SO ₄ | 29 |
| | NaCl | 13 |
| | γ-FeOOH | 2 |

Table 19: Solid-state experiments to evaluate the effect of residues on iron corrosion. Compounds 1 and 2 were mixed and exposed to the given RH at 20°C in the climate chamber.

| Compound 1 | Compound 2 | RH (%) |
|--|------------|-----------|
| Fe | - | 75 and 90 |
| Na ₂ SO ₄ | - | 75 and 90 |
| Na ₂ SO ₄ | Fe | 75 and 90 |
| FeSO ₄ ·7H ₂ O | - | 75 |
| FeSO ₄ ·4H ₂ O | - | 75 |
| FeSO ₄ ·7H ₂ O | Fe | 75 |
| FeSO ₄ ·4H ₂ O | Fe | 75 |
| FeSO ₄ ·4H ₂ O/FeSO ₄ ·7H ₂ O/NaCl | Fe | 75 |

6.2.2 Results – formation of residues

Results of the evaporation tests are shown in Table 18. Evaporation of Na₂SO₃ solution produced partial oxidation of SO₃²⁻ leaving a Na₂SO₄/Na₂SO₃ mixture. Evaporating freshly mixed FeCl₂/Na₂SO₄ solution produced a ferrous sulphate/sodium chloride mixture (Table 18). After standing for several weeks in a stoppered volumetric flask in the laboratory the FeCl₂/Na₂SO₄ solution formed natrojarosite (NaFe₃(SO₄)₂(OH)₆).

The NaOH/Na₂SO₃/FeCl₂·4H₂O solution precipitated a greenish solid immediately upon mixing. Subsequent evaporation of the solution produced either Na₆(CO₃)(SO₄)₂/Na₂SO₄/NaCl/γ-FeOOH for high concentration of NaOH/Na₂SO₃ or Na₂SO₄/NaCl/γ-FeOOH for low NaOH/Na₂SO₃ concentrations (Table 18). In neither instance was NaOH identified as a product of evaporation. The appearance of carbonate ions for the formation of burkeite (Na₆(CO₃)(SO₄)₂) results from the reaction of sodium hydroxide with dissolved carbon dioxide. No ferrous sulphate appeared in alkaline solutions, with ferrous ions precipitating initially to a precipitate assumed to be a green rust and then oxidising to γ-FeOOH.

6.2.3 Results – the effect of residues on iron corrosion

In solid phase tests at 75% RH and 20°C neither anhydrous Na₂SO₄ nor iron powder showed detectable weight gain (Figure 61). The weight gain of Na₂SO₄/Fe was slight over a 16 day period (Figure 61) with a few very small visible nodules of orange-brown corrosion products.

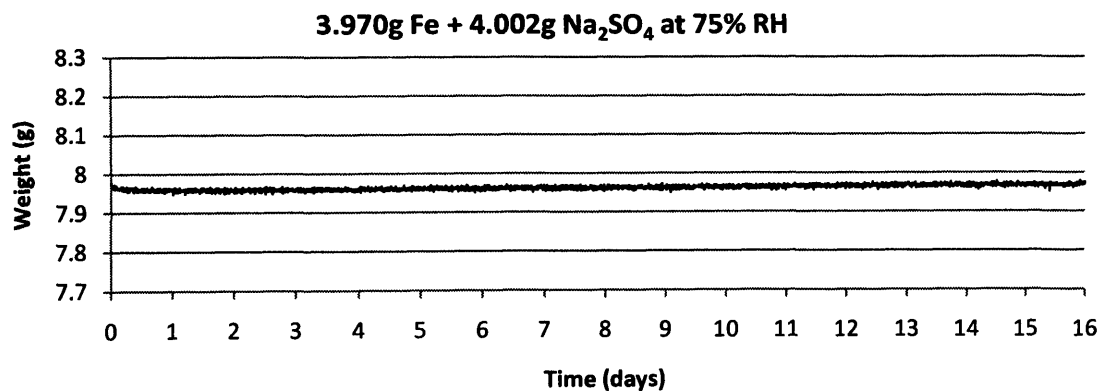
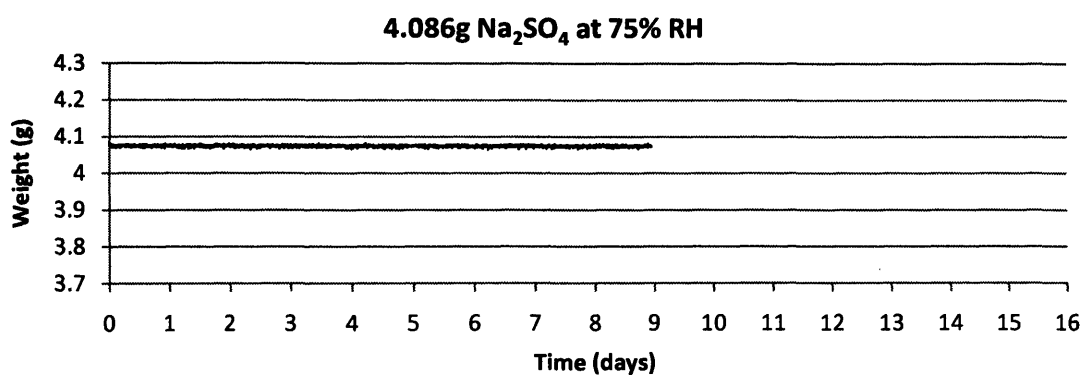
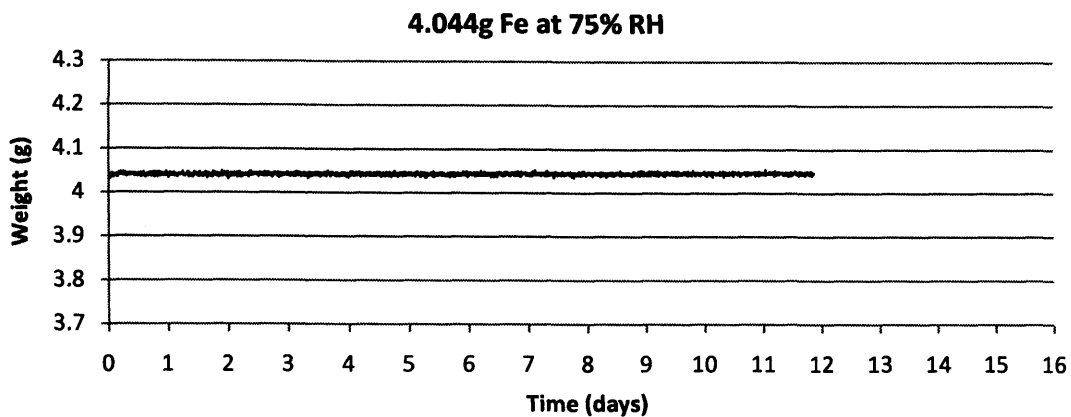


Figure 61: Weight measurements of Fe, Na₂SO₄ and a mix of both at 75% RH. Weight gain for the mixture (bottom graph) is minimal over 16 days.

Anhydrous Na₂SO₄ exposed to 90% RH hydrated rapidly (Figure 62) producing a mix of liquid and solid Na₂SO₄ in less than 24 hours. A Na₂SO₄/Fe mixture was slower to hydrate (Figure 62) but small quantities of iron corrosion product were observed within a day. These were insufficient for XRD analysis.

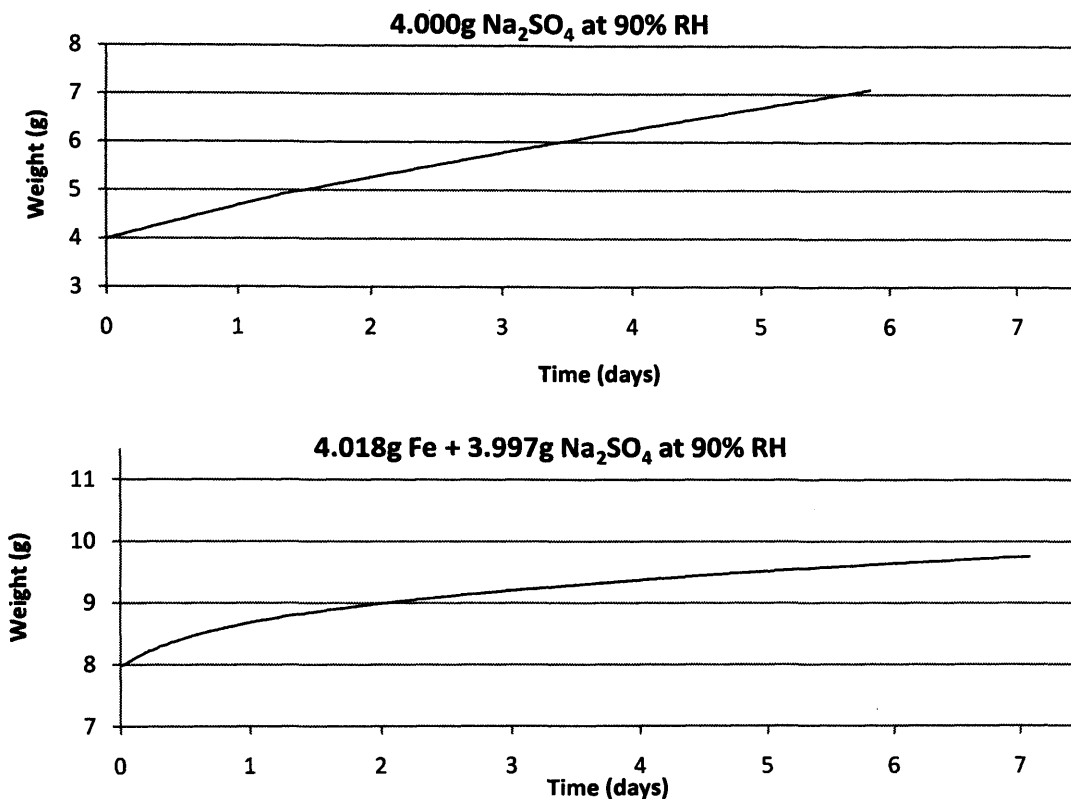


Figure 62: Weight measurement of Na₂SO₄ and Fe/Na₂SO₄ at 90% RH. Hydration is rapid in both cases.

Exposing FeSO₄·7H₂O to 75% RH 20°C showed no weight gain over 7 days (Figure 63). This is not surprising, as the maximum hydration state of FeSO₄ is 7, and it does not deliquesce until around 95% RH (Table 20). In the same conditions a FeSO₄·7H₂O/Fe mixture slightly increased in weight, although after eight days visual inspection could not identify iron corrosion products. This suggests that when mixed with iron at 75% RH, FeSO₄·7H₂O may cause slow corrosion of iron, but this is very limited at this RH. Longer periods of exposure may allow corrosion products to be detected.

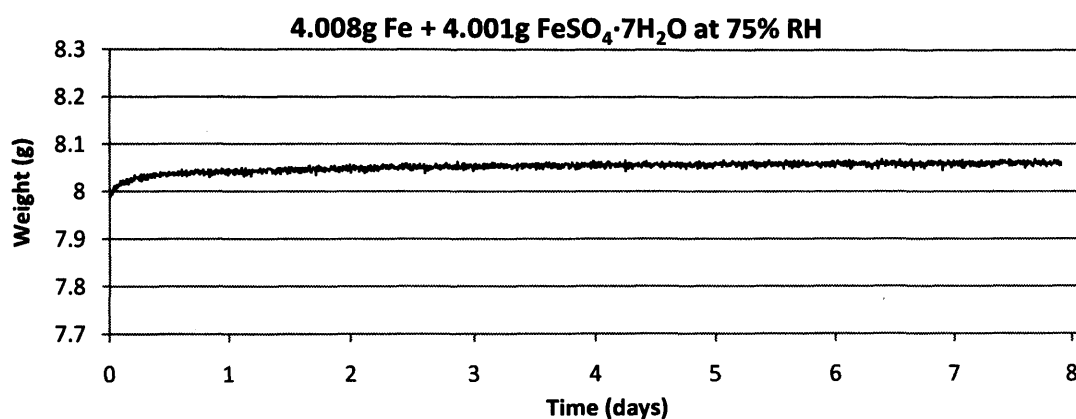
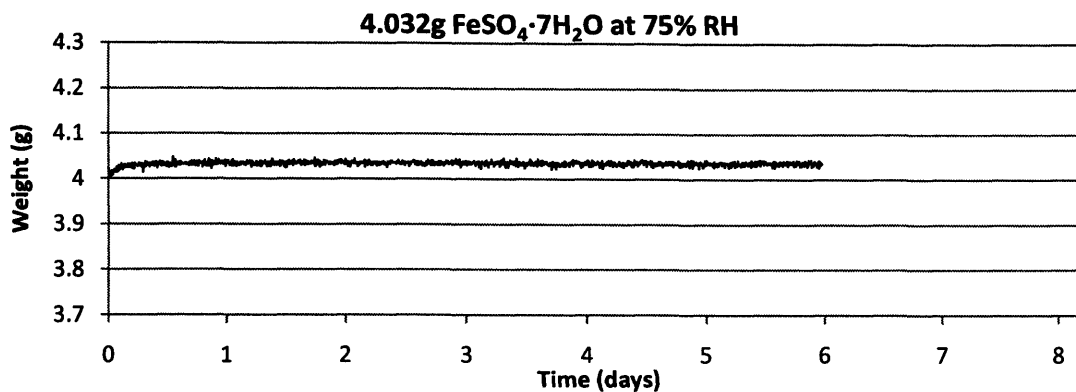


Figure 63: Weight measurements for FeSO₄·7H₂O and Fe/FeSO₄·7H₂O. The 7-hydrate does not gain noticeable weight. Very slow weight gain is occurring in the mixture.

As FeSO₄·7H₂O did not cause significant corrosion of iron at 75% RH, FeSO₄·4H₂O was hydrated to examine if the change to FeSO₄·7H₂O caused corrosion. Hydration of FeSO₄·4H₂O at 75% RH was rapid, completing within one day and gaining no further weight (Figure 64). When mixed with iron powder, weight gain was slow and continued to increase over a 33 day period, slowing down and flattening after 30 days. Corrosion was not visible on the sample. The majority of the weight gain is hydration, which is occurring much more slowly than FeSO₄·4H₂O on its own.

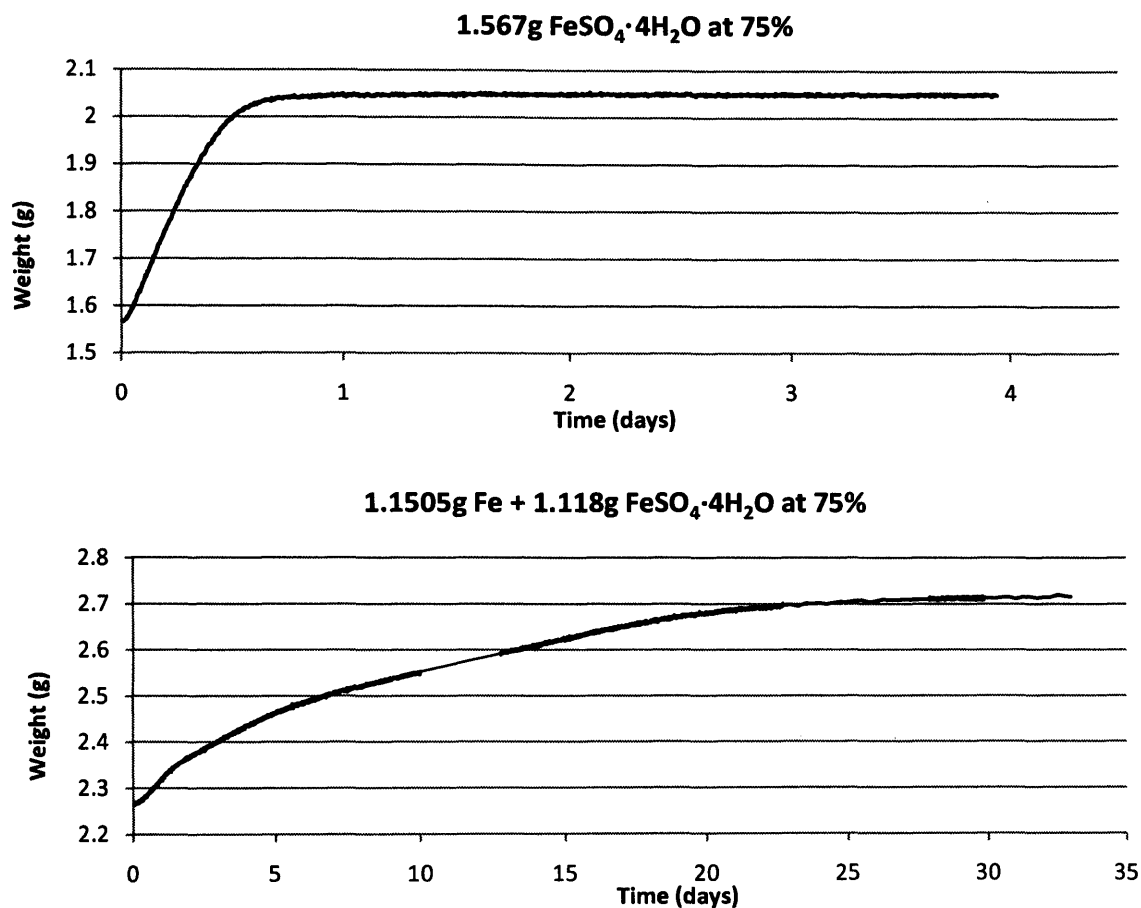


Figure 64: Hydration of FeSO₄·4H₂O and Fe/FeSO₄·4H₂O at 75% RH. Hydration of ferrous sulphate is complete within 1 day with no further weight change. The mixture gains weight more slowly. The line has been extrapolated in two places due to failure of the software to record for short periods of time during this test.

FeSO₄·4H₂O/FeSO₄·7H₂O/NaCl, produced by solution evaporation from 1M FeCl₂·4H₂O/1M Na₂SO₄ (Table 18), was mixed with an equal weight of iron powder and exposed at 75% RH to see if the addition of c. 30% NaCl increased corrosion compared to sulphate compounds. Corrosion was readily visible within hours and weight gain was rapid and continuous (Figure 65). Corrosion was ongoing and greater than for any of the sulphate-containing compounds studied in these experiments.

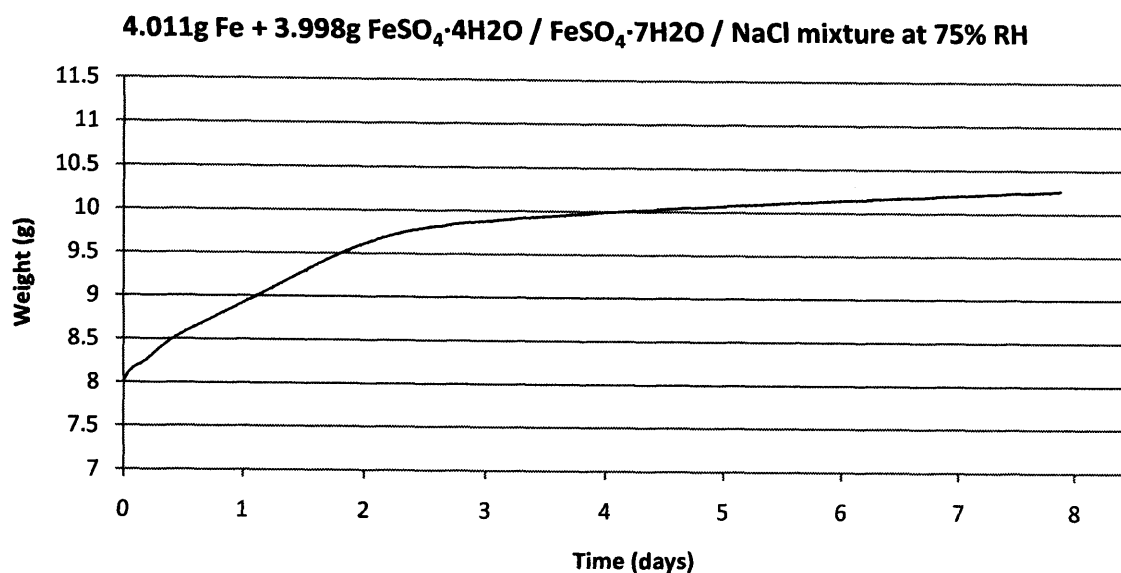


Figure 65: Weight gain caused by including NaCl in a mixture of Fe and FeSO₄. At 75% RH weight gain is rapid and continuous, with much greater weight gain than any other test.

6.2.4 Discussion

Many of the compounds formed by evaporation are hygroscopic (Table 20). NaOH is not included in Table 20, as no solid NaOH was identified in any evaporate.

Table 20: Transition RH and deliquescence RH for the compounds in this study. RH values are given for 20°C. Note that the only hydrated form of NaCl, NaCl·2H₂O, is not stable at atmospheric pressure above a temperature of 0.1°C, and is therefore not relevant to this study. References: ¹Steiger & Asmussen 2008, ²Chou et al. 2002, ³Ehlers & Stiles 1965, ⁴Linnow & Steiger 2007

| Compound | Transition RH (%) | Hydrated form | Deliquescence RH (%) |
|--|---------------------|---|----------------------|
| Na ₂ SO ₄ (thenardite) | 76.4 ¹ | Na ₂ SO ₄ ·10H ₂ O (mirabilite) | 95.6 ¹ |
| FeSO ₄ ·4H ₂ O (rozenite) | c. 60% ² | FeSO ₄ ·7H ₂ O (melanterite) | c. 95% ³ |
| NaCl (halite) | N/A | N/A | 75.4 ⁴ |

Incomplete oxidation of Na₂SO₃ upon drying probably results from high SO₃²⁻ concentration and speedy evaporation. Formation of both FeSO₄·4H₂O and FeSO₄·7H₂O from the

evaporating $\text{FeCl}_2/\text{Na}_2\text{SO}_4$ solution was most likely the result of partial dehydration of $\text{FeSO}_4 \cdot 7\text{H}_2\text{O}$ during storage. The modelling tests suggest that NaCl is the most problematic residue, but levels of chloride ions should be low in objects after desalination compared to the concentration of sulphate ions. Similarly, all the evaporated solutions in these tests are likely to contain more ferrous ions than occur on desalinated objects after treatment, as ferrous ions are removed or fixed by the treatment.

Although chloride remaining after alkaline sulphite treatment might be expected to be deep seated at the metal surface, adsorbed onto $\alpha\text{-FeOOH}$ and contained in $\beta\text{-FeOOH}$, formation of small amounts of NaCl cannot be discounted as solutions concentrate during drying and it readily formed during drying of solutions tested here. However, no ferrous chloride was detected after evaporation of $\text{FeCl}_2/\text{Na}_2\text{SO}_4$ solution, and since $\text{FeCl}_2 \cdot 4\text{H}_2\text{O}$ corrodes iron at very low humidity, this is a welcome result (Watkinson & Lewis 2005a).

Formation of natrojarosite ($\text{NaFe}_3(\text{SO}_4)_2(\text{OH})_6$) from $\text{FeCl}_2/\text{Na}_2\text{SO}_4$ solution after several weeks should not be a worry for alkaline sulphite treated objects. Formation of jarosite minerals requires acidic conditions (Baron & Palmer 1996), making them unlikely products of alkaline treatment. Additionally, being stable (Navrotsky et al. 2005) and non-hygroscopic they do not pose a corrosion risk (Vaniman et al. 2008).

6.2.4.1 Sodium sulphate

Sodium sulphate was shown to offer a limited corrosion threat at 75% RH. It exists mainly as anhydrous Na_2SO_4 (thenardite) and $\text{Na}_2\text{SO}_4 \cdot 10\text{H}_2\text{O}$ (mirabilite) (Table 20). The phase transition RH for Na_2SO_4 is reported as 76.4% RH at 20°C (Steiger & Asmussen 2008). The test results agree with this as anhydrous Na_2SO_4 was stable at 75% RH (Figure 61). It did produce very minor corrosion of iron over a 17 day period at 75% RH (Figure 61), but this may reflect the chamber RH fluctuation of $\pm 1\%$ producing a very small amount of corrosion as the phase transition point to $\text{Na}_2\text{SO}_4 \cdot 10\text{H}_2\text{O}$ is approached. Longer test periods may reveal whether this is the case.

Deliquescence of Na_2SO_4 occurs at 95.6% RH (Table 20), but some liquid was observed during hydration of Na_2SO_4 at 90% RH. This facilitated rapid corrosion of iron within a short time (Figure 62). Hydration of the $\text{Na}_2\text{SO}_4/\text{Fe}$ mix was slower than for Na_2SO_4 alone; this is probably due to adhesion of iron powder to the Na_2SO_4 crystals reducing the diffusion rate

of water to the crystal (Linnow et al. 2006). Pragmatically, the risk to iron from Na_2SO_4 residues can be interpreted as being very limited below 75% RH from the results presented here. Although the corrosion risk is much greater as the deliquescence RH is approached and an electrolyte solution is formed, this will occur only at RH close to the deliquescence point and is therefore unlikely in iron storage, and easy to control by maintaining RH less than 75%.

Formation of Na_2SO_4 or $\text{Na}_2\text{SO}_4 \cdot 10\text{H}_2\text{O}$ during drying from a solution depends on environmental RH and temperature (Steiger & Asmussen 2008). At RH > 40%, $\text{Na}_2\text{SO}_4 \cdot 10\text{H}_2\text{O}$ crystallizes and then dehydrates to Na_2SO_4 . At RH < 15% only anhydrous Na_2SO_4 forms and between 15-40% RH both phases occur simultaneously. Above 32.4°C only anhydrous Na_2SO_4 forms (Rodriguez-Navarro et al. 2000). This suggests that drying objects at low RH will ensure immediate formation of safe Na_2SO_4 and above this the $\text{Na}_2\text{SO}_4 \cdot 10\text{H}_2\text{O}$ initially formed will convert to safe Na_2SO_4 as long as the RH is maintained under the hydration point.

The crystallization of Na_2SO_4 may offer the threat of physical damage in porous substrates like corrosion matrices. Pressure created by Na_2SO_4 crystallisation at low RH can be high (Steiger & Asmussen 2008) and $\text{Na}_2\text{SO}_4 \cdot 10\text{H}_2\text{O}$ crystallisation produces large volume increases (Rodriguez-Navarro et al. 2000; Steiger & Asmussen 2008). The degree of solution supersaturation and the pore morphology determine which compounds will form, the crystal volume and the extent of any resulting damage. There is no quantitative data about corrosion product porosity and geometry, and so it is difficult to determine whether archaeological iron containing Na_2SO_4 solution will be damaged by pressure and volume increases during drying.

6.2.4.2 Ferrous sulphate

Ferrous sulphate was only identified as an evaporation product from non-alkaline solutions. In the presence of NaOH, Fe^{2+} is converted to green rust, probably GRII in this case due to the presence of sulphate ions (Refait et al. 2003a). It then oxidised to lepidocrocite (Table 18). It is only if pH of objects is returned to neutral e.g. through rinsing that FeSO_4 could form during drying. The corrosion threat from FeSO_4 was nevertheless examined as it has previously been suggested as a hazardous residue of alkaline sulphite treatment.

Ferrous sulphate is not reported naturally in anhydrous form. Although $\text{FeSO}_4 \cdot \text{H}_2\text{O}$ does occur in nature (Hemingway et al. 2002), it is not possible to convert $\text{FeSO}_4 \cdot 4\text{H}_2\text{O}$ into $\text{FeSO}_4 \cdot \text{H}_2\text{O}$ even using completely dry air (Ehlers & Stiles 1965). $\text{FeSO}_4 \cdot 5\text{H}_2\text{O}$ and $\text{FeSO}_4 \cdot 6\text{H}_2\text{O}$ are not thought to be stable (Hemingway et al. 2002). It is $\text{FeSO}_4 \cdot 4\text{H}_2\text{O}$ (rozenite) and $\text{FeSO}_4 \cdot 7\text{H}_2\text{O}$ (melanterite) that occur most readily (Hemingway et al. 2002). Their phase transition RH has been reported as ranging from 15% to 95% RH (25°C), but most values cluster around 60% RH (20°C) (Chou et al. 2002). Above 60% RH ferrous sulphate is said to be hygroscopic and to significantly increase corrosion risk (Jones 1996: 401). It deliquesces around 95% RH (Table 20).

At 75% RH $\text{FeSO}_4 \cdot 7\text{H}_2\text{O}$ did not absorb water nor did it cause noticeable corrosion of iron over a 12 day period (Figure 63), although longer time periods may detect slow corrosion. The hydration of the $\text{FeSO}_4 \cdot 4\text{H}_2\text{O}/\text{Fe}$ mixture at 75% RH took much longer, but weight gain did not continue at a significant pace after hydration was complete (Figure 64). The phase transition to $\text{FeSO}_4 \cdot 7\text{H}_2\text{O}$ did not appear to cause significant corrosion of iron. It is possible that minor corrosion occurred during the phase transition, but this was much less significant than that observed when chloride ions were present (Figure 65). If hydration of $\text{FeSO}_4 \cdot 4\text{H}_2\text{O}$ to $\text{FeSO}_4 \cdot 7\text{H}_2\text{O}$ proceeds via a dissolution-precipitation pathway, rather than solid state transformation, the dissolution phase may provide enough dissolved ions to form an electrolyte to support corrosion, but once hydration is complete, $\text{FeSO}_4 \cdot 7\text{H}_2\text{O}$ is not a significant threat to iron. Constant humidity fluctuations around the 60% RH boundary could cause corrosion, as the transition between the 4 and 7 hydrate occurs, but this requires further investigation. Even if this is the case, this RH is significantly higher than the RH at which residual chloride ions and compounds cause corrosion, from 15% RH (Watkinson & Lewis 2005a). The presence of chloride ions in objects is a much greater risk than the presence of sulphate ions.

6.2.5 Conclusion on risk from treatment residues

This initial investigation of the occurrence and corrosion impact of residues from alkaline sulphite treatment suggests that ferrous sulphate and sodium sulphate residues offer minor corrosion risks to iron at 75% RH. Sodium sulphate was the most abundant residue, but it did not significantly increase iron corrosion below 75% RH. Ferrous sulphate did not form in

alkaline conditions, and their supposed formation on objects suggested in previous literature requires thorough investigation. The only iron sulphates detected were ferrous sulphates formed from non-alkaline solution, and these may offer a minor corrosion risk at 75% RH, although corrosion was not observed in significant quantities. By far the most aggressive corrosion accelerator was sodium chloride. It produced rapid and continuous corrosion of iron at 75% RH, much greater than any of the sulphate compounds tested. Based on the laboratory models studied here, it can be reconsidered whether attempts to wash out treatment residues are necessary and whether they are likely to be more damaging than beneficial for the long-term survival of archaeological iron treated by alkaline sulphite.

The experiments carried out represent only an initial investigation of the results of drying alkaline sulphite and the possible implications of crystalline sulphate residues on iron corrosion at a set RH. Further examination of a range of solution concentrations dried at various temperatures and RH, and more thorough testing of residues at various RHs would offer greater insight into the formation of compounds and their behaviour to follow on from this initial study.

6.3 The effect of rinsing

6.3.1 Methodology

Although a full examination of the effects of rinsing could not be carried out, several nails were immersed in deionised water at room temperature to see if any immediate impact of rinsing could be observed. The nails were from the site of Billingsgate (BWB83) and had been immersed in alkaline sulphite solution (0.1M NaOH/0.05M Na₂SO₃) for three weeks prior to rinsing. 100 ml of deionised water was used to rinse each nail. A Hanna HI-2210 pH meter with combined electrode and automatic temperature compensation was used to monitor progress at 1 to 10 minute intervals, and the rinsing water was changed when pH stabilised. Three nails were exposed to rinsing, two without stirring, and one using a magnetic stirring rod in the base of the container.

6.3.2 Results

Figures 66, 67 and 68 show the results of rinsing for the three objects tested.

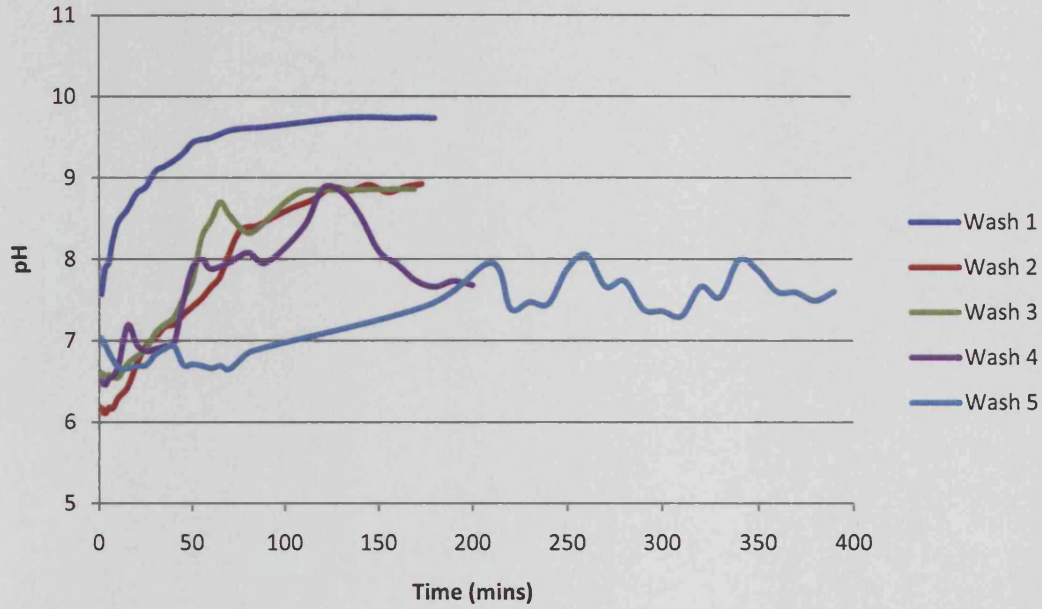


Figure 66: pH changes as a result of rinsing Nail 1 in deionised water. The rinse water was not stirred.

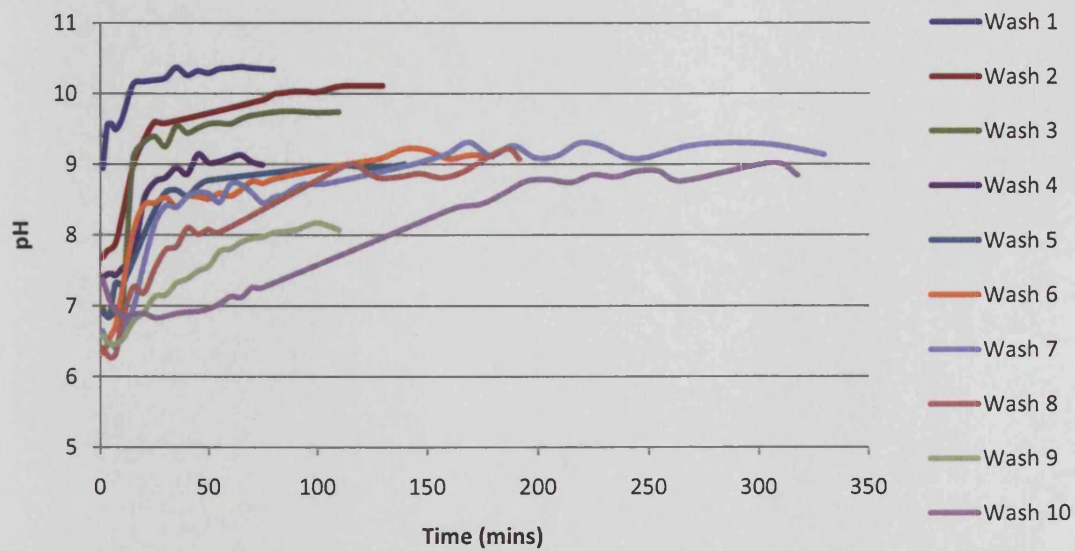


Figure 67: pH changes as a result of rinsing Nail 2 in deionised water. The rinse water was not stirred.

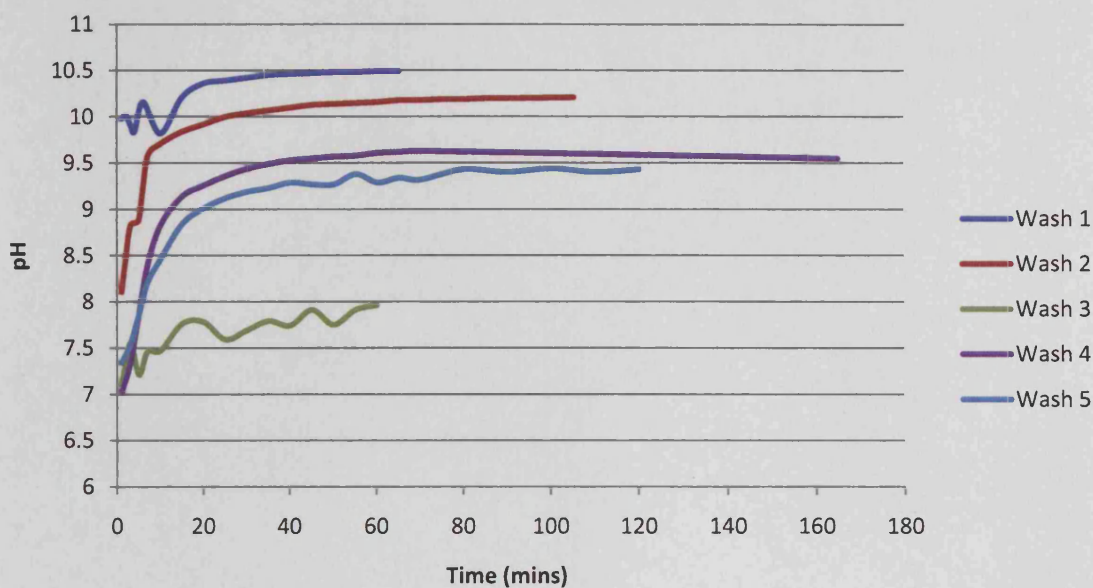


Figure 68: pH change as a result of rinsing Nail 3 in deionised water. The rinse water was stirred using a magnetic stirring rod.



Figure 69: Rinsing nail 2, showing development of orange corrosion on the surface after rinsing. The product was very powdery and non-adherent and identified as lepidocrocite.

Nail 1 reached roughly neutral pH after five changes of the rinsing water (Figure 66), while Nail 2 was still increasing the water to pH 9 after ten rinse solutions (Figure 67). Stirring

seemed to smooth out the pH measurement (Figure 68), but no obvious increase in the speed of neutralisation could be detected. The rate of pH increase in the solution was rapid in the first few rinse baths, and slowed in subsequent baths as expected for a diffusion-controlled process.

After two to three hours of immersion in deionised water, orange corrosion products began to form on the object and in the water (Figure 69). The development of this corrosion product was quite substantial if nails were left in the rinse solution overnight. The corrosion product was powdery, and could easily be removed with a scalpel or by brushing. Raman spectroscopy was used to identify this corrosion product (see Appendix 2.2.3 for details of method). In all three cases, the powder was identified as lepidocrocite, γ -FeOOH.

The appearance of lepidocrocite after several hours in the rinsing solution suggests that corrosion has been restarted by the rinsing procedure. This is not surprising, as oxygenated water has been introduced into the object. Formation was quite rapid and occurred in many places over the objects. Although the lepidocrocite could be easily removed, its formation indicates that rinsing in oxygenated water risks restarting the corrosion processes that have been halted during deoxygenated treatment. The lepidocrocite formation is unsightly and would require removing before an object could be stored or placed on display. A further danger is that, if the desalination treatment itself was not properly completed, rinsing could allow the mobilisation of remaining chloride ions which would then move back towards the anodic metal as corrosion restarts. This brief evaluation suggests that more thorough testing of the potential risks of rinsing is needed to fully understand whether it is beneficial or damaging to objects.

6.4 Summary

The simple qualitative assessment of the physical changes occurring to objects from desalination treatment is not conclusive, nor could the mechanisms by which these changes occur be elucidated. Nevertheless, the analysis shows that serious damage was less common than expected. The majority of the objects survived the treatment with no significant alteration to the appearance or integrity of the corrosion products, and only 2% suffered complete fragmentation. All the treatments gave similar results, including higher temperature treatment. The fragmentation of objects appears to be most strongly

influenced by the condition of the object and the amount of handling. This information can be integrated into an assessment of overall treatment outcome and risk (see Chapter 7).

Risk from sulphate-containing treatment residues appears to be quite limited in comparison to soluble chloride. The main residue from alkaline sulphite treatment is likely to be sodium sulphate, which has little effect on corrosion of iron except at high humidity above its hydration point (76.4% RH). Ferrous sulphate hydration did cause corrosion, but ferrous sulphate is an unlikely treatment residue in alkaline conditions. The sulphate compounds tested all had a much smaller impact on iron corrosion than chloride ions. Further work is needed to confirm the results, but the risk posed to objects from treatment residues is less than that from chloride ions, and should therefore not be considered a barrier to applying desalination treatment. The small possibility of risk from treatment residues may be an acceptable trade-off in reducing the risk from chloride-induced corrosion. This is encouraging, as the small-scale tests of rinsing suggested that this may restart corrosion and cause the formation of unsightly lepidocrocite on the surface of objects. If sulphate residues are not a significant risk, the need for laborious and possibly dangerous rinsing can be reconsidered. A full study of the risks from rinsing and whether rinsing is beneficial in removing treatment residues is recommended.

Chapter 7 – General discussion

In determining risk we must assess whether the intended treatment, if successful, would actually increase or maintain value. We need to know what the probability of an adverse outcome is and how this will affect value. We need to know the probabilities of unintentional consequences and determine their effect on value.

Ashley-Smith 1999: 288

7.1 Experimental treatment

The three experimental treatments (dNaOH, AS20 and AS60) showed similar patterns of extraction and efficiency in removing chloride ions from objects. Chloride was extracted at various rates; the majority of objects reached the specified completion criteria (< 10 ppm in final two treatment solutions) within 96 days at room temperature, and within 56 days at 60°C. Although the heated treatment completed more quickly, the overall extraction rate of chloride from the objects was not significantly improved; statistical analysis showed no significant difference in the mean extraction % of the three treatments. This suggests that there is no advantage in heating treatments in terms of chloride extraction, but there are benefits in reducing treatment time by increasing the diffusion rate.

There was no difference in the treatment effectiveness of the two deoxygenation methods (nitrogen gas or sodium sulphite), showing that either method is capable of deoxygenating the solution sufficiently to halt corrosion and promote the release of chloride. The longer time needed for nitrogen gas to deoxygenate the solution (via positive pressure) was not detrimental to the performance of the treatment.

The site from which the objects originated did play a role in the effectiveness of treatment. Nails from the coastal site of Bornais had significantly higher chloride levels than the other two sites, but it was the site of Caerwent that had the lowest average extraction % and retained higher levels of residual chloride. The nails from this site also had the highest number of objects which did not complete the treatment within the time. The most likely explanation is that there is some factor in the corrosion morphology or material of

Caerwent nails which impeded the ability of treatment to extract chloride, by slowing down the diffusion rate and/or containing higher levels of bound or inaccessible chloride.

The mean extraction % of all three treatments was 77%, with a standard deviation of 22%. This is less than in the previous study by Al-Zahrani (1999), where both alkaline deoxygenated treatments had a mean extraction % of over 97%, and a standard deviation of less than 3%. Two possible explanations are suggested for this difference:

- Some samples in this study achieved 99% extraction rate, and so it is possible that the objects selected by Al-Zahrani all achieved this. It would suggest that there were very low levels of bound chloride present, and that none of the objects had inaccessible areas of chloride ions. Such a sample does not represent the full variety of object morphologies and extraction efficiency as demonstrated in this study.
- The method used by Al-Zahrani to digest iron objects may have been flawed. Objects were digested for 3 days using a water bath to heat the acid (D. Watkinson, *pers.comm.* 26/05/2010), and this may have resulted in loss of chloride ions due to volatilization of HCl.

The latter is the most likely explanation for the apparently high and consistent extraction rate of Al-Zahrani's treatments. The data in this study is closer to that in other studies of alkaline treatments which have measured residual chloride content (Watkinson 1982, 1996). The results of Al-Zahrani (1999) are unlikely to represent an accurate picture of the ability of treatments to extract chloride ions.

7.2 Location, nature and effect of residual chloride

The analysis of cross-sections by scanning electron microscope (SEM) was able to identify where residual chloride was located and which types of chloride could or could not be extracted. Slag inclusions, which were found more prevalently in the Caerwent nails, harboured soluble chloride ions which were not accessible to the treatment solution. A second factor was the thickness of the corrosion products. Although this could not be measured reliably, nails from Caerwent displayed the deepest corrosion profiles, and these harboured chloride ions in small pockets at the interface with the metal core. Both deep corrosion profiles and chloride along slag inclusions could have contributed to the poorer performance of Caerwent nails. However, nails from all three sites were found to contain

low levels of chlorine within the corrosion product structure after treatment. Although its concentration could not be measured accurately, the levels were much lower than those found in untreated objects, where high concentrations of chloride in an apparently soluble form caused fresh corrosion products to appear on the polished surfaces of the cross-sections. This did not occur where chloride was located within the corrosion matrix in low concentrations.

Although it could not be definitely identified, the low levels of chloride found in the corrosion products of treated objects are most likely to be bound within the structure of akaganéite which has formed within the corrosion product structure. Treatments did not appear to be able to remove this. Surface-adsorbed chloride is known to enhance corrosion of objects, while the role of bound chloride in the tunnels is less certain. Tunnel-bound chloride may be of concern if akaganéite is metastable and transforms at a later date to release the chloride. Desalination treatments which are able to extract chloride ions from the tunnel structure of akaganéite could be considered to be preferable over those that do not.

Tests of the effects of treatment solutions on synthetically produced akaganéite under various conditions showed that treatment solutions were able to convert some of the akaganéite into goethite and, in some cases, hematite, and that this conversion was greater in alkaline conditions than in deionised water. However, the full transformation of akaganéite that was anticipated from the previous work of Al-Zahrani (1999) did not occur. The maximum conversion in this study was c. 50%. At room temperature conversion was limited to c. 20%. Heated solutions effected the transformation more quickly (within 24-48 hours), increased the proportion of transformation and altered the products of the transformation in some cases. Seeding with other corrosion products (goethite and magnetite) did not increase the amount of transformation, and in some cases appeared to retard it.

The results of the study lead to the conclusion that heated treatments under certain solution conditions do increase the transformation of akaganéite, and should therefore lead to the release of more chloride. This effect could not, however, be readily discerned in the treatment of objects. The appearance of chlorine-bearing crystalline corrosion products

identified on treated samples by SEM-EDX suggested that akaganéite remained on objects after treatments, although it could not be confirmed.

Two possible conclusions can be drawn. First, although transformation of synthetic akaganéite is possible under certain treatment conditions, it may not occur on objects. The transformation of all corrosion products depends strongly on local conditions, and synthetic corrosion products may not be sufficiently similar to objects to allow extrapolation of the results. Only a study of transformations of corrosion products on objects can resolve this question. The other possibility is that some transformation of akaganéite does occur on objects, but the additional release in chloride is minimal compared to the total extraction. The difference between heated and room temperature treatment should have resulted in a greater conversion of akaganéite (by about 25 to 30%), but this effect was not discernable from the overall variability within each treatment. This suggests that the actual amount of akaganéite bound in objects is small compared to the soluble and adsorbed chloride. The additional transformation of akaganéite by some treatment solutions may not be a particularly important factor in determining the overall extraction efficiency of treatments.

The distinction between free and bound chloride is important when considering the meaning of the residual chloride content of the objects, which in this study was measured by digestion. Digestion cannot discern between bound and free chloride, nor are chloride ions evenly distributed throughout the object. As has been known for some time and was confirmed by SEM analysis, chloride ions in objects are highly localised. Nevertheless, residual chloride was the best available method for assessing the overall performance of treatments in terms of their chloride extraction ability. Some of this residual chloride is almost certainly bound chloride. If we assume that bound chloride does not play a significant role in corrosion promotion, then an object may contain some residual chloride and yet be unlikely to experience the type of rapid and detrimental corrosion caused by soluble chloride ions. Chloride ions up to 0.6 wt% can also be adsorbed onto the surface of goethite (Al-Zahrani 1999) and are not expected to have an effect on corrosion rate in this form. Not all residual chloride is therefore of concern in increasing corrosion.

An examination of the accelerated corrosion results sheds some light on this issue. The results of subjecting objects to highly corrosion-promoting conditions showed that the

response of an object to these conditions was dependent not just on its chloride content, but also on whether or not it had been treated. Untreated objects with similar overall chloride content to treated objects always tended to show a greater response to the accelerated corrosion conditions, both visually and by increased weight, even at relatively low chloride content at which treated objects were stable during the period of the test. Most of the treated objects did not gain significant weight during the tests, although there were exceptions, most of which related to incomplete treatments. Treated objects usually had chloride content less than about 500 ppm. If we assume that a treated object that does not show weight gain has had all the soluble chloride removed, then the residual chloride is likely to represent bound chloride, and this appears to be present in concentrations up to 500 ppm.

The accelerated corrosion study cannot be related directly to the behaviour of objects at room temperature and lower or fluctuating RH. The conditions in the test were highly corrosive, particularly in the use of high RH, which could promote corrosion reactions which do not occur at lower RH (Thickett 2005). However, it is the first attempt to compare the corrosion behaviour of treated and untreated objects where the chloride content of the objects is known. Although it is not possible to establish any direct quantitative relationship between chloride content and corrosion rate or say how much longer a treated object would survive, it has been established that in the majority of cases, properly treated objects are much less likely to corrode than untreated objects. Given how aggressive the accelerated conditions were, it was not surprising that many of the untreated objects corroded dramatically, but many of the treated objects showed very little sign of change, or changed only a little compared to similar untreated objects. As ambient conditions are much less corrosive than those in the test, the apparent stability of treated objects under the test conditions must translate into a similar stability under less damaging ambient conditions, although slow corrosion could occur over longer periods of time if bound chloride is slowly released from akaganéite.

Despite the fact that residual chloride content measured by digestion is not a reflection of the localised nature of chloride ions in objects, and the difficulties in using a weight gain methodology with accelerated corrosion, the tests have provided confirmation of the positive impact of desalination treatment on corrosion behaviour, supporting the general

conclusions of collection surveys (Keene & Orton 1985; Selwyn & Logan 1993; Keene 1994; Loeper-Attia & Weker 1997). The existence of a positive correlation between higher corrosion susceptibility and higher chloride content has been confirmed, and this can form the basis of further studies of corrosion rates of objects.

7.3 Probability of treatment outcomes

A model was set out in Chapter 3 of various possible value outcomes from treatment, combining the short-term outcome of damage during treatment with the long-term prospects for object stability. As a theoretical model, it allows the data from this study to be evaluated in terms of the long-term outcome for the lifespan and value of iron objects. Because of the problems with some of the data (discussed below) this is not intended as an actual prediction of long-term outcomes, but rather to present a mechanism by which treatment data can be combined and analysed in a quantitative way to facilitate improved discussion.

Data to calculate the overall outcomes of treatment includes the likelihood of treatments causing short-term damage (Chapter 6) and the long-term stability of objects as suggested by residual chloride content (Chapter 4).

Table 21: Probability of treatment outcomes calculated using short and long-term outcome data developed in this study.

| | | | dNaOH | AS20 | AS60 | Overall |
|---------|--------|--------------|--------------------|-------------------|-------------------|------------------|
| Outcome | Damage | Long-term | P _{dNaOH} | P _{AS20} | P _{AS60} | P _{All} |
| V2 | None | Poor | .1679 | .0276 | .0496 | .0897 |
| V3 | None | Optimum | .2336 | .3519 | .2852 | .2898 |
| V4 | Some | Optimum | .08 | .1479 | .1748 | .1218 |
| V5 | Some | Poor | .0575 | .0116 | .0304 | .0377 |
| V6 | Total | N/A | .0208 | .0208 | 0 | .0167 |
| V7 | None | Intermediate | .3285 | .3105 | .2852 | .3105 |
| V8 | Some | Intermediate | .1125 | .1305 | .1748 | .1305 |

To calculate the probability of each of the treatment outcomes in Figure 5, V2 – V8, the probability of damage and the probability of long-term success is combined by multiplying the probability for each category of short and long-term outcome. The results are given in Table 21 and shown graphically in Figure 70. In the graph the outcomes are arranged in approximate order from most favourable (V3) to least favourable (V6). Long-term outcome has been prioritised in terms of favourability, i.e. V4 (some damage but optimum long-term outcome) is considered more favourable than V7 (no damage but only intermediate stability improvement).

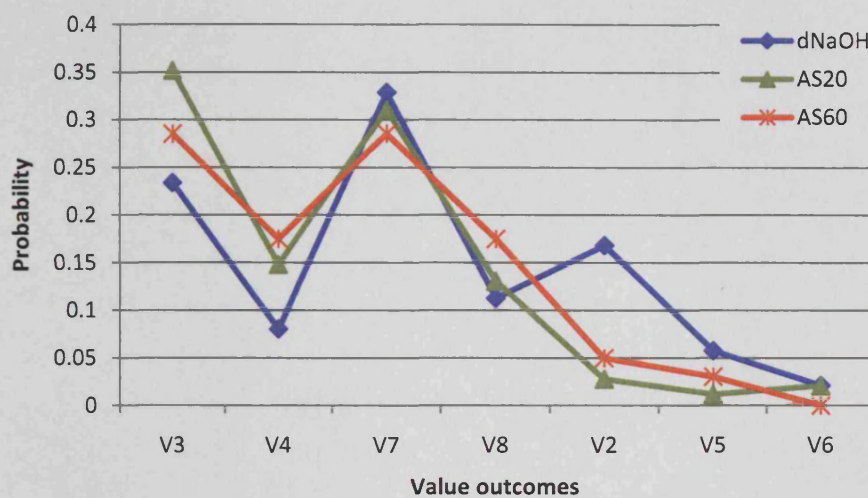


Figure 70: Graphical representation showing the probability of the treatment outcomes in order of decreasing desirability (left to right).

According to the data in this study, the most likely outcome is either V3 or V7, depending on which treatment is considered (Figure 70). The probability of the optimal outcome (V3 – no damage during treatment and less than 200 ppm residual chloride) is .2898 overall, with a maximum probability of .3519 for AS20 treatment (Table 21). The next most favourable outcome, with no damage during treatment and a reduction of chloride ion levels to less than 1000 ppm (V7), out of the ‘high risk’ zone suggested by North and Pearson (1978a), has a probability of .3105 (Table 21). Together, these two most favourable outcomes have a probability of greater than .6.

The two most negative outcomes (V5 and V6) are the least probable in all cases (Figure 70). The combined probability of the two least favourable outcomes is around .05, an order of

magnitude smaller than the two most favourable outcomes. V2, which is an overall neutral outcome, also has a low probability of just .08 (Table 21).

Comparing the three treatments, there is some variation between the three treatments, but no clear pattern emerges as to which is more favourable, and this reflects the analysis in Chapter 4 that the differences between the three treatments were not statistically significant.

Referring to Figure 5 (Chapter 3), apart from V5, V6 and V2, all the other outcomes represent some improvement in the overall lifespan of the object, and its ability to retain more value by time T2. Taking all these favourable outcomes together, the probability of making some improvement to an object by desalination treatment is about .86.

The probability of a drop in value is equivalent to a measurement of risk to the object (Ashley-Smith 1999). The calculated probability that the desalination treatment of an object will be unsuccessful (outcomes V2, V5 and V6) is about .13, seven times less likely than any of the favourable outcomes. The data suggests that approximately one in ten objects will not benefit from treatment. This figure includes objects where no change occurs compared to untreated objects (V2). This cannot be included in a calculation of risk, as no value has been lost due to the treatment. Without V2 included, the risk of the two most damaging outcomes V5 and V6 is only .05, or one object in every twenty treated.

These probability calculations can only provide a rough guide to the relative frequency of treatment outcomes. Much will depend on individual objects and their prior condition. Which outcomes are accepted as successful will also be dependent on individual situations. For very fragile or rare objects, any damage occurring during treatment may be more severe than for less important objects, and so the consideration of damage will play a greater role in treatment decisions. These judgements can only be made by conservators in individual situations.

However, the analysis does show that a positive outcome from treatment is reasonably likely, and that the severest forms of damage and/or treatments that do not improve the stability of the objects are quite unlikely. This is a useful way of assessing the possible effects of treatment using data analysis as the basis of the evaluation rather than anecdotal

outcome. It is an improvement by permitting quantitative assessment of the outcomes of treatment, and has only been possible due to the large number of samples and the statistical robustness of the data in this study.

The use of the damage categorisation (Chapter 6) to calculate treatment outcomes is problematic, as the methodology used to assess the data was crude and qualitative only. Damage is a complex issue, and could not be fully assessed in this study. The use of this data to assess treatment outcomes must be approached with caution. However, it has been demonstrated that such an approach is possible. This is intended to point the way to a more quantitative evidence-based evaluation of treatments and the risks involved, and stimulate discussion of the level of risks that may be acceptable during treatment.

A further problem with the probability calculations is the lack of a quantitative link between the residual chloride data that has been used as a proxy measure for long-term outcome, and the actual corrosion rate of objects in ambient conditions. This undermines the credibility of the outcome analysis, as it is not known whether the boundary chloride values are an accurate measure for predicting the long-term stability of objects. If a quantitative link can be established between residual chloride levels, corrosion rates, and the long-term stability of objects, treatment data can be used to predict treatment outcomes with more accuracy using an approach such as the one demonstrated here.

Chapter 8 – Conclusion

Passive methods involving control of the environment will prolong the useful life of objects... However, there are a number of circumstances where chemical intervention is necessary to reduce rates of decay, in which case treatment should be sooner than later.

Ashley-Smith 1999: 302

8.1 Conclusions from experimental work

This thesis has fulfilled its main aim in providing a large and quantitative data set on the effectiveness of alkaline deoxygenated desalination treatments. Digestion of treated objects allowed quantitative assessment of the results of chloride extraction from archaeological iron objects. This has been supplemented by work on the risks of treatment to object coherence, the possible risks from treatment residues, and the function of treatment solutions in removing chloride from the corrosion product akaganéite. Methods for examining the link between chloride content and corrosion rate were tested, and a study under accelerated corrosion conditions provided an initial assessment of that relationship.

Desalination treatment is not capable of removing all the chloride ions in an object. It is capable of removing enough chloride to reduce the susceptibility of many objects to rapid corrosion. As the accelerated corrosion test showed, around 77% of the treated objects did not show any weight gain or signs of visual corrosion under the harsh accelerating conditions during the period of the test. This does not definitively prove that no corrosion has occurred, but there was a clear difference between the magnitude of the corrosion experienced by treated and untreated objects, with many of the untreated objects experiencing catastrophic damage within the test period.

The outcome of treatment for an individual object is difficult to predict, but using the large sample in this study it is possible to estimate the likelihood that treatment will reduce chloride content and increase lifespan. The suggestion that desalination treatments are often damaging and offer little benefit in stabilising iron has not been substantiated by this

thesis, although much more work on the relationship between chloride ion levels and actual object corrosion rates is required to confirm and extend the data presented here.

The main conclusions of the experimental work are as follows:

- Alkaline deoxygenated desalination treatments extract between 60-99% of chloride ions from the majority of objects.
- Heating treatment solutions decreased the length of the treatment, but had no significant effect on increasing overall chloride extraction.
- Residual chloride levels in 87% of objects were less than 1000 ppm after treatment, and 42% achieved chloride content of less than 200 ppm. This represents a significant reduction in chloride content and should significantly improve the stability of objects.
- Treated objects were much less susceptible to corrosion under accelerated corrosion conditions. 77% of the treated objects showed no weight gain or visual corrosion under the test conditions.
- A positive correlation between chloride levels and corrosion rate was observed by accelerated corrosion testing, but it was not possible to extrapolate to corrosion behaviour in ambient conditions.
- Akaganéite can be transformed by alkaline solutions, but the amount of transformation is subject to numerous variables which require further assessment. It was not possible to ascertain whether transformation occurs on objects.
- Only 2% of objects experienced destructive fragmentation during treatment. 69% of objects experienced no change during treatment.
- Sulphate residues from alkaline sulphite solutions may cause some limited corrosion behaviour at elevated RH, but their effect is insignificant compared to the risk from chloride ions.
- The overall outcome of treatment is likely to produce some improvement in the stability and lifespan of objects in 86% of cases, based on the analysis of the available data.

8.2 Decision-making in iron conservation

Conservators perceive actions that may result in change or damage to objects as high risk. Risk aversion is appropriate in conservators and museum professional because of the responsibility they bear in preserving heritage for the future, but it may result in failure to carry out treatments that would be beneficial to objects and collections. Bad experiences with desalination treatments in the past may increase the perception of risk from treatment (Appelbaum 2007: 376).

Decision-making in conservation must involve an analysis of the costs, benefits and risks of the various conservation options available, e.g. through decision trees (Caple 2000) and risk analysis (Ashley-Smith 1999). As discussed in Chapter 3, the use of dehumidified storage has become the default strategy for iron conservation in Britain, as it appears to be low-risk and fulfils the principle of minimum intervention. If preventive conservation methods fail to deliver acceptable levels of preservation for iron, then this strategy must be revised. Preventive methods only stabilise iron if properly maintained. If maintenance is not possible, the use of preventive methods alone is a high-risk strategy, potentially exposing objects to damaging conditions on a regular basis.

For chloride-contaminated objects, moderate RH conditions of 35-40% are not sufficient to prevent corrosion induced by the high hygroscopicity of akaganéite and the presence of soluble chloride ions. If dry storage at 12% RH cannot be maintained to preserve these objects, desalination treatment could be used to reduce the susceptibility of these objects to corrosion and increase their lifespan.

Immersion in aqueous solution does carry risks, particularly for objects that are already fragile, and it is acknowledged that this is a concern. Nevertheless, risk arising from desalination must be balanced against the very real risk to objects when environmental control is insufficient to stabilise iron objects. Objects are damaged when humidity conditions are not low enough to prevent corrosion reactions, and this damage can be as bad as or worse than that occurring during desalination. When dehumidification in a box or showcase fails, every object in that container is then at risk. In a storage box, excessive RH may go unnoticed for several years, and by the time it is detected, objects may be too damaged to warrant further treatment or repair. Desalination treatments can be targeted

towards those objects most able to withstand the wet treatment procedure, and the risk of damage can be mitigated by protection of the object during treatment, careful monitoring and thorough documentation. Improvements in treatment method such as lower solution concentrations and methods of protecting objects during treatment (Selwyn & Argyropoulos 2005) have also helped to reduce the risk of desalination.

8.3 When should objects be treated?

Objects known to be contaminated with high levels of chloride ions will benefit more from early treatment. The objects will be less fragmented, thus reducing the risk of damage during the treatment. If treatment is carried out before objects are dried after excavation, it may be possible to extract more chloride before the formation of akaganéite has occurred. Treating early also preserves more of the total value of an object (Ashley-Smith 1999).

This suggestion rejects the idea that interventive treatment should only be used when less intrusive methods have proved inadequate. By the time it is recognised that an object is not sufficiently protected by passive means, it may already be too late to preserve the original value. If it is not possible to maintain proper environmental control for objects, then desalination of objects should be considered as early as possible to maximise the preservation of value.

Equally, a blanket policy of desalination treatment would be neither time nor resource efficient, and lead to objects being treated that do not require it. For freshly acquired material, an assessment of whether chloride contamination is likely to be a problem should be made, preferably before the material arrives to allow preparation time and resource allocation. Various methods have been trialled for assessing soil aggressiveness towards metal artefacts (Wagner et al. 1997; Wagner et al. 1998; Gerwin & Baumhauer 2000), but although higher chloride levels in soils are likely to lead to higher chloride levels in objects and more corrosion (Nord et al. 2005), the relationship between individual objects and their soil environment may be too complex to allow prediction based on soil chloride measurements. Digestion of several small and archaeologically unimportant iron objects (e.g. undated, context-less bulk iron) may be a better method of indicating whether objects are likely to be at risk from chloride ion corrosion. Some environments, e.g. coastal sites are

highly likely to produce severely contaminated objects, and desalination methods immediately after excavation should certainly be considered for these.

Objects already in museum collections which are found to be unstable and fragmenting require assessment of whether desalination is likely to benefit the object sufficiently to outweigh the risk. A decision will also be based on whether 12% RH can be achieved consistently, but where this is not possible, desalination treatment can be considered as a viable option, as an unstable object will continue to corrode and lose value if no action is taken.

Desalination treatment may also be considered for objects which cannot be displayed in dehumidified conditions, either because environmental control is not possible in the display area, or because objects are part of a mixed display where low RH conditions would harm the other materials. These cases can only be evaluated on an individual basis, but a desalination treatment could form part of a strategy for dealing with such issues.

8.4 Recommendations for treatment and storage

All three desalination treatments tested in this study performed in similar ways and had similar overall outcomes. Selecting a treatment from the three tested here can therefore be made on practical grounds. Heating the treatment to 60°C reduced the treatment time by around one-third without increasing the risk of damage to objects. If rapid treatment is desired, heated treatment can be recommended. Alkaline sulphite with a concentration of 0.1M NaOH and 0.05M Na₂SO₃ performed well at both room temperature and at 60°C, and the recommendation of the Swiss National Museum (Schmidt-Ott & Oswald 2006) to reduce alkaline sulphite treatment to these concentrations can be supported.

Reducing to 0.05M Na₂SO₃ reduces the quantity of chemical residues, particularly of the sulphate-containing residues which have previously caused concern. The results of the modelling study here suggested that sulphate-containing residues were unlikely to be problematic, as Na₂SO₄ is likely to be the most common residue and does not increase iron corrosion below 75% RH. No recommendation can be made on whether rinsing is necessary; further work is needed. If treatment residues are of concern, the nitrogen-deoxygenated 0.1M sodium hydroxide treatment is a suitable alternative, although it is more difficult to carry out this treatment at elevated temperatures due to the set-up of the gas

deoxygenation system (Appendix 1.3.1). Nitrogen gas is inexpensive and simplifies issues of chemical disposal of sulphite-containing solutions.

It is strongly recommended that the chloride content of treatment solutions be monitored. As discussed in Chapter 4, objects must be desalinated to completion (that is, to at least less than 10 ppm, and preferably to less than 5 ppm in final two baths) to maximise the likelihood of optimum stability improvement. Objects that do not complete treatment are more likely to experience later corrosion. Measurement of chloride ion concentration does make desalination treatment more laborious. Several methods of chloride ion determination are available (Wang et al. 2008), but all require additional time, effort and equipment to carry out, and have different levels of accuracy. Nevertheless, monitoring of treatment progress is essential in achieving the best possible outcome.

If treatments are completed until only very low chloride levels remain, the risk to objects from RH greater than the critical RH of 15% is likely to be significantly reduced. Objects that have had the majority of the chloride ions removed will be less susceptible to low RH corrosion and will be at less risk if storage conditions are exceeded or objects are moved to uncontrolled spaces. Because the treatment outcome for individual objects cannot be predicted with absolute certainty, it is not possible to say that treated objects are no longer at any risk from chloride ions. When a large group of objects is treated, the data in this study suggests that a small percentage will retain sufficient chloride to cause corrosion, but there is no method for determining which objects will be stable after treatment and which will not, except long-term observation. However, even if objects are not completely stabilised by treatment, their lifespan should be extended by the treatments. Removing chloride ions must be beneficial to objects, even if some residual chloride ions remain. Corrosion rates should be slower after treatment as less chloride is present, and so the risks of corrosion occurring during storage failure are also lowered.

8.5 Further work

There are several areas which would benefit from further research to follow on from the work presented in this thesis.

- The link between chloride content and corrosion rate requires a significant and extended study. Although a positive correlation was established by the accelerated

corrosion test, a study under ambient conditions is necessary to properly evaluate the improvement that desalination treatments make to object stability. Oxygen depletion as a measure of corrosion rate could be used to do this.

- The effect of treatment solutions on corrosion products and morphology should be studied. A detailed examination with SEM-EDX on cross-sections before and after treatment would be an initial step. This could be supplemented with other methods of analysis such as hardness testing to understand the effect of immersion on the composition and structural coherence of corrosion layers.
- The treatment of synthetic akaganéite in this study contradicted earlier work. A full-scale study of akaganéite transformation under a wider range of conditions and examining a wider range of variables is necessary to explain this difference and determine which treatment solutions are likely to transform akaganéite on objects. A study of object corrosion products which identifies akaganéite before and after treatment is necessary.
- An initial study of treatment residues has suggested that the risk from chemical residues may not be as significant as previously thought. The formation of residues in objects should be determined, alongside further testing of the effect they have on iron corrosion. Tests on the effectiveness of rinsing on removing chemical residues should also be carried out.

Bibliography

- Al-Zahrani, A. A. (1999). Chloride ion removal from archaeological iron and beta-FeOOH. Unpublished PhD Thesis, University of Wales, Cardiff.
- Angelini, E., E. Barberis, P. Bianco, F. Rosalbino and L. Ruatta (1998). Effect of burial in different soils on the decay of iron artifacts: Laboratory investigation. Metal 98 : proceedings of the international conference on metals conservation, Draguignan-Figanières, France, 27-29 May 1998. ed. W. Mourey and L. Robbiola. London, James & James: 106-110.
- Antony, H., S. Perrin, P. Dillmann, L. Legrand and A. Chausse (2007). "Electrochemical study of indoor atmospheric corrosion layers formed on ancient iron artefacts." Electrochimica Acta 52(27): 7754-7759.
- Aoki, S. (1987). Conservation of excavated iron objects in Japan. Recent Advances in the Conservation and Analysis of Artifacts. ed. J. Black. London, Summer Schools Press: 93-98.
- Appelbaum, B. (2007). Conservation Treatment Methodology. Oxford, Butterworth-Heinemann.
- Argyropoulos, V., L. S. Selwyn and J. A. Logan (1997). Developing a conservation treatment using ethylenediamine as a corrosion inhibitor for wrought iron objects found at terrestrial archaeological sites. Metal 95: Proceedings of the International Conference on Metals Conservation, Semur en Auxois, 25-28 Sept. 1995. ed. I. D. MacLeod, S. L. Pennec and L. Robbiola. London, James & James: 153-158.
- Arnould-Pernot, P., C. Forrieres, H. Michel and B. Weber (1997). Peut-on Dechlorurer les Objets Archeologiques Ferreux avec les Plasmas d'Hydrogene? Metal 95: Proceedings of the International Conference on Metals Conservation, Semur en Auxois, 25-28 Sept 1995. ed. I. D. MacLeod, S. L. Pennec and L. Robbiola. London, James & James: 147-152.
- Ashley-Smith, J. (1999). Risk assessment for object conservation. Oxford, Butterworth-Heinemann.
- Askey, A., S. B. Lyon, G. E. Thompson, J. B. Johnson, M. Cooke and P. Sage (1993). "The corrosion of iron and zinc by atmospheric hydrogen chloride." Corrosion Science 34: 233-247.
- Baron, D. and C. D. Palmer (1996). "Solubility of jarosite at 4-35°C." Geochimica et Cosmochimica Acta 60(2): 185-195.
- Bartz, A. E. (1988). Basic Statistical Concepts (3rd edition). New York, Macmillan.
- Beaudoin, A., M.-C. Clerice, J. Francoise, J.-P. Labbe, M.-A. Loeper-Attia and L. Robbiola (1997). Corrosion d'Objets Archeologiques en Fer apres Dechloruration par la Methode au Sulfite Alcalin; Caracterisation Physico-Chimique et Retraitement Electrochimique. Metal 95: Proceedings of the International Conference on Metals Conservation, Semur en Auxois, 25-28 Sept 1995. ed. I. D. MacLeod, S. L. Pennec and L. Robbiola. London, James & James: 170-177.
- Berducou, M. (1996). Introduction to Archaeological Conservation. Historical and Philosophical Issues in the Conservation of Cultural Heritage. ed. N. Stanley Price, M. K. Talley and A. Melucco Vaccaro. Los Angeles, J. Paul Getty Trust: 248-259.

- Bertholon, R. (2004). The location of the original surface, a review of the conservation literature. Metal 01: Proceedings of the International Conference on Metals Conservation, Santiago, Chile. ed. I. D. MacLeod, J. M. Theile and C. Degrigny. Perth, Western Australian Museum: 167-179.
- Bertholon, R. (2007). Archaeological metal artefacts and conservation issues: long-term corrosion studies. Corrosion of metallic heritage artefacts: Investigation, conservation and prediction for long-term behaviour. ed. P. Dillmann, G. Béranger, P. Piccardo and H. Matthiesen. Cambridge, Woodhead: 31-40.
- Bland, P. A., S. P. Kelley, F. J. Berry, J. M. Cadogan and C. T. Pillinger (1997). "Artificial weathering of the ordinary chondrite Allegan: Implications for the presence of Cl- as a structural component in akaganeite." American Mineralogist **82**(11-12): 1187-1197.
- Bradley, S. (1988). The Stabilisation of Iron (Internal Report). London, The British Museum.
- Butler, G. and J. G. Beynon (1967). "The corrosion of mild steel in boiling salt solutions." Corrosion Science **7**: 385-404.
- Cai, J., J. Liu, Z. Gao, A. Navrotsky and S. L. Suib (2001). "Synthesis and anion exchange of tunnel structure akaganeite." Chemistry of Materials **13**(12): 4595-4602.
- Cai, J. P. and S. B. Lyon (2005). "A mechanistic study of initial atmospheric corrosion kinetics using electrical resistance sensors." Corrosion Science **47**(12): 2956-2973.
- Caple, C. (2000). Conservation Skills: Judgement, Method and Decision Making. London, Routledge.
- Carpenter, J. and I. D. MacLeod (1993). Conservation of Corroded Iron Cannon and the Influence of Degradation on Treatment Times. International Council for Museums Committee for Conservation 10th Triennial Meeting, Washington DC. ed. J. Bridgland. Paris, James and James: 759-766.
- Chambaere, D. G. and E. Degraeve (1985). "The Beta-FeOOH to Alpha-Fe₂O₃ Phase-Transformation - Structural and Magnetic Phenomena." Physics and Chemistry of Minerals **12**(3): 176-184.
- Chitty, W. J., P. Dillmann, V. L'Hostis and C. Lombard (2005). "Long-term corrosion resistance of metallic reinforcements in concrete - a study of corrosion mechanisms based on archaeological artefacts." Corrosion Science **47**(6): 1555-1581.
- Chou, I. M., R. R. Seal and B. S. Hemingway (2002). "Determination of melanterite-rozenite and chalcantite-bonattite equilibria by humidity measurements at 0.1 MPa." American Mineralogist **87**(1): 108-114.
- Cole, I. S., T. H. Muster, D. Lau and W. D. Ganther (2004). Some recent trends in corrosion science and their application to conservation. Metal 04: Proceedings of the International Conference on Metals Conservation Canberra, Australia 4-8 October 2004. ed. J. Ashton and D. Hallam. Canberra, National Museum of Australia: 2-16.
- Cornell, R. M. and R. Giovanoli (1988). "Acid Dissolution of Akaganeite and Lepidocrocite - the Effect on Crystal Morphology." Clays and Clay Minerals **36**(5): 385-390.
- Cornell, R. M. and R. Giovanoli (1990). "Transformation of Akaganeite into Goethite and Hematite in Alkaline Media." Clays and Clay Minerals **38**(5): 469-476.
- Cornell, R. M. and R. Giovanoli (1991). "Transformation of Akaganeite into Goethite and Hematite in the Presence of Mn." Clays and Clay Minerals **39**(2): 144-150.
- Cornell, R. M. and U. Schwertmann (2003). The Iron Oxides: Structure, Properties, Reactions, Occurrences and Uses, 2nd edition. Weinheim, Wiley-VCH.
- Cronyn, J. M. (1990). The Elements of Archaeological Conservation. London, Routledge.

- Cudennec, Y. and A. Lecerf (2005). "Topotactic transformations of goethite and lepidocrocite into hematite and maghemite." Solid State Sciences **7**(5): 520-529.
- de Faria, D. L. A., S. S. Venancio and M. T. de Oliveira (1997). "Raman microspectroscopy of some iron oxides and oxyhydroxides." Journal of Raman Spectroscopy **38**: 873-878.
- de Graaf, M. J., R. J. Severens, L. J. van IJendoorn, F. Munnik, H. J. M. Meijers, H. Kars, M. C. M. van de Sanden and D. C. Schram (1995). "Cleaning of iron archaeological artefacts by cascaded arc plasma treatment." Surface and Coatings Technology **74-75**: 351-354.
- de Vivies, P., D. Cook, M. Drews, N. Gonzalez, P. Mardikian and J. B. Memet (2007). Transformation of akaganeite in archaeological iron artefacts using subcritical treatment. Metal 07: Interim Meeting of the ICOM-CC Metal Working Group, Volume 5: Protection of Metal Artefacts, 17-21 September 2007, Amsterdam. ed. C. Degriigny, R. van Langh, I. Joosten and B. Ankersmit. Amsterdam, Rijksmuseum: 26-30.
- Drews, M. J., P. De Vivies, G. Nestor, N. Gonzalez and P. Mardikian (2004). A study of the analysis and removal of chloride in samples from the Hunley. Metal 04: Proceedings of the International Conference on Metals Conservation Canberra, Australia 4-8 October 2004. ed. J. Ashton and D. Hallam. Canberra, National Museum of Australia: 247-260.
- Dünnwald, J. and A. Otto (1989). "An investigation of phase transitions in rust layers using Raman Spectroscopy." Corrosion Science **29**(9): 1167-1176.
- Duncan, S. J. (1988). The nature of chloride corrosion on iron: a review. London, The British Museum.
- Dussere, F. (1997). Peut-on Concevoir le Plasma comme un Traitement de Masse? Metal 95: Proceedings of the International Conference on Metals Conservation, Semur en Auxois, 25-28 Sept 1995. ed. I. D. MacLeod, S. L. Pennec and L. Robbiola. London, James & James: 138-146.
- Eggert, G. (2009). Rust never sleeps: Saving our ferrous finds for the next millennium. Lecture given at UCL Institute of Archaeology, 21st October 2009. London.
- Eggert, G. and B. Schmutzler (2009). Lässt sich die Konservierung von Eisenfunden 'auf Standard' bringen? kulturGUTerhalten: Standards in der Restaurierungswissenschaft und Denkmalpflege. ed. P. von Zabern. Berlin, Staatliche Museen zu Berlin: 91-95.
- Ehlers, E. G. and D. V. Stiles (1965). "Melanterite-rozenite equilibrium." American Mineralogist **50**: 1457-1461.
- Ellis, J., R. Giovanoli and W. Stumm (1976). "Anion exchange properties of b-FeOOH." Chimia **30**: 194-197.
- Evans, U. R. and C. A. J. Taylor (1972). "Mechanism of atmospheric rusting." Corrosion Science **12**: 227-246.
- Fowler, P. J. (1992). The Past in Contemporary Society: Then, Now. London, Routledge.
- Frini, A. and M. El Maaoui (1997). "Kinetics of the formation of goethite in the presence of sulfates and chlorides of monovalent cations." Journal of Colloid and Interface Science **190**(2): 269-277.
- Ganiaris, H. (2009). 30 years of iron conservation at the Museum of London. Archaeological Iron: Reflection and Outlook, 11th September 2009, London, Unpublished conference paper.

- Garcia, K. E. (2005). "On the Rust Products Formed on Weathering and Carbon Steels Exposed to Chloride in Dry–Wet Cyclical Processes." Hyperfine Interactions **161**: 127-137.
- Gasteiger, S. (2008). "Nachhaltige Konservierung archäologischer Eisenfunde durch Natrium-Sulfit Entsalzung." Jahrbuch der Bayerischen Denkmalpflege Band 60/61: 19-24.
- Génin, J. M. R., A. A. Olowe, N. D. Benbouzid-Rollet, D. Prieur, M. Confente and B. Resiak (1992). "The simultaneous presence of green rust 2 and sulfate reducing bacteria in the corrosion of steel sheet piles in a harbour area." Hyperfine Interactions **69**(1-4): 875-878.
- Gerwin, W. and R. Baumhauer (2000). "Effect of soil parameters on the corrosion of archaeological metal finds." Geoderma **96**(1-2): 63-80.
- Gil, M. L. A., A. Santos, M. Bethencourt, T. Garcia, S. Fernandez-Bastero, A. Velo and L. Gago-Duport (2003). "Use of X-ray and other techniques to analyse the phase transformation induced in archaeological cast iron after its stabilisation by the electrolytic method." Analytica Chimica Acta **494**(1-2): 245-254.
- Gilberg, M. R. and N. J. Seeley (1981). "The identity of compounds containing chloride ions in marine iron corrosion products: A critical review." Studies in Conservation **26**: 50-56.
- Gilberg, M. R. and N. J. Seeley (1982). "The Alkaline Sodium Sulphite Reduction Process for Archaeological Iron: A Closer Look." Studies in Conservation **27**: 180-184.
- Graedel, T. E. and R. P. Frankenthal (1990). "Corrosion mechanisms for iron and low alloy steels exposed to the atmosphere." Journal of the Electrochemical Society **137**: 2385-2394.
- Grossman, A. K. (2006). Keeping it together: conservation, context and cultural materials. The Object in Context: Crossing Conservation Boundaries - Contributions to the Munich Congress 28 August - 1 September 2006. ed. D. Saunders, J. H. Townsend and S. Woodcock. London, IIC: 1-6.
- Guilminot, E., N. Huet, D. Neff, P. Dillmann, C. Rémazeilles, P. Refait, S. Réguer, L. Bertrand, F. Nicot, F. Mielcarek, J. Rebière and F. Mirambet (2008). Dechlorination of archaeological iron artefacts: dechlorination efficiency assessment assisted by physico-chemical analytical high-tech methods. Preprints of the ICOM 15th Triennial Meeting, New Delhi, 22 - 26 September 2008. ed. J. Bridgland. New Delhi, Allied Publishers. **1**: 418-426.
- Hemingway, B. S., R. R. Seal and I.-M. Chou (2002). Thermodynamic Data for Modeling Acid Mine Drainage Problems: Compilation and Estimation of Data for Selected Soluble Iron-Sulfate Minerals. Reston, United States Geological Survey Open-File Report 02-161.
- Hjelmhansen, N., J. van Lanschot, C. D. Szalkay and S. Turgoose (1992). Electrochemical monitoring of archaeological iron artifacts during treatment. 3rd International Conference on Non-Destructive Testing, Microanalytical Methods and Environmental Evaluation for Study and Conservation of Works of Art, Viterbo, Italy, October 4-9. Brescia, Italy, Italian Society for Nondestructive Testing: 361-373.
- Hjelmhansen, N., J. Van Lanschot, C. D. Szalkay and S. Turgoose (1993). "Electrochemical Assessment and Monitoring of Stabilization of Heavily Corroded Archaeological Iron Artifacts." Corrosion Science **35**(1-4): 767-774.
- Ishikawa, T., Y. Kondo, A. Yasukawa and K. Kandori (1998). "Formation of magnetite in the presence of ferric oxyhydroxides." Corrosion Science **40**: 1239-1251.

- Ishikawa, T., S. Miyamoto, K. Kandori and T. Nakayama (2005). "Influence of anions on the formation of beta-FeOOH rusts." Corrosion Science **47**: 2510-2520.
- Jones, D. A. (1996). Principles and Prevention of Corrosion. Upper Saddle River, Prentice Hall.
- Kamimura, T., S. Nasu, T. Segi, T. Tazaki, H. Miyuki, S. Morimoto and T. Kudo (2005). "Influence of cations and anions on the formation of beta-FeOOH." Corrosion Science **47**(10): 2531-2542.
- Kaneko, K. and K. Inouye (1979). "Adsorption of water on FeOOH as studied by electrical conductivity measurements." Bulletin of the Chemical Society of Japan **52**(2): 315-320.
- Kaneko, K. (1993). Surface Chemistry of FeOOH Microcrystals. Current Problems in the Conservation of Metal Antiquities. Tokyo, Tokyo National Research Institute of Cultural Properties: 55-70.
- Kanji, G. K. (1993). 100 Statistical Tests. London, SAGE Publications.
- Keene, S. and C. Orton (1985). "Stability of treated archaeological iron: an assessment." Studies in Conservation **30**: 136-142.
- Keene, S. (1994). Real-time survival rates for treatments of archaeological iron. Ancient & Historic Metals: Conservation and Scientific Research. ed. D. A. Scott, J. Podany and B. Considine. Marina del Rey, Getty Conservation Institute: 249-264.
- Keene, S. (2002). Managing Conservation in Museums, 2nd edition. Oxford, Butterworth-Heinemann.
- Keiser, J. T., C. W. Brown and R. H. Heidersbach (1982). "The Oxidation of Fe₃O₄ on Iron and Steel Surfaces." Corrosion **38**(7): 357-360.
- Keller, P. (1970). "Eigenschaften von (Cl,F,OH)₂Fe₈(O,OH)₁₆ und Akaganeit." Neues Jahrbuch Mineralogie **113**: 29-49.
- Knight, B. (1982). Why do some iron objects break up in store? Conservation of Iron: Maritime Monographs and Reports No. 53. ed. R. W. Clarke and S. M. Blackshaw. London, National Maritime Museum: 50-51.
- Knight, B. (1997). The stabilisation of archaeological iron; past, present and future. Metal 95: Proceedings of the International Conference on Metals Conservation, Semur en Auxois, 25-28 Sept. 1995. ed. I. D. MacLeod, S. L. Pennec and L. Robbiola. London, James & James: 36-40.
- Kotzamanidi, I., E. Sarris, P. Vassiliou, C. Kollia, G. D. Kaniias, G. J. Varoufakis and S. E. Filippakis (1999). "Effect of heat treatment in reducing plasma environments on chloride ion removal and corrosion of oxidised steel artefacts." British Corrosion Journal **34**(4): 285-291.
- Kotzamanidi, I., P. Vassiliou, E. Sarris, A. Anastassiadis, L. Filippaki and S. E. Filippakis (2002). "Effects of plasma cleaning and conservation treatment on the corrosion layer of corroded steel - XRD evaluation." Anti-Corrosion Methods and Materials **49**(4): 256-263.
- Kranzler, G. and J. Moursund (1999). Statistics for the Terrified (2nd edition). Upper Saddle River, Prentice Hall.
- Kwon, S. K., S. Suzuki, M. Saito and Y. Waseda (2005). "Influence of foreign ions on the atomic scale structure of ferric oxyhydroxides." Corrosion Science **47**(10): 2543-2549.
- Lide, D. R., Ed. (1996). CRC Handbook of Chemistry and Physics, 77th edition. Boca Raton, CRC Press.

- Linnow, K., A. Zeunert and M. Steiger (2006). "Investigation of sodium sulfate phase transitions in a porous material using humidity- and temperature-controlled X-ray diffraction." Analytical Chemistry **78**(13): 4683-4689.
- Liu, J. and Y. Li (2008). "The study of immersion chloride extraction of iron artifacts." Materials and Corrosion **59**(1): 52-55.
- Loeper-Attia, M.-A. and W. Weker (1997). Dechloruration d'Objets Archeologiques en Fer par la Methode du Sulfite Alcalin a l'IRRAP. Metal 95: Proceedings of the International Conference on Metals Conservation, Semur en Auxois, 25-28 Sept 1995. ed. I. D. MacLeod, S. L. Pennec and L. Robbiola. London, James & James: 162-166.
- Mathias, C. (1994). "A conservation strategy for a Seventeenth-century archaeological site at Ferryland, Newfoundland." Journal of the International Institute for Conservation - Canadian Group **19**: 14-23.
- Mathias, C., K. Ramsdale and D. Nixon (2004). Saving archaeological iron using the Revolutionary Preservation System. Metal 04: Proceedings of the International Conference on Metals Conservation, Canberra, Australia, 4-8 October 2004. ed. J. Ashton and D. Hallam. Canberra, National Museum of Australia: 28-42.
- Matthiesen, H., L. R. Hilbert and D. J. Gregory (2003). "Siderite as a corrosion product on archaeological iron from a waterlogged environment." Studies in Conservation **48**(3): 183-194.
- McGowan, G. and J. Prangnell (2006). "The Significance of Vivianite in Archaeological Settings." Geoarchaeology **21**(1): 93-111.
- Merriman, N. and H. Swain (1999). "Archaeological Archives: Serving the Public Interest?" European Journal of Archaeology **2**(2): 249-267.
- Monnier, J., L. Bellot-Gurlet, L. Legrand, P. Dillmann, S. Réguer, D. Neff and I. Guillot (2007). The long term indoor atmospheric corrosion of iron: rust layer characterisation. Metal 07: Interim Meeting of the ICOM-CC Metal Working Group, Volume 2: Innovative Investigation of Metal Artefacts, 17-21 September 2007, Amsterdam. ed. C. Degryny, R. van Langh, I. Joosten and B. Ankersmit. Amsterdam, Rijksmuseum: 47-54.
- Muñoz Viñas, S. (2005). Contemporary Theory of Conservation. Oxford, Elsevier Butterworth-Heinemann.
- Navrotsky, A., F. L. Forray and C. Drouet (2005). "Jarosite stability on Mars." Icarus **176**: 250-253.
- Navrotsky, A., L. Mazeina and J. Majzlan (2008). "Size-Driven Structural and Thermodynamic Complexity in Iron Oxides." Science **319**: 1635-1638.
- Neff, D., S. Réguer, L. Bellot-Gurlet, P. Dillmann and R. Bertholon (2004). "Structural characterization of corrosion products on archaeological iron: an integrated analytical approach to establish corrosion forms." Journal of Raman Spectroscopy **35**(8-9): 739-745.
- Neff, D., P. Dillmann, L. Bellot-Gurlet and G. Beranger (2005). "Corrosion of iron archaeological artefacts in soil: characterisation of the corrosion system." Corrosion Science **47**(2): 515-535.
- Neff, D., L. Bellot-Gurlet, P. Dillmann, S. Réguer and L. Legrand (2006). "Raman imaging of ancient rust scales on archaeological iron artefacts for long-term atmospheric corrosion mechanisms study." Journal of Raman Spectroscopy **37**(10): 1228-1237.

- Nelson, M. C. and B. Shears (1996). "From the Field to the Files: Curation and the Future of Academic Archaeology." Common Ground 1(2): http://www.nps.gov/history/archeology/Cg/vol1_num2/files.htm Accessed 28/04/2008.
- Nord, A. G., K. Tronner, E. Mattsson, G. C. Borg and I. Ullen (2005). "Environmental threats to buried archaeological remains." Ambio 34(3): 256-262.
- North, N. A. and C. Pearson (1975). Alkaline sulfite reduction treatment of marine iron. ICOM Committee for Conservation, 4th Triennial Meeting Venice, 75/13/3. Paris, International Council of Museums: 1-14.
- North, N. A. and C. Pearson (1978a). Methods for treating marine iron. ICOM Committee for Conservation 5th Triennial Meeting, Zagreb, 78/23/3. Paris, International Council of Museums: 1-10.
- North, N. A. and C. Pearson (1978b). "Washing methods for chloride removal from marine iron artifacts." Studies in Conservation 23: 174-186.
- North, N. A. (1982). "Corrosion products on marine iron." Studies in Conservation 27: 75-83.
- North, N. A. and I. D. MacLeod (1987). Corrosion of metals. Conservation of Marine Archaeological Objects. ed. C. Pearson. London, Butterworths: 68-98.
- Novakova, A. A., T. S. Gendler, N. D. Manyurova and R. A. Turishcheva (1997). "A Mossbauer spectroscopy study of the corrosion products formed at an iron surface in soil." Corrosion Science 39(9): 1585-1594.
- Oddy, W. A. (1987). A New Method for the Conservation of Iron: Ionophoresis in a Non-Aqueous Electrolyte. Recent Advances in the Conservation and Analysis of Artifacts. ed. J. Black. London, Summer Schools Press: 155-158.
- Oguzie, E. E., I. B. Agochukwu and A. I. Onuchukwu (2004). "Monitoring the corrosion susceptibility of mild steel in varied soil textures by corrosion product count technique." Materials Chemistry and Physics 84: 1-6.
- Oh, S. J., S. J. Kwon, J. Y. Lee, J. Y. Yoo and W. Y. Choo (2002). "Oxidation of Fe²⁺ ions in sulfate-and chloride-containing aqueous medium." Corrosion 58(6): 498-504.
- Olowe, A. A., P. Refait and J. M. R. Genin (1990). "Superparamagnetic behaviour of goethite prepared in sulphated medium." Hyperfine Interactions 57(1-4): 2037-2043.
- Oswald, N. (1997). In Search of the Lost Surface. 10 Years of Active Hydrogen Research: An attempt to Convert Destructive Criticism into Improvements of the Plasma Method. Metal 95: Proceedings of the International Conference on Metals Conservation, Semur en Auxois, 25-28 Sept 1995. ed. I. D. MacLeod, S. L. Pennec and L. Robbiola. London, James & James: 133-137.
- Ouahman, R., R. Rahouadj and P. Fluzin (1997). Traitement de Stabilisation du Fer par le Sulfite Alcalin: Modelisation de la Diffusion des Ions Cl⁻. Metal 95: Proceedings of the International Conference on Metals Conservation, Semur en Auxois, 25-28 Sept 1995. ed. I. D. MacLeod, S. L. Pennec and L. Robbiola. London, James & James: 167-169.
- Ouyang, W. Z., C. C. Xu, L. J. Yue and F. Wang (2004). "A study of localised corrosion within occluded cells on a simulated cast iron artefact in chloride solution." Anti-Corrosion Methods and Materials 51(4): 259-265.
- Ouyang, W. Z. and C. C. Xu (2005). "Studies on localized corrosion and desalination treatment of simulated cast iron artifacts." Studies in Conservation 50(2): 101-108.
- Phillips, J. L. (1999). How to think about statistics (6th edition). New York, W.H. Freeman.

- Pye, E. (2001). Caring for the Past: Issues in conservation for archaeology and museums. London, James & James.
- Refait, P. and J. M. R. Génin (1994). "The Transformation of Chloride-Containing Green Rust One into Sulfated Green Rust 2 by Oxidation in Mixed Cl⁻ and SO₄²⁻ Aqueous-Media." Corrosion Science **36**(1): 55-65.
- Refait, P., S. H. Drissi, J. Pytkiewicz and J.-M. R. Génin (1997). "The anionic species competition in iron aqueous corrosion: role of various green rust compounds." Corrosion Science **39**: 1699-1710.
- Refait, P. and J.-M. R. Génin (1997). "The mechanisms of oxidation of ferrous hydroxychloride beta-Fe₂(OH)₃Cl in aqueous solution: the formation of akaganeite vs goethite." Corrosion Science **39**: 539-553.
- Refait, P., M. Abdelmoula and J.-M. R. Génin (1998). "Mechanisms of formation and structure of Green Rust one in aqueous corrosion of iron in the presence of chloride ions." Corrosion Science **40**(9): 1547-1560.
- Refait, P., G. A. M. Abdelmoula and J. M. R. Génin (2003a). "Coprecipitation thermodynamics of iron(II-III) hydroxysulphate green rust from Fe(II) and Fe(III) salts." Corrosion Science **45**: 659-676.
- Refait, P., J. B. Memet, C. Bon, R. Sabot and J. M. R. Génin (2003b). "Formation of the Fe(II)-Fe(III) hydroxysulphate green rust during marine corrosion of steel." Corrosion Science **45**(4): 833-845.
- Réguer, S., P. Dillmann, F. Mirambet and L. Bellot-Gurlet (2005). "Local and structural characterisation of chlorinated phases formed on ferrous archaeological artefacts by μ XRD and μ XANES." Nuclear Instruments & Methods in Physics Research Section B-Beam Interactions with Materials and Atoms **240**(1-2): 500-504.
- Réguer, S., P. Dillmann and F. Mirambet (2007a). "Buried iron archaeological artefacts: Corrosion mechanisms related to the presence of Cl-containing phases." Corrosion Science **49**(6): 2726-2744.
- Réguer, S., D. Neff, L. Bellot-Gurlet and P. Dillmann (2007b). "Deterioration of iron archaeological artefacts: micro-Raman investigation on Cl-containing corrosion products." Journal of Raman Spectroscopy **38**(4): 389-397.
- Réguer, S., F. Mirambet, E. Dooryhee, J.-L. Hodeau, P. Dillmann and P. Lagarde (2009). "Structural evidence for the desalination of akaganeite in the preservation of iron archaeological objects, using synchrotron X-ray powder diffraction and absorption spectroscopy." Corrosion Science **51**: 2795-2802.
- Rémazeilles, C. and P. Refait (2007). "On the formation of beta-FeOOH (akaganeite) in chloride-containing environments." Corrosion Science **49**(2): 844-857.
- Rémazeilles, C., D. Neff, F. Kergourlay, E. Foy, E. Conforto, E. Guilminot, S. Réguer, P. Refait and P. Dillmann (2009). "Mechanisms of long-term anaerobic corrosion of iron archaeological artefacts in seawater." Corrosion Science **51**: 2932-2941.
- Rinuy, A. and F. Schweizer (1981). "Methodes de conservation d'objets de fouilles en fer: etude quantitative comparee de l'elimination des chlorures." Studies in Conservation **26**: 29-41.
- Rinuy, A. and F. Schweizer (1982). Application of the alkaline sulphite treatment to archaeological iron: A comparative study of different desalination methods. Conservation of Iron: Maritime Monographs and Reports No. 53. ed. R. W. Clarke and S. M. Blackshaw. London, National Maritime Museum: 44-49.

- Rodriguez-Navarro, C., E. Doehne and E. Sebastian (2000). "How does sodium sulfate crystallize? Implications for the decay and testing of building materials." Cement and Concrete Research **30**: 1527-1534.
- Rosenberg, G. A. (1917). Antiquites en Fer et en Bronze, leur Transformation...et leur Conservation. Copenhagen, Gyldendalske Boghandels Sortiment.
- Scharff, W. and I. Huesmann (1998). Conservation of archaeological metal artifacts: Thermal treatment methods for iron objects and temporary consolidation of fragile corrosion products with volatile binders. Metal 98 : proceedings of the international conference on metals conservation, Draguignan-Figanières, France, 27-29 May 1998. ed. W. Mourey and L. Robbiola. London, James & James: 155-161.
- Schmidt-Ott, K. and V. Boissonas (2002). "Low-pressure hydrogen plasma: An assessment of its application on archaeological iron." Studies in Conservation **47**(2): 81-87.
- Schmidt-Ott, K. (2004). Plasma-Reduction: Its Potential for Use in the Conservation of Metals. Metal 04: Proceedings of the International Conference on Metals Conservation, Canberra, Australia, 4-8 October 2004. ed. J. Ashton and D. Hallam. Canberra, National Museum of Australia: 235-246.
- Schmidt-Ott, K. and N. Oswald (2006). Alkaline Sulfite Desalination: Tips and Tricks. VDR conference handbook, "Archaeological Metal Finds - From Excavation to Exhibition". October 11-13th 2006, Mannheim, Germany: 17.
- Schmutzler, B. and N. Ebinger-Rist (2008). "The conservation of iron objects in archaeological preservation - Application and further development of alkaline sulphite method for conservation of large quantities of iron finds." Materials and Corrosion **59**(3): 248-253.
- Schwarz, H. (1965a). "Die theoretische Deutung der Eisen(II)-sulfat-Nester im atmosphärischen Rost." Werkstoffe und Korrosion **16**: 208-212.
- Schwarz, H. (1965b). "Untersuchungen über die Wirkung des Eisen(II)-sulfates beim atmosphärischen Rosten und beim Unterrosten von Anstrichen." Werkstoffe und Korrosion **16**: 93-103.
- Scott, D. A. and N. J. Seeley (1987). "The Washing of Fragile Iron Artifacts." Studies in Conservation **32**: 73-76.
- Scott, D. A. and G. Eggert (2009). Iron and Steel in Art. London, Archetype.
- Scully, J. C. (1990). The Fundamentals of Corrosion. Oxford, Pergamon.
- Selwyn, L. and V. Argyropoulos (2006). "Chlorine Determination in Archaeological Wrought Iron by Instrumental Neutron Activation Analysis." Journal of the Canadian Association for Conservation **31**: 3-12.
- Selwyn, L. S. and J. A. Logan (1993). Stability of Treated Iron: A Comparison of Treatment Methods. International Council for Museums Committee for Conservation 10th Triennial Meeting, Washington DC. ed. J. Bridgland. Paris, James and James: 803-807.
- Selwyn, L. S., P. J. Sirois and V. Argyropoulos (1999). "The corrosion of excavated archaeological iron with details on weeping and akaganéite." Studies in Conservation **44**: 217-232.
- Selwyn, L. S., W. R. McKinnon and V. Argyropoulos (2001). "Models for Chloride Ion Diffusion in Archaeological Iron." Studies in Conservation **46**: 109-120.
- Selwyn, L. S. (2004). Overview of archaeological iron: the corrosion problem, key factors affecting treatment, and gaps in current knowledge. Metal 04: Proceedings of the International Conference on Metals Conservation, Canberra, Australia, October 2004. ed. J. Ashton and D. Hallam. Canberra, National Museum of Australia: 294-306.

- Selwyn, L. S. and V. Argyropoulos (2005). "Removal of chloride and iron ions from archaeological wrought iron with sodium hydroxide and ethylenediamine solutions." Studies in Conservation **50**(2): 81-100.
- Shanks, M. (1992). Experiencing the past: on the character of archaeology. London, Routledge.
- Shearman, F. (2003). Archaeological iron, conservation and collections care: CGM file note. BM Internal Report. London, British Museum.
- Skinner, T. (1980). The treatment of archaeological iron by the alkaline sulphite method. Conservation of Iron. ed. T. Bryce and J. Tate, National Museum of Antiquities of Scotland.
- Smith, L. (2006). Uses of Heritage. Abingdon, Routledge.
- Sonderman, R. C. (1996). "Primal Fear: Deaccessioning Collections." Common Ground **1**(2): http://www.nps.gov/history/archeology/Cg/vol1_num2/fear.htm Accessed 28/04/2008.
- Song, F. M., D. W. Kirk, J. W. Graydon and D. E. Cormack (2002). "Effect of ferrous ion oxidation on corrosion of active iron under an aerated solution layer." Corrosion **58**(2): 145-155.
- Stahl, K., K. Nielsen, J. C. Hanson, P. Norby, J. Z. Jiang and J. van Lanschot (1998). The akaganeite-hematite reaction on the possibilities for chloride removal from iron artifacts. 25 Years School of Conservation Preprints of Jubilee Symposium 18-20 May 1998. ed. K. Borchersen. Copenhagen, Det Kongelige Danske Kunstakademi, Konservatorskolen: 157-160.
- Stahl, K., K. Nielsen, J. Z. Jiang, B. Lebech, J. C. Hanson, P. Norby and J. van Lanschot (2003). "On the akaganeite crystal structure, phase transformations and possible role in post-excavational corrosion of iron artifacts." Corrosion Science **45**(11): 2563-2575.
- Stambolov, T. (1985). The Corrosion and Conservation of Metallic Antiquities and Works of Art: A Preliminary Survey. Amsterdam, Central Research Laboratory for Objects of Art and Science.
- Stanley-Price, N. P. (1989). Archaeology and conservation training at the international level. Archaeological Heritage Management in the Modern World. ed. H. Cleere. London, Unwin Hyman: 292-301.
- Steiger, M. and S. Asmussen (2008). "Crystallization of sodium sulfate phases in porous materials: The phase diagram Na₂SO₄-H₂O and the generation of stress." Geochimica Et Cosmochimica Acta **72**(17): 4291-4306.
- Stratmann, M. and K. Hoffmann (1989). "In situ Mößbauer spectroscopic study of reactions within rust layers." Corrosion Science **29**: 1329-1352.
- Tam, A. (2009). Reassessment of desalinated Anglo-Saxon iron objects from Garton, East Yorkshire at The British Museum. Institute of Archaeology. London, University College London. **MSc in Conservation for Archaeology and Museums (Unpublished dissertation)**.
- Thickett, D. (2005). Analysis of iron corrosion products with Fourier transform infra-red and Raman spectroscopies. Proceedings of the Sixth Infra-Red and Raman Users Group Conference (IRUG6), Florence, Italy, March 29th - April 1st 2004. ed. M. Picollo. Padua, Il Prato: 86-93.
- Thickett, D., S. Lambarth and P. Wyeth (2008). Determining the stability and durability of archaeological materials. 9th International Conference on Non-Destructive Testing of Art, Jerusalem, Israel, 25-30 May 2008.

- Thickett, D. and M. Odlyha (forthcoming). Iron storage: assessment of dry storage microenvironments for archaeological iron. The conservation of archaeological materials - current trends and future directions, Williamsburg, 2005.
- Turgoose, S. (1982a). "Post-Excavation Changes in Iron Antiquities." Studies in Conservation **27**: 97-101.
- Turgoose, S. (1982b). The nature of surviving iron objects. Conservation of Iron: Maritime Monographs and Reports No. 53. ed. R. W. Clarke and S. M. Blackshaw. London, National Maritime Museum: 1-7.
- Turgoose, S. (1985). "The corrosion of archaeological iron during burial and treatment." Studies in Conservation **30**: 13-18.
- Turgoose, S. (1993). Structure, composition and deterioration of unearthed iron objects. Current Problems in the Conservation of Metal Antiquities. Tokyo, Tokyo National Research Institute of Cultural Properties: 35-52.
- Tylecote, R. F. and J. W. B. Black (1980). "The Effect of Hydrogen Reduction on the Properties of Ferrous Materials." Studies in Conservation **25**: 87-96.
- Vaniman, D. T., D. L. Bish and S. J. Chipera. (2008). "Salt-hydrate stabilities and Mars sample return missions, Ground Truth from Mars, April 21-23 2008, Albuquerque, Mexico." <http://www.lpi.usra.edu/meetings/msr2008/pdf/4025.pdf> Retrieved 9 July, 2009.
- Vega, E., P. Dillmann and P. Fluzin (2004). A study on species transport in the corrosion products of ferrous archaeological analogues: A contribution to the modelling of iron long term corrosion mechanisms. Prediction of Long Term Corrosion Behaviour in Nuclear Waste Systems: Proceedings of the 2nd International Workshop, Nice, September 2004. ed. Andra: 128-140.
- Vega, E., P. Berger and P. Dillmann (2005). "A study of transport phenomena in the corrosion products of ferrous archaeological artefacts using O-18 tracing and nuclear microprobe analysis." Nuclear Instruments & Methods in Physics Research Section B-Beam Interactions with Materials and Atoms **240(1-2)**: 554-558.
- Wagner, D., F. Dakoronia, C. Ferguson, W. R. Fischer, C. Hills, H. Kars and R. Meijers (1997). "Soil Archive" Classification in Terms of Impacts of Conservability of Archaeological Heritage. Metal 95: Proceedings of the International Conference on Metals Conservation, Semur en Auxois, 25-28 Sept 1995. ed. I. D. MacLeod, S. L. Pennec and L. Robbiola. London, James & James: 21-26.
- Wagner, D. H. J., M. Kropp, W. R. Fischer and H. Kars (1998). A systematic approach to the evaluation of the corrosion load of archaeological metal objects. Metal 98 : proceedings of the international conference on metals conservation, Draguignan-Figanières, France, 27-29 May 1998. ed. W. Mourey and L. Robbiola. London, James & James: 80-86.
- Wang, Q. (2007a). "An Investigation of Deterioration of Archaeological Iron." Studies in Conservation **52**: 125-134.
- Wang, Q. (2007b). "Effects of relative humidity on the corrosion of iron: an experimental view." The British Museum Technical Research Bulletin **1**: 65-73.
- Wang, Q., S. Dove, F. Shearman and M. Smirniou (2008). "Evaluation of methods of chloride ion concentration determination and effectiveness of desalination treatments using sodium hydroxide and alkaline sulphite solutions." The Conservator **31**.
- Wang, Z., C. C. Xu, X. Cao and B. Xu (2007). "The morphology, phase composition and effect of corrosion product on simulated archaeological iron." Chinese Journal of Chemical Engineering **15(3)**: 433-438.

- Watkinson, D. (1982). An assessment of lithium hydroxide and sodium hydroxide treatments for archaeological ironwork. Conservation of Iron: Maritime Monographs and Reports No. 53. ed. R. W. Clarke and S. M. Blackshaw. London, National Maritime Museum: 28-40.
- Watkinson, D. (1983). "Degree of mineralization: its significance for the stability and treatment of excavated ironwork." Studies in Conservation **28**: 85-90.
- Watkinson, D. (1996). Chloride extraction from archaeological iron: comparative treatment efficiencies. Archaeological Conservation and its Consequences: Preprints of the Contribution to the Copenhagen Congress, 26-30 August 1996. ed. A. Roy and P. Smith. London, International Institute for Conservation: 208-212.
- Watkinson, D. and M. Lewis (2004). ss Great Britain iron hull: modeling corrosion to define storage relative humidity. Metal 04: Proceedings of the International Conference on Metals Conservation Canberra, Australia 4-8 October 2004. ed. J. Ashton and D. Hallam. Canberra, National Museum of Australia.
- Watkinson, D. and M. R. T. Lewis (2005a). The Role of beta-FeOOH in the Corrosion of Archaeological Iron. Materials Issues in Art and Archaeology VII. ed. P. B. Vandiver, J. L. Mass and A. Murray. Warrendale, PA, Materials Research Society of America Symposium: 103-114.
- Watkinson, D. and M. R. T. Lewis (2005b). "Desiccated Storage of Chloride-Contaminated Archaeological Iron Objects." Studies in Conservation **50**: 241-252.
- Watkinson, D. and A. Al-Zahrani (2008). "Towards quantified assessment of aqueous chloride extraction methods for archaeological iron: de-oxygenated treatment environments." The Conservator **31**: 75-86.
- Watkinson, D. and M. Tanner (2008). SS Great Britain: Conservation and Access - Synergy and Cost. Conservation and Access: Contributions to the London Congress, 15-19 September 2008. ed. D. Saunders, J. H. Townsend and S. Woodcock. London, International Institute for Conservation of Historic and Artistic Works: 109-114.
- Weiser, H. B. and W. O. Milligan (1935). "X-ray studies on the hydrous oxides. V. Beta ferric oxide monohydrate." Journal of the American Chemical Society **57**: 238-241.
- Weissenrieder, J., C. Kleber, M. Schreiner and C. Leygraf (2004). "In situ studies of sulfate nest formation on iron." Journal of the Electrochemical Society **151**(9): B497-B504.
- Wiesner, I., B. Schmutzler and G. Eggert (2007). The desalination of archaeological iron objects with hydroxylamine. Metal 07: Interim Meeting of the ICOM-CC Metal Working Group, Volume 5: Protection of Metal Artefacts, 17-21 September 2007, Amsterdam. ed. C. Degriigny, R. van Langh, I. Joosten and B. Ankersmit. Amsterdam, Rijksmuseum: 110-114.
- Williams, J. (2009). The Use of Science to Enhance our Understanding of the Past, National Heritage Science Strategy Report 2, <http://www.heritagesciencestrategy.org.uk> retrieved 17/05/2010.
- Wood, M. (2003). Making Sense of Statistics: A Non-mathematical Approach. New York, Palgrave Macmillan.
- Zucchi, F., G. Morigi and V. Bertilasi (1977). Beta iron hydroxide formation in localized active corrosion of iron artifacts. Corrosion and Metal Artefacts. ed. B. F. Brown, W. Burnett, T. Chase et al, National Bureau of Standards: 103-106.

Appendix 1: Experimental methods

1.1 Manufacturing akaganéite

There are many methods available of manufacturing akaganéite (Cornell & Schwertmann 2003). The method chosen for this study was that used by Al-Zahrani (1999), and produces akaganéite via a solid-state reaction between pure iron and ferrous chloride ($\text{FeCl}_2 \cdot 4\text{H}_2\text{O}$). This method was preferred for this study as it occurs more slowly and does not involve the use of solutions, heating or other processes which do not occur on archaeological iron objects.

100 g each of pure iron powder and ferrous chloride were mixed together in open Petri dishes. The dishes were placed in a humidification chamber with a saturated solution of sodium carbonate (Na_2CO_3) which produced a relative humidity of $92\% \pm 5$. The door of the chamber was regularly opened to allow influx of oxygen in an attempt to prevent the formation of magnetite as occurred with Al-Zahrani (1999). The samples were regularly mixed with a metal spatula.

X-ray diffraction analysis after 4 months confirmed that akaganéite had formed. There was no trace of pure iron remaining, but some excess ferrous chloride was detected. The akaganéite was split into two samples and was washed using a Buchner funnel, one in acetone and the other in deionised water. Further XRD assay confirmed that both these methods were able to remove the excess ferrous chloride.

It is possible that the washing process removed some of the adsorbed chloride. Two samples from both acetone-washed and water-washed akaganéite were dissolved in nitric acid (see Appendix 1.4) to allow the chloride ion content to be determined. Both the acetone-washed samples contained a total of 7.8% chloride ions. The water-washed samples contained 7.0% and 7.4% respectively, suggesting that there had been a small amount of chloride removal during the washing process with water. The amount removed was minimal compared to the total amount of chloride in the akaganéite samples.

Once rinsed through, the akaganéite samples were allowed to dry in ambient conditions, and then lightly ground in an agate mortar to break up aggregated particles. They were then

stored in screw-top glass jars. A third XRD assay two years after manufacture showed that there had been no transformation of the akaganéite under the storage conditions.

1.2 Transformation experiments

Glass vials (volume 28 ml) were labelled and 1 g (± 0.005) of the corrosion product (akaganéite, goethite, magnetite) was weighed out. Where a corrosion product mixture was used, the mixture was prepared by weighing out the correct amount of each corrosion product and then grinding together in a large agate mortar until thoroughly mixed. 25 ml of the solution (NaOH or alkaline sulphite) was added to each vial using a pipette. The vials were sealed with rubber caps. Room temperature samples were placed in a tray and kept in the laboratory (15-20°C, 35-75% RH). Heated samples were placed in a standard oven (Make, model). This did not have independent temperature control, so a thermometer was placed inside and the oven adjusted until the desired temperature was maintained (60°C). This temperature was probably maintained to $\pm 5^\circ\text{C}$, and all the vials were kept together and in the same part of the oven to keep conditions the same for all samples. Vials were shaken once per day during the first week, and at least twice a week for the rest of the experiments, except for room temperature vials, which were shaken approximately once a week for the first eight months and not thereafter.

After the allotted time, samples were removed from oven and allowed to cool. The powder was separated from the solution using filter paper (Whatman No. 4), using 0.1M NaOH to rinse out residues. The samples were allowed to dry in ambient conditions (15-20°C, 35-75% RH) for 1 – 2 days, and then the powder was brushed off the filter paper into screw-top glass vials for analysis. Analysis was usually carried out within one month.

1.3 Desalination of objects

Objects were desalinated individually. Each nail was weighed into a screw-top HDPE flask with a volume of 125 ml. Solutions were changed by removing the nail from the container using plastic tweezers, pouring the solution out into a 250 ml glass beaker, rinsing the container and nail with deionised water and adding to the previous solution, and then replacing the nail and adding fresh solution using a measuring cylinder. While the solutions were prepared for chloride measurement, the beakers were covered with Parafilm 'M' laboratory film or watch glasses.

1.3.1 Nitrogen-deoxygenated NaOH

The treatment solutions had a volume of 100 ml (dNaOH). The flasks were left open and placed in Stewart boxes which had been divided into individual compartments to hold each flask and prevent accidental spillage. Holes were cut in the lids of the Stewart boxes and piping fed through. Joints were sealed with Plumbers Mate, a water-resistant putty which could easily be moulded to hold the tubing in place. The tubes were connected to the nitrogen gas cylinder as shown in Figure 71. A gas bubbler was connected to the exit tube on the right of Figure 71 so that gas flow could be monitored. The lids of the Stewart boxes were sealed with electricians tape rather than Plumbers Mate, as they needed to be regularly opened to change solutions and measure oxygen concentration in the solutions. There was some leakage from the boxes, but gas flow was regulated to constantly maintain a positive pressure of nitrogen within the boxes so that no oxygen would diffuse in. The set up is shown in Figure 72. The nitrogen cylinder was changed when empty as indicated by the dial on the regulator. One cylinder lasted approximately three weeks.

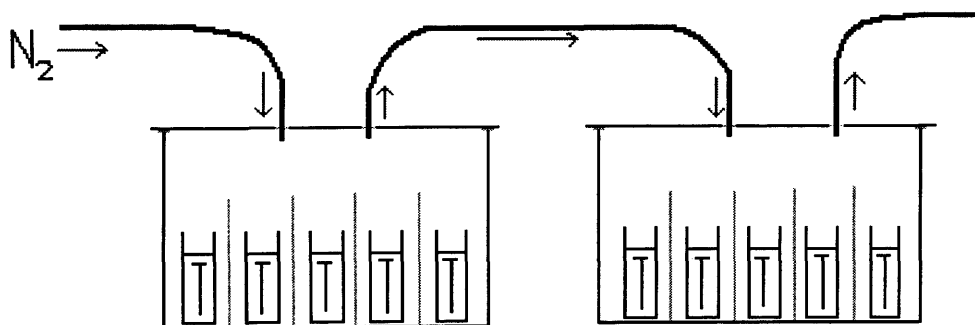


Figure 71: Diagram of set-up for dNaOH treatment.

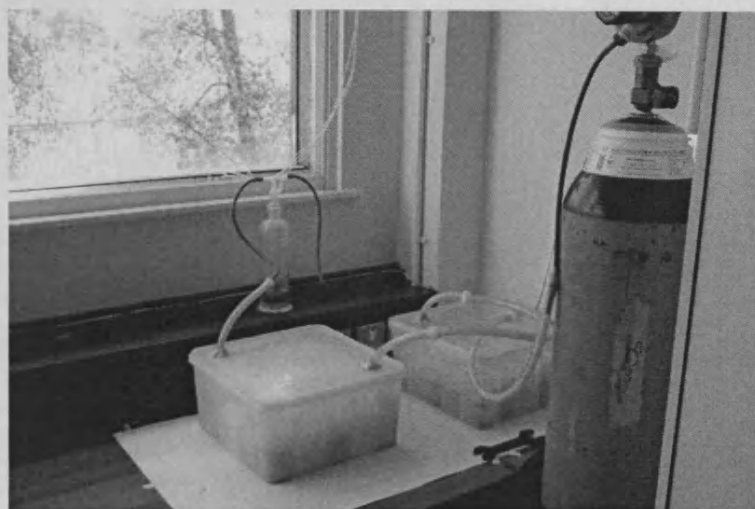


Figure 72: Nitrogen-deoxygenated desalination in progress. The gas from the cylinder (right) flows through both Stewart boxes and out via the gas bubbler at the back.

1.3.2 Alkaline sulphite

The same HDPE bottles were used for alkaline sulphite treatments after thorough washing and rinsing with deionised water. 120 ml of solution was used for both alkaline sulphite treatments to minimise the amount of air remaining in each flask. Lids were screwed on tightly to reduce oxygen ingress. This was sufficient to maintain deoxygenated conditions for each bath. Solution changes were carried out in the same manner as for dNaOH. For room temperature alkaline sulphite, the flasks were placed on the bench in the laboratory (temperature 28-25°C). Heated alkaline sulphite was placed in the oven on metal trays for easy handling, and allowed to cool to room temperature before changing the solutions.

1.4 Digestion of objects

Each nail was placed in a container, either a glass beaker (150-250 ml sizes) or a high-density polyethylene (HDPE) flask (120-250 ml sizes). The exact weight of the material in the container was recorded by zeroing the balance with the empty container before adding the nail and any associated flakes.

5M nitric acid (AnaLar grade) was diluted from concentrated (69%) nitric acid. Deionised water was used throughout, and all containers were thoroughly washed with deionised water to ensure that no chloride ions were present. The diluted nitric acid was then added to each container in sufficient quantity to cover the nail completely. Fizzing was sometimes observed as reactions between the acid and the corrosion products or adhering soil

minerals occurred. Containers were covered with watch glasses, Parafilm 'M' Laboratory Film or a screw cap in the case of the polypropylene flasks. The containers were placed in trays and kept in the fume cupboard during the duration of the dissolution process. The nails were stirred at regular intervals to break them up and aid the dissolution process. Stirring rods were rinsed back into the container to keep all the chloride ions. No heat was used to prevent the evaporation of hydrochloric acid (HCl). Dissolution took an average of 6-8 weeks at room temperature. Those containers with screw tops sometimes formed a brown gas on opening; this was nitrous oxide. Some objects began to form brown precipitates, which dissolved if more acid was added.

Total dissolution could not be achieved in all cases. Objects with a substantial metal core sometimes retained some of this core even after 8 weeks in nitric acid. As the vast majority of chloride ions are located in the corrosion products and at the metal/corrosion interface, it was assumed that objects which only had solid metal remaining had completed dissolution. The core was removed and rinsed. Other objects had remaining soil minerals which formed a residue in the solution. These were ignored and filtered out during the preparation process (see Appendix 2.3).

In a very few cases, dissolution of the corrosion products was not complete within 8 weeks. This tended to be objects with very thick corrosion products which contained little or no metal. This occurred with CAE_20 and CAE_40.1 and CAE_40.2. In the case of CAE_20, it was left for 1 year, after which dissolution was complete. Due to time considerations CAE_40.1/40.2 could not be left for this period of time and was excluded from the study.

To prepare digested nails for chloride ion measurement, the ferrous/ferric ions need to be removed. This was achieved by adding an excess of 3M NaOH, stirring with a glass rod until all the ferrous ions were precipitated as $\text{Fe}(\text{OH})_2$, a gel-like brown precipitate. The solutions were filtered using Whatman No. 1 filter paper. The filtrate was rinsed several times using deionised water, retaining all the rinse water to add to the sample solution. This method was that used by Al-Zahrani (1999), who showed that no chloride ions were retained by the $\text{Fe}(\text{OH})_2$ precipitate. Salt crystals which sometimes appeared on the filter paper during drying were tested but did not contain any chloride ions. These are likely to have been sodium carbonate precipitated from the excess sodium hydroxide during drying.

Once the ferrous/ferric ions were removed, the solutions were treated as given in Appendix 2.3.4.

1.5 Climate chamber tests

The climate chamber is a Vötsch VC4018 climatic chamber with temperature and humidity control. It is controlled via an attached computer. Tests show that conditions are maintained to within $\pm 0.1^\circ\text{C}$ and $\pm 0.5\%$ RH. When starting experiments, conditions are achieved within several hours (depending on difference between set parameters and external conditions) and can be maintained for at least six weeks as long as the water reservoir is replenished regularly.

A Mettler AJ100 analytical balance ($\pm 0.0001\text{g}$) was placed inside the chamber and connected to a computer to provide dynamic recording of weight change. Data was recorded to a text file and then copied into Microsoft Excel for graphing. The climate chamber causes vibration during operation which affects the balance. This was minimised by weighting the shelf with lead weights. Because of the vibration, the balance records a different weight when the chamber is operating, and so the weight of the sample cannot be read off directly from the graph. However, changes in weight are readily observable from the overall shape of the graph.

A 100g weight was placed on the balance and the chamber was run at 20°C and 75% RH for 15 days (Figure 73). The graph shows that although the balance was affected by the vibration of the chamber up to $\pm 0.008\text{ g}$, there was no overall drift in the readings.

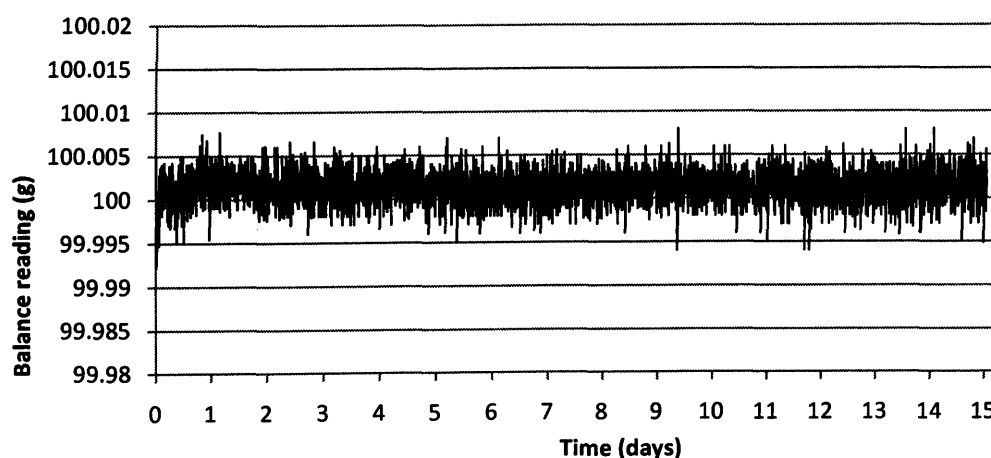


Figure 73: Testing weight measurements in climate chamber using 100g weight.

Appendix 2: Analytical methods

2.1 X-ray diffraction

2.1.1 Sample preparation

A small amount of the corrosion product mixture is ground in an agate mortar until very fine. A sub-sample is placed on a silicon chip and dispersed using a few drops of acetone, using the back of a scalpel blade to ensure even dispersion. The acetone is allowed to evaporate until dry, leaving a flat dispersion of powder on the chip. The chip is placed in the sample holder and analysed.

2.1.2 XRD method

XRD analysis was carried out at 40kV and 30mA, using Cu K α radiation from a copper anode. The measurement range was 5° to 75°, with a total time of 5 minutes. Data was exported to PANalytical X'Pert HighScore for analysis, including background and peak determination. The software matched peaks to stored profiles for mineral substances. These were scored based on the goodness of fit with the obtained profile. Once best-fit patterns had been used to establish which compounds were present in the sample, patterns were used which included a Relative Intensity Rating (RIR). These were not always the best-fit patterns, but allowed approximate proportions of the compounds present to be obtained quickly. Because the patterns used to obtain the proportions are not the best-fitting, the proportions are subject to an estimated 10% error. This was confirmed by running control samples of known akaganéite/goethite mixes which were prepared and analysed. Figure 74 shows the discrepancy between the actual proportions and those calculated by RIR. The scale of the error depends on the quantity of the products, and is an average of 10%. The proportion of akaganéite is always underestimated compared to goethite.

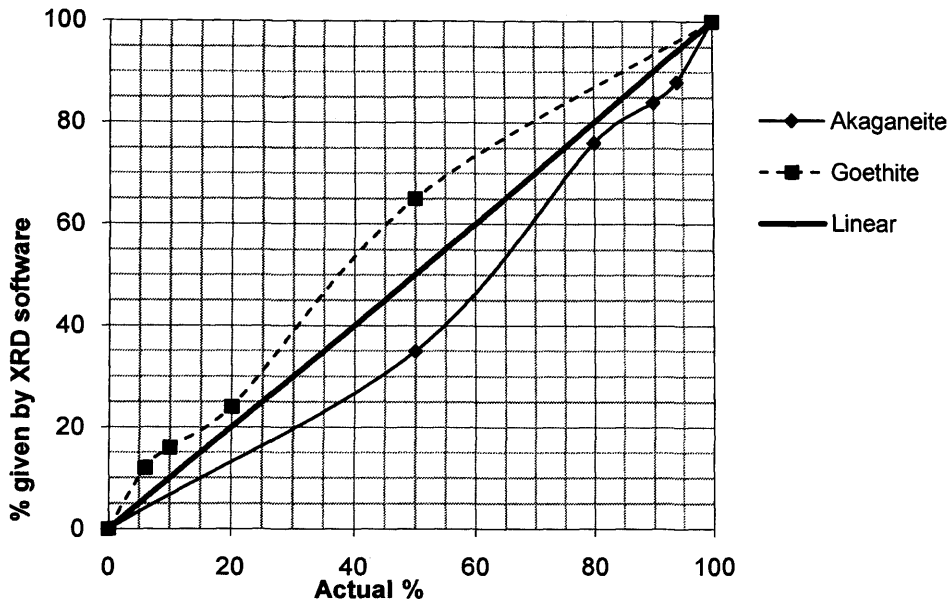


Figure 74: XRD analysis of standardised goethite/akaganéite mixtures.

2.2 Cross-section analysis

2.2.1 Sample preparation

Cross-sections for analysis were cut from the halved nails. A transverse section of several millimetres width was cut from near the original cut face using an ISOMET diamond saw and an oil-based lubricant (Buehler ISOCUT). The nail was wrapped in tissue before screwing into the holder to minimise removal of outer corrosion products and damage to the nail; however, some outer corrosion products were removed during the cutting procedure. The oil lubricant was removed from the samples by rinsing in Industrial Methylated Spirits (IMS) and the nails were dried with cool air blasts.

The cross-sections were set in epoxy resin with the freshly cut side as the side to be analysed. Once dry, the samples were ground using silicon carbide papers and polished using diamond paste down to 1 µm finish. White spirit was used as the lubricant throughout to prevent removal of chloride ions. Once polishing was completed, the white spirit was removed using a few drops of IMS and the samples were dried using compressed air.

Finally, the cross-sections were carbon-coated. For Raman analysis, the carbon coating was removed by repolishing the sample with 1 μm diamond paste as above.

2.2.2 SEM analysis method

Scanning electron microscopy (SEM) was carried out at The British Museum in the Department of Conservation and Scientific Research. The instrument is a Hitachi S-4800 field emission SEM equipped with energy dispersive X-ray spectrometry (EDX). The instrument is capable of magnifications from x60 to x50000, but for this study the maximum magnification used was x4500. The instrument was run at an accelerating voltage of 20 kV. Both SE and backscattered electrons were used as required. EDX analysis and mapping was carried out with a Silicon Drift detector (SDD) INCAx-act for X-ray detection and Oxford Instruments INCA software. Single spot analysis ran for 90 seconds, maps for between 1 and 3 hours depending on the size of the field. The detection limit for chlorine is c. 0.2%, with a relative precision of 10% which decreases as the detection limit is approached, and the mapping resolution was 512x416 pixels.

2.2.3 Raman microscopy

Raman microscopy was used on several of the cross-sections and other corrosion product samples to identify the chloride-containing products which were detected with the SEM. The analysis was carried out at The British Museum (Department of Conservation and Scientific Research) using a Jobin Yvon Infinity spectrometer equipped with a green laser (532 nm with maximum power of 1.2 mW at the sample). The analysis was run with a reduced laser power of 0.3 mW to avoid burning the sample. The analytical spot size was c. 5 μm in diameter. Spectra were compared with the in-house reference database and published data.

2.3 Chloride measurement

Chloride measurement was carried out using a Radiometer Analytical PHM250 specific ion meter with a mercury/mercury sulphate reference electrode (REF621) and a chloride-specific electrode (ISE25Cl). The meter is able to detect chloride down to a concentration of c. 0.5 ppm, although its ability to detect low concentrations depends on the calibration

solutions used. PHM250 is equipped with autoread and calibration functions, such that once calibrated, the meter calculates chloride ion concentration from the measured mV.

Calibration was carried out using standard NaCl solutions diluted from 0.1M (3544 ppm) NaCl solution made up from an ampoule. Deionised water was used throughout for dilution and washing of beakers and pipettes. Concentration of calibration solutions ranged from 3.5 to 354.4 ppm depending on the sample concentration. Because the relationship between measured mV and chloride concentration is logarithmic, meter inaccuracy results is minimised at lower concentrations, so concentrations above 354 ppm were avoided. Where sample concentrations fell outside of the calibration range, the meter was the sample was diluted to fit into the range.

All samples were pH adjusted prior to measurement to fall within the range 5.5 to 7. Although the specific ion meter is capable of taking accurate ion measurements in a large pH range (0-14), the calibration solutions were roughly neutral pH and so the samples were adjusted to the same range to minimise any differences. All samples and standard solutions had an ionic adjustment buffer added (0.5M acetic acid/0.5M ammonium acetate in deionised water) to minimise activity effects.

Two measurement methods were used to determine chloride ion concentration. For treatment solutions, direct measurement was used, which was able to give accurate and repeatable readings ($\pm 10\%$) with only one calibration. A standard addition method was adopted for solutions from digested nails, as these were heavily contaminated with other ions, and caused drift in the reference electrode. The method of measurement in each type of solution is given below.

2.3.1 In alkaline solutions

pH was adjusted using 5M nitric acid and 3M NaOH until in the range 5.5 to 7.0. The final volume of the solution was measured using a measuring cylinder (± 1 ml). A 10 ml sample was drawn using a pipette. 1 ml of the buffer solution was added. The meter was calibrated with at least four standard solutions, and sample measurements made directly. Two measurements were taken from each sample, and the values averaged. If there was more than 10% discrepancy between the two readings, a third reading was obtained. The

electrodes were rinsed for 20 seconds between each reading in deionised water, and dried gently using a Kimwipe tissue before immersing in the next solution. Standard solutions were measured at regular intervals, and the meter recalibrated if electrode drift exceeded 10%.

2.3.2 In sulphite-containing solutions

Sulphite ions (SO_3^{2-}) interfere with chloride measurement, and must be oxidised to sulphate ions (SO_4^{2-}) before the chloride concentration can be measured. Sulphite ions were oxidised using hydrogen peroxide (30% solution). 2 ml hydrogen peroxide was added per 100 ml of sample solution, and left to stand overnight until excess peroxide had decomposed. The sample was then treated as for alkaline solutions.

2.3.3 In sulphide-contaminated solutions

Some of the treatment solutions were contaminated with sulphide ions, particularly those that came from waterlogged contexts (BWB83 samples). Sulphide ions also interfere with chloride measurement by destabilising the electrodes and preventing stable readings from being acquired. Sulphide ions were removed by acidifying the solutions to less than pH 1 using 5M nitric acid, and then placing in a vacuum chamber overnight or leaving in a fume cupboard for several days. This removes sulphide ions by drawing off hydrogen sulphide gas. Once completed, the samples were pH adjusted to the range 5.5-7 using 3M NaOH and treated as above.

2.3.4 In solutions from digested nails

The solutions from digested nails contained an array of contaminants which could not be identified, but which destabilised the electrode and caused significant and rapid drift from the calibrated readings. To combat this, the standard addition method was adopted, which uses an additional internal standard in each sample to account for changes in the electrode potential. Samples were treated as above (neutralised, volume measured, 10 ml sample taken and buffer added). The meter was calibrated as normal using at least four standard solutions. An initial reading is taken from the sample. 0.5 ml of 0.1M standard solution (3544 ppm) is then added to the sample and a second reading taken. The PHM250 automatically calculates the concentration of the sample using the difference recorded from

the addition of a known quantity of chloride ions to account for electrode drift. Using this method usually produced very precise readings with less than 5% difference between repeated measurements on the same sample solution. As it is a more time-consuming method, however, it was only used when direct measurement was affected by unacceptable levels of drift.

2.4 pH measurement

pH measurement and adjustment were carried out using either a Electronic Instruments 7065 pH/mV meter at Cardiff University or a Hanna HI-2210-02 at The British Museum. Meters were calibrated with two standard pH buffers depending on whether acidic or alkaline measurements were taken, using pH 7, 4 and 9.2 buffer solutions. Both meters were operated using a combined pH electrode. When adjusting pH, the sample solution was swirled while adding 5M nitric acid or 3M NaOH using a pipette until the pH was in the correct range. The pH electrode was rinsed into the sample solution to retain all the chloride ions, and dried using a Kimcare wipe before immersing in the next sample. Temperature was either adjusted manually (Cardiff University) or automatically using an attached temperature probe (BM).

Appendix 3: Statistical methods

The statistical methods used in this thesis are standard statistical tests. This section briefly summarises the methods used for those not familiar with statistical methods and discusses the limitations of the methods used. References which were used to select and inform the use of statistics in this study were Bartz (1988) and Kanji (1993), with supplementary guidance from Kranzler and Moursund (1999), Wood (2003) and Phillips (1999). Statistics were calculated using Microsoft Excel.

3.1 Descriptive statistics

Descriptive statistics are those which describe a given set of data. The most important aspects of the data sets in this study are the measures of central tendency and the measures of distribution or variability.

3.1.1 Measures of central tendency

Measures of central tendency include the mean (sometimes called the average), the median and the mode. The mean is the most common measure of central tendency, and is calculated by summing the individual values (x) and dividing by the number of values (N), or using the =AVERAGE function in Excel. The median is the middle value when all the values are placed in ascending order (=MEDIAN), and the mode is the most common value in a given data set (=MODE). Many of the data sets in this study did not have a mode, so mean and median were used to describe central tendency.

In a normal distribution or bell curve, the mean and median are the same (Fig x). Any difference between the mean and the median suggests that the dataset is skewed (i.e. non-normal). Skewed distributions were common in this study. The mean is more significantly affected by the skew, as it takes account of all the values and therefore is more affected by high or low outliers than the median. In a skewed distribution, the median is the more accurate descriptor of the central tendency of the dataset.

3.1.2 Measures of distribution

The measures of distribution used in this study include the total range, interquartile range and standard deviation. The range is given by subtracting the lowest from the highest value. Although it describes the total dataset, like the mean it is significantly affected by high and

low outliers. The standard deviation is calculated by the following formula, where $\sum x^2$ is the sum of the squared scores, N is the number of scores, and m is the mean of the distribution (Bartz 1988).

$$S = \sqrt{\frac{\sum x^2}{N} - m^2}$$

In Excel, =STDEV is used to calculate standard deviation. Although it is less affected by outliers than the range, the standard deviation relies on the mean as a measure of central tendency, and therefore may not be suitable for skewed distributions.

The interquartile range is the range of the central 50% of the values in the dataset, i.e. the values that lie 25% either side of the median. Because it is based on the median, it is not strongly affected by outliers and is therefore a more appropriate measure to use for skewed distributions.

3.2 Inferential statistics

Inferential statistics are those that infer relationships within or between datasets. They always relate to a null hypothesis, which is formulated for each test. In this study, the null hypothesis is always that there is no relationship between the variables being analysed. The null hypothesis is refuted if the calculated value from the test lies above a critical value, which may be found in published tables. For this study, tables in Bartz (1988) and Kranzler and Moursund (1999) were used. If a calculated value falls above the critical value, then the null hypothesis is rejected. Different critical values are available for different levels of significance; that is, for example, at a .05 significance level, the probability of the obtained result being a random occurrence is 5 in 100, and at .01 significance level, 1 in 100.

3.2.1 Correlation (Pearson Product Moment, r)

The Pearson Product Moment Correlation Coefficient (r) is a measure of the linear relationship between two variables (e.g. between extraction % and residual chloride content). It is calculated by the formula below, or by using the =PEARSON function in Excel:

$$r = \frac{N\sum xy - (\sum x)(\sum y)}{\sqrt{[N\sum x^2 - (\sum x)^2][N\sum y^2 - (\sum y)^2]}}$$

Values of r can be anything from 0 to 1, where 0 is no correlation at all and 1 is a perfect linear correlation. Positive values of r indicate that an increase in one variable produces an increase in the other, whereas negative values of r indicate that an increase in one variable produces a decrease in the other. Where the critical value of r (r_{crit}) is exceeded at a particular significance level, the relationship between the two variables is significant, i.e. they are related. The closer the value of r is to 1, the stronger the relationship is. However, this does not necessarily imply causation.

The Pearson correlation coefficient is intended for use with roughly normal distributions. However, it can be used with skewed distributions provided that the sample size is large and the skew is not too large. For this study, the sample number when calculating r was always over 100, and so the Pearson correlation coefficient is sufficiently robust to be used as a measure of correlation.

3.2.2 Coefficient of variation (r^2)

The coefficient of variation (r^2) follows on from the Pearson Product Correlation. It is a measure of how much of the difference in one variable is accounted for by a change in the related variable. It is simply calculated by squaring r , or by using the =RSQ function in Excel. It may also be calculated using the trend line plotting tool on scatter graphs of the data. A low r^2 value suggests that although the two variables are related, the relationship is not very strong (e.g. a r^2 of 0.21 means that 21% of the variability in one measure is accounted for by variability in the other, while an r^2 of 0.95 means that 95% of the variability in one is accounted for by variability in the other). The closer r^2 is to 1, the more strongly the two variables are connected.

3.2.3 Analysis of variance (ANOVA) (F)

The analysis of variance (ANOVA) test is a method of comparing datasets with each other. It tests to see whether the differences between datasets are greater than can be accounted for by the variability within each dataset. It is an extended version of the t-test which compares the means of two datasets, but cannot be used for greater numbers of datasets. The ANOVA test is a method of comparing more than two datasets with each other. The test uses the variance, which is a measure of the variability of a dataset based on the squared

deviation from the mean. By comparing the variance within each dataset (i.e. the deviation of each score from the mean) with the variance between groups (i.e. the deviation of the mean of each dataset from the total mean of all datasets) it can be established whether the datasets are significantly different from each other. The calculated value F is the ratio of the variance between the groups to the variance within groups. If the null hypothesis that there is no significant difference between the means of the three groups is true, then the F ratio will equal 1. The larger F is, the more significant the difference between the means is. Critical values of F are given in statistical tables, and an F value larger than the critical value indicates that the difference between the means of the groups is not accounted for by the variance within each group.

Calculating F is a complex procedure and will not be explained here. The reader is referred to Bartz (1988) for full explanation of the ANOVA test, and to Kranzler and Moursund (1999) for a simplified method of calculation.

Because the ANOVA test depends on the mean of the datasets, it may be problematic when used with skewed distributions, where the mean is not an accurate representation of the central tendency. In this study, therefore, ANOVA tests are approached with caution. Where the value of F is only slightly higher than the critical value, the results must be carefully evaluated. In many cases, however, the median and the mean are sufficiently similar to allow the results of the ANOVA test to be used, especially when F is very large. It is used here as an indication of where significant differences may lie.

Once the null hypothesis has been rejected, a post-hoc analysis is required to determine which of the means in the ANOVA test is responsible for the positive result. The method used here is the Scheffé test to calculate C given in Kranzler and Moursund (1999) to compare pairs of means. Where significant values of C are obtained, the difference between the two means is significant. The Scheffé method was used only where it was not obvious from the mean/median which of the datasets was significantly different.

3.2.4 Chi-squared test (X^2)

The chi-squared test is used for non-parametric data; that is, data where individual values are grouped together rather than having individual scores. The test determines whether the

number in each group is significantly different from those that would be expected if the distribution were random. Its use in this thesis was limited to determination of whether change frequency was differently distributed among the three treatments. The test is described in Bartz (1988) and calculates whether the number of values in each category is different from those expected if the distribution occurred only by chance. One limitation of this test is that no cell should have an expected value of less than 1 and less than 20% of the cells should have expected values of less than 5. The table of change categories as given in Chapter 5 violates the first limitation, and so for the chi-squared test categories C and D were combined to avoid having expected values less than 1. However, the second limitation is still violated, as 3 out of 9 remaining cells have expected values less than 5. According to Bartz (1988) however, there is no agreement on how important this assumption is. As two of the three cells had expected values very close to 5 (4.8), the chi-squared test was applied. Although the results need to be treated with caution given the violated of this assumption, the very low level of χ^2 compared to the critical value suggests that the rejection of the null hypothesis is valid in this case.

